The Anatomical Origins of Migratory Dendritic Cells in the Intestine

Stephanie Ailsa Houston
BSc, MRes

Submitted in fulfilment of the requirement for the degree of
Doctor of Philosophy

Institute of Infection, Immunity and Inflammation
College of Medical Veterinary and Life Sciences
University of Glasgow

December 2013

Abstract

The intestine is exposed to a vast array of harmless dietary antigen as well as an enormous community of commensal bacteria. Alongside this harmless antigen, pathogens can enter the body via the intestinal mucosal surface. The intestinal immune system must discriminate between pathogens and innocuous antigens. Dendritic cells (DCs), present in the small intestine (SI) and colon, are fundamental in controlling intestinal immune responses; they migrate to the mesenteric lymph node (MLN) and prime effector or regulatory T cells. Furthermore, DCs direct the immune response in the gut-associated lymphoid tissues (GALT), the Peyer's patches (PP) and isolated lymphoid follicles (ILFs).

The aim of this work was to determine the anatomical origins of DCs in the MLN. First, the anatomical organisation of lymphatic vessels draining to the MLN from the SI and colon was investigated. Second, DC migration in mice lacking specific GALT was explored. Finally, the migration of DCs from PPs to the MLN was investigated. To achieve these aims, DC migration was studied using a variety of labelling methods, mice that lacked specific GALT were employed, and surgical procedures were used to collect DCs from the thoracic duct.

Here, I demonstrate the anatomical segregation of DCs that migrate to the MLN from the SI and colon. This was reflected in differences in DC subset composition and antigen presentation in the SI and colon-draining nodes of the MLN. Separate analysis of MLN nodes will allow a more refined understanding of intestinal immune responses. All but one DC subset, $CD103^-CD11b^-$ DCs, were still present in pseudo-afferent lymph from mice lacking both PPs and ILFs. This subset is therefore likely to originate from either PPs or ILFs. Surprisingly, $CD103^+CD8\alpha^+$ DCs were present in these mice, showing that many $CD8\alpha^+$ DCs were resident in the lamina propria and are not limited to lymphoid tissue. Four DC subsets are able to migrate from the intestine in PP-null mice, suggesting that $CD103^-CD11b^-$ DCs migrate specifically from ILFs. I then demonstrated that DCs migrate from PPs to the MLN. These migrating PP DCs expanded in response to a DC specific growth factor and their migration depended on CCR7 and S1P. These cells may play an important role in driving immune responses in the MLN and their manipulation could lead to advances in controlling intestinal immune responses.

Acknowledgments

Firstly I would like to thank my PhD supervisor Dr Simon Milling for his help and support over the last three and a half years. You have encouraged me to think for myself and given me the confidence to try new things, and make mistakes! I am particularly thankful for the time you have spent reading and correcting this thesis.

I would also like to thank the other original member of 'team mouse', Vuk. You were the best mouse cannulation teacher I could have had, even though I had to put up with your dodgy music choices! You have kept me right throughout my PhD, with help designing experiments and providing perspective (and Gin) when things weren't going so well. I also appreciate you taking the time to read this thesis and providing many helpful comments.

I must also thank Prof Allan Mowat for his encouragement and challenging comments in Lab Meetings, as well as reminding me of long forgotten papers. I would also like to thank Dr Oliver Pabst, who kindly welcomed me into his lab in Hannover to complete a set of experiments. You were genuinely interested in all the experiments I completed and were very kind during my visit. My thanks also go to Prof Jim Brewer, Prof Paul Garside and Prof Peter Lane for providing me with various mouse strains that have helped me complete extremely interesting experiments. I would also like to extend my gratitude to Carl Ware and his laboratory for providing me with key reagents, without which I could not have completed my studies anywhere near as quickly. I also want to acknowledge the Integrative Mammalian Biology programme for my scholarship.

I also need to extend my gratitude the other 'Mowlings' past and present. Pamela you've made me laugh a lot over the last few years. Thanks for putting up with me- it couldn't have been easy! I would like to thank you for reading bits of my thesis too. Lotta many thanks for whispering to my computer and making it work, I really couldn't have managed without your help. I would also like to thank Dawn and Aude for their help when I first joined the lab. Charlie I would like to thank for inspiring me to keep working, even in the midst of a

hangover- I don't know how you do it! Calum thank you for your guidance and your help with experiments over the last few years. I'd also like to thank Tamsin and Alberto for their encouragement. Together you've all made work an enjoyable place to be, and I'm sure we will remain good friends. I would also like to thank members of the Pabst Lab, particularly Anika for giving me somewhere to live in Hannover! I would like to extend my gratitude to Olga and Milas for their help with experiments while in Germany.

I must also thank staff at the CRF, particularly Tony, Dennis, Joanne, Dougie and Sandra. My thanks also go to Jim for giving me help and advice with microscopy and to Diane for all her FACS assistance.

I am very lucky to have a lovely group of friends who have helped me to escape from my PhD when necessary. Thanks to the Dunoon Crew for continually having the best house parties and the most excellent chat, and a special thanks to our adopted Sandra for being a very understanding flatmate. I would also like to thank Lauren, Jane, Anna, Jenny and Jodie for much drunken hilarity over the last few years, you stopped me from going mental. Thanks to The Yawns for giving me lots of excuses to go out, drink pints of red wine, and forget all about my PhD.

I would also like to thank my family, without your support I'm sure this wouldn't have been possible- in fact I probably wouldn't have managed to go to University in the first place. To my parents, Marion and David, for always believing I could do whatever I chose, and for helping me to achieve this. Thanks to my siblings Alison, Gavin and Suzanne. Sorry I've been so grumpy over the last few months!

Extra thanks go to Sean, thanks for putting up with my many freak-outs during my PhD and for not minding when I'm about 3 hours late! You've kept me sane over the last few years and always made me laugh. I could not have done this without you.

Authors Declaration

I declare that, except where reference is made to the contribution of others, this thesis is the result of my own work and has not been submitted for any other degree at the University of Glasgow or any other institution.

Signature: ..... Printed name: Stephanie Ailsa Houston .....

List of Abbreviations

A	
Ab	Antibody
Ag	Antigen
AhR	Aryl hydrocarbon receptor
ALDH	Aldehyde dehydrogenase
ALN	Axillary lymph node
ANOVA	Analysis of variance
APC	Antigen presenting cell
B	
BCA	Bicinchoninic acid assay
BLN	Brachial lymph node
BM	Bone marrow
BMDC	Bone marrow derived Dendritic Cell
BSA	Bovine serum albumin
C	
CD	Crohn's Disease
cDC	Conventional dendritic cell
cDNA	Complementary DNA
CDP	Common dendritic cell progenitor
CFSE	Carboxyfluorescein succinimidyl ester
CHO	Chinese hamster ovary
CP	Cryptopatch
cLP	Colonic lamina propria
CLP	Common lymphoid precursor
CMP	Common myeloid progenitor
CLN	Cervical Lymph Node
coMLN	Colonic draining mesenteric lymph node
coMLNx	Colonic draining mesenteric lymphadenectomy
CRF	Central research facility
CSF-1	Monocyte colony-stimulating factor
CSF-2	Granulocyte-macrophage colony stimulating factor
CT	Cholera Toxin
CTL	Cytotoxic T lymphocyte
CTLA-4	Cytotoxic T lymphocyte antigen 4
D	
DC	Dendritic cells
DMBA	7,12-Dimethylbenz(a)anthracene
DMEM	Dlbecco's modified Eagle's medium
DSS	Dextran sodium sulphate
E	
ESAM	Endothelial cell-selective adhesion molecule
EDTA	Ethylenediaminetetraacetic aci
F	
FACS	Fluorescence activated cell sorting
FBS	Foetal bovine serum
FCS	Foetal calf serum
fDC	Follicular dendritic cell
FITC	Fluorescein isothiocyanate
Flt3	Fms-like tyrosine kinase
Flt3L	Fms-like tyrosine kinase ligand
Foxp3	Forkhead box protein P3
FSC	Forward scatter
FTY720	Fingolimod
G	
GALT	Gut-associated lymphoid tissue
GF	Germ free
GFP	Green fluorescent protein
GP-2	Glycoprotein-2
GMP	Granulocyte-macrophage progenitor
H	
HA	Hyaluronic acid
HBSS	Hank's balanced salt solution
HSC	Haematopoetic stem cell

I	
i.v.	Intravenous
IBD	Inflammatory bowel disease
ICAM-1	Intercellular adhesion molecule-1
IEL	Intraepithelial lymphocyte
IFN	Interferon
Ig	Immunoglobulin
IL	Interleukin
ILC	Innate lymphoid cell
ILF	Isolated lymphoid follicle
ILN	Inguinal lymph node
iNOS	Inducible nitric oxide
int	Intermediate
iTregs	Inducible regulatory T cells
J	
JAM-A	Junctional adhesion molecule A
L	
LN	Lymph node
LP	Lamina propria
LPS	Lipopolysaccharide
LT	Lymphotoxin
LTα1β	Lymphotoxin α1β2
LTβR	Lymphotoxin β receptor
LTβR-Ig	Lymphotoxin β receptor fusion protein
LTi	Lymphoid tissue inducer cell
LTo	Lymphoid tissue organiser cell
LYVE-1	Lymphatic vessel endothelial hyaluronan receptor
LysoDC	Lysozyme expressing dendritic cell
M	
M cell	Microfold cell
MAdCAM-1	Mucosal vascular addressin cell adhesion molecule 1
MDP	Monocyte-dendritic cell progenitor
MHC	Major histocompatibility complex
MLN	Mesenteric lymph node
MLNX	Mesenteric lymphadenectomy
mRNA	Messenger RNA
N	
NALT	Nasal associated lymphoid tissue
NK	Natural killer
NOD	Nucleotide-binding oligomerization domain receptors
NOD-1	Nucleotide-binding oligomerization domain-containing protein 1
O	
OVA	Ovalbumin
P	
PAMP	Pathogen associated molecular pattern
PBS	Phosphate buffered saline
PCR	Polymerase chain reaction
pDC	Plasmacytoid dendritic cell
PE	Phycoerythrin
PerCP	Peridinin-chlorophyll-protein
PP	Peyer's patch
PRR	Pattern recognition receptor
R	
R848	Resiquimod
RA	Retinoic acid
RALDH	Retinaldehyde dehydrogenase
RBC	Red blood cell
RNA	Ribonucleic acid
RPMI	Roswell Park Memorial Institute-1640 medium
RORγt	RAR-related orphan receptor gamma
S	
S1P	Sphingosine-1 phosphate
S1PR	Sphingosine-1 phosphate Receptor
SD	Standard deviation
SEM	Standard error of the mean
SI	Small intestine
sIgA	Secretory IgA
siLP	Small intestinal lamina propria
SILT	Solitary intestinal lymphoid tissues

	siMLN	Small intestinal draining mesenteric lymph node
	siMLNx	Small intestinal draining mesenteric lymphadenectomy
	SMP	Splanchnic mesodermal plate
	SPF	Specific pathogen free
	SSC	Side scatter
T		
	TALT	Tear duct associated lymphoid tissue
	TCR	T cell receptor
	TDC	Thoracic duct cannulation
	Tfh	Follicular T helper cell
	TGF	Transforming growth factor
	Th	T helper cell
	TLR	Toll-like receptor
	TNF	Tumour necrosis factor
	Treg	T regulatory cell
	TRANCE	TNF-related activation-induced cytokine, RANKL
	TRANCER	TRANCE Receptor, RANK
	TRIP	TRAF-interacting protein
U		
	UC	Ulcerative colitis
	UEA-1	Ulex europaeus agglutinin-1
	UV	Ultraviolet
V		
	VCAM-1	Vascular cell adhesion protein-1
	VE-Cadherin	Vascular endothelial cadherin
Y		
	YFP	Yellow fluorescent protein

Chapter 1: Introduction

1.1 Dendritic Cells- A Brief Introduction

Dendritic cells (DCs) are specialised antigen presenting cells (APCs), which are essential for the induction and direction of an adaptive immune response. The term dendritic cell was coined in 1973 by Steinman and Cohn, who described a unique group of cells in the murine lymph nodes (LNs) and Peyer's patches (PP) (Steinman and Cohn, 1973). Since this first account, the role of DCs in the immune system has been much investigated. It has become clear that DCs form a link between the innate and adaptive immune responses and represent an immunological communication system between peripheral tissues and organised secondary lymphoid tissues.

DCs are present in the majority of tissues and organs throughout the body. They act as sentinels, continuously sampling their environment. They process antigen, undergo maturation and migrate from the periphery into organised lymphoid tissues by the lymphatic system. This is an essential step in the life cycle of a DC. Once in the draining LN they can interact with cells of the adaptive immune system required to initiate the immune response. This occurs in both the steady-state and during inflammation, and can result in immunological tolerance or the initiation of an immune response.

The extensive research into DCs has revealed that this term describes a heterogeneous population of cells, covering distinct subsets of DCs distinguishable by their expression of different surface markers, tissue distribution and functions. There are three major types of DCs: conventional DCs (cDCs), plasmacytoid DCs (pDCs) and follicular DCs (fDCs). fDCs are wholly different from cDCs and pDCs, they are not haematopoietic cells and present antigen in an MHC independent manner (Cyster et al., 2000; El Shikh et al., 2009; Tew et al., 2001). Their main function is to maintain immunological memory in B cell follicles of secondary lymphoid organs (Aguzzi and Krautler, 2010). As fDCs are distinct from cDCs and pDCs, and have not been the subject of my experiments, they will not be discussed further.

cDCs and pDCs are both present in peripheral tissue and both can prime naïve T cells (Kadowaki et al., 2001). cDCs are highly phagocytic while pDCs have poor phagocytic capacity. cDCs are able to migrate from the peripheral tissues to the LNs where they present antigen to naïve T cells. The migration of pDCs in afferent lymphatics is disputed. However, it is has been shown that pDCs are able to migrate to peripheral LNs via the blood (Ochando et al., 2006; Pascale et al., 2008; Yrlid et al., 2006b). Given the unique role that cDCs play in initiating and propagating the immune response and their ability to migrate from the periphery to the draining LNs, cDCs are being investigated further in this project.

1.2 Dendritic Cell Development

DCs in the periphery have a limited lifespan and must be continually replaced by circulating precursors. The precise origins of DCs and their differentiation programmes are complex and are only beginning to be fully understood. Models suggest that cDCs derive from committed cDC progenitors that develop in the bone marrow (BM) and travel via the blood to lymphoid organs and nonlymphoid organs, where they differentiate into mature cDCs (Fogg et al., 2006; Geissmann et al., 2010). Two distinct cell lineages can be recognised in the BM, myeloid and lymphoid. DCs represent a unique cell as they can be derived from both myeloid and lymphoid lineages (Manz et al., 2001). However, the majority of DCs in all compartments, except for the thymus, are derived from myeloid precursors (Liu and Nussenzweig, 2010; Naik, 2008).

The development of DCs in BM involves the differentiation of haematopoietic stem cells (HSC) through a number of morphologically distinct intermediate stages. At each stage there is a progressive lineage commitment and cells lose the potential to give rise to other cell types. The HSC is able to give rise to common myeloid progenitors (CMP) and the granulocyte macrophage progenitor (GMP). The CMP gives rise to the DC and monocyte precursor (MDP). The MDP no longer has granulopoietic potential and is characterised by the expression of c-kit, fms-like tyrosine kinase 3 (Flt3) and CX3CR1. This precursor is the first that is dedicated to the myeloid lineage (Fogg et al., 2006). Following the MDP there is likely to be a common DC progenitor (CDP), which can give rise to pDCs and DCs although its position remains controversial (Auffray et al., 2009; Naik et al.,

2007; Onai et al., 2007). Previous work suggested that monocytes were able to differentiate into DCs following transendothelial migration, while monocytes that remained in the subendothelial matrix differentiated into macrophages (Randolph et al., 1998). However, it has become clear that there is actually a DC-committed precursor that is independent of monocytes. The CDP has been shown to give rise to pDCs directly, and to the pre-cDC that can differentiate into cDCs but not pDCs (Diao et al., 2006; Fogg et al., 2006; Naik et al., 2006). This process is depicted in Figure 1.1.

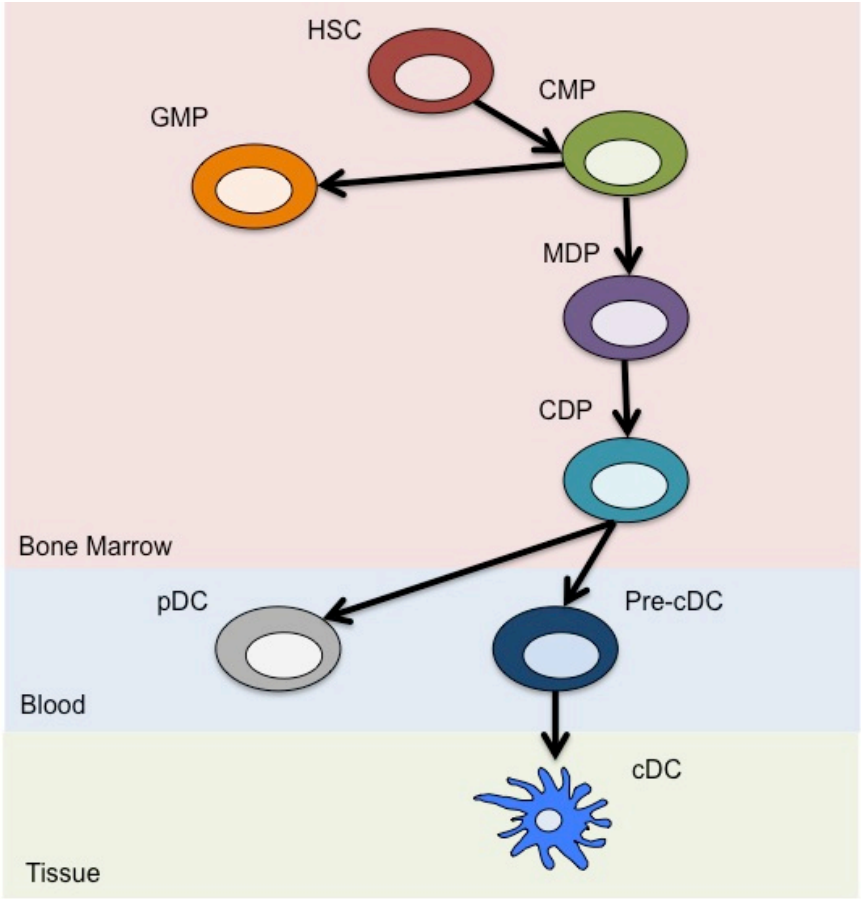

Figure 1-1 Dendritic Cell Development.

DCs in BM differentiate from haematopoietic stem cells (HSC). The HSC gives rise to the common myeloid progenitors (CMP) or the granulocyte macrophage progenitor (GMP). The CMP gives rise to the DC and monocyte precursor (MDP). Following the MDP there is likely to be a common DC progenitor which can give rise to pDCs and DCs. The MDP has been shown to give rise to pDCs directly, and to the pre-cDC that can differentiate into cDCs but not pDCs.

1.2.1 Cytokines Involved In Dendritic Cell Development

FLt3 and its ligand Flt3L are essential for the development of DCs in mice and humans (Naik et al., 2007). Various cell types constitutively secrete Flt3L including endothelial cells and activated T cells. However, the expression of the Flt3 receptor is restricted to the DC lineage. *In vitro* the addition of Flt3L to BM is sufficient to drive the differentiation of DCs, which closely resemble physiologically relevant populations of DCs in the steady-state (Naik et al., 2005). The loss of Flt3 expression in haematopoietic cells results in the loss of the ability of these cells to differentiate into DCs (Karsunky et al., 2003), a feature that can be rescued by increased expression of Flt3 in progenitors (Onai et al., 2006). The injection or induced expression of Flt3L in mice leads to a massive expansion of DCs in lymphoid and non-lymphoid organs, including the intestine (Schulz et al., 2009). Consistently, mice that are deficient in Flt3 or Flt3L have greatly reduced numbers of pDCs and cDCs in lymphoid organs (McKenna et al., 2000).

Another growth factor that has been implicated in the generation of DCs is granulocyte macrophage-colony stimulating factor (GM-CSF, CSF-2). It is widely used for the *in vitro* generation of DCs from BM (Inaba et al., 1992). However, the DCs produced following culture with CSF-2 are functionally and morphologically different to cDCs isolated *ex vivo* (Inaba et al., 1992). Unlike Flt3L, CSF-2 has been implicated in controlling the development of inflammatory DCs (Inaba et al., 1992). However, it does not appear to be necessary in the development of steady-state DCs in lymphoid organs. Instead, it may be required as an additional growth factor in some non-lymphoid tissues, but only for some subsets of DCs (Bogunovic et al., 2009). Further work will be required to fully determine the role of CSF-2 as a growth factor for DCs in non-lymphoid tissues.

Monocyte-colony stimulating factor (M-CSF, CSF-1) is an essential cytokine for the development of macrophages, however its role in the development of DCs remains uncertain. Although it was initially suggested that it was dispensable for the development of DCs, recent work has suggested that it may play a role. Data from CSF-1R green fluorescent protein (GFP) reporter mice indicated that the CSF-1R was expressed in most DCs present in lymphoid organs. However the exact correlation of the level of GFP expression with CSF-1R remains unclear

(MacDonald et al., 2005). Mice lacking CSF-1 had reduced numbers of DCs, however CSF-1 null mice also had reduced spleen size, which may perhaps explain the lower numbers of DCs (Naik, 2008).

Taken together the data from these studies show that Flt3 is essential for the development of cDCs and pDCs under steady-state conditions, whereas CSF-2 and CSF-1 play a more minor role.

1.3 Conventional Dendritic Cell Subsets

DCs can be divided into several groups and subsets. Here I will introduce some of these DC subsets. A more detailed account of migratory DC subsets in the context of the intestine will be presented in subsequent sections.

Phenotypically, DCs have a forward and side scatter profile similar to monocytes and express the haematopoeitc marker CD45, the integrin CD11c and major histocompatibility complex class II (MHCII). DCs were first described in the mouse spleen and further subsets of DCs were also initially described here (Vremec et al., 1992). These subsets are considerably different, both in the expression of many genes, and functionally they appear to be specalised for different aspects of antigen presentation. Mouse splenic DCs were originally divided into two subsets based upon their expression of CD8α (Vremec et al., 1992). CD8α^+ DCs were also CD205$^+$, CD11b$^-$ and CD172a$^-$. In comparison CD8α^- DCs are CD205$^-$, CD11b$^+$ and CD172a$^+$. This CD8α^- subset could further be divided into subsets based upon the expression of CD4. CD8α^+ DCs do not express CD4 (Vremec et al., 2000). These subsets have also been described within the resident DC compartment in LNs, although LNs also contain migratory populations from non-lymphoid organs such as the intestine, lung or skin (Annacker et al., 2005).

As well as these DC subsets being phenotypically distinct, they are found in different areas of lymphoid organs and are functionally different. While CD8$^+$ DCs are found in T cell zones, CD8$^-$ DCs are present in marginal zones (Steinman et al., 1997). Upon stimulation these CD8$^-$ DCs are able to migrate into T cell regions (Reis e Sousa et al., 1997). Functionally CD8α^+ DCs play a fundamental role in antiviral responses, in the response to intracellular pathogens, and are

the most efficient DC subset for the uptake of apoptotic cells (Iyoda et al., 2002). The CD8α^+ DC subset is specialised for the presentation of exogenously-derived antigen on MHC class I by a process known as cross presentation during which antigen is presented to CD8$^+$ T cells (den Haan et al., 2000) (Schnorrer et al., 2006). Upon activation CD8α^+ DCs produce IL-12, making them capable of driving the development of Th1 T cells and cytotoxic T cell responses from CD8$^+$ T cells (Yamazaki et al., 2008). As well as this, CD8α^+ DCs can produce transforming growth factor β (TGF-β) and have been shown to be more efficient in the induction of forkhead box P3 (Foxp3$^+$) regulatory T cells (Yamazaki et al., 2008). Therefore, these cells are ideally specialised to play a role in the induction of peripheral self-tolerance by capturing self-antigens and presenting them to naïve CD4$^+$ and CD8$^+$ T cells using the cross presentation pathway (Belz et al., 2002).

In comparison to CD8α^+ DCs, CD8α^- DCs are less well characterised. They have been shown to have an overall better capacity for phagocytosis (Leenen et al., 1998), and *in* vivo they appear to preferentially present antigen via MHCII (Yamazaki et al., 2008). CD8α^-CD4$^-$ DCs are able to prime CD4$^+$ T cells resulting in a tolerogenic response by their production of IL-10 via a TGF-β dependent mechanism (Zhang et al., 2005). This DC subset is not able to stimulate CD8$^+$ T cells as well as CD8α^+ DCs. In addition when a TLR agonist was used to stimulate CD8α^-CD4$^-$ DCs they induced the development of CD4$^+$ Th1/Th17 T cells (Zhang et al., 2010). Key differences between CD8α^+ DCs and CD11b$^+$ DCs are summerised in Figure 1.2.

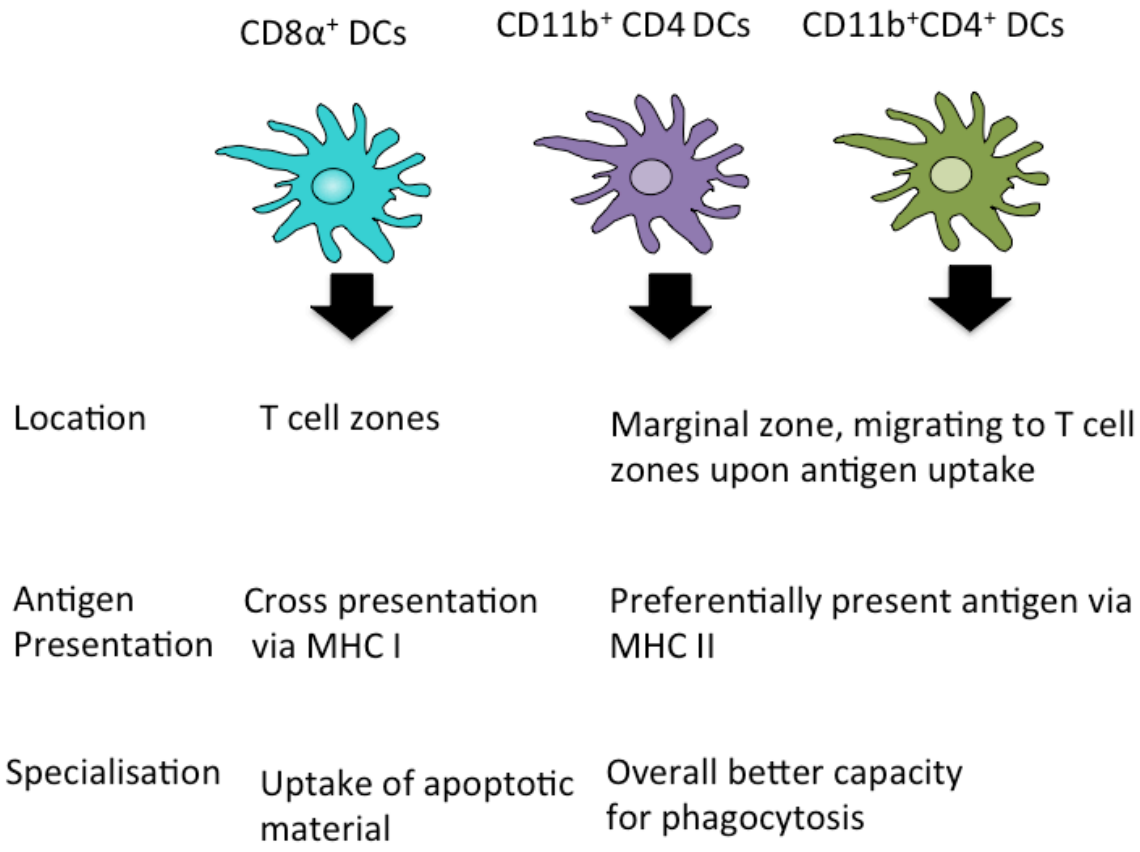

Figure 1-2 Functions of Dendritic Cell Subsets

Phenotypically distinct subsets of DCs have been described, $CD8\alpha^+CD11b^-CD4^-$ DCs, $CD8\alpha^-CD11b^+CD4^-$ DCs and $CD8\alpha^-CD11b^+CD4^+$ DCs. $CD8\alpha^+$ DCs are found mainly in T cell zones within a lymph node, while $CD11b^+$ DCs have been described residing within the marginal zone of a LN and migrating into T cell zones upon antigen uptake. $CD8\alpha^+$ DCs are able to cross-present antigen via MHC I, while $CD11b^+$ DCs preferentially present antigen on MHC II. Additionally $CD8\alpha^+$ DCs are the most efficient subset for the uptake of apoptotic cells, while $CD11b^+$ DCs have an enhanced capacity for phagocytosis.

1.4 Plasmacytoid Dendritic Cells

Plasmacytoid DCs (pDCs) are developmentally, phenotypically and functionally distinct from cDCs. They display MHCII, CD4, B220 and low levels of CD11c. They are specalised for mounting rapid type 1 IFN responses to nucleic acids that can be derived from viruses, bacteria or dead cells (Tang et al., 2010). *In vivo* depletion of pDCs results in abrogated production of IFN-α in response to cytomegalovirus infection (Dalod et al., 2002). Therefore pDCs play an essential role in anti-viral innate immune responses. Furthermore, pDCs promote the antiviral activity of other cells, including cDCs, NK cells, T cells and B cells. For example during infection with HIV, pDCs induce the maturation of cDCs via the

production of type 1 IFNs and TNF-α (Fonteneau et al., 2004). There is also evidence that pDCs play a role in autoimmunity; chronically activated pDCs and the high levels of IFN-α they produce have been implicated in the pathogenesis of systemic lupus erythematosus and psoriasis (Tang et al., 2010).

1.5 Pattern Recognition By Dendritic Cells

In the periphery DCs act as sentries, continually sampling the environment. As well as transporting endocytosed material to secondary lymphoid organs, DCs are able to monitor this matter by their expression of pattern recognition receptors (PRRs). These are activated by molecular motifs associated with foreign antigens not normally found in the mammalian host known as pathogen associated molecular patters (PAMPs). The best-characterised family of PRRs are the Toll-like receptors (TLRs), which are capable of recognising motifs on a wide range of bacterial, viral, fungal and parasitic pathogens (Takeda and Akira, 2005). In the presence of a pathogen there is an increase in the capacity of DCs to activate the adaptive immune system due to their activation of by TLRs and other PRRs.

To date there have been 13 different members of the TLR family identified. They can be divided into two separate groups based upon their location within the cell and the type of agonist they are able to respond to. TLRs 1, 2, 4, 5, 6, 10 and 11 are present on cell surfaces and recognise extracellular agonists. In comparison, TLRs 3, 7, 8 and 9 are found on intracellular membranes and mostly recognise nucleic acids. Although TLRs 12 and 13 have been cloned from the murine genome, their function is still under investigation. All TLRs, except for TLR3, rely on the adaptor protein MyD88, while TLR3 signals through the adaptor protein TRAF-interacting protein (TRIP) (Tabeta et al., 2004).

TLR expression varies between DC subsets; pDCs express high levels of TLR7 and TLR9 (Edwards et al., 2003). CD8α^+ DCs have been shown to express TLR3, and are able to respond to apoptotic cells with the addition of poly I:C (Schulz et al., 2005). This mechanism presumably allows CD8α^+ DCs to survey apoptotic cells for the presence of a viral infection. CD8α^+ DCs do not express detectable TLR7 (Edwards et al., 2003), thus the activation of these DCs by RNA which is normally present in host apoptotic cells is prevented.

1.6 Dendritic Cell Migration

DCs are present in non-lymphoid tissues including the intestine, lung and skin. These are vulnerable sites where pathogens can enter, and DCs play an essential role in mediating the immune response to pathogens. This is fundamental to the initiation and propagation of the immune response, and indeed is the rate-limiting factor in the process (Teoh et al., 2009). DCs reside in an immature state in the periphery. They sample antigen, and migrate out of the tissue into draining LNs via the afferent lymphatics. This allows DCs to migrate into LNs where they are able to interact with naïve T cells, steps that are imperative for DCs to complete their maturation process.

The lymphatic system has a dual purpose, not only is it required for fluid uptake and drainage but it is also essential for leukocyte migration. It is a hierarchical system comprising small blind-ended capillaries in the peripheral tissues that join larger collector ducts, which in turn drain into lymph nodes. Efferent lymph, leaving lymph nodes in the abdominal viscera drains into the cisterna chyli and thoracic duct, eventually emptying into the venous system in the neck. Lymph flows exclusively from the periphery towards the draining LNs. As DCs are found in only afferent lymphatics and not efferent lymphatics, it appears that once DCs have arrived in the LN they do not travel any further but die there. This is unlike lymphocytes that are able to migrate from LNs in efferent lymphatics and return to the circulation.

Capillaries of the lymphatic system have an unusual structure, the endothelial junctions of these cells overlap with oak leaf morphology. These areas of overlap function as primary valves. Recent work has further revealed a structure in which the scalloped edges of the leaflets form junctions in a button-like arrangement (Baluk et al., 2007). These button junctions constitute pores, and allow the easy passage of fluids as well as being the site of leukocyte entry (Lynch et al., 2007). Adherens and tight junction proteins such as claudins, vascular endothelial (VE)-cadherin, zona-occludens, junctional adhesion molecule A (JAM-A) and the endothelial selective adhesion molecules (ESAM) are expressed at the borders of the lymphatic vessel, while CD31 and the lymphatic

hyaluronan (HA) receptor lymphatic vessel endothelial hyaluronan receptor-1 (LYVE-1) are expressed at the tips.

The exact mechanism by which DCs gain access to lymphatics is unclear, however it has been suggested that areas of high CCL21 concentrations forms complexes with type IV collagen at the basement membrane of initial lymphatics. Migrating DCs then contact these CCL21 puncta before actually transmigrating into the lymph vessel lumen from these points (Tal et al., 2011). DCs from $CCR7^{-/-}$ mice, which are unable to migrate from peripheral tissues, have been seen to migrate randomly around initial lymphatics but fail to dock with and transmigrate into these vessels (Ohl et al., 2004; Tal et al., 2011). Once inside, DCs crawl along the inner surface of the lymphatic endothelium, and by sensing lymph flow, they receive guidance cues that allow for directed downstream migration. Finally, once DCs reach the larger collecting vessels they drift freely in lymph (Alvarez et al., 2008).

The overall mechanism of DC migration into lymphatic vessels involves a number of chemokines. The interaction between CCR7 expressed upon DCs and its ligands CCL21 and CCL19 is the most widely studied and crucial interaction (Ohl et al., 2004; Randolph, 2001). The deletion of CCR7 results in a complete absence of migratory DCs in draining LNs, while deletion of both CCL19 and CCL21 leads to defects in lymphatic trafficking (Gunn et al., 1999; Mori et al., 2001). As well as CCR7 and its ligands there is evidence that adhesion to the lymphatic vessel endothelium and transmigration involves other receptors, such as intercellular adhesion molecule-1 (ICAM-1), vascular cell adhesion molecule-1 (VCAM-1) or E-selectin (Johnson et al., 2006; Johnson and Jackson, 2008). These are reviewed in (Jackson, 2009). However, it is clear that the interaction of CCR7 with its ligands is the primary interaction for mediating DC migration into the lymphatics (Braun et al., 2011).

CCR7 is also involved in guiding migrating DCs within the LN, although this process is not completely understood. For example, although several integrins are highly expressed upon DCs, peripheral DCs do not appear to require these for traveling into and within the LN cortex. CCR7 is believed to be involved in

guiding DCs deeper into the cortex where CCL19 and CCL21 are most strongly expressed around HEVs (Braun et al., 2011).

The mobilisation and migration of DCs from some tissues is also likely to involve Sphingosine-1 Phosphate (S1P) (Czeloth et al., 2005; Idzko et al., 2006). S1P is a small soluble bioactive lipid metabolite that has been detected throughout eukaryotes (Spiegel and Milstien, 2003). There are five distinct S1P receptors (S1PR1-5), which are expressed throughout the immune system (Rosen et al., 2009). The discovery of the immunosuppressive drug FTY720 that acts upon four of the five S1PRs (not S1PR2) has allowed the functions of these S1PRs to be examined in further detail (Brinkmann et al., 2002; Mandala et al., 2002). S1PRs are coupled to various heterotrimeric G-proteins allowing them to mediate diverse functions, which are reviewed by (Rosen et al., 2007; Rosen et al., 2013; Sanchez and Hla, 2004). S1PR1 facilitates T cell trafficking at multiple stages of T cell development, including thymocyte egress into periphery, egress of mature T cells out of lymph nodes during systemic trafficking as well as after immune activation and retention of T cells in non-lymphoid tissues. The interaction between S1P and S1PR1 has been shown to be essential for the exit of lymphocytes into lymphatic vessels (Cyster, 2005; Cyster and Schwab, 2012). T cells expressing S1PR1 are able migrate towards an S1P gradient. T cells from S1PR1 deficient mice fail to egress from the thymus and peripheral lymphoid organs. The interaction between S1P and S1PR1 appears to act by overcoming CCR7 and CXCR5 signals, which mediate cell retention (Pham et al., 2008; Sinha et al., 2009). Using S1PR1 deficient T cells, or mice in which the lymphatic endothelium is S1PR1 deficient, it was shown that treatment of the T cells to inhibit CCR7 and CXCR5 retention signals have restored lymphocyte egress through the cortical sinuses, even in the absence of the S1P and S1PR1 signalling axis (Pham et al., 2010; Pham et al., 2008). Effector T cells eventually re-express S1PR1 and thereby egress from the lymph node to the lymph and into the peripheral tissues

DCs are able to express all five S1PRs (Czeloth et al., 2007), which can mediate a range of functions from endocytosis to affecting DC polarisation of T cells when exposed to bacterial products (Idzko et al., 2002; Maeda et al., 2007). Importantly, S1PRs are likely to play a key role in DC trafficking. The position of

33D1$^+$ DCs within the spleen has been shown to depend upon S1PR1, although these DCs display S1PR1 at much lower levels compared to T cells (Czeloth et al., 2007). Additionally, upon their maturation some subsets of intestinal DCs have been shown to upregulate S1PR1 and S1PR3, which resulted in an increased capacity for these DCs to migrate towards S1P (Czeloth et al., 2005; Rathinasamy et al., 2010). Therefore, it is likely that S1P and S1PR signalling will play an important role in DC trafficking from the periphery to the draining LN.

The migration of DCs from the periphery to the draining LNs happens in both the steady state and can be enhanced by the presence of proinflammatory stimuli. The intravenous (i.v) administration of LPS, or the oral administration of the TLR7/8 agonist Resiquimod (R848), induced a major increase in DC migration, leaving peripheral tissues virtually devoid of DCs (Yrlid et al., 2006c). These effects are dependent upon the systemic production of TNF-α. DC migration from the skin can be enhanced following contact sensitisation and is dependent upon CD40-CD40L interaction (Moodycliffe et al., 2000). During inflammation endothelial cells may upregulate the expression of some adhesion molecules, such as CX3CL1. CX3CL1 has been shown to be upregulated by dermal lymphatic endothelial cells following treatment with TNF-α or FITC skin painting leading to increased dermal DC migration from the skin (Johnson and Jackson, 2013). Additionally, CCL21 is rapidly secreted by lymphatic endothelial cells in response to treatment with TNF-α, providing a mechanism by which there is increased DC migration to draining LNs following inflammation (Johnson and Jackson, 2010). This demonstrates how the immune response can respond quickly in the presence of a pathogen.

1.7 Antigen Uptake and Presentation

DCs are able to take up a diverse array of antigens, which they can present to naïve T cells on either MHC class I or MHC class II. Immature, but not mature DCs, are specialised for antigen uptake. This occurs via endocytosis, with most immature DCs exhibiting three types of endocytosis; macropinocytosis, phagocytosis and clathrin-mediated endocytosis (Mellman and Steinman, 2001). Macropinocytosis and phagocytosis are related process that both depend upon actin assembly. Phagocytosis is triggered by the attachment of extracellular

particles to surface receptors that then initiate particle uptake. This is a particularly efficient mechanism for the generation of antigenic peptides, and is probably the most physiologically relevant form of antigen uptake (Inaba et al., 1998).

Following antigen uptake, antigens are degraded and loaded onto MHC molecules. The intracellular pathways for peptide loading and presentation by DCs have been analysed in detail and are reviewed by Guermonprez *et al*. and Blum *et al*. (Guermonprez et al., 2002), (Blum et al., 2013). Here, I will give a brief account of antigen presentation by DCs.

Initially, DCs were described to present antigen to $CD4^+$ T cells via MHCII. Peptide loading on MHCII molecules begins with the synthesis of MHCII dimers in the endoplasmic reticulum (Cresswell, 1996). These then pass through the Golgi body and are then transported to the endocytic pathway, which contain antigen taken up by DCs (Villadangos et al., 1999). MHCII dimers become able to bind antigen under the control of H2-M and H2-O (Kropshofer et al., 1999). Once stabilized by loading with peptide derived from antigen, the MHCII/antigen complex is then transported to the plasma membrane.

Most peptides presented via MHCI are generated from ubiquitinated proteins. However, some subsets of DCs, namely $CD8\alpha^+$ DCs, are able to carry out cross presentation. This is a process that involves presentation of peptide derived from exogenous antigen presented on MHCI to $CD8^+$ T cells. Cross presentation is essential for the generation of cytotoxic T cell responses against tumours and intracellular pathogens. There have been two main pathways described for the cross presentation; TAP independent and TAP dependent (Yewdell et al., 1999). Like presentation via MHCII, TAP independent cross presentation requires MHCI molecules to access in the endocytic pathway. The TAP dependent pathway requires a membrane pathway linking the lumen of endocytic compartments in the cytosol (Rodriguez et al., 1999).

Taken together, these specalised mechanisms for antigen uptake and presentation can begin to account for the unique role played by DCs in the generation of an adaptive immune response.

1.8 Dendritic Cell Interactions with the Adaptive Immune Response

After infection with a pathogen, an important function of DCs is to communicate the type of immune response necessary to successfully clear the infecting organism. They perform this by their interactions with cells of the adaptive immune response such as T and B cells. It is therefore essential to understand the biology of DC:T cell and DC:B cell interactions.

1.8.1 $CD4^+$ T Cells

$CD4^+$ T cells play a central role in many types of immune responses. They are able to orchestrate immune responses to a variety of pathogens in a number of ways. For example, by providing help to B cells to make antibodies, by supporting $CD8^+$ T cell responses, or by regulating macrophage function. Additionally, they are able to regulate and suppress immune responses to control autoimmunity and to adjust the magnitude and persistence of responses. These various functions can be achieved through the differentiation of naïve $CD4^+$ T cells by presentation of their cognate antigen by DCs, with the context by which the DC presents antigen being crucial (Zhu and Paul, 2008).

The differentiation of $CD4^+$ T cells is highly regulated, and there are at least three different signals required for their differentiation into effector cells. The first signal is provided by DCs presenting exogenously derived antigen cells via MHC class II. This complex is recognised by a particular T cell clone and interacts with T cell receptor (TCR) $\alpha\beta$ and CD4 molecules on the T cells. This interaction results in the activation of the naïve $CD4^+$ T cell, but it does not commit this to a specific lineage (Zhu and Paul, 2008). The second signal is also provided by DCs. This involves the binding of costimulatory molecules such as CD86 and CD80 on DCs to the activatory CD28, or the inhibitory cytotoxic T lymphocyte antigen 4 (CTLA-4) on $CD4^+$ T cells, controlling T cell activation (Lenschow et al., 1996). Further signals, are required for full T cell activation. These come from the interaction between CD40 on DCs and CD40L on naïve T cells (Behrens et al., 2004; Mosmann and Coffman, 1989). Together signals one and two lead to IL-2 production by the T cell needed for the clonal expansion of the T cells. If T cells do not receive both signals they enter a state of anergy rather than becoming

fully activated. This provides a mechanism by which peripheral self-tolerance can be maintained, essential because not all self reactive T cells are deleted in the thymus during T cell development.

Signal three is provided by cytokines secreted by DCs, directing the differentiation of $CD4^+$ T cells into different lineages. Originally $CD4^+$ T cells were viewed as having two major fates, T helper 1 (Th1) cells or Th2 cells. Th1 cells express T-bet and produce IFN-γ, and require IL-12 derived from either DCs or innate cells. Th2 cells express Gata3 and produce IL-4; they require IL-4 for their development, which may be derived from basophils, eosinophils, mast cells or $\gamma\delta$ T cells (Voehringer et al., 2004; Woerly et al., 2002; Zuany-Amorim et al., 1998). The Th1 response is important for the activation macrophages, the clearance of intracellular pathogens and the activation of naïve $CD8^+$ T cells. Th2 cells produce IL-2, IL-5, IL-10 and IL-13 and are involved in allergic responses. These cytokines have important roles in the production of IgE, the recruitment of basophils and eosinophils. Therefore, the Th2 response is mainly involved in the clearance of extracellular pathogens.

However, the Th1/Th2 paradigm does not explain some aspects of immunity and autoimmunity. The discovery of regulatory T cells (Tregs) was key to understanding mechanisms of autoimmunity (Josefowicz and Rudensky, 2009). There are two distinct types of Tregs, natural Tregs (nTregs) and inducible Tregs (iTregs). nTregs are generated from the thymus and are distinct from iTregs, which are generated from naïve $CD4^+$ T cells in the periphery (Geiger and Tauro, 2012). The differentiation of iTregs from naïve T cells requires TGF-β, which induces the expression of Foxp3. Foxp3 is specifically induced only on iTregs and is required for their maintenance in the peripheral immune compartment. Although there are differences in the development of nTregs and iTregs, both produce IL-10 and TGF-β. These inhibitory cytokines are important in maintaining tolerance and controlling inflammatory responses.

More recently Th17 cells have become a focus of attention due to the role they play in the pathogenesis of various autoimmune diseases, including rheumatoid arthritis, multiple sclerosis, and inflammatory bowel disease (Wilke et al., 2011). RORγt is the master regulator for Th17 cells, which produce IL-17 and

express IL-23R on their surface. Their differentiation requires TGF-β and IL-6 that can be produced by DCs, which induces RORγt expression on $CD4^+$ T cells (Mangan et al., 2006). They have been proposed to play a role in the protection against extracellular bacteria, protozoa and fungi. In the steady-state the largest population of Th17 cells is found in the intestinal mucosa, and the development of this population is largely dependent upon the colonisation of commensal microbiota (Ivanov et al., 2008).

Follicular helper T cells (Tfh) are the most recently described lineage of T cells. They are found in the germinal centers of lymphoid tissues and are found close to B cells. They are defined by the expression of Bcl6 and IL-21, and provide B cell help by promoting class switching (Crotty, 2011; Fazilleau et al., 2009). The development of Th subsets is outlined in Figure 1.2.

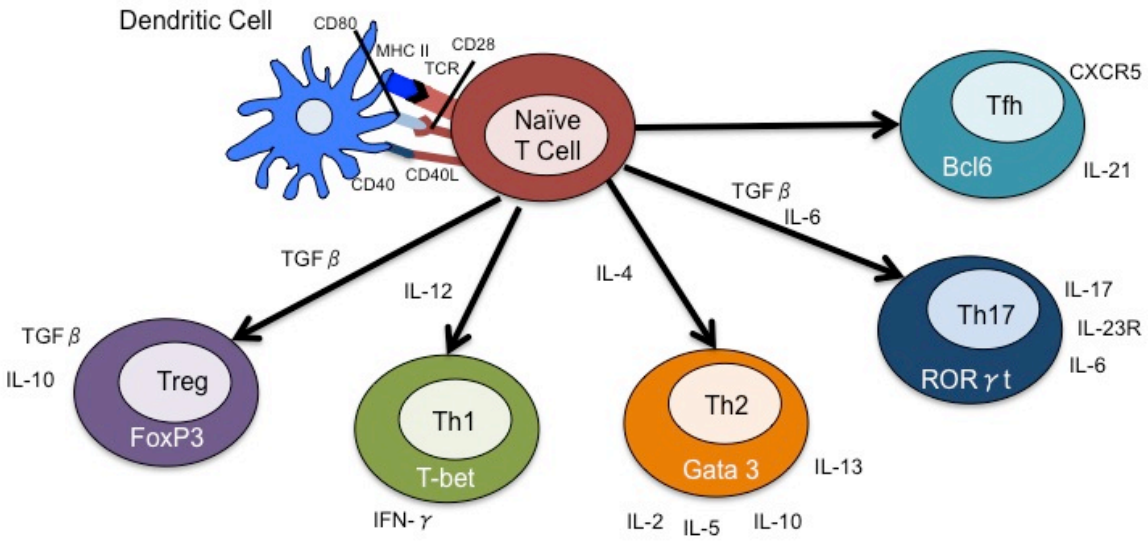

Figure 1-3 Development of T helper Subsets

Dendritic cells present antigen on MHCII to the T cell receptor on naïve T cells. This is accompanied by co-stimulation by the interaction by CD80/86 to CD28 or CTLA-4 and CD40 and CD40L on naïve T cells. Cytokines secreted by DCs, direct the differentiation of $CD4^+$ T cells into different lineages. Th1 cells express T-bet and produce IFN-γ, and require IL-12 for their development. Th2 cells express Gata3 and produce IL-4; they require IL-4 for their development, they produce IL-2, IL-5, IL-10 and IL-13. The differentiation of Tregs requires TGF-β; Tregs express Foxp3 and produce IL-10 and TGF-β. Th17 cells require TGF-β and IL-6 for their development and their master regulator is RORγt. They produce IL-17, IL-23R and IL-6. Tfh cells express Bcl6 and produce CXCR5 and IL-21.

There is increasing evidence of flexibility between T helper subsets (Murphy and Stockinger, 2010; O'Shea and Paul, 2010). For example not all cytokines are

selectively produced by different subsets of Th cells some are more widely expressed. As such, IL-10 was originally considered to be a Th2 cytokine. But more recent work has shown that Th1, Tregs and various innate immune cells can also produce IL-10 (Saraiva and O'Garra, 2010). It is also now becoming clear that some populations of T helper cells can change their phenotype during and after development. For instance, during differentiation of Tregs, the presence of IL-6 switches the development of Tregs to Th17 cells. Thus under inflammatory conditions in the presence of IL-6 inflammatory Th17 cells are produced, but under non-inflammatory conditions, Tregs are induced (Dons et al., 2012). Furthermore the differentiation of Th17 can be inhibited, and the production of Tregs increased, in the presence of retinoic acid (RA). RA is produced by intestinal DCs and acts directly on T cells enhancing TGF-β signaling while inhibiting IL-6 signalling (Jaensson et al., 2008). The Treg phenotype can, however, be plastic and fully differentiated Tregs can lose the expression of Foxp3 and produce proinflamatory cytokines such as IFN-γ (Oldenhove et al., 2009). Another example of plasticity is provided by Th2 cells that can express T-bet and IFN-γ during a viral infection (Hegazy et al., 2010). However, the most flexible subset appears to be Tfh, which have been shown to convert to Th1, Th2 or Th17 *in vitro,* and *in vivo* Tregs can become Tfh cells (Lu et al., 2011; Tsuji et al., 2009).

Taken together these data show the flexibility of $CD4^+$ T cells, which is likely to be advantageous in terms of host defense. However further information is required and as there is no simple way to determine stability versus plasticity this may be challenging.

1.8.2 $CD8^+$ T cells

DCs also play an important role in priming $CD8^+$ T cells. Unlike $CD4^+$ T cells, the range of phenotypes of effector cells is limited. Upon activation, all $CD8^+$ T cells become cytotoxic T lymphocytes (CTLs). Classically $CD8^+$ T cells recognise antigen presented via MHC class I molecules. MHC class I molecules are present on the surface of all nucleated cells in the body and present peptides from endogenously derived antigens. This provides a mechanism by which the immune response can specifically recognise cells infected with intracellular

pathogens or tumour cells. The $CD8^+$ T cell can then destroy the aberrant cell to circumvent the spread of the infection or cancer, whilst avoiding killing healthy bystander cells (Kurts et al., 2010). This restriction is potentially problematic in one situation; naïve $CD8^+$ T cells must be primed by APCs, usually DCs, before they can exert their cytotoxic actions. Therefore, if DCs were not able to present peptides derived from exogenous antigens of MHC class I, they would not be able to activate the naïve $CD8^+$ T cell, unless the DCs themselves were infected. This ability of DCs to present exogenous antigen via MHC class I to $CD8^+$ T cells is termed cross presentation (Heath and Carbone, 2001). This allows the priming of naïve $CD8^+$ T cells by DCs, which is essential in the response to viral infections and some bacterial infections (Kurts et al., 2010).

There are two ways by which DCs are able to activate CTL responses. Under inflammatory conditions DCs are activated by TLR binding resulting in their maturation. Mature DCs then interact with naïve $CD8^+$ T cells resulting in their production of IL-2, which stimulates their expansion. This type of CD8 T cell DC interaction is rare and only occurs under specific circumstances. More often DCs are provided with help from $CD4^+$ effector T cells (Wu and Liu, 1994). Upon $CD4^+$ T cell recognition of cognate antigen on the surface of DCs, there is upregulation of costimulatory molecules such as CD80 and CD86 on the surface of the DC (Schoenberger et al., 1998). These DCs are then more potent stimulators of $CD8^+$ T cell differentiation.

1.8.3 B Cells

DCs are able to indirectly and directly provide proliferation and survival signals to B cells. DCs are able to induce the development of T helper cells that then influence B cell maturation (Qi et al., 2006). Alternatively, a population of DCs can present intact antigen to B cells directly (Colino et al., 2002; Wykes et al., 1998). Following intravital multiphoton microscopy DCs in the LN paracortex were shown to interact with migrating B cells *in vivo* (Qi et al., 2006). DC-B cell interactions have been shown to lead to B cell activation via increased cell-to-cell contact times (Qi et al., 2006). This may provide a mechanism by which B cells can rapidly mount antibody responses.

1.9 Lymphoid Tissue Development

Lymphoid organs can be divided into three major categories, primary, secondary and tertiary based upon specific functional criteria. Primary lymphoid organs, the thymus and bone marrow, are responsible for the formation of the primary repertoire of lymphocyte effector cells. Secondary lymphoid organs are involved in the coordination of the immune response. They concentrate foreign antigen in specific areas and facilitate the interaction between APCs and antigen specific lymphocytes. LNs are located throughout the body and support a quick and effective immune response. Tertiary lymphoid tissues are comparable to secondary lymphoid organs, but they emerge under inflammatory conditions. The development of secondary lymphoid organs is predetermined during embryogenesis, while tertiary lymphoid organs can arise under environmental influences and are not restricted to specific developmental areas or anatomic locations. Here I will discuss the development of secondary and tertiary lymphoid organs, mainly within the context of the intestine.

1.9.1 Lymph Node Development

The anatomically distinct tissues designed to facilitate an adaptive immune response are secondary lymphoid organs. Secondary lymphoid organs include the network of LNs throughout the body, the spleen, and PPs. The development of secondary lymphoid organs is a highly controlled and ordered process initiated during embryogenesis. The development of lymphoid organs does not happen simultaneously, but sequentially (Figure 1.3). This was demonstrated using timed injections of lymphotoxin-β receptor immunoglobulin fusion proteins (LTβR-Ig) that can inhibit the formation of lymphoid organs. For example, injections at day 12.5 of embryonic development (E12.5) prevented the development of all LNs and PP, while injections at E15.5 allowed the formation of brachial and axillary LNs (Rennert et al., 1996). The mechanism by which LTβR-Ig acts is outlined below in Figure 1.3.

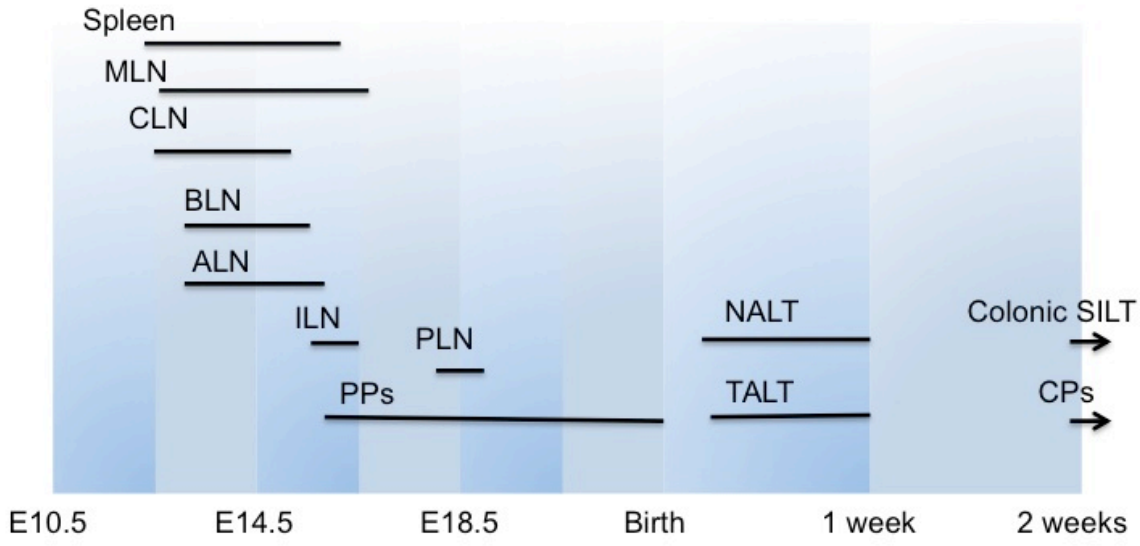

Figure 1-4 Timeline of the Sequential Development of Secondary Lymphoid Organs.

Mesenteric lymph nodes (MLN) develop between E10.5 and E15.5, cervical lymph nodes (CLN) between E11.5 and E14, brachial lymph nodes (BLN) between E12 and E15, axillary lymph nodes (ALN) between E12 and E15, inguinal (ILN) between E16 and E16.5, PPs between E16 and birth and popliteal lymph nodes (PLN) between E17 and E17.5. In comparison, nasal-associated lymphoid tissue (NALT) and tear duct-associated lymphoid tissue (TALT) develop post birth. Cryptopatches (CPs) develop from two weeks post birth, and these can then develop into isolated lymphoid follicles (ILFs) under environmental influences. Colonic solitary intestinal lymphoid tissue (SILT) develops around two weeks after birth (Adapted from (Mebius, 2003)).

The earliest event during LN development is the formation of lymph sacs, and these were considered to be a necessary requirement for the development of LNs (Kelly and Scollay, 1992; Mebius et al., 1997; Mebius et al., 1996). During the first phase of LN development *Prox1* expressing endothelial cells form lymph sacs at precise positions in the developing embryo (Wigle and Oliver, 1999). However, more recently, using *Prox1* deficient and *Prox1* conditional knock out animals, it was demonstrated that the formation of lymph sacs was not the triggering factor in the development of LNs (Vondenhoff et al., 2009b). Instead it was suggested that LN morphogenesis was initiated by the expression of CXCL13 by RA producing neurons (van de Pavert et al., 2009), which attract lymphoid tissue inducer (LTi) cells. Despite this recent work, the signals that trigger LN morphogenesis are still poorly understood. Therefore further work is required to fully determine the identity of signals that control the initiation of LN development.

The first cells that colonise developing secondary lymphoid organs and the principal cells involved in their development are LTi cells (Mebius et al., 1997).

LTi cells are a subset of innate lymphoid cells (ILCs). ILCs lack specific antigen receptors, but produce effector cytokines and play important roles in not only the formation of lymphoid tissue but also in tissue homeostasis and in immunity to infectious microorganisms. The study of the development and functions of ILCs is a rapidly expanding field and is discussed in detail elsewhere (Spits et al., 2013; Spits and Cupedo, 2012). Here I will focus on the development and functions of LTi cells in the context of secondary lymphoid organ development. LTi cells are believed to develop from a foetal liver progenitor defined as $CD3^-$, $CD4^-$, $cKit^+$, IL-$7R\alpha^+$ and $\alpha4\beta7^+$. Between E9.5 and E16.5 they colonise the developing embryo (Rennert et al., 1996; Veiga-Fernandes et al., 2007). In RORγt deficient mice or in mice lacking the helix-loop-helix inhibitor Id2, LTi cells are not generated and these mice lack all LNs, PPs and isolated lymphoid follicles (ILFs) (Eberl and Littman, 2004; Yokota et al., 1999). RORγt is a ligand-dependent nuclear hormone receptor that is expressed only on LTi cells during embryogenesis, as well as on cells that develop post-natally such as Th17 cells and RORγt^+ ILCs that are distinct from LTi cells (Cella et al., 2009; Satoh-Takayama et al., 2008). LTi cells are defined as $CD4^+CD3^-IL7\alpha^+cKit^+$, they can be identified by their expression of RORγt, lymphotoxin-$\alpha1\beta2$ (LT$\alpha1\beta2$), IL-7Rα and the absence of lineage markers (Mebius et al., 1997). The transfer of LTi cells can rescue the development of PPs in $CXCR5^{-/-}$ mice that have abrogated PP development (Finke et al., 2002), demonstrating the requirement of these cells in the development of secondary lymphoid organs (Fukuyama and Kiyono, 2007).

The interaction of LTi cells with lymphoid tissue organiser (LTo) cells is crucial in the development of secondary lymphoid organs. LTo cells are mesenchymal cells that give rise to the stromal cell subsets that are present in mature lymph nodes (Cupedo et al., 2004). During lymphoid tissue organogenesis LTo cells express the lymphotoxin-β receptor (LTβR) which interacts with LT$\alpha1\beta2$ expressed by LTi cells (Honda et al., 2001; Yoshida et al., 2002a). Injections of LTβR-Ig inhibit this interaction. The interaction between LTi cells and LTo cells triggers the maturation of LTo cells and begins a positive feedback loop involving LT$\alpha\beta$/LTβR signalling that promotes and sustains lymphoid organ formation. Briefly, LTo signalling via LTβR induces the expression of TNF-related activation induced cytokine (TRANCE, also known as TNFSF11 and RANKL) and IL-7, which results in increased LT$\alpha1\beta2$ expression by newly arriving LTi cells and therefore increased

signalling via LTβR (Honda et al., 2001; Mebius, 2003; Yoshida et al., 2002a). The maturation of LTo cells results in the increased expression CCL19, CCL21, CXCL13, IL-7, VCAM-1 and ICAM-1 which support the attraction and retention of more haematopoietic cells, leading to LN growth (Cuff et al., 1999; Mebius, 2003). This process is depicted in Figure 1.4. Cytokines and chemokines are essential in the development of LNs, demonstrated by the combined ablation of CXCL13, CCL21 and CCL19 or CCR7 and CXCR5 resulting in the lack of LN and PP development (Luther et al., 2003; Ohl et al., 2003). The induction of the lymphangiogenic factor VEGF-C by LTo cells promotes the link between developing LNs and the lymphatic vasculature (Vondenhoff et al., 2009a). Subsequently, these structures can become colonised by lymphocytes resulting in the development of a highly organised lymphoid organ.

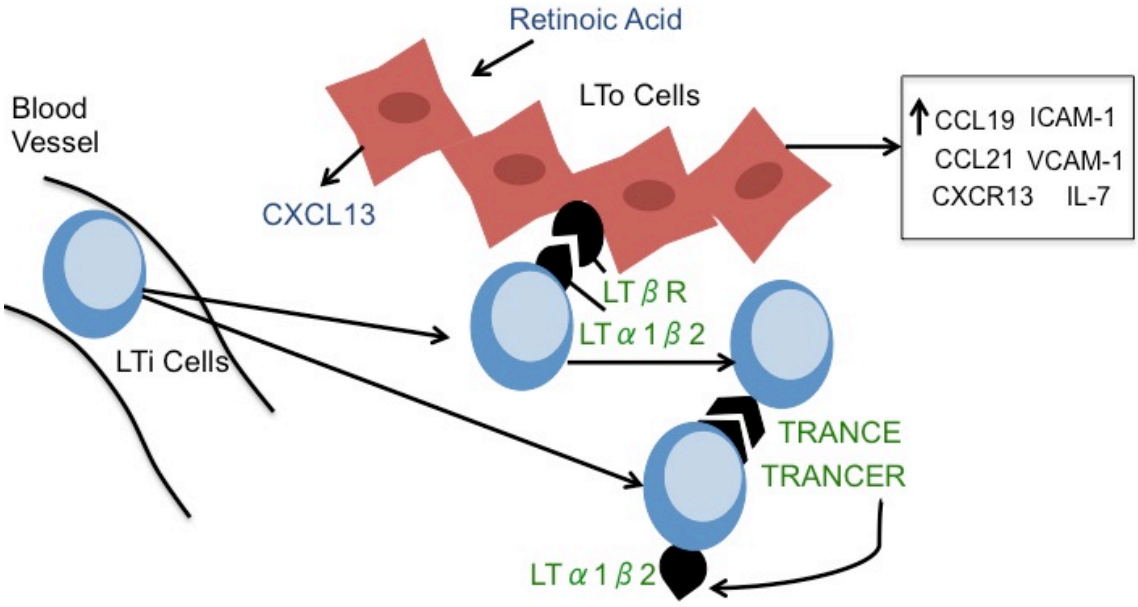

Figure 1-5 Lymph Node Development.

Retinoic acid is released resulting in the gathering of lymphoid tissue organiser (LTo) cells, which in turn release CXCL13. This results in lymphoid tissue inducer (LTi) cells leaving the blood vessels and the interaction between LTβR on LTo cells and LTα1β2 on LTi cells. This starts a positive feedback loop via the induction of TRANCE. It also leads to the maturation of LTo cells that produce CCL19, CCL21, CXCR13, ICAM-1, VCAM-1 and IL-7. The interaction between TRANCE and TRANCER results in the increased expression of LTα1β2 on newly arriving LTi cells, resulting the attraction of further haematopoietic cells leading to the growth of the lymph node.

1.10 Splenic Development

The development of the spleen is distinct from other secondary lymphoid tissues, as LTi cells are not necessary for their initial splenic development, demonstrated by the presence of a spleen in RORγt$^{-/-}$ and Id2$^{-/-}$ animals (Eberl, 2005; Yokota et al., 1999). Instead the initial event in splenic development is the formation of the splanchnic mesodermal plate (SMP) that forms at E12 (Mebius and Kraal, 2005). The spleen is then colonised at E12 by LTi cells following an upregulation of VCAM-1 on LTo cells (Withers et al., 2007) (Mebius et al., 1997). Lymphotoxin dependent signals from LTi cells then regulate T cell organisation; thereafter the development of splenic white pulp is more similar to the development of other secondary lymphoid organs (Withers et al., 2007). However additional lymphotoxin independent signals are also necessary for the organisation of T cell zones in the spleen, which may account for the fact that RORγt$^{-/-}$ and Id2$^{-/-}$ mice have aberrant segregated B and T cell areas (Eberl, 2005; Yokota et al., 1999).

1.11 Mesenteric Lymph Node Development

The development of the mesenteric lymph node (MLN) is likely to require additional chemokines compared to the development of other peripheral LNs. For example, mice lacking CXCL13 or CXCR5 do not develop peripheral LNs, yet MLNs, facial and cervical LNs develop normally. The combined elimination of CXCL13, CCL19 and CCL21, or their receptors CXCR5 and CCR7 prevents the development of all LNs except the MLNs (Ansel et al., 2000; Luther et al., 2003; Ohl et al., 2003). Furthermore MLNs, but not PPs or other peripheral LNs develop in LTβ-deficient mice, which are deficient for the LTα1β2 ligand of LTβR. The mechanism by which MLNs form in these animals was proposed to be due to the expression of LIGHT which can act as a substitute for LTβ in the formation of MLNs (Alimzhanov et al., 1997; Scheu et al., 2002).

1.12 Peyer's Patch Development

Although there is much overlap between LN development and PP development, there are some key differences. Unlike LNs that develop at defined positions in the body, PPs develop at inconsistent locations and in varying numbers along the

anti-mesenteric axis of the SI. Similar to LN development the initial step in PP organogenesis involves the colonisation of LTi cells. This occurs at E12.5 and is initially restricted to the duodenum and caecum, but by E15.5 these LTi cells are distributed evenly throughout the intestinal wall. Aggregates of these cells form 1 day later, leading to the formation of PP primordia (Hashi et al., 2001; Veiga-Fernandes et al., 2007). Therefore PP primordia appear to have a stochastic distribution, distinct from LNs that develop at precise locations.

As outlined above, signalling between LTi and LTo cells results in the upregulation of LTα1β2 via the interaction between TRANCE and its receptor TRANCER. This results in the survival and differentiation of LTi cells, and in line with this TRANCE deficient embryos have reduced numbers of LTi cells (Kim et al., 2000). However TRANCE signalling is not required for PP development (Dougall et al., 1999), and LTo cells from PPs do not express TRANCE. Although they were able to generate PPs, TRANCE deficient animals showed decreased numbers of B cells within PPs. Another pair of molecules that play different roles in the development of LNs and PPs are IL-7 and IL-7R; IL-7R$\alpha^{-/-}$ mice lack PPs, but brachial, axillary LNs and MLNs all develop normally until the neonatal stage (Adachi et al., 1998; Mebius, 2003). Furthermore, the tyrosine kinase receptor RET is also involved to differential degrees in LNs and PP formation. RET is expressed by a subset of cells that are similar to LTi cells, but they express CD11c. These cells are essential for haematopoietic cell clusters, and in RET$^{-/-}$ mice LTi clusters are missing (Veiga-Fernandes et al., 2007). It has been proposed that the activation of RET on these CD11c^{+} cells leads to the induction of LTα1β2 expression, which interacts with LTβR on LTo cells leading to the attraction and retention of LTi cells in the PP. Although CD11c^{+} cells are commonly found in developing PPs, few can be found in developing LNs (Adachi et al., 1998). Therefore, further work is required to determine the role these CD11c^{+} haematopoietic cells play in the development of LNs outwith the intestine. There are also differences between the levels of expression of transcription factors and cytokine expression on LTo cells from PPs and LNs, although the functional consequences of this are not yet clear (Okuda et al., 2007). Taken together these data support the concept that LN and PP development are controlled differently, however further work is required to fully determine the different pathways of PP and LN development.

1.13 Development of Mucosal Associated Lymphoid Tissues

Secondary lymphoid tissues also include several mucosal associated lymphoid tissues, such as the nasopharynx-associated lymphoid tissue (NALT), tear duct-associated lymphoid tissue (TALT), cryptopatches (CP) and ILFs. In contrast to PPs and LNs, the development of these lymphoid tissues occurs after birth. A population of LTi cells is likely to play a role in their development and is present in adult mice. These adult LTi cells express OX40 ligand and CD30 ligand, unlike LTi cells found in developing embryos (Eberl and Littman, 2004; Kim et al., 2005). Their ontogeny is also different; foetal RORγt$^+$ LTi cells mature in the foetal liver but in the adult RORγt$^+$ cells are BM derived and matured outwith the BM and in a notch2-dependent manner (Possot et al., 2011).

The cellular and molecular interactions required for the development of these mucosal associated lymphoid tissues are beginning to be elucidated. The formation of TALTs and NALTs occurs independently of LTβR-mediated signalling, however the development of NALTs requires Id2 suggesting there may be a role for LTi cells (Fukuyama et al., 2002; Nagatake et al., 2009).

The largest populations of adult LTi cells are found in the intestinal lamina propria (LP) within CPs (Lane et al., 2009; Pabst et al., 2006). CPs are small aggregates of cells, which contain immature lymphocytes and DCs (Kanamori et al., 1996). CPs form within the LP around two weeks after birth (Kanamori et al., 1996). Current evidence suggests that CPs do not continually develop throughout adulthood (Velaga et al., 2009), but these small clusters are able to develop into ILFs (Pabst et al., 2006; Pabst et al., 2005; Taylor et al., 2007). ILFs are organised lymphoid structures that possess distinct B and T cell areas, an epithelium containing M cells and are able to take up bacteria (Lorenz and Newberry, 2004). Collectively CPs and ILFs are commonly referred to as solitary intestinal lymphoid tissues (SILT). The process of the expansion of CPs into ILFs involves an increase in the size of the CP and an influx in B cells. There is a requirement for the microbiota in this process, as it is reduced in germ-free (GF) animals (Pabst et al., 2006) and signaling from dietary ligands via the aryl hydrocarbon receptor (AhR) is likely to play a role. Signalling between LTβR and LTα1β2 is also required, as timed injections of LTβR-Ig during the first two

weeks of birth can prevent the formation of CPs and therefore ILFs (Bouskra et al., 2008). DCs have also been proposed to play a role in the formation of ILFs via the production of CXCL13. In CXCL13 deficient animals there was no transformation of CPs into ILFs and the source of this CXCL13 was attributed to DCs (McDonald et al., 2010). RORγt expression is also required for the development of SILT, as mice lacking RORγt do not develop CPs or ILFs (Eberl and Littman, 2004). In order for a CP to expand into an ILF, the expression of CCR6 by B cells is essential. Therefore it is likely that its ligand CCL20 plays a role in attracting B cells to CPs (McDonald et al., 2007). CCL20 can be expressed by epithelial cells that overlay follicles, perhaps in response to LTα1β2 signalling (Randall et al., 2008). Additionally, commensal bacteria in the intestine can induce CCL20 production by crypts resulting in the formation of ILFs by CPs sensing the microbiota via nucleotide-binding oligomerisation domain protein 1 (NOD1) (Bouskra et al., 2008). Therefore ILF formation can be viewed as inducible; furthermore upon treatment with antibiotics to reduce commensal bacteria the generation of ILFs was reduced. Therefore, the continuing expansion and reduction of ILFs to CPs and vice versa is likely to represent equilibrium between the intestinal immune system and commensal bacteria (Eberl, 2005) (Figure 1.5).

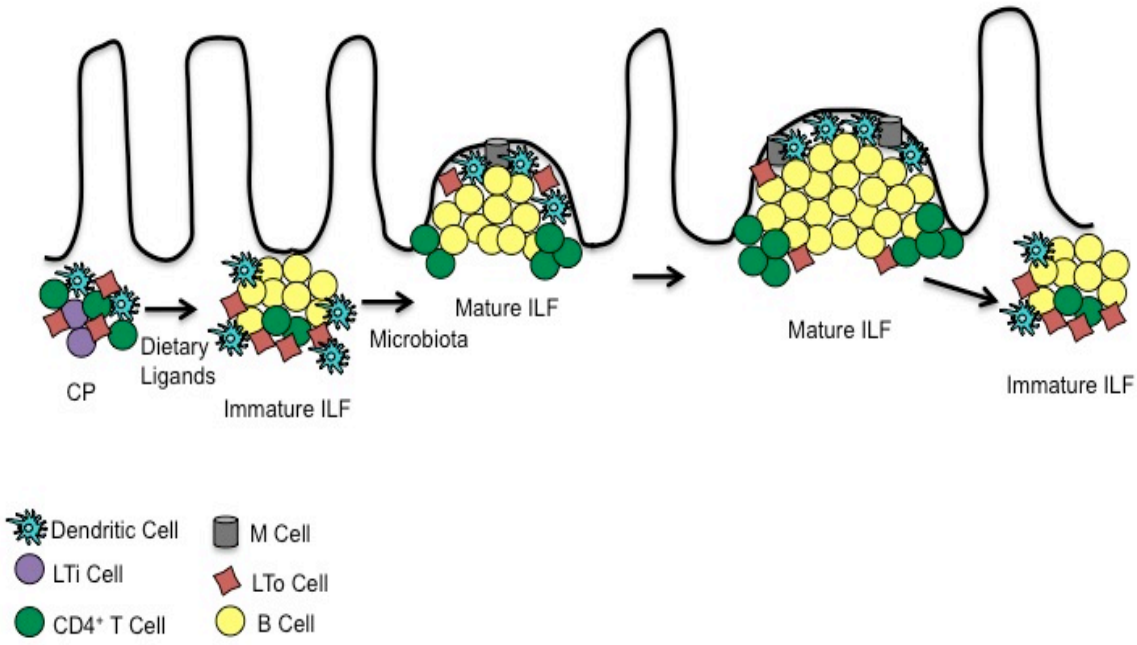

Figure 1-6 The Development of Cryptopatches and their Expansion into Isolated Lymphoid Follicles.

Dietary ligands signal via the aryl hydrocarbon receptor (AHR) on lymphoid tissue inducer (LTi) cells, resulting in the formation of a cryptopatch (CP). CPs develop into immature isolated lymphoid follicles (ILFs) upon further AHR signaling and NOD1 signalling from microbiota, they recruit T and B cells via LTβR and LTα1β2, CXCL13 and CCR6. Mature ILFs promote the formation of IgA plasmablasts. Once challenges from the microbiota are reduced, mature ILFs become immature ILFs. Adapted from (Knoop et al., 2011).

Here I have described the development of lymphoid tissue in the SI, however the situation in the colon is different. Similar to the SI the colon contains two developmentally distinct lymphoid tissues, which have only recently been described (Baptista et al., 2013). Colonic patches are similar to PPs in that they develop during embryogenesis, a process that was likely to be dependent upon LTi cells that were detected in the developing colonic patch. Further similarities were evidenced by the requirement of CXCL13 and LTα for the development of colonic patches and PPs. Colonic patches also contained distinct B and T cell areas, but unlike PPs these distinct areas did not segregate into organised areas until after birth (Baptista et al., 2013; Hashi et al., 2001). Therefore, there are likely to be some differences in the way the development of colonic patches and PPs develop. Recent work also identified colonic SILT that developed post-natally, however these structures are distinct from SI ILFs, demonstrated by the development of colonic SILT in $CXCL13^{-/-}$ mice that do not contain SI ILFs

(McDonald et al., 2010). They also do not depend upon TRANCE for their development (Knoop et al., 2011). Instead the development of colonic SILT appears to be dependent upon CCR6 and CCL20 signalling. Furthermore colonic SILT development is not dependent upon the microbiota, while the development of SI ILFs is dependent on commensal bacteria (Baptista et al., 2013; Kweon et al., 2005). While it has been suggested that the development of colonic SILT is dependent upon the presence of LTi cells, RORγt$^{-/-}$ mice contain lymphoid tissue specifically in their colon (Baptista et al., 2013; Lochner et al., 2011). Whether RORγt independent lymphoid structures represent these colonic SILT or a tertiary lymphoid structure, which develops in the colon when there are no other lymphoid tissues, remains unclear. Further research into these colonic structures is required to determine their developmental cues and the molecular mechanisms that govern this development.

1.14 Formation of Tertiary Lymphoid Organs

Tertiary lymphoid organs resemble ILFs, with organised B and T cell compartments and can produce effector B and T cells (Lee et al., 2006; Moyron-Quiroz et al., 2006; Nasr et al., 2007). However, tertiary lymphoid organs only develop under conditions of inflammation (Lochner et al., 2011). When these are formed at the site of a pathogenic infection, such as during influenza infection of the lungs, they can contribute to the generation of a protective response (Moyron-Quiroz et al., 2004). However tertiary lymphoid organs have also been reported at sites where there is presentation of autoantigens, such as in the pancreas of non-obese diabetic (NOD) mice, and in this case they may lead to the propagation of tissue damage (Anderson and Bluestone, 2005). The generation of tertiary lymphoid organs was reported to be similar to that of secondary lymphoid organs, with CXCL13 playing a role by attracting B cells (Dejardin et al., 2002). But in contrast to the formation of LNs, tertiary lymphoid organs can develop in RORγt$^{-/-}$ animals, via an LTi independent pathway in response to environmental factors (Lochner et al., 2011) (Lee et al., 2006).

1.15 The Intestinal Immune System

The intestine has a surface area over 200 times that of the skin. It primarily functions to process foodstuffs and to allow the absorption of nutrients and water. The intestine is constantly exposed to a vast array of harmless antigen from dietary agents and an enormous community of commensal bacteria, which outnumber human cells in the body by ten times (Macpherson et al., 2009). Alongside this harmless antigen most pathogens enter the body via a mucosal surface such as the intestine (Mowat, 2003). Therefore, the intestinal immune system has to discriminate between pathogenic material and harmless antigen, and then mount an appropriate immune response. In order to fulfil this essential task, the intestinal immune system has evolved to become the largest and most complex part of the immune system. A breakdown in the discrimination between harmful and harmless antigen by the intestinal immune system can result in the development of pathogenesis in the form of inflammatory bowel disease (IBD) or coeliac disease (CD). Due to their unique ability to stimulate primary immune responses DCs play an essential role in the intestinal immune system. They are also able to determine the outcome of the immune response; therefore they also play a vital role in maintaining the delicate balance between immunity and tolerance in the intestine.

1.15.1 Antigen Uptake in the Intestine

The mucosal surfaces of the digestive system are covered by an epithelial barrier, consisting of only a single layer of epithelial cells that separate the external gut lumen from the underlying LP. This epithelial layer has a high cellular turnover and contains proliferating cells, which replace those that are lost and shed into the lumen. Intestinal epithelial cells are derived from stem cells, which, in the SI, are located in crypts near the base of the villi. These intestinal stem cells give rise to distinct cell lineages; enterocytes, goblet cells, enteroendocrine cells, and Paneth cells (Bjerknes and Cheng, 1999; Hermiston and Gordon, 1995). These cells migrate towards the tip of the villus, except Paneth cells that remain in the crypt and produce defensins, lysozyme and phospholipase A2 (Ayabe et al., 2000; Wilson et al., 1999). Although the colon lacks villi there is a similar replacement of epithelial cells from the crypt, however Paneth cells are only produced in the proximal colon (Chang and

Leblond, 1971). A physiochemical barrier is maintained by the intestinal epithelium, via the production of mucus from goblet cells and antimicrobial peptides from Paneth cells. Thus, contact between the contents of the gut lumen and the epithelium is limited. When intact, the intestinal epithelium largely prevents the passive entry of large particulate antigen and bacteria. Small soluble molecules may pass the epithelium by non-mediated inactive passive diffusion (Travis and Menzies, 1992). However, effective immune surveillance of the mucosal surface requires the transport of intact macromolecules and microorganisms across the epithelial barrier to cells such as DCs. Several mechanisms for antigen uptake in the intestine have been described and will be outlined below.

1.15.2 M Cell Mediated Antigen Uptake

Microfold (M) cells are atypical epithelial cells that are specialised for the transport of large particulate antigens and microorganisms across the epithelial barrier. M cells are located on the follicle-associated epithelium (FAE) of the PPs and ILFs (Borghesi et al., 1999; Neutra et al., 1996). Although some previous reports have suggested that M cells are present within the villous epithelium (Jang et al., 2004; Vallon-Eberhard et al., 2006), more recent work has suggested that these represent a functionally immature M cell which is unlikely to play a role in antigen sampling in the villi (Kobayashi et al., 2012). The FAE has fewer mucus-producing goblet cells and lysozyme producing Paneth cells, making it easily accessible from the gut lumen. M cells internalise particulate antigen via endocytosis in clathrin-coated vesicles, actin-dependent phagocytosis, or macropinocytosis (Neutra et al., 2001; Owen, 1999). Unlike DCs or macrophages, M cells transcytose the internalised antigen rather than targeting it for degradation. This delivers antigen to DCs, macrophages or B cells in the M cell basolateral pocket, which may involve intercellular communication channels (Hase et al., 2009b). Therefore, this mechanism appears to be specialised for the uptake of intestinal bacteria and large particulate antigens.

In order to mediate the uptake of specific microorganisms M cells express a range of molecules. For instance, murine M cells express glycoconjugates that can bind *Ulex europaeus* agglutinin (UEA)-1 (Chionh et al., 2009). Another example is glycoprotein-2 (GP-2) that is expressed on the surface of M cells and

binds to FimH, which is expressed by many commensal and pathogenic enterobacteria (Hase et al., 2009a). M cells also express the C5a receptor that binds proteins that are similar to outer membrane protein H expressed by *Yersinia enterocolitica (Kim et al., 2011).* Some studies have also suggested that M cells express an IgA specific receptor that binds to the constant regions of secretory IgA (sIgA), although the receptor has not yet been identified (Mantis et al., 2002; Mantis et al., 2011; Rey et al., 2004). As ILFs and PPs produce large amounts of IgA, this may be a mechanism to regulate and allow the coexistence of commensal bacteria and preventing the development of aberrant immune responses. M cells continually sample antigen in the steady-state and this can be increased upon exposure to microbial products. For example injections of peptidoglycan from *Staphylococcus aureus* or *Streptococcus pneumoniae* into the intestinal lumen have been shown to increase the transport of microparticles across the FAE (Chabot et al., 2006; Meynell et al., 1999).

As M cells represent a point of entry into the host, some pathogens exploit M cells to cause infection. For example, *Yersinia* species are able to produce invasin that specifically binds to integrin-β1 on M cells, facilitating its entry into M cells (Clark et al., 1998). *Listeria monocytogenes* produces internalin B and *Salmonella enterica* utilises a secretion system to specifically target M cells, although the specific receptors for their uptake have not yet been identified (Chiba et al., 2011; Jones et al., 1994). It has also been suggested that prions selectively gain access to M cells, although the mechanism by which this is achieved is yet to be determined (Donaldson et al., 2012) and other studies suggested prions were able to access the intestine independently of M cells (Jeffrey et al., 2006; Mishra et al., 2004). There is great interest in understanding M cell receptors and their signalling mechanisms in order to improve oral vaccine delivery systems. However, further work will be required in order to fully elucidate the mechanisms involved in antigen acquisition and transport by M cells.

1.15.3 Dendritic Cell Uptake of Luminal Antigen

In addition to M-cell mediated antigen uptake, it was proposed that CD11c-expressing cells associated with the gut epithelium in the LP were a population of DCs capable of capturing luminal bacteria directly (Rescigno et al., 2001).

The presence of trans-epithelial dendrites on this subset of mononuclear cells was confirmed using transgenic mice expressing the GFP in place of CX3CR1, with heterozygous mice functioning as reporter mice (Jung et al., 2000). Fluorescence imaging hinted trans-epithelial dendrites mediated the uptake of *S. enterica,* as the number of trans-epithelial dendrites in the terminal ileum increased after Salmonella challenge and this response was markedly reduced in CX3CR1 deficient mice (Niess et al., 2005). The formation of trans-epithelial dendrites is dependent upon the expression of CX3CR1 (Niess et al., 2005). Furthermore, following administration of fluorescently labelled *Escherichia coli* in CX3CR1 deficient animals there were fewer bacteria recovered from the MLN. The number of trans-epithelial dendrites was increased after the introduction of TLR ligands and was reduced in mice given broad-spectrum antibiotics or mice lacking the TLR adaptor molecule MyD88 (Chieppa et al., 2006; Niess et al., 2005; Vallon-Eberhard et al., 2006). Together these observations were the basis of the suggestion that *in vivo* $CX3CR1^+$ cells in the LP extended trans-epithelial dendrites to sample bacteria from the gut lumen.

However, association of bacteria with a cell does not necessarily mean that these cells have actively sampled the bacteria. Further evidence began to call into question the physiological role played by these antigen sampling $CX3CR1^+$ cells. Upon inoculation with *Aspergillus fumigatus,* for instance, pathogen uptake was not affected in the absence of $CD11c^+$ cells, or in CX3CR1 deficient mice that also lack trans-epithelial dendrites (Vallon-Eberhard et al., 2006). Additionally, the presence of trans-epithelial dendrites appears to be mouse strain dependent. Trans-epithelial dendrites have also been observed in CD11c-GFP and MHCII-GFP reporter mice although their position remains controversial due to substantial differences in the distribution of dendrites in comparison to CX3CR1 reporter mice (Chieppa et al., 2006; Niess et al., 2005).

Although there was some variation in reports regarding the importance of trans-epithelial dendrites in the adaptive immune response, it was generally assumed that epithelial-associated $CX3CR1^+$ mononuclear LP DCs were able to acquire luminal antigen via trans-epithelial dendrites and transport it to the MLN via lymphatics. However, more recent evidence has definitively shown that the majority of $CX3CR1^+$ $CD11c^+$ cells do not represent DCs; instead these are more

likely to represent a population of sedentary macrophages (Schulz et al., 2009). CX3CR1^{+} LP cells and cDCs arise from different progenitors and serve different functions. Subsets of DCs which express CD103 appear to confer typical properties of the intestinal immune response such as the ability to migrate to the draining LN and are able to present antigen to naïve T cells, although genuine CD103^{-} DCs expressing intermediate levels of CX3CR1 are also present and behave in a similar manner to CD103^{+} DCs (Bain et al., 2013; Cerovic et al., 2012; Schulz et al., 2009). Upon further characterisation, the CX3CR1^{hi} CD11c^{+} cells also appeared to express F4/80, CD14 and CD64; markers commonly used to identify macrophages (Bain et al., 2013; Schulz et al., 2009; Tamoutounour et al., 2012). Additionally, in comparison to CD103^{+} DCs, CX3CR1^{hi}CD11c^{+} cells were inefficient at inducing the proliferation of naïve T cells as assessed by a thymidine incorporation assay (Schulz et al., 2009). Finally, the CX3CR1^{hi} intestinal cells are monocyte-derived and CSF-1 dependent, while the CD103^{+} DCs arise from preDCs and are dependent on the growth factor FLt3L (Bain et al., 2013; Bogunovic et al., 2009; Tamoutounour et al., 2012; Varol et al., 2009). Therefore, it is likely that CX3CR1^{hi} CD11c^{+} cells are a gut resident population of macrophages, not of a population of migratory DCs. LP-resident cells expressing intermediate levels of CX3CR1 are heterogeneous and contain a mix of sedentary macrophages and a population of Flt3-dependent DCs capable of migrating in intestinal lymph (Bain et al., 2013; Cerovic et al., 2012). This CX3CR1 expression by DCs was notably lower than that expressed by CX3CR1^{hi} macrophages (Cerovic et al., 2012). Recently, Diehl *et al*. reported that a CX3CR1^{hi} population of cells were also able to migrate to the MLN, in a CCR7 dependent manner, in the steady-state and following *Salmonella* infection (Diehl et al., 2013). However, in our hands, we find only the CX3CR1^{int} population of bona-fide DCs (which lack the expression of macrophage markers F4/80, CD14 and CD64 and share an ontogeny with CD103^{+} DCs) migrate in the steady-state following thoracic duct cannulation (TDC) and mesenteric lymphadenectomy (MLNx) (Cerovic et al., 2012) (V.Cerovic, personal communication). It is possible that Diehl *et al*. have misclassified CX3CR1^{int} cells as CX3CR1^{hi} cells, thus leading to the conclusion that macrophages migrate to the MLN. However we, and others, have shown this does not occur in the steady-state (Cerovic et al., 2012; Schulz et al., 2009). The ability of CX3CR1$^{hi/+}$ cells to migrate under conditions of inflammation has also been reported during DSS induced colitis, although the origin of these cells

is unclear (Zigmond et al., 2012). Such migration of CX3CR1 expressing cells under conditions of inflammation may represent an interesting pathway by which antigen can gain access to the MLN, and therefore deserves much further investigation.

Recently, Farache *et al*. crossed CX3CR1$^{GFP/+}$ mice with CD11c-YPF mice in order to determine whether bona-fide DCs were able to extend trans-epithelial dendrites. These studies used 2-photon microscopy to identify CD11c^{YFP+}CX3CR1^{GFP-} cells that they correlate with CD103^{+} DCs (Farache et al., 2013). Interestingly these cells were responsive to CSF-2, a marker more commonly associated with the expansion of macrophages, although is likely to act as an accessory for the expansion of some subsets of CD103^{+} DCs (Bogunovic et al., 2009) (Greter et al., 2012). The authors showed that CD11c^{YFP+}CX3CR1^{GFP-} cells were able to internalise non-invasive *Salmonella* and that these cells were less efficient than CX3CR1^{GFP+} at the uptake of soluble OVA. However, they do not directly show CD103^{+} DCs extending dendrites. Interestingly, recent work by McDole *et al*. did not identify the formation of trans-epithelial dendrites, although they used the same mouse model as Farache *et al*. (McDole et al., 2012). Instead the authors identified CD11c^{YFP+}CX3CR1^{GFP-} cells forming goblet cell associated antigen passages, which were visible after the intraluminal injection of rhodamine dextran. In contrast to previous reports, the authors do not suggest that DCs are acquiring antigen from the gut lumen, but from the LP. However, it is contradictory to previous reports, which used flow cytometry to show that after intraluminal injection of fluorescently labelled ovalbumin the majority of fluorescent antigen was taken present in CX3CR1^{+} cells in the LP, not CD103^{+} DCs (Schulz et al., 2009). Furthermore following FITC dextran administration a larger population of SSC^{lo} cells, distinct from CD103^{+} DCs, appeared to be positive for FITC dextran (McDole et al., 2012). Therefore the relevance of antigen uptake via goblet cell associated antigen passages requires further investigation.

Recently Lelouard *et al*. described a population of CD11c^{+}CX3CR1^{+} DCs which express lysosome M and are able to extend dendrites that capture fluorescent micropartices or *S. typhimurium* (Lelouard et al., 2012; Lelouard et al., 2010). Unlike previous mechanisms described for DC subsets in the villus epithelium

that describe dendrites extending paracellularly between epithelial cells, these "LysoDC" extend dendrites in a transcellular manner and sample via M cell pores. Briefly, there is a cytoskeleton rearrangement in both the M cell and the LysoDC which allows the LysoDC to extend through a transcellular pore created by the M cell, without breaking the integrity of the epithelial barrier. Although the authors have designated these $CD11c^{+}CX3CR1^{+}$Lysozyme M^{+} cells as DCs, it is unclear if these are genuine DCs or a population of macrophages. Although the authors showed that $CD11c^{+}CX3CR1^{+}$Lysozyme M^{+} cells had the highest expression of CD11c, MHCII and costimulatory molecules the ability of these cells to migrate, present antigen and stimulate the proliferation of naïve T cells has not yet been addressed.

The observations outlined above describe a number of studies using 2-photon microscopy for the direct observation of DCs *in situ*. However it is important to remember that during experimental imaging there is likely to be tissue disruption in order to immobilise the intestine for the imaging. Furthermore disruption to the mucus layer caused by the injection of large volumes of fluid, or resulting from imaging experiments, may force contact between the epithelium and luminal contents. Therefore further work must be completed in order to determine the functional relevance of these antigen uptake mechanisms.

1.15.4 Antigen Uptake Via the Neonatal Fc Receptor

Under specific circumstances, enterocytes have also been shown to mediate antigen sampling in the SI. Enterocytes are mainly involved with food absorption, but they are also able to express the neonatal Fc receptor (FcRn) until adulthood (Dickinson et al., 1999). Human FcRn has been shown to mediate the transport of IgG across the epithelium and can transfer IgG together with its cognate antigen as an immune complex across the intestinal epithelial barrier. Antigen is then passed to DCs and presented to T cells in the MLN (Yoshida et al., 2004; Yoshida et al., 2006). More recent work has demonstrated the importance of this pathway for some pathogens. For instance, there was enhanced epithelial invasion of *Helicobacter heilmannii* following infection in FcRn deficient mice (Ben Suleiman et al., 2012). Therefore this pathway may

represent a process by which antigen that has previously raised an IgG response may swiftly be captured and processed.

1.16 Dendritic Cell Subsets in the Intestine

1.16.1 Dendritic Cell Subsets in the Lamina Propria

DCs in the LP have been principally defined by their co-expression of CD11c and MHC class II. However, the use of only these markers to define distinct intestinal DC subsets is complex as CD11c is also expressed on functionally distinct macrophages, along with CX3CR1, F4/80 and CD64 (Bain et al., 2013; Cerovic et al., 2012; Tamoutounour et al., 2012). Subsequently, in addition to CD11c and MHCII, CD103 has been used as a de facto marker of DCs in both the siLP and cLP (Johansson-Lindbom et al., 2005; Rivollier et al., 2012; Schulz et al., 2009). However we have shown that following TDC there are four functionally and phenotypically distinct subsets of DC identified by their expression of CD103 and CD11b, including two $CD103^-$ subsets (Cerovic et al., 2012). Corresponding DC subsets were also identified in the siLP, and CD103 and CD11b have also been used to identify DC subsets in the cLP (Rivollier et al., 2012).

The majority of $CD103^+$ DCs in the siLP express CD11b, but some $CD103^+$ siLP DCs express CD8α instead of CD11b (Fujimoto et al., 2011; Jakubzick et al., 2008). In comparison in the cLP the ratio between these two DC subsets is reversed, with $CD103^+CD11b^-$ DCs being the largest population and $CD103^+CD11b^+$ comprising a smaller population (Denning et al., 2007). As $CD8\alpha^+$ has previously been used to identify DCs as lymphoid-tissue resident cells, this was a surprising finding (Jakubzick et al., 2008). Determining whether $CD103^+CD8\alpha^+$ DCs are a contamination from intestinal lymphoid tissue or are a population genuinely present in the LP is essential for elucidating the function of this DC subset. In addition to the two subsets of $CD103^+$ DCs, there are also $CD103^-CD11b^+$ DCs and $CD103^-CD11b^-$ DCs present in the intestinal lymph and siLP (Cerovic et al., 2012). Both of these $CD103^-$ DC subsets express CCR7, expand in response to FLt3L, present antigen to naïve T cells and express the DC restricted transcription factor Zbtb46 (Cerovic et al., 2012; Satpathy et al., 2012). Interestingly $CD103^-$ $CD11b^+$ DCs also express intermediate levels of CX3CR1, but do not express other macrophage-associated markers such as F4/80 or CD64.

Although these distinct DC subsets originate from the same pre-cDC precursor (C.L Scott, personal communication), the development of different subsets requires specific factors. For example, $CD103^+CD11b^+$ DCs require CSF-2 for their development, demonstrated by their selective impairment in CSF-2R-deficient mice (Greter et al., 2012). $CD103^+CD11b^+$ DCs are also dependent upon Notch-2 and IRF4 for their development, but $CD103^+CD11b^-$ DCs development is unaffected by the absence of these factors (Lewis et al., 2011; Persson et al., 2013). In contrast, $CD103^+CD11b^-CD8\alpha^+$ DCs require Batf3 and IRF-8 for their development, but $CD103^+CD11b^+$ DCs are unaffected in the absence of these transcription factors (Edelson et al., 2010). The ontogeny of $CD103^-$ DC subsets is less clear, although it has been shown that these cells develop from the common pre-cDC precursor (Schraml et al., 2013) and they are unaffected by conditional IRF4 depletion (Persson et al., 2013).

1.16.2 Functions of Dendritic Cell Subsets in the Lamina Propria

In order for DCs to perform their major function of initiating an adaptive immune response, their migration to the draining LN is crucial. In the steady-state DCs from the intestine constitutively migrate through the lymphatics to the MLN where they present peripherally derived antigen to T cells (Pugh et al., 1983; Wilson et al., 2008). This is essential for the induction of oral tolerance, and following pathogen stimulation DCs can also initiate an adaptive immune response (Milling et al., 2007; Worbs et al., 2006). Additionally it has been demonstrated in rats that microbial stimuli can influence the migration and maturation of DCs. Upon oral administration of the TLR7/8 agonist R848 there is a dramatic increase in DCs migrating from the LP to T cell areas of the MLN in a TNF-α dependent manner. This demonstrates that the presence of pathogenic microbial products can increase the rate of DC migration to the MLN, presumably resulting in a more rapidly induced adaptive immune response (Yrlid et al., 2006c).

The migration of DCs from the LP to the draining MLN is a CCR7 dependent process. In $CCR7^{-/-}$ mice the numbers of $CD103^+$ DCs are reduced in the MLN but not in the LP (Jang et al., 2006; Johansson-Lindbom et al., 2005; Ohl et al.,

2004). $CD103^+$ DCs accumulate with delayed kinetics in the MLN compared to the LP in BrdU pulse chase experiments, indicating that $CD103^+$ LP DCs represent a migratory DC population in the LP (Jaensson et al., 2008). Furthermore, using confocal microscopy to study lymphatic vessel *in vivo* and flow cytometry to assess DC subsets in draining MLN-afferent lymph, it was directly shown that LP derived $CD103^+$ DCs make up the major population of DCs in murine draining lymph (Schulz et al., 2009). Additionally $CX3CR1^{hi}$ expressing cells cannot be detected in the draining lymph either in the steady-state or following administration of R848, providing further evidence to support the hypothesis that these cells are not DCs (Schulz et al., 2009).

Additionally, the migration of DCs from the LP to the MLN may be influenced by pDCs. Following the oral administration of the TLR 7/8 ligand R848 there is a rapid mobilisation of DCs from the LP into intestinal lymph (Yrlid et al., 2006c). However, some DC subsets obtained from intestinal lymph are unable to respond directly to R848, as they do not express TLR7 or TLR8 (Yrlid et al., 2006a). Instead it has been shown that after oral application of R848 intestinal pDCs are required for the mobilisation of DCs from the LP. This effect is likely to be mediated by TNF-α (Wendland et al., 2007; Yrlid et al., 2006a).

1.16.3 Peyer's Patch Dendritic Cells

In the PPs there are three major populations of $CD11c^+$ DCs; $CD11b^+$ in the subepithelial dome, $CD8\alpha^+$ in the inter-follicular regions and $CD11b^-CD8\alpha^-$ DCs which are found throughout the PPs except in the germinal centres (Iwasaki and Kelsall, 2000; Iwasaki and Kelsall, 2001). More recently within the $CD11b^-CD8\alpha^-$ subset, a subset of $CX3CR1^+$ DCs which also express lysozyme was described (LysoDCs) (Lelouard et al., 2010). These were located only in the subepithelial dome. More recent work has used CD103 as a marker to define DC subsets within the SI and colon, and indeed some $CD103^+$ DCs have been identified in the PPs however the majority of DCs in the PPs are $CD103^-$ (Bogunovic et al., 2009; Jaensson et al., 2008).

The anatomical location of PPs DCs is dependent upon the expression of various chemokines and their receptors. As revealed by in situ hybridisation all three

subsets of PP DCs express CCR7 (Iwasaki and Kelsall, 2000). In the steady state $CD11b^+$ DCs express CCR6 and CCR1, in addition to CCR7, and so migrate towards CCL20 and CCL19. CCL20 is constitutively expressed by epithelial cells in the follicle associated epithelium leading to the hypothesis that $CD11b^+$ DCs are constantly recruited to the subepithelial dome (Cook et al., 2000; Zhao et al., 2003). In accordance with this it was reported that $CD11b^+$ DCs were severely reduced or completely absent in the subepithelial domes of CCR6 deficient mice or following in vivo antibody neutralisation of CCL9 (Cook et al., 2000; Varona et al., 2001). In comparison, $CD8\alpha^+$ DCs constitutively express CCR7, but not CCR6, and so are able to migrate towards CCL19 and CCL21, but not CCL20 (Iwasaki and Kelsall, 2000). CCL19 and CCL21 are constitutively expressed in the inter-follicular region suggesting that $CD8\alpha^+$ DCs are resident in the inter-follicular region. The chemokines responsible for the migration and localisation of $CD11b^-$ $CD8\alpha^-$ DCs have not yet been identified.

Upon *in vivo* activation with the soluble tachyzoite antigen from *Toxoplasma gondii* (STAg) $CD11b^+$ and possibly some $CD11b^-CD8\alpha^-$ DCs migrated from the subepithelial dome into the inter-follicular regions, where T cell priming can occur. This correlated with an upregulation of CCR7 and a downregulation of CCR6 upon overnight culture (Iwasaki and Kelsall, 2000). These support the hypothesis that activation of DCs in the subepithelial dome, as would occur following exposure to microorganisms entering via M cells, results in the upregulation of CCR7 and migration to the inter-follicular regions by the upregulation of CCR7 where T cell priming can occur.

In the steady-state DCs are present in the follicle-associated epithelium in smaller numbers than in the subepithelial dome. Oral administration of cholera toxin, cholera toxin B-toxin, *Escherichia coli* heat labile toxin or *Salmonella typhimurium* infection can induce an influx of DCs from the subepithelial dome into the follicle-associated epithelium (Anosova et al., 2008). It was also shown that PP DCs in the subepithelial dome that express CCR6 appear to migrate into the follicle-associated epithelium, where they form clusters with antigen specific $CD4^+$ T cells. Furthermore the activation and expansion of specific T cells was dependent upon CCR6 (Salazar-Gonzalez et al., 2006). These CCR6-expressing DCs were not recruited to the intestinal LP, suggesting that these DCs

may have specific functions in organised lymphoid tissues, where the CCR6 ligand is constitutively expressed.

1.16.4 Functions of Peyer's Patch Dendritic Cell Subsets

It has been shown that PP CD11b$^+$ DCs produced relatively low levels of IL-12 and IFN-γ upon stimulation with *Staphylococcus aureus* (Iwasaki and Kelsall, 2001). Compared to CD8α^+ or CD8α^-CD11b$^-$ DCs, however, CD11b$^+$ DCs from PPs produced high levels of IL-10, and induced naïve T cells to differentiate into IL-10 producing T cells. In comparison, CD8α^+ and CD11b$^-$CD8α^- DCs produced IL-12 and little or no IL-10 under the same conditions (Iwasaki and Kelsall, 2001). These studies support the hypothesis that in the steady state PP CD11b$^+$ DCs produce IL-10 and possibly TGF-β upon interaction with naïve T cells causing their differentiation into Th2 cells producing IL-4, IL-10 and TGF-β.

Several characteristics have been attributed to CD8α^+ and CD11b$^-$CD8α^- DCs. Following reovirus infection dome region CD11b$^-$CD8α^- DCs take up viral antigens from dying infected epithelial cells. As CD11b$^-$CD8α^- DCs have been shown in vitro to produce high levels of IL-12 it is likely these cells go on to drive a Th1 type response (Fleeton et al., 2004). CD8α^+ DCs also present viral antigen to T cells, although it is still unclear if this is the result of direct viral antigen uptake or the cross presentation of antigen transported into the T cell zone by other DC subsets (Fleeton et al., 2004).

All subsets of PPs DCs, but not splenic or DCs from other tissues, are able to induce the expression of the mucosal homing receptor $\alpha4\beta7$ and CCR9 on T cells in vitro (Mora et al., 2003). Upon adoptive transfer of PPs DCs, primed CD8$^+$ T cells preferentially migrate to mucosal lymphoid tissues (Mora et al., 2005). This demonstrates that DCs from peripheral tissues are able to imprint T cells with tissue-specific homing receptors. The ability to imprint gut homing T cells is dependent upon the generation of the vitamin A metabolite retinoic acid (RA) by DCs (Iwata et al., 2004).

The PP is also the primary site for the production of IgA, which prevents invading pathogens and commensal bacteria from binding to the intestinal epithelium and

neutralises their toxins to maintain homeostasis at the mucosal surface (Cerutti, 2008; Tezuka and Ohteki, 2010). Accumulating evidence indicates that DCs are critical to the synthesis of IgA. For instance, PP DCs produce TGF-β and IL-6, facilitating the switching of TLR-activated B cells from IgM to IgA expression; this also causes the generation of IgA plasmablasts. Following the retention or upregulation of CCR9 and α4β7, and the downregulation of CXCR5 expression, IgA^+ plasmablasts migrate from the PP to the gut LP where they further differentiate into IgA plasma cells (Cerutti and Rescigno, 2008). Vitamin A levels have also been shown to be associated with IgA responses in the intestine, with vitamin A deficiency leading to reduced levels of IgA (Stephensen, 2001). Furthermore, it has been demonstrated that the ability of DCs from the PP to promote T-cell-independent class switching to IgA can be attributed to the combined effects of RA and IL-5 or IL-6 (Mora et al., 2006).

1.16.5 Dendritic Cell Subsets in Isolated Lymphoid Follicles

Previously, the phenotype of ILF DCs has been investigated by manually separating ILFs from all other intestinal tissues, followed by flow cytometry (McDonald et al., 2010). This study showed that the majority of $CD11c^+$ cells within the ILF were $CD11b^-$, although the authors did not report on the expression of CD103 in the ILF-derived DCs (McDonald et al., 2010). The phenotype of DCs in the ILF has also been investigated using immunohistochemistry (Jaensson et al., 2008; McDonald et al., 2010). Jaensson *et al*. showed that the majority of DCs within ILFs are $CD103^-$, although some were $CD103^+$. This suggests that there are likely different subsets present within the ILF, although due to their small size determining these subsets using flow cytometry or immunohistochemistry will be challenging.

1.16.6 Functions of Dendritic Cells Within Isolated Lymphoid Follicles

ILFs are distinct anatomical structures in the intestine, which contribute to the intestinal mucosal immune system by acting as inducible sites for the generation of adaptive immunity. DCs that originate here are likely to have been exposed to a different immune and antigenic environment than LP- or PP-derived DCs. This specialised environment could generate the features that distinguish the ILF-DCs

from the other migrating intestinal DC populations. Due to their small size little has been done to elucidate the specific functions of ILF DCs. However, like PP DCs, they are likely to be specialised for inducing B cell class switching as ILFs have been shown to play a compensatory role in producing antigen specific IgA in PP-null mice (Glaysher and Mabbott, 2007; Lorenz and Newberry, 2004). The ILF generation of IgA has been shown to be independent of T cell help, therefore the DCs present in the ILF can present antigen to B cells directly (Tsuji et al., 2008). However this did not rule out the ability of DCs to present antigen to T cells, which are present in ILFs.

1.17 Functions of Dendritic Cells in the Mesenteric Lymph Nodes

Both in the steady state and under conditions of inflammation the MLN is home to several populations of $CD11c^+$ DCs. It contains the four migratory DC subsets arriving from the LP, and perhaps DCs from the PPs and ILFs, as well as DCs that have developed from blood borne precursors. The expression of CD103 on DCs is likely to mark many of the DCs arriving from the LP. However not all migratory DCs are $CD103^+$ some are $CD103^-$ (Cerovic et al., 2012). DCs in the MLN have the ability to generate gut-homing T cells, therefore naïve T cells primed here will preferentially localise their effects in the intestine.

1.17.1 Oral Tolerance

Oral tolerance is the state of local and systemic immune unresponsiveness that is induced by the oral administration of innocuous antigen, such as food protein. This state of hyporesponsiveness to fed antigen prevents unnecessary inflammation and hypersensitivity to harmless antigen. Oral tolerance can be transferred from one animal to another via the transfer of Tregs, or can be abolished by the depletion of $Foxp3^+$ T cells (Hadis et al., 2011; Zhang et al., 2001). The MLN, specifically the migration of DCs to the MLN, is essential for the generation of oral tolerance. CCR7 deficient mice demonstrate this; where intestinal DCs cannot migrate to the MLN, are unable to mount a T cell response in the MLN, cannot generate $Foxp3^+$ Tregs, and thus are defective in their ability to generate oral tolerance (Johansson-Lindbom et al., 2005; Worbs et al., 2006). Of the migratory DCs in the MLN it is likely to be $CD103^+$ rather than $CD103^-$ DCs

that play a major role in the induction of tolerance. This was demonstrated after the oral administration of ovalbumin (OVA), where purified $CD103^+$ but not $CD103^-$ MLN DCs to induced OVA-specific T cell response *in vitro* (Coombes et al., 2007; Jaensson et al., 2008). *In vivo* the depletion of either $CD103^+CD11b^+$ or $CD103^+CD11b^-$ DCs does not result in a decrease in the number of responding T cells in the LP (Edelson et al., 2010; Persson et al., 2013; Welty et al., 2013). A reduction in intestinal regulatory T cells was only observed when animals lacked all $CD103^+$ intestinal DCs. Therefore there is likely to be some degree of functional overlap between $CD103^+CD11b^+$ and $CD103^+CD11b^-$ DCs in the induction of tolerance (Welty et al., 2013).

It has been suggested that $CD103^+$ DCs are conditioned by epithelial cell derived factors to promote a tolerogenic response. The interaction between E-cadherin expressed by epithelial cells and CD103 on DCs, along with factors such as TGF-β, IL-10, RA, TSLP, PGE2 and VIP can condition DCs (Annacker et al., 2005; Coombes and Powrie, 2008; Coombes et al., 2007; McDonald et al., 2012; Rimoldi and Rescigno, 2005). This appears to facilitate DCs to drive a regulatory type response in the intestine, by fostering the conversion of naïve T cells recognising innocuous antigen into $Foxp3^+$ Tregs (Coombes et al., 2007).

It has also been proposed that pDCs play a role in the generation of oral tolerance (Goubier et al., 2008). Depletion of pDCs using the pDC specific Gr1 mAb resulted in abrogated induction of oral tolerance to a hapten as well as reducing systemic tolerance to OVA (Goubier et al., 2008). However as intestinal pDCs are unable to migrate to the draining MLN, it is unlikely these are acting in a similar manner to cDCs from the SI (Yrlid et al., 2006b). The liver can also function of a site of soluble oral antigen presentation due to the way in which it receives soluble antigen in the bloodstream from the portal vein (Yang et al., 1994). The authors noticed that the transfer of pDCs from the liver of animals fed with specific antigen to naïve mice resulted in the suppression of delayed type hypersensitivity responses (Goubier et al., 2008). As the pDC depletion used by the authors was systemic, it may be that pDCs may induce anergy or deletion of antigen specific T cells, possibly $CD8^+$ T cells in the liver or perhaps the GALT (Goubier et al., 2008; Dubois et al., 2009).

1.17.2 Functions of Retinoic Acid in Dendritic Cells

The MLN is a site of enhanced Treg differentiation and T cells primed at this site are induced to express the gut homing receptors CCR9 and $\alpha4\beta7$ (Coombes et al., 2007; Johansson-Lindbom et al., 2003). These properties have been shown to be dependent upon the ability of intestinal DCs to generate the vitamin A metabolite RA (Coombes et al., 2007; Iwata et al., 2004). In the intestine vitamin A is obtained from the diet, which is oxidised to retinal by alcohol dehydrogenase (ADH) and then further to RA by aldehyde dehydrogenase (ALDH) (Mora et al., 2008). DCs express Aldh1a2, which encodes retinaldehyde dehydrogenase 2 (RALDH2), an enzyme that converts retinal to RA (Coombes et al., 2007). $CD103^+CD11b^+$, $CD103^+CD8\alpha^+$ and $CD103^-$ DC subsets have all been shown to possess ALDH activity, and thus the ability to metabolise vitamin A (Cerovic et al., 2012). Therefore they have the potential to generate gut tropic T cells, and perhaps $Foxp3^+$ Tregs cells.

1.17.3 The Generation of $Foxp3^+$ Regulatory T Cells in the Mesenteric Lymph Node

DCs are able to promote the development of $Foxp3^+$ Tregs. In this process TGF-β facilitates the generation and maintenance of $Foxp3^+$ Tregs, and RA is an essential cofactor. In the absence of exogenously added TGF-β, OVA-loaded $CD103^+$ DCs from the MLN, but not $CD103^-$ DCs, were able to induce the generation of $Foxp3^+$ Tregs from naïve T cells (Coombes et al., 2007; Jaensson et al., 2008). One of the possible reasons for the functional difference between $CD103^+$ and $CD103^-$ MLN-derived DCs may be the ability of $CD103^+$ DCs to produce higher levels of TGF-β than $CD103^-$ DCs although the $CD103^+$ DCs would be likely to be derived from the LP with $CD103^-$ DCs being a combination of blood derived DCs and some immunogenic migratory $CD103^-$ from the LP. Specifically $CD103^+$ DCs express higher levels of tissue plasminogen factor latent TGF-β binding protein 3 and ALDH, which play roles in the efficient secretion and activation of TGF-β (Coombes et al., 2007). When cultures of $CD103^+$ MLN-derived DCs were incubated with naïve T cells in the presence of TGF-β and synthetic RA inhibitors, the induction of $Foxp3^+$ Tregs were completely abrogated, indicating that RA is an essential cofactor to increase the rate of Treg induction mediated by TGF-β. RA alone has little effect upon Foxp3 expression, therefore it has

been suggested that there is cooperation between the TGF-β and RA pathways (Balmer and Blomhoff, 2002). It was also shown that $CD103^+$ and $CD103^-$ MLN-derived DCs were equally potent in generating $Foxp3^+$ Tregs from naïve $CD4^+$ T cells in the presence of exogenous TGF-β and RA (Coombes et al., 2007).

1.17.4 The Induction of Gut Homing Receptors on T Cells by Dendritic Cells

Another key step in the development of oral tolerance is the generation of gut homing T cells. Tissue-selective trafficking of T lymphocytes is guided by a combination of adhesion molecules and chemokines. Upon activation in the MLN by DCs, T cells can upregulate CCR9 and α4β7 integrin endowing these cells with the capacity to home to the SI (Jaensson et al., 2008; Johansson-Lindbom et al., 2005). Consequently CCR9 deficient $CD8^+$ T cells have severely impaired access to SI epithelium. The key role played by the of the expression of gut homing molecules on T cells is demonstrated by a decreased ability to generate oral tolerance in CCR9 or β7 deficient mice (Cassani et al., 2011; Wagner et al., 1996), although other groups have found that CCR9 deficient animals may generate normal oral tolerance (A. Mowat, personal communication).

The ability to cause the retention or upregulation of CCR9 and α4β7 is mediated by MLN-derived $CD103^+$ DCs. Conversely $CD103^-$ DCs from MLN failed to induce CCR9 expression on T cells (Johansson-Lindbom et al., 2005). However we have shown that $CD103^-$ DCs from intestinal lymph can result in CCR9 expression in responding T cells, although to a lower extent (Cerovic et al., 2012). This property appears to be due to the increased capacity of SI $CD103^+$ DCs to generate RA, which itself is sufficient to induce CCR9 and α4β7 expression on activated T cells (Coombes et al., 2007). Additionally the ability of DCs to induce α4β7 and CCR9 was partially inhibited with the retinal dehydrogenase inhibitor citral (Iwata et al., 2004). RA acts on the heterodimeric retinoic acid receptor (RAR) expressed in T cells, causing the induction of CCR9 and α4β7 expression. This interaction, along with antigen dose, has been shown to influence the expression of CCR9 in T cells (Svensson et al., 2008). The ability to generate gut-tropic α4β7 T cells, however, appears to be less dependent on high levels of RA. Both $CD103^+$ and $CD103^-$ DCs are able to generate similar

numbers of $CD8^+$ T cells expressing $\alpha4\beta7$, although $CD103^+$ DCs were still more efficient that their $CD103^-$ counterparts (Jaensson et al., 2008; Johansson-Lindbom et al., 2005).

Recent work by Haddis *et al*. has shown that, in order to generate effective oral tolerance MLN derived Tregs undergo a secondary expansion upon their arrival to the siLP (Hadis et al., 2011). However, in the presence of cholera toxin (CT) this expansion was abrogated suggesting that intestinal inflammation prevents the generation of a tolerogenic response. The authors showed that in the steady-state the expansion of Tregs in the siLP required CX3CR1, specifically the production of IL-10 from CX3CR1 macrophages in the intestine (Hadis et al., 2011). Similarly, the production of IL-10 in the colon is required to maintain Tregs in the colon (Murai et al., 2009).

1.17.5 Initiation of an Adaptive Immune Response By Dendritic Cells

Despite their ability to induce a tolerogenic response, intestinal DCs retain functional plasticity and can induce the differentiation of effector T cells. There is some evidence showing that TLR stimulation is likely to be responsible for the ability of DCs to switch between generating Tregs and initiating an active immune response, although much further work is required to fully elucidate how this occurs. Upon TLR5 stimulation $CD103^+CD11b^+$ DCs are able to produce IL-23 and stimulate IFN-γ and IL-17 production from responding T cells (Kinnebrew et al., 2012). Similarly, $CD103^+$ DCs from lymph respond to TLR2 stimulation by producing IL-12p40 and IL-6 resulting in IFN-γ producing effector T cells (Cerovic et al., 2012). Intriguingly, $CD103^-$ DCs from the MLN and lymph appear to have a more immunogenic phenotype and prime IFN-γ and IL-17 producing effector T cells in the absence of overt stimulation (Cerovic et al., 2012). Therefore in the absence of TLR stimulation there is a small subset of DCs that retain an immunogenic phenotype.

Recently work has begun to determine the effect of individual DC subsets on the immune response. Depletion of $CD103^+CD11b^+$ DCs results in a reduction of Th17 cells in the siLP, which was dependent upon the ability of $CD103^+CD11b^+$ DCs to produce IL-6 (Lewis et al., 2011; Persson et al., 2013). Furthermore, following

stimulation with the TLR5 ligand flagellin $CD103^+CD11b^+$ DCs can induce the differentiation of IgA-producing B cells, independent of GALT. Furthermore, $CD103^+CD11b^+$ DCs supported the development of antigen specific Th17 cells and Th1 cells following TLR5 stimulation (Uematsu et al., 2006) (Cerovic et al., 2012).

Like other CD8α expressing DCs, $CD103^+CD11b^-$ DCs are able to cross-present antigen and prime effector $CD8^+$ T cells. The ability to cross-present antigen and generate CTL responses against tumours and intracellular pathogens is limited to these $CD8\alpha^+$ DCs. Analogous populations to $CD103^+CD11b^-$ DCs in the rat have been shown to take up apoptotic cells in the LP and transport them to the MLN (Huang et al., 2000). It is likely that $CD103^+CD11b^-$ DCs in the mouse also act to take up apoptotic cells and present this to $CD8^+$ T cells. Previously, we have shown that $CD103^+CD11b^-$ DCs have ALDH activity and are able to induce CCR9 expression in responding T cells. Therefore these $CD103^+CD11b^-$ DCs may contribute to peripheral tolerance by sampling dying cells and generating regulatory T cells in response to self-antigen. Alternatively, $CD103^+CD11b^-$ DCs may take up virally infected cells and communicate this with the MLN. As such, $CD103^+CD11b^-$ DCs express TLR3, TLR7 and TLR9 therefore they are able to respond to microbial challenge. Upon TLR stimulation $CD103^+CD11b^-$ DCs were able to produce IL-12p40, and produce antigen-specific IFN-γ producing CTLs that lead to the development of SI inflammation (Fujimoto et al., 2011) (V. Cerovic, personal communication).

$CD103^-CD11b^+$ DCs are the only subset able to prime the development of IFN-γ and IL-17 producing T cells, even without stimulation. In comparison, $CD103^-CD11b^-$ DCs induce only IL-17 production from $CD4^+$ T cells (Cerovic et al., 2012). However, much further research is required to determine the function of these newly described subsets of intestinal DCs.

1.18 Hypothesis and Aims

Understanding the functions of DCs in the MLN is a vital area of research if DCs are to be targeted by orally-delivered adjuvants, the details of how they influence immune responses must be determined. Recent findings regarding $CD103^+$ and $CD103^-$ DCs have revealed much about their phenotype and function. However, there are still fundamental gaps in the understanding of the roles played by intestinal DC subsets *in vivo*.

I sought to determine the anatomical origins of the DCs that migrate to the MLN, including all the recently described migratory DC subsets in the intestine. I hypothesised there would be differences in the endpoint of migration of DCs between the SI and colon, and that DC might migrate to the MLN from both the siLP and GALT. Using an array of surgical and labelling techniques, and mouse models, I was able to test these hypotheses and provide an up to date analysis of the origins of each of the DC subsets in the intestine.

In the first results chapter, Chapter 3, I sought to compare the migration of DCs from the SI and colon to the MLN. Most current research examines the entire MLN, as a reflection of both the SI and colon. However, as these organs are physically and functionally different, and contain distinct cell populations, I hypothesised that there would be significant differences in the lymphatic drainage of DCs to different areas of the MLN. In Chapter 4 I aimed to describe the contribution of DCs from SI-associated lymphoid tissue to total DC migration. Two mouse models were employed and compared. One lacked both PPs and ILFs and the other lacked only PPs, I suggest there would be differences in the composition of DC subsets between the two mouse models. In Chapter 5 I intended to determine if DCs can migrate from PPs to the MLN, using two labelling techniques. The question of whether DCs migrate from PPs and ILFs to the MLN has been a long-standing area of controversy, but based upon previous research I postulated that DCs were able to migrate from PPs to the MLN (Macpherson and Uhr, 2004). By performing this set of experiments I hoped to determine the routes of migration of DCs from the SI, SI-associated lymphoid tissues, and the colon to the MLN. This will provide new insights into DC biology

in the intestine, and is essential to determine the potential for targeting these cells to regulate mucosal immune responses.

Chapter 2: Materials and Methods

2.1 Animals

Mice were maintained under specific pathogen free (SPF) conditions at the Central Research Facility (CRF) located at the University of Glasgow or at the Central Animal Facility at the Hannover Medical School. Mice were used between 6 and 20 weeks, unless otherwise stated. C57Bl/6 mice were obtained from Harlan (Bicester, Oxfordshire/University of Glasgow), or from Charles River (Koln, Sulzfeld/Hannover Medical School). Table 1 outlines mouse strains used throughout these studies. All strains were on the C57Bl/6 background. Procedures were performed in accordance with UK Home Office Regulations (University of Glasgow), or in accordance with institutional guidelines and were approved by the institutional review board of the Hannover Medical School.

Table 2-1 Details of Mouse Strains

Strain	Source
C57Bl/6 (B6, CD45.2$^+$)	Harlan, Charles River
C57Bl/6.SJL (CD45.1$^+$; Ly5.1$^+$)	Kindly provided by Prof. Allan Mowat (University of Glasgow)
CB57Bl/6 (CD45.1$^+$/CD45.2$^+$)	Generated by crossing C57Bl/6 mice with C57Bl/6.SJL
OT-I (CD45.2$^+$) **C57Bl/6-Tg(TcraTcrb)1100Mjb/J**	Kindly provided by Prof. Allan Mowat (University of Glasgow)(Hogquist et al., 1995)
OT-I (CD45.1$^+$)	Generated by crossing OT-I CD45.2$^+$ mice with C57Bl/6.SJL
OT-I (CD45.1$^+$/CD45.2$^+$)	Generated by crossing OT-I CD45.2$^+$ mice with C57Bl/6.SJL
OT-II (CD45.2$^+$) **B6.Cg-Tg(TcraTcrb)425Cbn/J**	Kindly provided by Prof. Allan Mowat (University of Glasgow)(Barnden et al., 1998)
OT-II (CD45.1$^+$/CD45.2$^+$)	Generated by crossing OT-II CD45.2$^+$ mice with C57Bl/6.SJL
OT-II (CD45.1$^+$)	Generated by crossing OT-II CD45.2$^+$ mice with C57Bl/6.SJL
Kaede (CD45.2$^+$) **Tg(CAG-KikGR)33Hadj/J**	Kindly provided by Prof. James Brewer and Prof Paul Garside (University of Glasgow)(Tomura et al., 2008)
CX3CR1$^{gfp/gfp}$ **(B6.129P-Cx3CR1$^{tm1Litt/J}$)**	Kindly provided by Prof. Allan Mowat (University of Glasgow) (Jung et al., 2000)
RORγt$^{neo/neo}$CD3$\varepsilon^{-/-}$	Kindly provided by Prof. Peter Lane (University of Birmingham)(Sun et al., 2000)
CD3$\varepsilon^{-/-}$	Kindly provided by Prof. Peter Lane (University of Birmingham)(Wang et al., 1994)
CCR7$^{-/-}$ **B6.129P2(C)-Ccr7^{tm1Rfor}/J**	Kindly provided by Dr Oliver Pabst (Hannover Medical School)(Forster et al., 1999)
EDG3$^{-/-}$	Kindly provided by Dr Oliver Pabst (Hannover Medical School)(Kono et al., 2004)
232-4 **IFABP-tOVA**	Kindly provided by Prof. Leo Lefrancois (University of Connecticut)(Vezys et al., 2000)

Generation of Peyer's Patch Free Mice

HEK293 cells stably transfected with LTβR-Ig were obtained from Dr Oliver Pabst at the Hannover Medical School. These cells were cultured in Dulbecco's Modified Eagle Medium (DMEM, Life Technologies, CA, USA) supplemented with 5% ultra low IgG foetal calf serum (FCS, Gibco, Life Technologies) and 1% penicillin/streptomycin (Gibco) in a cell culture incubator at 37°C with 5% CO_2 in a tissue culture flask with a surface area of 175 cm^2 (Corning, Sigma-Aldrich, Poole, UK). Cells were passaged twice a week once they were confluent. Media was removed and cells were washed with PBS (Gibco, Life Technologies). Cells were detached from the tissue culture flask by treatment with 4mls 0.25% trypsin and 0.5 mM Ethylenediamineteraacetic acid (EDTA) (Life Technologies) for 1 minute, before adding 10ml DMEM (Life Technologies) supplemented with 5% FCS (Gibco) and 1% penicillin/streptomycin (Gibco). Cells were collected, centrifuged at 400g for 5 minutes and resuspended in DMEM supplemented with 5% ultra low IgG FCS (both Gibco) and dilutions of 1/5 to 1/10 were passaged into new tissue culture flasks (Corning). Supernatants were then sterilised by passing them through a 0.2μm cell filter (Corning).

The LTβR-Ig was purified from the supernatants of cell cultures using protein A sepharose columns (Amersham Biosciences, NJ, USA). LTβR-Ig was loaded onto a protein A sepharose column (Amersham Biosciences) containing approximately 2ml of protein A beads (Amersham Biosciences) by running 5-10l of cell culture supernatant through the column. The column was washed with PBS and the loaded protein was eluted by 4ml of 0.1M Citrate, pH 3.5, into a mixture of 700 μl of 0.5 M Na_2HPO_4 and 300μl Tris, pH9.5. The buffer conditions were changed by using gel filtration desalting columns (PD-10 GE Healthcare, Life Sciences, Buckinghamshire, UK) eluting the protein in pure PBS. The protein solution was concentrated by ultra-filtration with Microsep centrifugal devices (PALL Life Sciences, NY, USA) with a 30kDa cut off, centrifuged at 7,500xg. Protein concentration was determined by bicinchonicic acid assay (BCA) protein assay, performed as per manufacturers instructions (Thermo-Fisher Scientific, MA, USA). Briefly, Bovine Serum Albumin (BSA) standards (Thermo-Fisher Scientific) from 0 to 25μg/ml in 0.5 μg/ml steps were prepared and 300μl of the Coomassie Reagent from the BCA (Thermo-Fisher Scientific) was added to the BSA standards

(Thermo-Fisher Scientific) and sample for 10 minutes at room temperature. The absorbance of each of the samples was determined using a plate reader at 595nm. The protein concentration was then determined based upon the standard curve. The integrity of the LTβR-Ig was confirmed using SDS-PAGE. Briefly, samples were loaded onto a Nu-PAGE Bis-Tris Pre-cast gel (Life Technologies) along with a molecular weight ladder (Life Technologies). The sample was run in Nu-PAGE MES SDS running buffer (Life Technologies). The gel was washed in deionised water and the protein was detected by incubation with 20mls SimplyBlue SafeStain (Life Technologies) at room temperature with gentle shaking. The gel was washed again and photographed. To deplete mice of PPs, two intravenous injections of 200 μg of purified LTβR-Ig, into pregnant females at E14 and E16 were performed.

2.2 Surgical Procedures

2.2.1 Mesenteric Lymphadenectomy

The MLNx procedure was adapted from established protocols (Milling and MacPherson, 2010) (Cerovic et al., 2012). Animals underwent anaesthesia via inhalation of isolflurane (Abbot Laboratories Ltd, IL, USA), subsequently shaved and treated with subcutaneous analgesics Carprofen (Rimadyl; Pfizer, NY, USA) and Buprenorphine (Vetergesic; Reckitt Benckiser Healthcare, Berkshire, UK); diluted to dose rates of 0.1ml/100g and 0.15 ml/100g respectively. An abdominal midline incision was made in mice aged 5-6 weeks, and the intestine exposed. During MLNx, all visible MLNs located above the superior mesenteric vein were removed by blunt dissection with the intestine being replaced upon completion. For partial MLNx specific parts of the MLN, which drain either the SI (siMLNx) or colon (coMLNx), were removed and the intestine replaced. The muscle layer was sutured with 6.0 vicryl absorbable sutures (Johnson and Johnson, NJ, USA) and the skin closed using surgical clips (Autoclip Wound Clip System, Harvard Apparatus, MA, USA).

2.2.2 Thoracic Duct Cannulation

5-6 weeks after the MLNx procedure, thoracic duct cannulation (TDC) was performed. Except in RORγtCD3ε deficient mice, as these were already lacking

MLNs therefore MLNx was not performed in these animals. Mice were gavaged with 300μl olive oil (Tesco, Hertfordshire, UK) 30 minutes prior to the procedure to assist lymphatic visualisation. Animals underwent inhalation anaesthesia, as previously described, and an incision of around 2-3cm was made from the xiphisternum towards the spine. A polyurethane cannula (2Fr, Harvard Apparatus) was inserted into the thoracic duct, fixed in place using surgical glue, and exteriorised between the ears. The muscle layer was then stitched, and the skin was held together with surgical glue. The cannula was then fed into a Covance harness (Harvard Apparatus). Pseudo-afferent lymph was collected on ice overnight in PBS supplemented with (25U/ml) Heparin (Wockhardt, Mumbai, India).

2.2.3 Photoconversion of Kaede Mice

Following laparotomy and reflection of the SI onto a sterile swab as described for the MLNx procedure, photoconversion was performed. This technique was adapted from established protocol (Schmidt et al., 2013). For PP photoconversion all visible and accessible PPs were converted. Black card with a density greater than 280 microns (Rymans, Cheshire, UK) was used to cover intestinal tissues and to prevent exposure of the UV light source (405nm UV LED, Amazon, WA, USA) to the surrounding LP. Every accessible PP was exposed to the UV light source for 2 minutes. This process is represented in Figure 2.1. For SI or colon photoconversion, the PPs and any superfluous tissue were protected from UV light using black card (Rymans). 2-3cm sections of SI or colon were exposed to UV light for 2-3 minutes, as depicted in Figure 2.2. The intestine was replaced; the muscle layer sutured and the skin closed using surgical clips as previously described.

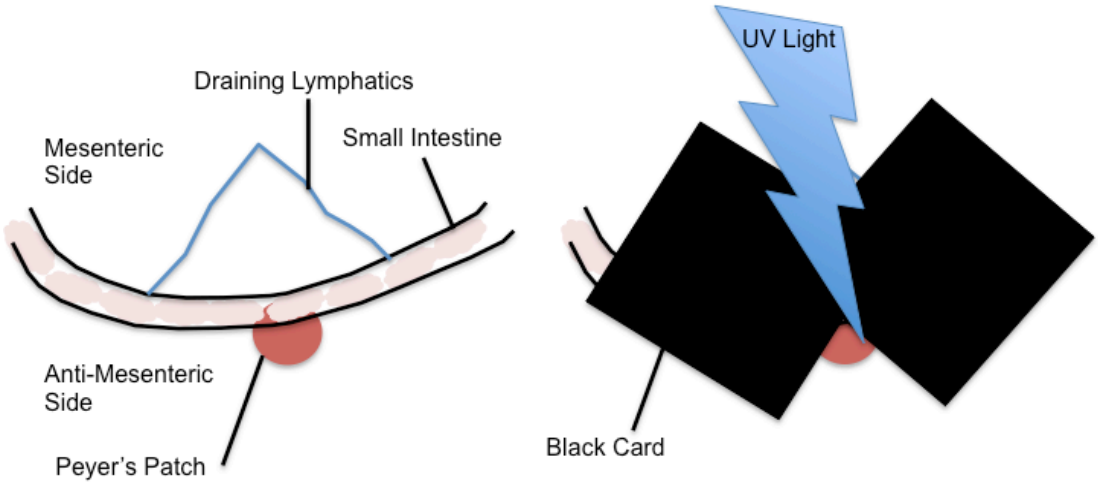

Figure 2-1 Peyer's Patch Photoconversion

Following the induction of anaesthesia via inhalation of isolflurane the intestine was exposed and reflected onto a sterile swab. The intestine was manipulated with cotton swabs to ensure that the Peyer's patch (PP) to be photoconverted was lying at the outermost edge of the small intestine (SI), without any SI underneath the PP. Black card was then placed on top of the SI, and some of the PP, before UV light was shone on the PP for 2 minutes. This process was repeated for every accessible PP in the SI. The intestine was then replaced, the muscle layer stitched, and the wound closed with surgical clips. The animal was then allowed to recover.

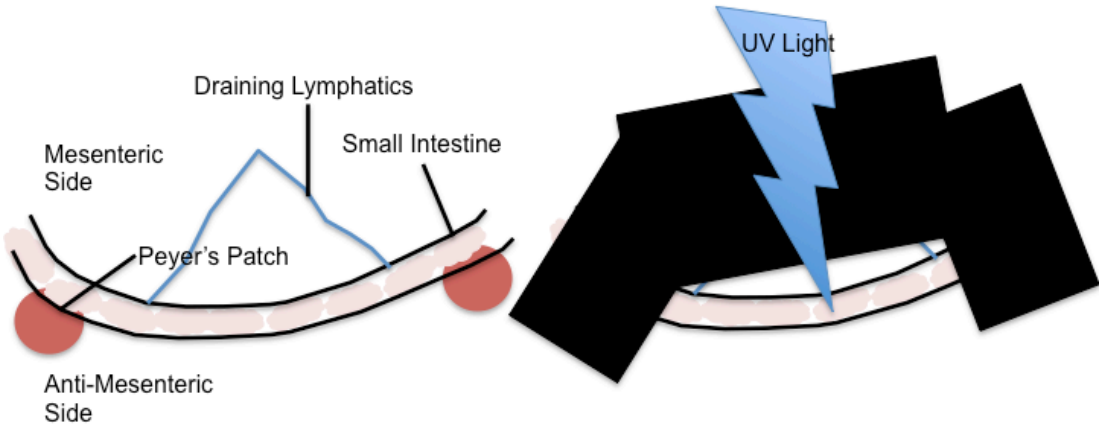

Figure 2-2 Small Intestine Photoconversion

Following the induction of anaesthesia via inhalation of isolflurane the intestine was exposed and reflected onto a sterile swab. The intestine was manipulated with cotton swabs to ensure that the Peyer's patches (PP) were lying at the outermost edge of the small intestine (SI). Black card was then placed on top of the PPs, mesentery and colon before UV light was shone on the section of the SI for 2-3 minutes. This process was repeated for the length of the SI or colon. The intestine was then replaced, the muscle layer stitched, and the wound closed with surgical clips. The animal was then allowed to recover.

2.2.4 FITC Injections

For the injection of FITC into PPs, mice were first anaesthetised using Ketamine and Rompun (both Bayer Healthcare, Leverkusen, Germany) (100mg/kg and 10mg/kg for Ketamine and Rompun respectively administered by intraperitoneal injection). Laparotomy was performed and intestines reflected onto a sterile swab. 1mg/ml FITC (Sigma Aldrich) was microinjected using a CO_2 powered micro-injector (PLI-100, Harvard Apparatus) into every visible PP. The intestine was replaced, and the muscle layer and skin sutured. Gavage of cholera toxin (CT) (10μg, Sigma Aldrich), R848 (10μg, Sigma Aldrich) or Fingolimod (FTY720) (20μg, LC Laboratories, MA, USA) where appropriate was performed after FITC injection was completed and the animal was recovered.

2.2.5 Subserosal Injections of Evan's Blue

Animals were anaesthetised with Isoflurane as previously described, a midline incision was made and intestines were reflected onto a dampened swab. The intestine was held gently with fine forceps and Evans Blue (2% solution, Sigma Aldrich), up to 30μl per injection site, was injected into the subserosal layer using a Micro-fine syringe (30G, BD Biosciences, NJ, USA).

2.2.6 Swiss Roll Sections of Intestine

Swiss roll sections of intestines were prepared as previously described (Moolenbeek and Ruitenberg, 1981; Pabst et al., 2006). Briefly, mice were anaesthetised using Isoflurane as previously described, 7-8cm sections of intestine were excised, cut longitudinally along the anti-mesenteric axis, intestinal contents were gently removed and a layer of Tissue-Tek O.C.T (Bayer) was applied to the luminal side of the intestine. Sections of intestine were rolled and snap frozen in O.C.T over isopentane (VWR, PA USA) on dry ice. Animals were then sacrificed. Blocks were stored at -80°C until use.

2.3 Reagents

Where indicated, cells were cultured in complete RPMI consisting of: RPMI 1640 medium supplemented with 5% FCS, 2mM L-glutamine, 100U/ml penicillin, 100μg/ml streptomycin and 50μM 2-mercaptoethanol (all Gibco). FACS buffer was used to re-suspend cells for FACS staining, this consisted of PBS supplemented with 2mM EDTA and 1% FCS (all Gibco).

Recombinant human Flt3L (Amgen, Seattle, USA) was injected intraperitoneally at 10μg per mouse per day for 10 days.

2.4 Cell Isolation

2.4.1 Isolation of Thoracic Duct Leukocytes

Lymph collected overnight on ice in PBS and 20U/ml Heparin was passed through a 40-μm-cell strainer (BD Biosciences), and red blood cells (RBCs) were lysed with 3ml ammonium chloride potassium (ACK) lysis buffer (Sigma Aldrich) for 1 minute and lysis was quenched by the addition of 20mls complete RPMI. Cells were washed twice in complete RPMI and stained and analysed by flow cytometry or sorted by fluorescence-activated cell sorter using the FACSAria cell sorter (BD Biosciences).

2.4.2 Isolation of Small Intestine Lamina Propria Cells

To obtain leukocytes from the siLP, I used the established isolation laboratory protocol developed by the laboratory of Prof. Allan Mowat. The SI was excised and washed in Hanks' Balanced Salt Solution (HBSS, Gibco) supplemented with 2% FCS (Gibco), PPs and fat were excised from the tissue. The intestine was cut longitudinally, then further cut into 0.5cm sections. Tissue was shaken vigorously in HBSS/2% FCS and the supernatant was removed by pouring tissue and supernatant through a 50μm Nitex mesh (Cadisch and Sons, London, UK) with the tissue subsequently collected from the top of the mesh. The intestines were incubated twice in HBSS with 2 mM EDTA at 37°C with vigorous shaking for 20 minutes, with the tissue being washed in HBSS between each incubation by removal of the supernatant by pouring onto Nitex mesh and re-collection of the

tissue. Tissue was then digested with 1 mg/ml of Collagenase VIII (Sigma Aldrich) in complete RPMI at 37°C with vigorous shaking until the tissue was fully digested (approximately 15 minutes). Cells were passed through a 100μm filter (BD Biosciences) followed by a 40μm filter (BD Biosciences), washed twice in complete RPMI and kept on ice until use.

2.4.3 Isolation of Colonic Lamina Propria Cells

To obtain leucocytes from the cLP, pieces of colon were soaked in ice cold PBS. After removing all fat and faeces, the colon was opened longitudinally and cut into 0.5 cm sections. Tissue was shaken vigorously in HBSS/2% FCS and the supernatant was removed by pouring tissue and supernatant through a 50μm Nitex mesh (Cadisch and Sons) with the tissue sections subsequently collected from the top of the mesh. The intestines were incubated twice in HBSS with 2 mM EDTA at 37°C with vigorous shaking for 15 minutes, with the tissue being washed in HBSS between each incubation by removal of the supernatant by pouring onto Nitex mesh and re-collection of the tissue. Tissue was digested with 1.25mg/ml collagenase D, 0.85mg/ml collagenase V, 1mg/ml dispase and 30U/ml DNase in complete media for 30-40 minutes while shaking at 37°C. The resulting cell suspension was passed through a 40μm cell strainer (BD Biosciences) and then washed twice in complete RPMI. Cells were kept on ice until use.

2.4.4 Isolation of Lymph Node and Spleen Cells

LN and spleens were collected from mice and excess fat was removed. To obtain DCs, samples were collected in serum free RPMI, cut into small pieces, and digested using 50μg/ml of DNase and 0.4WunchUnits/ml of liberase (Roche) for 45 minutes in a shaking incubator at 37°C. After this, cells were passed through a 40μm cell strainer, washed, stained with antibodies and analysed by flow cytometry. RBCs in the spleen preparations were lysed by incubation with 5mls RBC lysis buffer (Sigma) for 5 minutes. Lysis was quenched with 40ml complete RPMI. To obtain T cells from LN and spleens, tissue was mashed through a 40μm filter (BD Biosciences), which was washed with 10ml complete RPMI. These samples were then treated in a similar manner to samples that had been digested using DNase and liberase.

2.5 Flow Cytometry

Cell surface staining was performed on freshly isolated cells resuspended in FACS buffer (PBS supplemented with 2mM EDTA and 5% FCS). Samples were stained in 12x75mm polystyrene tubes (BD Biosciences) with up to $10x10^6$ cells per 200μl of FACS buffer. Non-specific binding of antibodies to Fc receptors was blocked by the addition of Fc block (anti-CD16/CD32, Biolegend) diluted 1:200 for 10 minutes at 4°C. Required antibodies or isotype controls were then added to samples for 30 minutes at 4°C. Cells were then washed twice in FACS buffer. Where a biotin-conjugated antibody was used, cells were washed with FACS buffer, and further stained with a streptavidin-fluorochrome conjugate for 15 minutes at 4°C, and washed again before analysis. For a full list of antibodies see Table 2.2. To determine proportions of live and dead cells 20μl of 7-aminoactinomycin D (7AAD, Biolegend) was added to samples just prior to analysis. Alternatively, 1μl of fixable viability dye eFluor 780 (eBioscience) was added to samples in 1ml of azide and FCS free PBS for 30 minutes at 4°C prior to staining with antibodies. Samples were washed in FACS buffer and stained with antibodies as outlined above. All samples were acquired using either MACS Quant analyser (Miltenyi), or an LSR II (BD Biosciences), or sorted and analysed using the BD FACS Aria (BD Biosciences). All data analysis was carried out using FlowJo software (Tree Star).

Cells were prepared for sorting as described for flow cytometry analysis but under sterile conditions. When sorting DC subsets, cells were kept at all times in complete RPMI on ice. Cells were kept in complete RPMI for the entire duration of the sort, and they were sorted into complete RPMI.

Table 2-2 List of Antibodies

Antibody	Clone	Isotype	Source
CD3	17A2	Rat IgG2b	Biolegend
CD4	GK1.5	Rat IgG2b	Biolegend
CD8α	53-6.7	Rat IgG2a	Biolegend
CD11b	M1/70	Rat IgG2b	Biolegend
CD11c	N418	Hamster IgG	Biolegend
CD19	1D3	Rat IgG2a	Biolegend
CD45	30-F11	Rat IgG2b	Biolegend
CD45.1	A20	Rat IgG2a	Biolegend
CD45.2	104	Rat IgG2a	Biolegend
CD45R	M5/114.15.2	Rat IgG2b	Biolegend
CD64	X54-5/7.1	Mouse IgG1	Biolegend
CD80	16-10A1	Hamster IgG	BD Biosciences
CD86	GL1	Rat IgG2a	BD Biosciences
CD172a	P84	Rat IgG1	Biolegend
CD199 (CCR9)	9B1	Rat IgG2a	Biolegend
F4/80	BM8	Rat IgG2a	Biolegend
MHCII	M5/11.4.15.2	Rat IgG2b	Biolegend/ eBioscience
TCRVα2	B20.1	Rat IgG2a	Biolegend
Ly6C	HK1.4	Rat IgG2c	Biolegend
PDCA-1	129c	Rat IgG2b	eBioscience

2.6 Induction of DSS Colitis

An established protocol was used to induce colitis; mice received 2% dextran sodium sulphate (DSS) salt (reagent grade; MW 6,000-50,000kDa; MP Biomedicals Ohio, USA), in sterile drinking water for three days. Mice were monitored daily for weight change, rectal bleeding and diarrhoea. Mice that lost >20% of their initial bodyweight were sacrificed immediately in accordance with Home Office regulations. Some groups of mice were returned to normal drinking water following three days of the addition of DSS to drinking water to assess the recovery phase of disease. Mice were continually monitored daily for weight change, rectal bleeding and diarrhoea.

2.7 Adoptive Transfers

T cells were isolated from the spleen and MLN of donor OT-II CD45.1$^+$ mice or OT-I CD45.1$^+$/CD45.2$^+$ mice as previously described. Donor cells were labelled with 5μM Carboxyfluorescein succinimidyl ester (CFSE, Life Technologies) for 15 minutes at 37°C (Invitrogen). 5x10^6 CFSE-labelled donor cells were injected intravenously into congenic recipient mice in 100μl sterile PBS. 24 hours later the animal was gavaged with 10 mg of OVA protein. Proliferation was assessed by CFSE dilution by flow cytometry.

2.7.1 Proliferation Assay

To assess the ability of DC to prime naïve T cells, populations of DCs were FACS-purified from the lymph or MLN and described above and co-cultured with FACS-purified naïve (CD62L$^+$) CD4$^+$ or CD8$^+$ T cells of OT-II or OT-I mice respectively. Prior to co-culture, T cells were labelled with 5μM CFSE (Life Technologies) for 3 minutes before washing in complete RPMI. DC populations, except for DCs from 232-4 mice, were pulsed with 2mg/ml OVA protein for 2 hours, washed twice in complete RPMI and then co-cultured at varying ratios with 100,000 T cells for 3-4 days at 37°C with 5% CO_2. Following co-culture samples were stained with antibodies as described above. Samples were analysed by FACS and T cell proliferation was determined by CFSE dilution.

2.8 Generation of Bone Marrow Dendritic Cells

BM cells were isolated by flushing tibias and femurs from mice with complete RPMI, using a 26G needle attached to a 20 ml syringe. Cells were centrifuged at 380g for 5 minutes and the supernatant discarded. RBCs were lysed by resuspending the pellet in 3 mls RBC lysis buffer (Sigma) for 5 minutes. 40mls of complete RPMI was added and cells were centrifuged at 380 g for 5 minutes, the supernatant was discarded and cells were resuspended in 10mls of complete media. An aliquot of live cells was counted and cells were plated out in a 6 well plate at $1x10^7$ cells/well in the presence of 10% Flt3L-containing supernatant from CHO Flt3L cells. Cells were cultured at 37°C at 5% CO_2 for 7-9 days.

Mouse Flt3L transfected Chinese hamster ovary (CHO) cells were grown in flasks in $ProCHO_4$ media (Lonza, Basel, Switzerland) supplemented with 1x ProHT (Lonza), 2 mM L-glutamin, 100 U/ml penicillin and 100 µg/ml streptomycin (all Invitrogen) until confluence was achieved. Supernatant was harvested from the flasks, and filtered through a 0.2 µM filter (Millipore). The filtered supernatant was aliquoted and placed at -20°C until use.

For photoconversion studies, after 7 days of culture with FLt3L, BMDCs were harvested and spun down. The pellet was photoconverted for two minutes before being resuspended in 5mls of complete media and being returned to a flat-bottomed 6-well plate. 24 hours later cells were assessed by flow cytometry.

2.9 Preparation of Blood and Tissue Samples

Tail samples were prepared for PCR using the DNeasy blood and tissue kit (Qiagen) as per the manufacture's guidelines. Tail samples were digested overnight at 56°C with Proteinase K. DNA was purified by binding to the spin column membrane provided, washing and eluting in the elution buffer supplied. Samples of genomic DNA were stored at -20°C until use. Blood samples were incubated with 5mls RBC lysis buffer (Sigma) for 5 minutes at room temperature. Adding 40mls PBS subsequently quenched lysis. The sample was centrifuged at 380 g for 5 minutes and the pellet resuspended in 200µl PBS supplemented with 2% FCS. Cells from the blood sample were then labelled for FACS.

2.10 Polymerase Chain Reaction

RORγt$^{neo/neo}$CD3ε$^{-/-}$ and CD3ε$^{-/-}$ mice were genotyped before use for breeding. Genomic DNA was isolated from tail tips and was diluted by 50% prior to use in all polymerase chain reaction (PCR). Primers for the amplification of RORγt and neomycin were designed from the published murine RORγt and neomycin sequences using Primer-BLAST, the online primer design software. The sequences of the primers used are shown in Table 2.3. All PCR primers were synthesised by Integrated DNA Technologies. PCR reactions were performed in 25μl volumes using the Go-Taq PCR mix (Promega, WI, USA). Each PCR mix contained genomic DNA, 100nM primers (Integrated DNA Technologies, IA, USA), 0.2mM dNTPs, 5U/μl Go Taq polymerase, 5X reaction buffer and nuclease free water (all Life Technologies). The optimal annealing temperature of each primer was determined using an online biomath calculator for determining the Tm of oligomer (Table 2.3). Cycling parameters were: 95°C for 1 minute followed by annealing at the optimal annealing temperature (Table 2.3) for 30 seconds and elongation for 30 seconds at 72°C for 35 cycles. The PCR products were visualised by gel electrophoresis on a 1% agarose gel (Sigma-Aldrich) in 1X TAE with 2μl ethidium bromide (Life Technologies) per 100 ml gel. 10μl of the PCR reaction with 2μl of 6X loading dye (Life Technologies) were loaded into the gel along with 5μl DNA ladder (Life Technolgies) and 1μl 6X loading dye. Gels were run in 1X TAE buffer for approximately 1 hour, or until bands had reached the bottom of the gel, at 100mV. Gels were visualised by UV transillumination.

Table 2-3 List of Primer Sequences For Genotyping

Product	Forward Primer (5'-3')	Reverse Primer (5'-3')	Optimal Annealing Temperature
RORγt	ACAGAGACACCACCGGACATCT	TCGCTCCTACCTCACCGCTTT	52°C
Neomycin	AGCACTACTCGGAATGGAAG	AATATCACGGGTAGCCAACG	48°C

2.11 Immunohistochemical Labelling of Slides

Cryosections were cut at 8μm from blocks that had been snap frozen and kept in the -80°C using a cryotome (Thermo Electon Corporation, MA, USA) and mounted on slides which were stored at -80°C until use. For immunohistochemical labelling of slides, slides were fixed in ice-cold acetone for 10 minutes. The slides were allowed to air dry for 10 minutes before being rehydrated in PBS for 10 minutes. To prevent non-specific staining sections were blocked in PBS (Gibco) with 1% FCS (Gibco) for 15 minutes then washed in PBS for 10 minutes. To block endogenous biotin on sections an Avidin/Biotin blocking kit (Vector Laboratories, CA, USA) was applied to sections. Breifly, sections were blocked for 15 minutes with Avidin (Vector), washed in PBS (Gibco) for 10 minutes and blocked for a further 15 minutes with biotin (Vector). Slides were washed again in PBS for 10 minutes. Sections were then stained with 400-600 μl biotinylated anti-B220 diluted 1:200 or isotype control in PBS (Gibco) for at least 30 minutes at 4°C. Binding was detected using streptavidin Alexa Fluor 647 (BD Biosciences), diluted 1:200 in PBS (Gibco) for at least 30 minutes at 4°C in the dark. Slides were washed twice in PBS (Gibco) and allowed to dry before Vectasheild mounting medium with DAPI (Vector) was applied to sections and a coverslip placed on top. Sections were examined on an epifluorescence microscope (Imager Z.1, Carl Zeiss, Herts, UK) using AxioVision software (version 4.7).

2.12 Statistical Analysis

For comparison of means between two groups, data were analysed using a Student's *t*-test. For comparisons involving more than two data sets, a one way analysis of variance (ANOVA) was used with a Bonferroni post test. For multiple data sets with independent variables a two way ANOVA was used, with a Bonferroni post test to compare selected data sets. P-values <0.05 were considered significant. All statistical analysis was performed using Graphpad Prism (Graphpad).

Chapter 3: Comparison of Dendritic Cell Migration in the Small Intestine and Colon

The SI and colon are vastly different environments. Functionally, the SI is specialised for the uptake of food while the colon acts largely to reabsorb water. There is also a vast difference between the microbial load in the SI and colon, with up to 10, 000 times more bacteria present in the colon compared to the ileum (Hooper and Macpherson, 2010). Furthermore, diseases affecting each area vary; inflammatory bowel diseases mostly affect the colon, ulcerative colitis affects only the colon, and Crohn's Disease affects the colon and the terminal ileum.

Another specific difference between the SI and colon is in the type of immune responses induced in each area. For example the tolerance induced in the SI to food proteins generates both a local and a systemic response, while in the colon there is no systemic response to bacteria, meaning the immune system is only acting locally (Pabst and Mowat, 2012).

The MLN forms the largest group of lymph nodes in the body; they are not only the key site for induction of oral tolerance but also preserve systemic ignorance to intestinal commensal bacteria. Lymphatic drainage from the intestine was first examined over 50 years ago (Carter and Collins, 1974; Tilney N, 1971); it was suggested that afferent lymphatic vessels from different areas of the intestine drained to distinct parts of the MLN. These early findings describe only the lymphatic drainage and movement of lymphocytes; DCs had not yet been identified.

Due to differences between the SI and colon it is likely that the DC populations migrating from each area are different. However, much previous work has failed to make this distinction and has examined the whole MLN to understand the immune environment in both the SI and the colon (Cerovic et al., 2012; Laffont et al., 2010). An up to date investigation of lymphatic drainage is essential to

fully elucidate which nodes of the MLN drain lymph from the SI and colon, and to understand differences between DCs migrating from each of these tissues.

Practical difficulties make cells in the intestine difficult to label and track over extended periods of time, and enzymatic isolation of DCs from the intestine may affect their functions (Milling et al., 2010). Furthermore, there are challenges in elucidating the roles intestinal DCs and macrophages due to an overlap of phenotypic and functional features (Rivollier et al., 2012) (Bain et al., 2013) (Schulz et al., 2009) (Cerovic et al., 2012). Recent technical advances now enable us to investigate the anatomical segregation between the SI and colon, in the context of recent studies that describe four functionally distinct subsets of DCs (Cerovic et al., 2012).

3.1 Results

3.1.1 Identification of Small Intestinal and Colonic Draining Mesenteric Lymph Nodes

Due to differences in the primary function, immune responses, associated immune organs, diseases, and cell populations between the SI and colon it is likely that the type of DC migrating from each area will be different. Therefore, to investigate these differences in DC populations, it is essential to understand the anatomical details of the lymphatic drainage from the SI and colon.

To identify which part of the intestine supplies lymph to each of the nodes of the MLN chain, we examined the lymphatic drainage from the SI and colon. To achieve this, Evans blue dye was injected into the subserosal layer of either the SI or the colon of live anaesthetised mice. This allowed direct examination of the intestinal afferent lymphatic system and the draining MLNs. Five minutes after injection of dye into the SI, the draining afferent lymphatics and the three central LNs of the MLN chain stained blue and the afferent lymphatics were blue showing the draining lymphatics (Figure 3.1 B), compared to the control animal which did not contain any Evans blue dye (Figure 3.1 A). This identified these LNs as the SI draining LNs, the siMLNs. When Evans blue was injected subserosally into the proximal colon, the dye first reached the MLN located directly adjacent to the caecum (Figure 3.1 C). A second MLN also stained blue

following injection of dye into the proximal colon. This second colon-draining MLN was at the opposite end of the main MLN chain (Figure 3.1 C). Following Evans blue injection into the distal colon, the first MLN to stain blue was the lymph node located adjacent to the abdominal aorta (Figure 3.1 D). Together, these three nodes, at opposite ends of the MLN chain, adjacent to the caecum and the abdominal aorta, will be referred to as colonic MLN, coMLN. These draining MLNs are depicted in Figure 3.1 E.

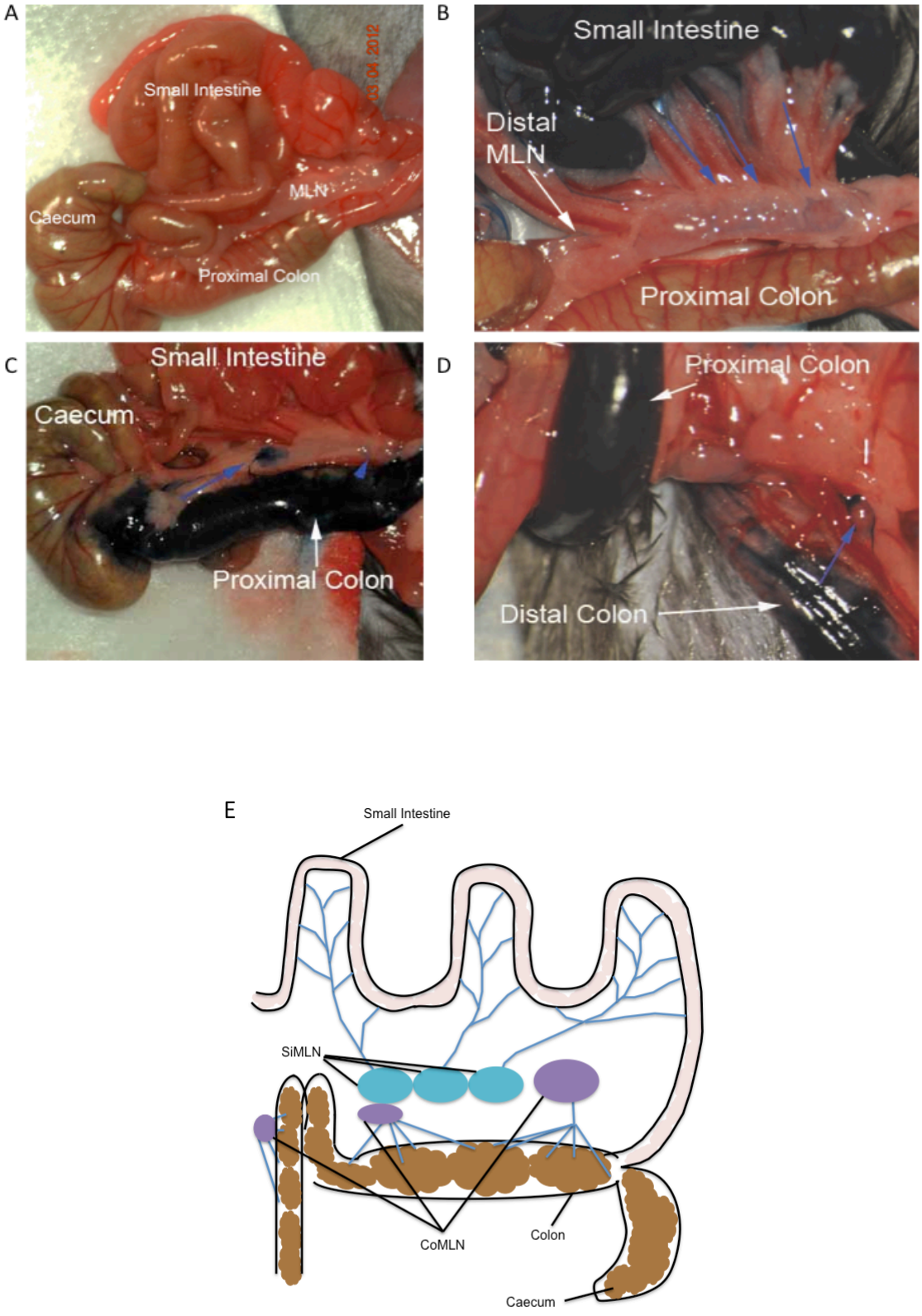

Figure 3-1 Subserosal Injection of Evans Blue Distinguishes Distinct Parts of the MLN Drain the Small Intestine and Colon.

The SI and colon of mice under terminal anaesthesia were visualised. Control mice that were not injected (A) or mice injected with Evans blue dye into the subserosal layer of the SI (B), proximal colon (C) and distal colon (D). 5 to 10 minutes after subserosal injection draining MLNs and the SI and colon were visualised and photographed. Blue Arrows indicate direction of lymph flow. Pictures represent 5-6 individual animals. Diagram depicting draining MLNs is shown in E, SI draining MLN (siMLN) are shown in blue and colonic draining MLN (coMLN) are shown in purple.

The coMLN and siMLN reproducibly acquired Evans blue after subserosal injection of the dye into the colon or SI. This indicated that these MLNs are each responsible for draining lymph from different regions of the intestine. As antigen is carried to the MLN by DCs, which then drive differentiation of antigen-specific naïve T cells, we next sought to identify the route of migration of DCs from the SI and colon to the MLN. In order to precisely observe the migration of DCs to specific regions of the MLN we used transgenic mice that constitutively express the photoconvertible kaede protein (Tomura et al., 2008).

Exposure of kaede to UV light induces a specific peptide cleavage and subsequent formation of a double bond within the kaede chromophore that changes its excitation and emission wavelengths. This results in a permanent change in the structure of the protein, resulting in the permanent labelling of these cells (kaede-red^{+} cells). However, cell proliferation can dilute the of photoconverted kaede with non-photoconverted kaede protein (kaede-green^{+} cells). Transgenic mice carry kaede cDNA under the CAG promoter; this results in the expression of kaede in all cells, with no abnormality in their growth and reproduction. The expression of kaede, combined with the photoconversion technique, has no effect upon the homing capacity of lymphocytes (Tomura et al., 2008).

Therefore, kaede mice were used here to investigate DC migration from the SI and colon to the MLN. After laparotomy, all accessible parts of the SI were exposed to low intensity UV light for two to three minutes. The PPs, MLN and the colon were not exposed to UV light. The siMLN and coMLN were examined 24 and 48 hours after exposure of kaede SI to UV light. Briefly, separate parts of the MLN were removed and enzymatically digested. Cells were stained with antibodies for flow cytometry and analysed. The gating strategy was consistent throughout the experiment. First large cells were gated, and live and B220^{-} cells were selected. Single, F4/80^{-} cells were further selected and MHCII^{hi}CD11c^{+} migratory DCs were gated (Figure 3.2 A). Previous reports have suggested that migratory DCs fall into the MHCII^{hi}CD11c^{+} group, while blood-derived DCs are MHCII^{+}CD11c^{hi} (Lambrecht et al., 1998). The expression of kaede-red^{+} on DCs was then observed (Figure 3.2 B) and compared to non-photoconverted MLNs (Figure 3.2 C). 24 hours after exposure of the SI to UV light, significantly more

photoconverted kaede-red^{+} DCs were present in the siMLN than in the coMLN after 24 hours (Figure 3.2 D and E). There were also significantly more kaede-red^{+} DCs in the siMLN compared to the coMLN after 48 hours (Figure 3.2 D) The percentage, but not number, of migratory DCs in the siMLN was decreased after 48 hours (Figure 3.2 D and E).

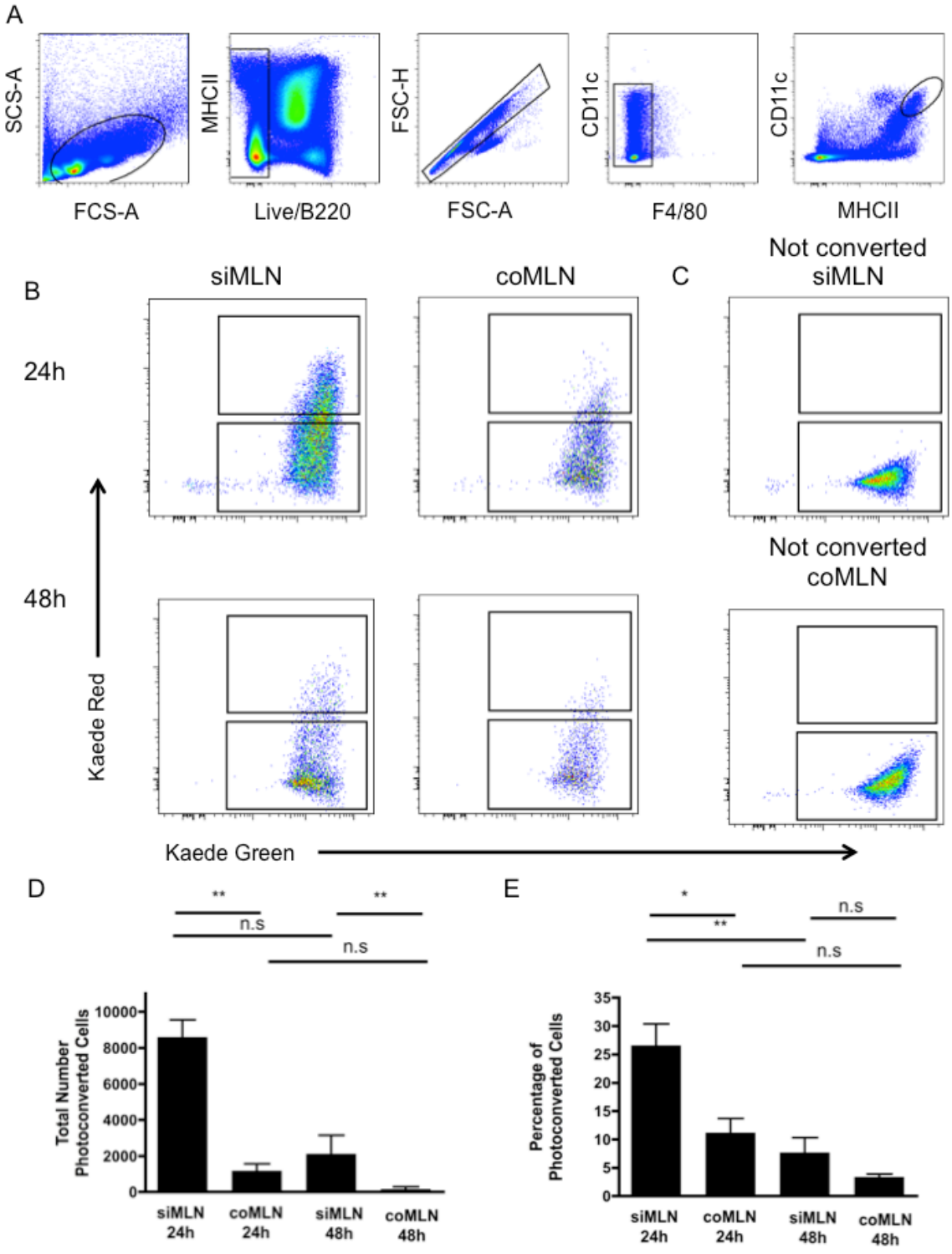

Figure 3-2 DCs Originating in the Small Intestine Drain to Specific Parts of the MLN.

The SI of photoconvertable kaede mice were exposed to UV light for 2-3 minutes, avoiding PP, and animals allowed to recover. The siMLN and coMLN were removed digested separately and stained for flow cytometry 24 hours and 48 hours later. Migratory DCs were gated as large, live, $B220^{-}$, single, $F4/80^{-}$, $CD11c^{+}MHCII^{hi}$ cells (A) and the number of photoconverted migratory DCs was observed (B). Gates for photoconverted cells were drawn based upon a non-converted control (C). Number and percentage of photoconverted DCs was compared between the siMLN and coMLN (D and E respectively). Results are representative of two separate experiments with similar results. A Two-Way ANOVA was performed and a Bonferroni posttest applied showing a significant difference between the siMLN and coMLN. Data are means and S.E.M, n=4, not significant (n.s), *$p<0.05$, ** $p<0.01$.

These data show that DCs from the SI preferentially drain to the siMLN. Next, DCs migrating from the colon were investigated. In this experiment, the colon was exposed to UV light for 2-3 minutes and the MLN and entire SI were protected from light. As before, the siMLN and coMLN were removed and digested 24 and 48 hours after exposure of the colon to UV light. The gating strategy was as follows; large, live, $B220^-$, single, $F4/80^-$ cells were selected and migratory DCs were gated ($MHCII^{hi}CD11c^+$) (Figure 3.3 A). The expression of kaede-red^+ in the migratory DCs was then investigated (Figure 3.3 B) and compared to the non-converted MLN (Figure 3.3 C).

24 hours after the exposure of the colon to UV light, significantly more kaede-red^+ cells were found in the coMLNs than in the siMLN. This result was mirrored after 48 hours, with there being significantly more kaede-red^+ cells present in the coMLNs than in the siMLNs (Figure 3.3 D and E). Therefore, as indicated by the data from the Evans blue experiments, DCs that originate in the SI drain to the centremost MLNs, while DCs that originate in the colon drain the specific MLN we describe here as coMLN.

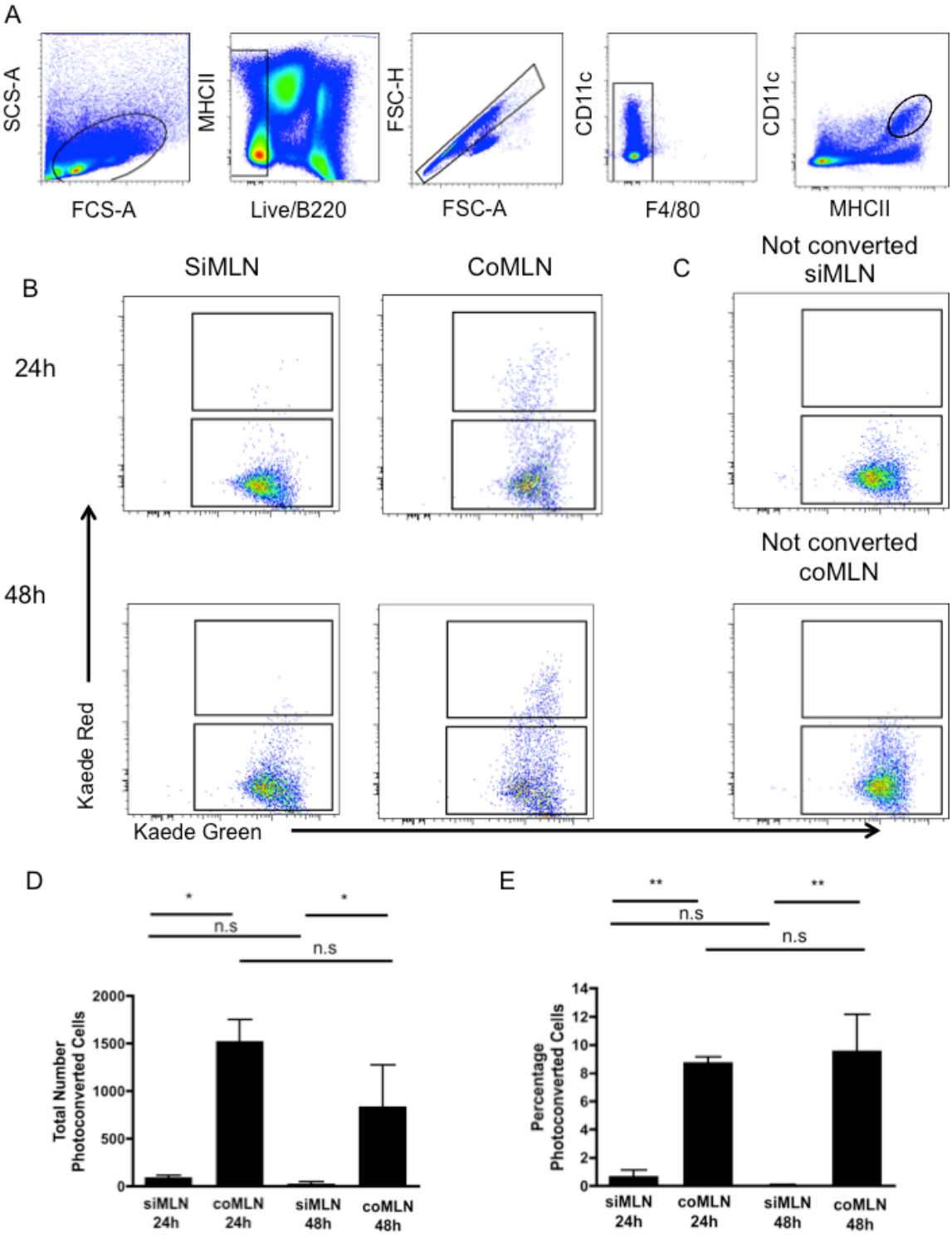

Figure 3-3 Dendritic Cells Originating in the Colon Drain to Specific Nodes of the MLN.

The colon of photoconvertable kaede mice was exposed to UV light for 2-3 minutes and animals allowed to recover. The siMLN and coMLN were removed digested separately and stained for flow cytometry 24 hours and 48 hours later. Migratory DCs were gated as large, live, $B220^{-}$, single, $F4/80^{-}$, $CD11c^{+}MHCII^{hi}$ cells (A) and the number of photoconverted migratory DCs was observed (B). Gates for photoconverted cells were drawn based upon a non-converted control (C). Number and percentage of photoconverted DCs was compared between the siMLN and coMLN (D and E respectively). Results are representative of two separate experiments with similar results. A Two-Way ANOVA was performed and a Bonferroni posttest applied showing a significant difference between the siMLN and coMLN. Data are means and S.E.M, n=4, not significant (n.s), *$p<0.05$, ** $p<0.01$.

3.1.2 Evaluation of Transgenic Kaede Mice to Monitor Dendritic Cell Migration

Previous reports using kaede mice suggest there are no effect of photoconversion upon the activation status of T cells and B cells (Tomura et al., 2008). However, previous work has concentrated upon lymphocytes and the effect of photoconversion upon these cells rather than DCs. Furthermore, the source of low power UV light differs between our experiments and others (Schmidt et al., 2013; Tomura et al., 2008). Therefore it was important to assess the level of activation induced by photoconversion of kaede DCs in our hands. The level of activation of DCs can be assessed by investigating the levels of expression of the co-stimulatory molecules CD80 and CD86 on DCs, which act to provide the necessary accessory signals for T cell activation. In order to perform this experiment, BMDCs were generated by the isolation of BM from the tibias and femurs of kaede mice. BM was cultured for seven days at 37°C with humanised Flt3L, to generate BMDCs (Naik et al., 2005). After seven days, BMDCs were harvested and either untreated, photoconverted, or stimulated with 1μg/ml or 10μg/ml of LPS. DCs were harvested 24 hours later and analysed by flow cytometry. Large live cells were gated and pDCs were removed by gating out $B220^+$ cells. Single cDCs were selected by gating $MHCII^+CD11c^+$ cells (Figure 3.4 A). The presence of kaede red was then analysed upon BMDCs (Figure 3.4 B), and the levels of the costimulatory molecules CD80 and CD86 were investigated on each group (Figures 3.4 C and D respectively). The percentage of $CD80^+$ and $CD86^+$ DCs were compared between DCs from animals that did not undergo photoconversion kaede-$green^+$ DCs, or animals that did undergo photoconversion kaede-red^- DCs and kaede-red^+ DC fractions, and cells stimulated with LPS (Figures 3.4 E and F respectively). This showed that there was a significant increase in the expression of both CD80 and CD86 on DCs that were stimulated with LPS compared with unstimulated cells. DCs that were exposed to UV light did not upregulate the expression of CD80 or CD86. Furthermore, the photoconversion of kaede in kaede-red^+ DCs did not change the expression of CD80 or CD86. Therefore, the photoconversion of cells in kaede mice does not activate DCs.

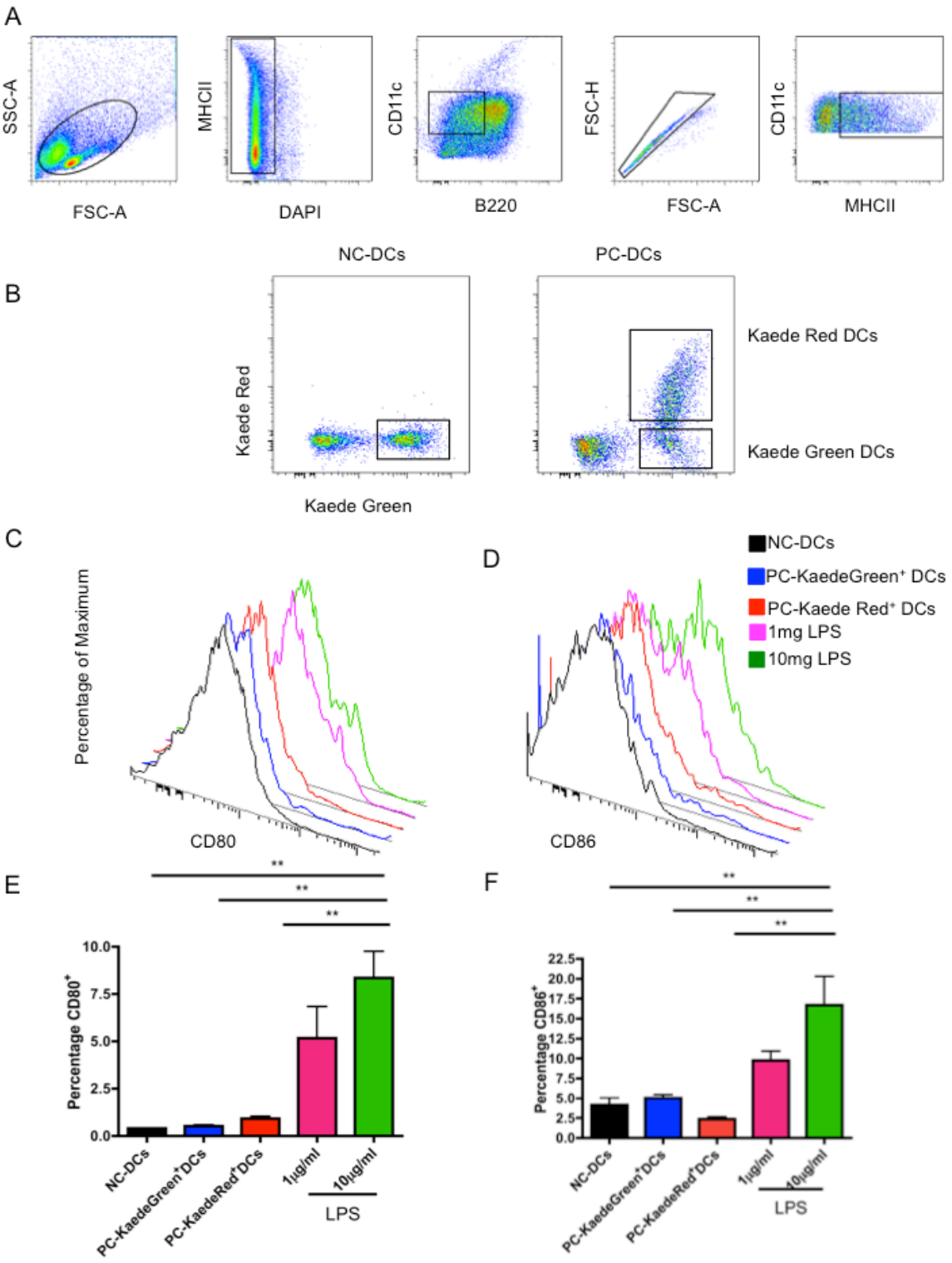

Figure 3-4 Photoconversion of kaede bone marrow derived DCs does not upregulate the expression of CD80 or CD86.

BM was isolated from tibias and femurs of kaede mice, and cultured with Flt3L for 7 days 37. BMDCs were harvested, not converted (NC) photoconverted (PC) or stimulated with 1 µg/ml or 10 µg/ml LPS. Photoconversion was performed on harvested cells in culture media for 2 minutes. All groups were returned to cell culture at 37°C and 24 hours later cells were analysed by flow cytometry. Selecting large, live, $B220^-$ single cells that were also $MHCII^+$ $CD11c^+$ gated DCs (A). The expression of kaede-red was compared on groups (B) and the levels of CD80 (C and E) and CD86 (D and F) were compared for each group. A One-Way ANOVA was performed with a Bonferroni post test, data are means and S.E.M, n=3, *p<0.05 and **p<0.01.

3.1.3 Comparison of Levels of MHCII Expression Upon Migratory and Resident Dendritic Cell Subsets in the Mesenteric Lymph Nodes

These results indicate that the low power UV light we used to switch the kaede cells is unlikely to affect DC activation. The kaede mice therefore appear to be a useful tool to monitor the constitutive DC migration from the intestine. In our previous gating strategy in the MLN we selected MHCII^{hi}CD11c^{+} DCs as migratory DCs. Previous work with lung and dermal DCs has suggested that the MHCII^{hi}CD11c^{+} DCs present in lymph nodes represent a migratory subset of DCs (Kamath et al., 2002). This gating strategy has also been used in the MLN to identify migratory DCs (Persson et al., 2013). However there is no direct evidence that the MHCII^{hi}CD11c^{+} DCs in the MLN have actually migrated from the intestine. Therefore, to confirm the phenotype of the migratory DCs in the MLN, the presence of kaede-red^{+} DCs within the phenotype of the "migratory" MHCII^{hi}CD11c^{+} DC gate was compared with the presence of kaede-red^{+} DCs within the "resident" MHCII^{+}CD11c^{hi} gate. Photoconversion was performed on either the SI or colon. 24 or 48 hours later the siMLN and coMLN were removed, digested, and analysed by flow cytometry. Cells were gated as before, with large, live, B220^{-}, single F4/80^{-} cells were defined as DCs. Migratory MHCII^{hi}CD11c^{+} DCs and resident, blood derived, DCs MHCII^{+}CD11c^{hi} were gated separately (Figure 3.5 A). The presence of kaede-red^{+} DCs amongst migratory and blood derived DCs after SI or colonic photoconversion was observed (Figure 3.5 B) and compared between groups (Figure 3.5 C). In the siMLN there were significantly more kaede-red^{+} DCs in the migratory gate compared to the resident gate 24 and 48 hours after photoconversion of the SI. This was mirrored in the coMLN where significantly more kaede-red^{+} DCs were found in the migratory DC gate compared to the resident DC group after 24 and 48 hours. Therefore, migratory DCs do express MHCII at higher levels than resident DCs, thus supporting the enrichment of migratory DCs based upon their expression of high levels of MHCII. In these experiments, there are no kaede-red^{+} DCs among the resident DCs in the MLN. Thus, all kaede-red^{+} DCs are derived from the intestinal tissue itself; photoconversion of DC precursors in blood vessels overlying intestinal tissue and subsequent migration to the MLN does not contribute the numbers of kaede-red^{+} cells in the MLN.

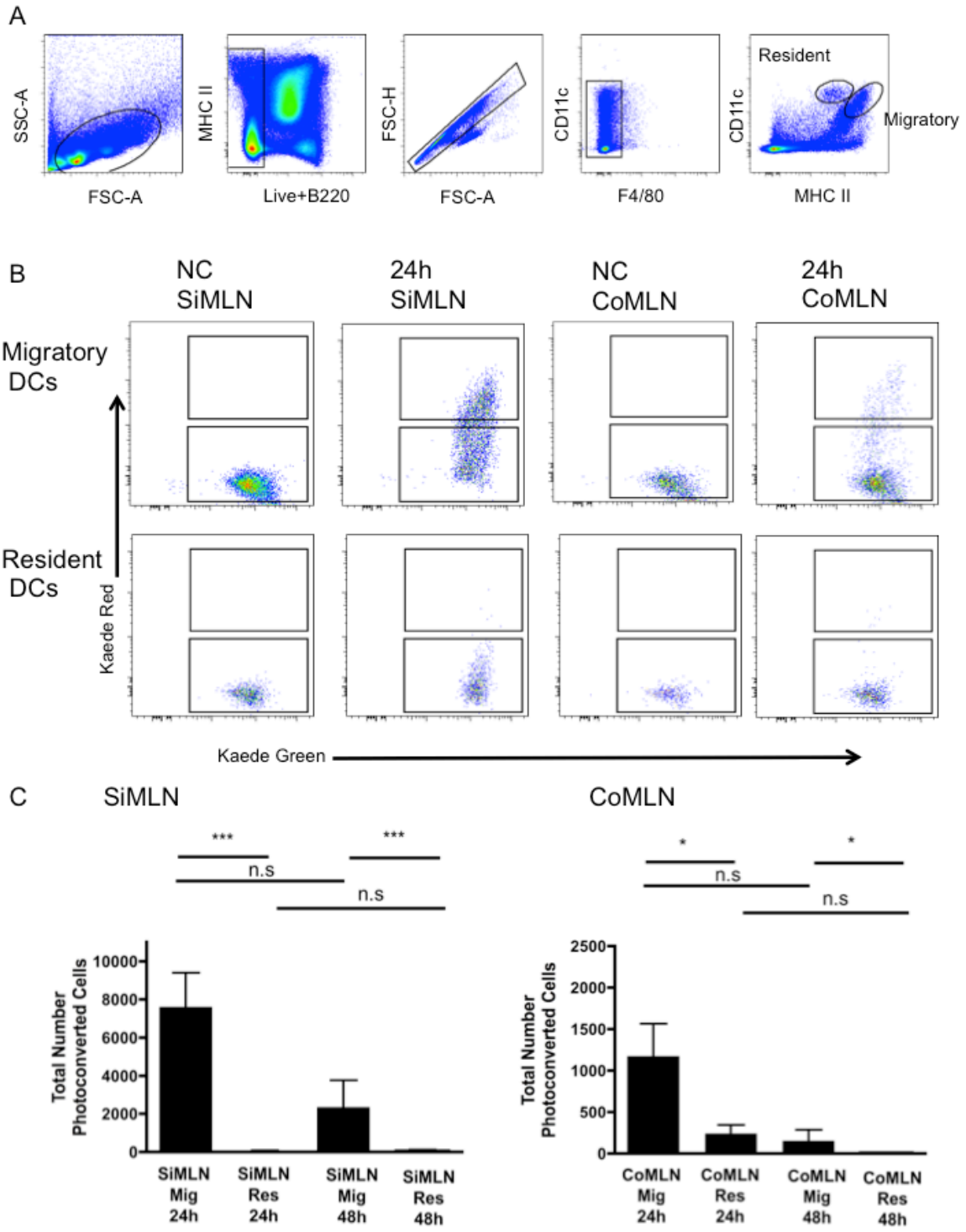

Figure 3-5 Migratory Photoconverted kaede-Red^{+} DCs in the Small intestine and Colon Express Higher Levels of MHCII in the MLN.

The SI and colon of photoconvertable kaede mice were exposed to UV light for 2-3 minutes and animals allowed to recover. The siMLN and coMLN were isolated, digested separately, stained and analysed by flow cytometry 24 and 48 hours after photoconversion. DCs were gated as large, live, B220^{-}, single, F4/80^{-} cells and migratory (Mig) DCs were CD11c^{+}MHCII^{hi} and resident (Res) DCs were gated as CD11c^{+}MHCII^{+} (A). The presence of kaede-red^{+} DCs in photoconverted animals was compared between Mig and Res DCs based and gates were drawn based upon a non-converted control (NC) (B). Total numbers of kaede-red^{+} DCs were compared between Mig and Res DC populations in the SiMLN and CoMLN (C). A Two-Way ANOVA was performed and a Bonferroni posttest applied. Data are means and S.E.M, n=4, not significant (n.s), *p<0.05, *** p<0.001.

3.1.4 Comparison of Dendritic Cell Subsets in the Small Intestine, Colon, Small Intestinal and Colonic Draining Mesenteric Lymph Nodes

As our previous work indicated that there was anatomical segregation between the SI and colonic draining lymph nodes, we sought to determine if there were differences between the DC populations within these lymph nodes. To provide necessary background information, we first examined the DC subsets in the SI and colon, from which the MLN DCs migrate. To examine the SI DCs, the SI was isolated, PPs were removed, the SI was digested and a single cell suspension generated. This was labelled for flow cytometry; large cells were gated, then $CD45^+$ live cells were selected, $F4/80^+$ macrophages were excluded and $MHCII^+$ and $CD11c^+$ single cells were selected (Figure 3.6 A). Four distinct DC subsets were then identified, based upon their expression of CD11b and CD103 (Figure 3.6 B). Our previous work identified four functionally distinct subsets of DCs migrating in pseudo-afferent lymph (Cerovic et al., 2012). Four phenotypically similar subsets were also identified in the small intestinal lamina propria (siLP). The most numerous siLP DC population was the $CD103^+CD11b^+$ subset. The second largest population was the $CD103^+CD11b^-$ that also expressed $CD8\alpha^+$. These two populations have previously been described in the siLP (Fujimoto et al., 2011). There were also two distinct populations of $CD103^-$ DCs in the siLP, the $CD103^-CD11b^+$ and the $CD103^-CD11b^-$ DCs. We showed these populations were genuine migratory DCs, present in pseudo-afferent lymph (Cerovic et al., 2012). There remains significant confusion regarding the precise identification of bona fide $CD103^-$ DC populations in the siLP. However using a macrophage specific markers such as F4/80, combined with data from TDC we are able to definitively identify four distinct DC subsets present in the siLP.

Next, DC populations in the colon were investigated. The colon was removed and a single cell suspension was generated by enzymatic digestion. A similar gating strategy to the SI was performed in order to identify DCs (Figure 3.7 A). This revealed three distinct subsets of DCs based upon the expression of CD103 and CD11b (Figure 3.7 B); these subsets have previously been described in the colonic lamina propria (cLP) and were similar to subsets in the siLP (Rivollier et al., 2012). However, there were some key differences between DC populations in the SI and colon. Firstly, the $CD103^-CD11b^-$ population was reduced in the

colon. This suggests that migratory DCs in the MLN with the $CD103^{-}CD11b^{-}$ phenotype are likely to have originated in the siLP. There are also differences between the SI and colon in the proportions of each subset. In the siLP the $CD103^{+}CD11b^{+}$ DCs were the most numerous, while in the cLP the $CD103^{+}CD11b^{-}$ is the largest population.

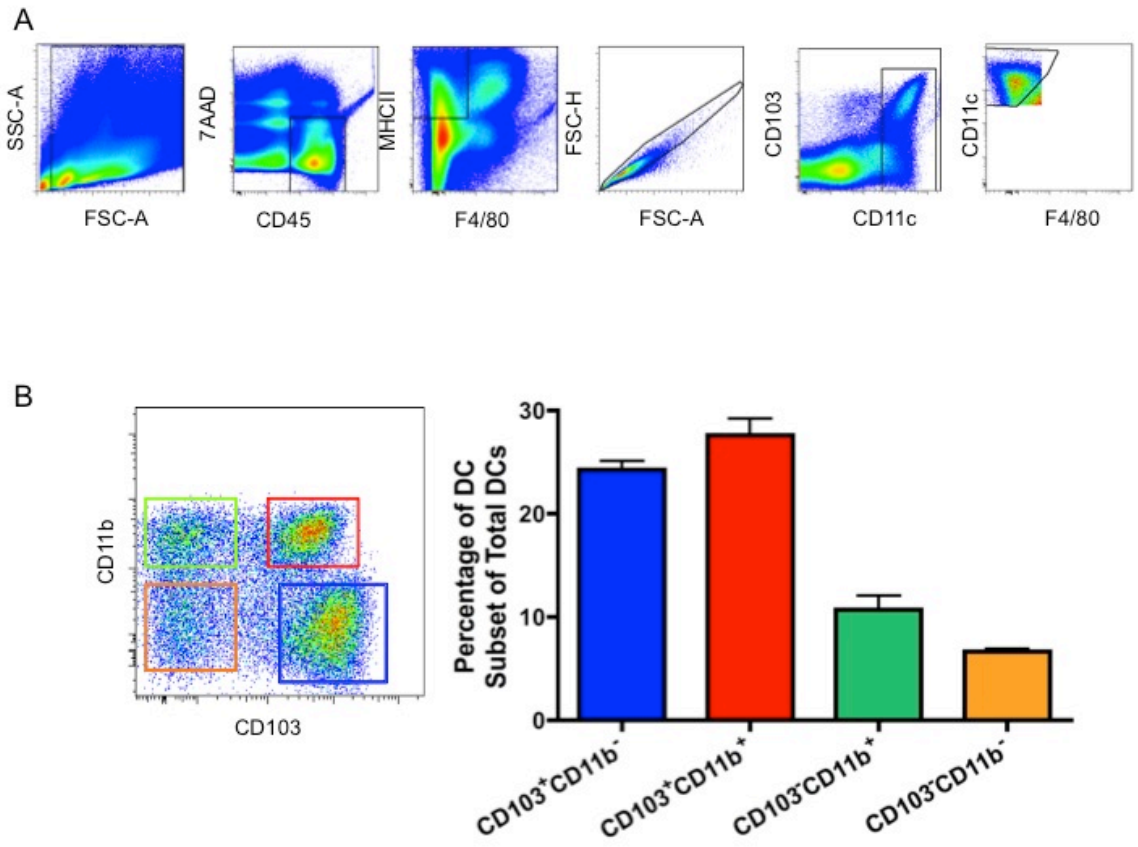

Figure 3-6 Four Distinct Subsets of DCs are Present in the Small Intestinal Lamina Propria.

Single cell suspension of SI lamina propria (siLP) cells were generated by the digestion of the SI without PPs and cells were analysed by flow cytometry. Large cells were gated and live leukocytes ($7AAD^{-}CD45^{+}$) were identified, $F4/80^{+}$ cells were excluded and $MHCII^{+}$ were gated. Doublets were excluded and $CD11c^{+}$ cells were gated and $F4/80^{+}$ DCs were excluded again (A). The resulting DCs were then further split into 4 populations based upon the expression of CD103 and CD11b (B). The percentage of each DC subset was compared. Data are means and S.E.M. n=6.

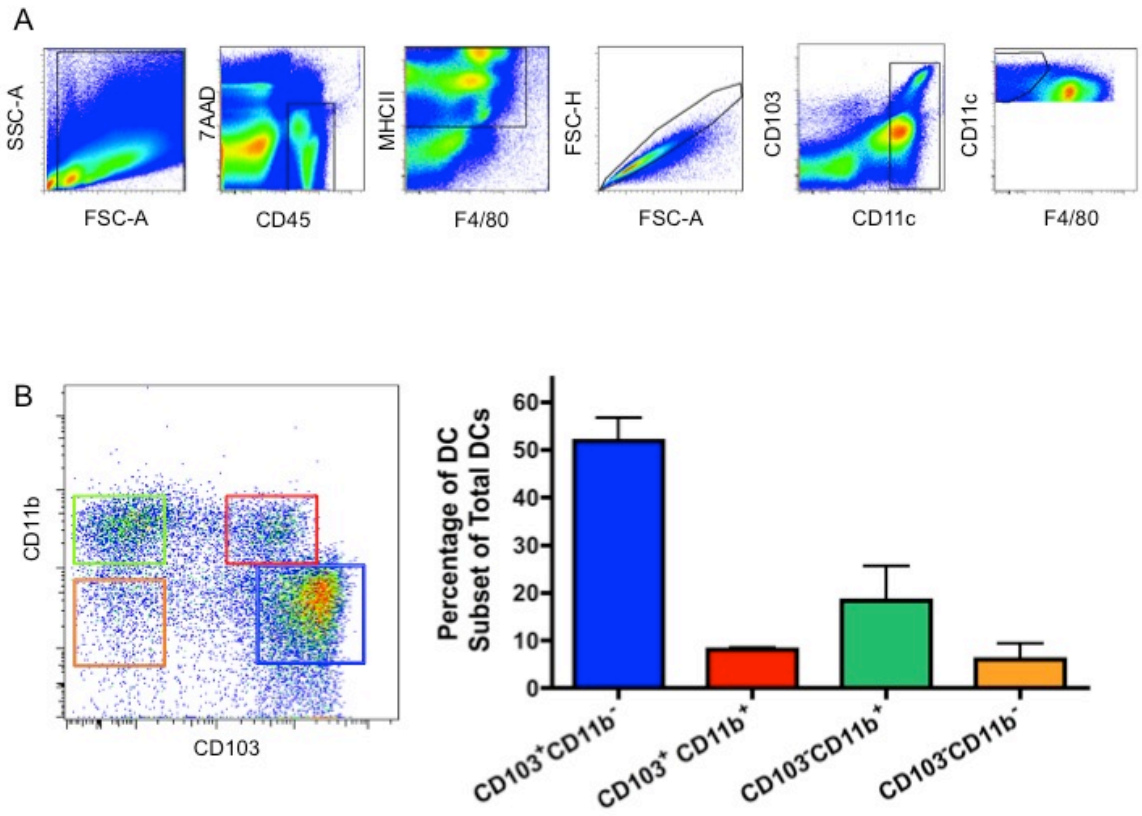

Figure 3-7 Three Distinct Subsets of DCs are Present in the Colonic Lamina Propria.

Single cell suspension of colonic lamina propria (cLP) cells were generated by the digestion of the colon and cells were analysed by flow cytometry. Large cells were gated and live leukocytes ($7AAD^{-}CD45^{+}$) were identified, and $MHCII^{+}$ were gated. Doublets were excluded and $CD11c^{+}$ cells were gated and $F4/80^{+}$ DCs were excluded (A). The resulting DCs were then further split into 4 populations based upon the expression of CD103 and CD11b (B). The percentage of each DC subset was compared. Data are means and S.E.M. n=6.

Having now defined the DC populations in the SI and colon, the DCs in the siMLN and coMLN were compared. The siMLN and coMLN were removed separately and digested. Using flow cytometry DC subsets were identified as follows; large, $7AAD^-$, $CD3^-$, $CD19^-$, single cells (Figure 3.8 A). $MHCII^{hi}CD11c^+$ cells were defined as migratory DCs (Figure 3.8 B) and $MHCII^+CD11c^{hi}$ cells were defined as resident DCs (Figure 3.8 C). Migratory and resident DCs were further separated into subsets based upon their CD103 and CD11b expression and compared with the siLP and the cLP DCs (Figure 3.8 D and 3.8 E, migratory and resident DCs respectively). The percentage of DCs in each subset, as a proportion of total cells, was compared between the siMLN and coMLN, for both migratory DC and resident DC (Figure 3.8 E and 3.8 F, migratory and resident DCs respectively). There was a significantly higher percentage of $CD103^-CD11b^+$ and $CD103^-CD11b^-$ among the migratory DCs in the siMLN compared to the coMLN. The reduction in $CD103^-CD11b^-$ DCs in the coMLN was unsurprising, as this subset of DCs was also missing from the cLP. Furthermore, there was a significantly higher percentage of $CD103^-CD11b^-$ DCs in the resident DC compartment of the coMLN compared to the siMLN. Again this was foreseeable finding; as this population of DCs was not migrating from the colon any $CD103^-CD11b^-$ DCs present in the coMLN had to be resident DCs from blood-derived precursors.

Our previous work showed that the $CD103^-CD11b^+$ subset of DCs migrating in lymph expressed intermediate levels of CX3CR1. As previously described, not all the investigators agree that intestinal DCs express CX3CR1 (Bain et al., 2013; Diehl et al., 2013; Rivollier et al., 2012; Schulz et al., 2009). However, as our TDC experiments data identify bona-fide migratory DCs, we can be confident in our observation that some DC subsets indeed express CX3CR1 (Cerovic et al., 2012). Using $CX3CR1^{+/GFP}$ mice, in which one of the genes encoding CX3CR1 has been replaced with GPF, the level of CX3CR1 expression on DC subsets in the siMLN and coMLN can be compared. siMLN and coMLNs were removed, digested and stained for flow cytometry. Migratory and resident DCs were gated as large, live, $B220^-$, $CD64^-$, $MHCII^{hi}CD11c^+$ or $MHCII^+CD11c^{hi}$ single cells. Four distinct subsets of DCs were identified and the levels of CX3CR1 were compared between DC subsets in the siMLN and coMLN on migratory (Figure 3.9 A) or resident DCs (Figure 3.9 B). In both the migratory and resident DC subsets there was no significant difference between the expression of CX3CR1 in $CD103^+CD11b^-$ DCs or

in $CD103^{-}CD11b^{-}$ DCs in the siMLN or coMLN. Previously, we identified the $CD103^{-}$ $CD11b^{+}$ DCs as expressing intermediate levels of CX3CR1. Consistent with this result, we found $CD103^{-}CD11b^{+}$ DCs to be expressing intermediate levels of CX3CR1 in the siMLN, the percentage of $CD103^{-}CD11b^{+}$ DCs expressing CX3CR1 significantly increased in the coMLN in both migratory and resident DCs. Although there was a significant increase in CX3CR1 expression in the coMLN, the levels of expression were at least one log lower than CX3CR1 expression on macrophages that can be described as $CX3CR1^{hi}$. Additionally, a significantly higher percentage of $CD103^{+}CD11b^{+}$ DCs in the coMLN expressed of CX3CR1 compared to the siMLN in both migratory, and to some extent the resident DC subsets. This was a surprising finding as our previous work had described $CD103^{+}CD11b^{+}$ DCs as CX3CR1 negative. This observation, however, was made using pseudo-afferent lymph from animals that retained some coMLN. Therefore, it is possible this phenotypic difference was not observed using our previous methods. An increase in the percentage of cells expressing CX3CR1 could represent an important difference in DCs from the SI and colon. Although the exact role of CX3CR1 remains to be established there is some evidence suggesting it is involved in cell survival (Landsman et al., 2009), therefore DCs from the colon may reflect environmental differences during the development of DCs from siMLN DCs via the expression of CX3CR1.

In order to confirm that there were differences in the migrating subsets of DCs from the siMLN and coMLN, partial MLNx was performed, followed by TDC. Partial MLNx involved the removal of only specific parts of the MLN. Although gating $CD11c^{+}MHCII^{hi}$ cells in the MLN allows us to identify DCs that are likely to be migratory, this is not definitive. For example, under conditions of inflammation all DCs in the MLN upregulate MHCII expression so that resident and migratory subsets can no longer be distinguished (Persson et al., 2013). MLNx followed by TDC is routinely performed our laboratory in order to isolate all migratory DCs from the intestine. Previously, during MLNx we removed all MLNs found adjacent to the proximal colon (Figure 3.10, lymph nodes routinely removed during MLNx marked in purple). Work described here, however, suggests these MLN are likely to drain both the SI and the proximal colon. Therefore, partial MLNx procedures were developed in order to allow the isolation of DCs from only the SI or colon by TDC. Briefly, siMLNx is the removal

of MLNs that drain the SI while the remaining coMLN are left intact. In contrast, coMLNx involves the removal of the MLNs that drain the colon, while the siMLN remain undamaged. Five to six weeks following partial MLNx TDC was performed as described and pseudo-afferent lymph was collected on ice overnight (Cerovic et al., 2012). Lymph cells were processed and analysed by flow cytometry, for the presence of DCs. DCs were observed by selecting large, live $CD19^-$, $MHCII^+CD11c^+$ cells (Figure 3.11 A), and the composition of DC subsets was compared between siMLNx and coMLNx animals (Figure 3.11 B and C). First the presence of DCs confirmed that the partial MLNx technique was effective. The MLNx procedure relies upon the reanastamosis of the afferent lymphatics from the intestine to the efferent lymphatics, this allows the flow of cells into the thoracic duct. As DCs are present following siMLNx and coMLNx this suggests that reanastamosis enables afferent lymphatics to drain to thoracic duct, allowing the isolation of migratory DCs even after removal of only a portion of the MLNs. Therefore, MLNs are connected to the lymph supply in parallel, not serially. There were significant differences between DC subsets from the siMLNx and coMLNx. First, there were significantly fewer $CD103^+CD11b^-CD8\alpha^+$ in the siMLNx lymph compared with coMLNx. This is a reflection of the composition of DC subsets in the SI and colon, where the numbers of $CD103^+CD11b^-CD8\alpha^+$ is far higher in the cLP compared to the siLP. Although there was not a significant difference in the MLN, there were fewer $CD103^+CD11b^-$ DCs in the siMLN compared to the coMLN. Additionally, there were more $CD103^+CD11b^+$ DCs in the siMLNx lymph compared to the coMLNx lymph. Although there were no significant differences between the numbers or percentages of either of the $CD103^-$ subsets, examination of DC subsets in the coMLNx lymph indicates that the $CD103^-CD11b^-$ subset is missing. This is the smallest subset and a bigger sample size may demonstrate that this loss is statistically significant. This may be expected because few $CD103^-CD11b^-$ DCs are found in the colon and coMLN.

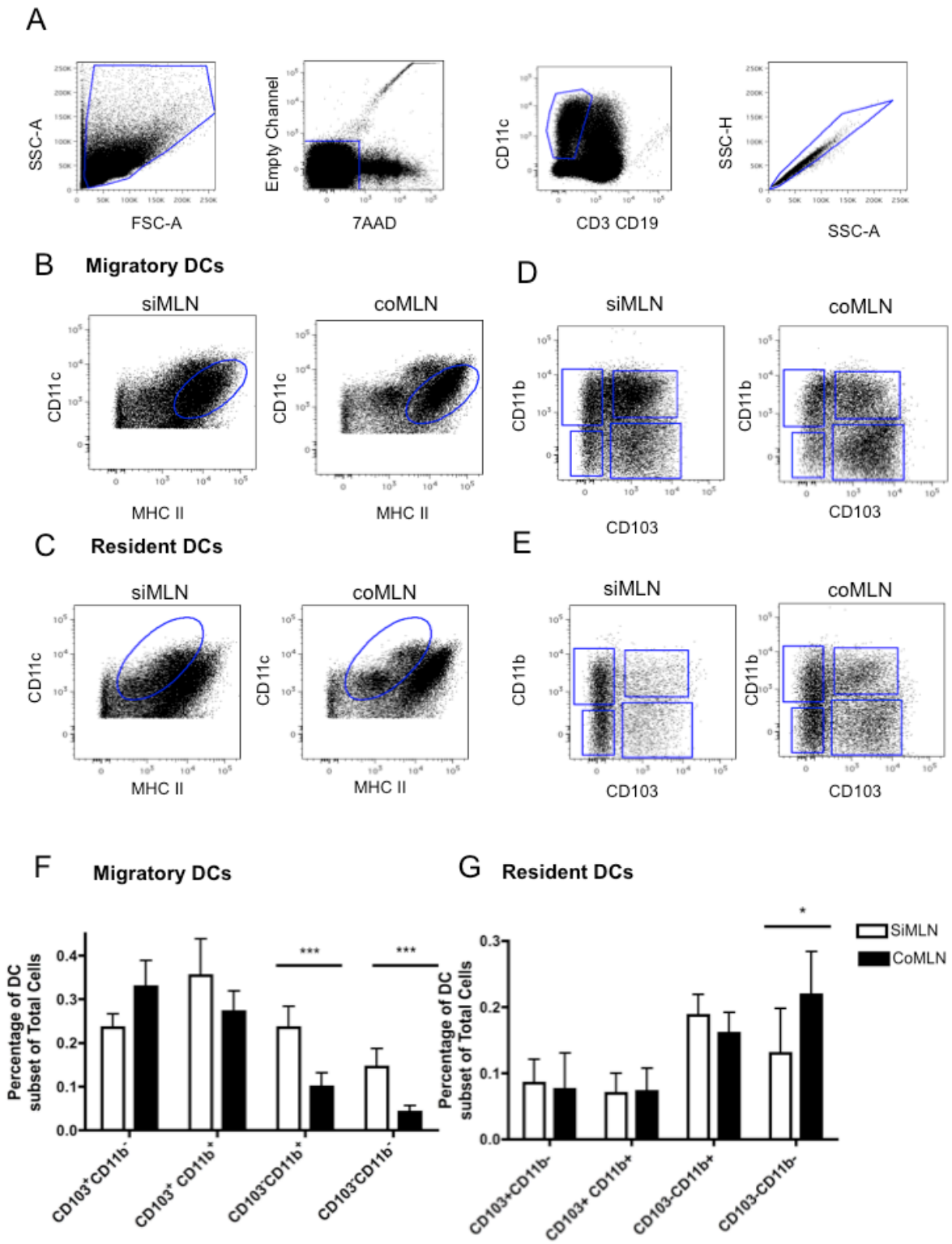

Figure 3-8 Dendritic Cell Subsets in Small Intestinal Draining MLN and Colonic Draining MLN.

Cells from the siMLN and coMLN were isolated and analysed by flow cytometry. Large, live cells were gated, $CD3^+$ $CD19^+$ cells and doublets were excluded (A). Migratory DCs ($MHCII^{hi}CD11c^+$, B) or resident DCs (MHC^+CD11c^{hi}, C) were selected and DC subsets, identified by their the expression of CD103 and CD11b, were compared between siMLN and coMLN migratory DCs (D) or resident DCs (E). The percentage of each DC subset of total cells was compared between DC subsets from the siMLN and coMLN in the migratory and resident DC compartments (F and G respectively). Data are means and S.E.M. The proportions of these populations were compared and results were analysed by Students *t* test, asterisks demote statistical significance, *p<0.05, **p<0.01, ***p<0.001, n=5.

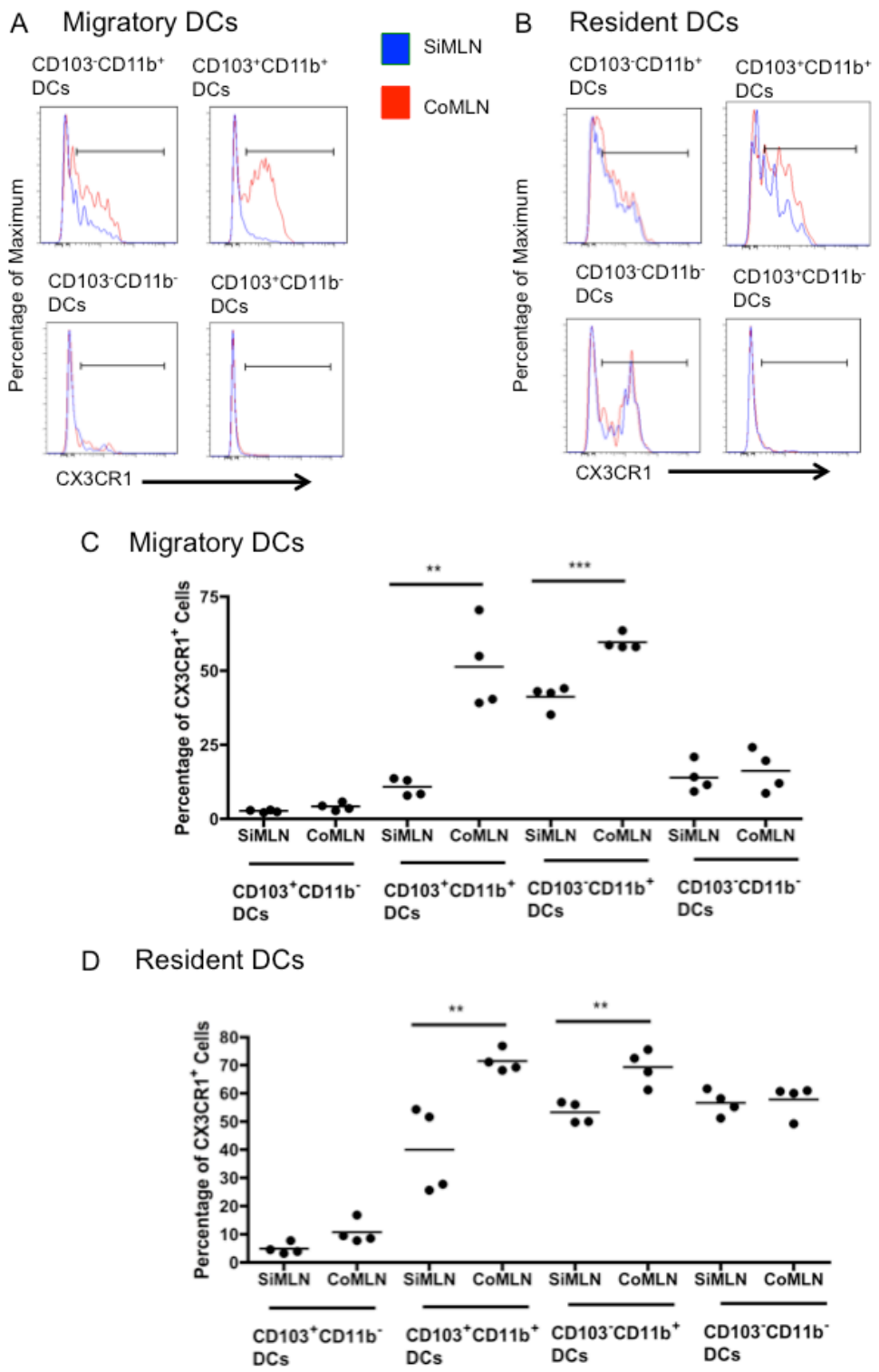

Figure 3-9 Expression of CX3CR1 on Migratory and Resident Dendritic Cell Subsets in siMLN and coMLN.

Cells from the siMLN and coMLN were isolated from CX3CR1$^{GFP/+}$ mice, digested and analysed by flow cytometry. Migratory and resident DCs were gated as B220^{-}, CD64^{-}, MHCII^{hi}CD11c^{+} or MHCII^{+}CD11c^{hi} single cells respectively. Four distinct DC subsets were identified by their expression of CD103 and CD11b. The expression of CX3CR1 was compared between migratory DC subsets (MHCII^{hi}CD11c^{+}, A and C) or resident DC subsets (MHC^{+}CD11c^{hi}, B and D). The percentage of CX3CR1^{+} cells were compared and results were analysed by Students *t* test, asterisks denote statistical significance each point represents an individual animal, *p<0.05, **p<0.01. Histograms are representative of 4 biological replicates.

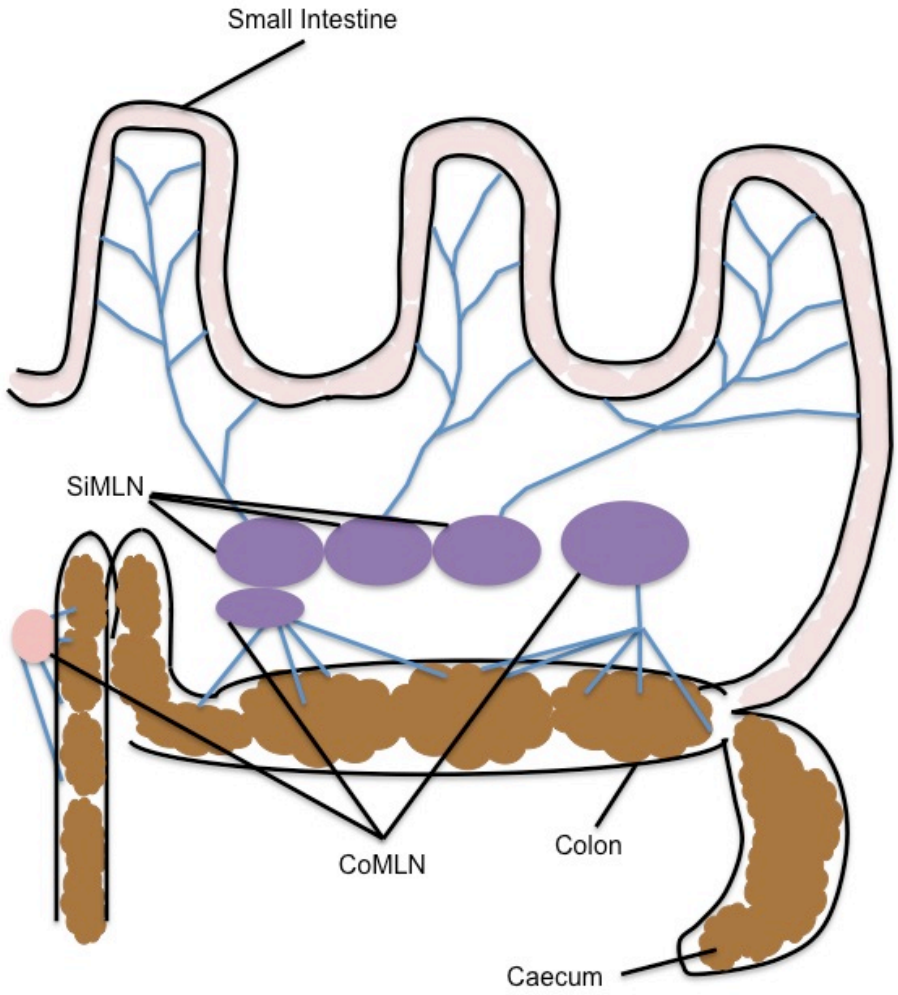

Figure 3-10 Small Intestine and Colon with Draining Mesenteric Lymph Nodes Normally Removed Following Mesenteric Lymphadenectomy.

The SI and colon drain to distinct parts of the MLN. Afferent lymphatics are depicted in blue. MLN normally removed during MLNx depicted in purple.

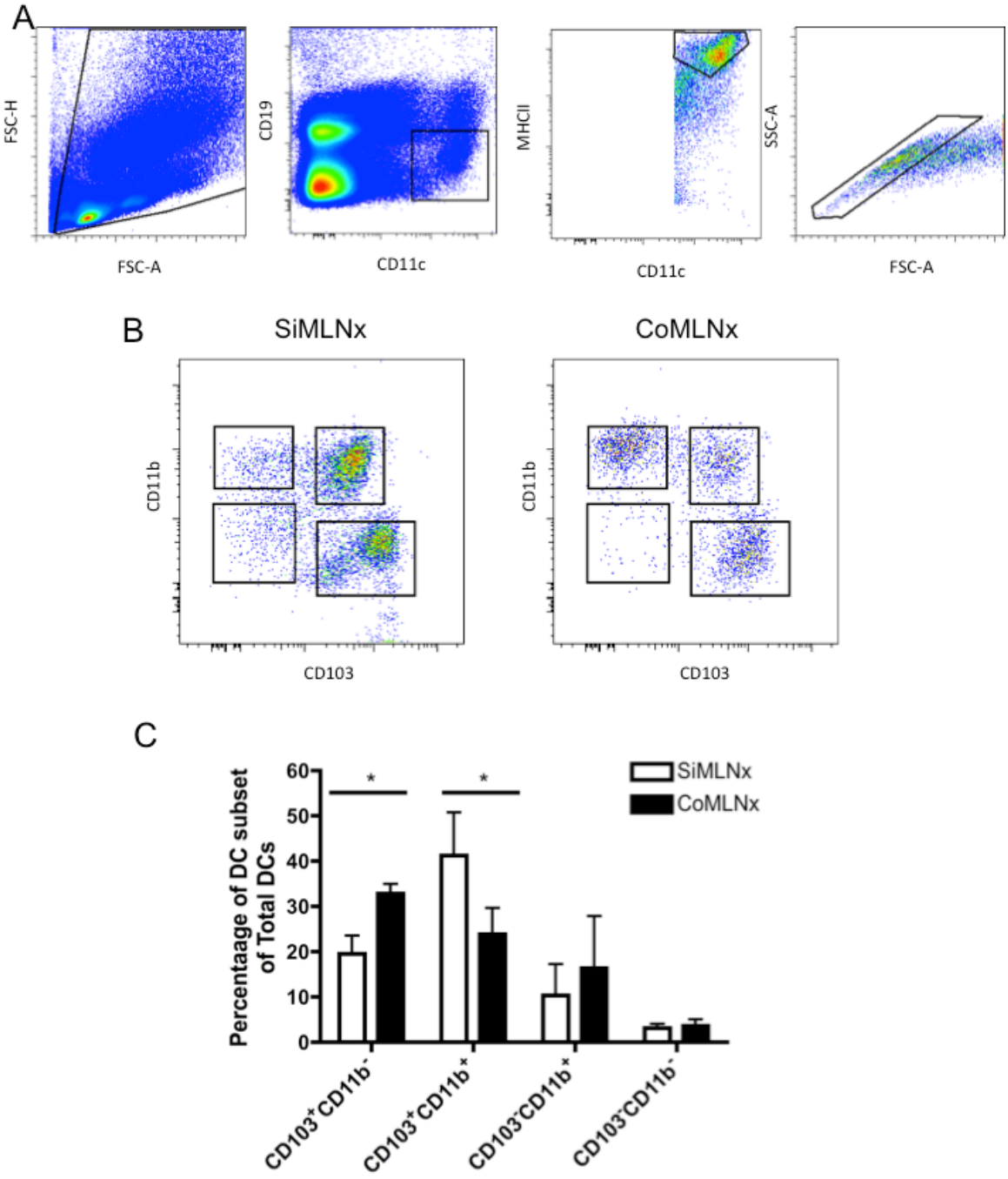

Figure 3-11 Dendritic Cell Subsets in the Lymph of siMLNx and coMLNx Mice.

Pseudo-afferent lymph was collected from mice that had undergone siMLN lymphadenectomy (siMLNx) or coMLN lymphadenectomy (coMLNx). Cells were analysed by flow cytometry; $CD19^-$, $CD11c^+MHCII^+$ single cells were selected (A) and DC subsets based upon the expression of CD103 and CD11b were compared (B). The percentage of the four distinct subsets was compared between siMLNx and coMLNx animals (C). Results were analysed by Students *t* test, asterisks denote statistical significance ($p^*<0.05$, n=5). Data are means and S.E.M. FACS plots representative of 5 independent biological replicates.

3.1.5 Comparison of Antigen Presentation by Small Intestinal and Colonic Draining Mesenteric Lymph Node Dendritic Cells *in Vitro*

To examine whether the siMLN and coMLN DCs have different functions, the ability of DCs from either the siMLN or coMLN were assessed for their ability to present antigen to naïve T cells. The ability to present antigen to naïve T cells is a defining property of DCs. Therefore, we chose to investigate if this property was dependent upon the anatomical origins of the DCs. Due to small numbers of DCs isolated following partial MLNx procedures, particularly coMLNx, total DCs from siMLNx'd or coMLNx'd animals were investigated rather than sorting each specific subset. Although specific DC subsets from the siMLN and coMLN are likely to be phenotypically and functionally different, functional differences arising due to differential subset composition in DCs from the siMLN or coMLN should be apparent as we are using DC subsets at ratios that are migrating to the lymph node. DCs isolated from following TDC of siMLNx and coMLNx animals were FACS purified, pulsed with OVA, washed and co-cultured with CFSE labelled FACS sorted naïve ($CD62L^+$) CFSE labelled OVA specific $CD8\alpha^+$ OT-I T cells. Proliferation was assessed three days later by measuring CFSE dilution (Figure 3.12 A). DCs from the siMLNx and coMLNx lymph were able to present antigen equally well to $CD8^+$ naïve T cells (Figure 3.12 B). Additionally, DCs from the siMLN and coMLN were able to drive the same percentage of cells to undergo at least three divisions (Figure 3.12 C).

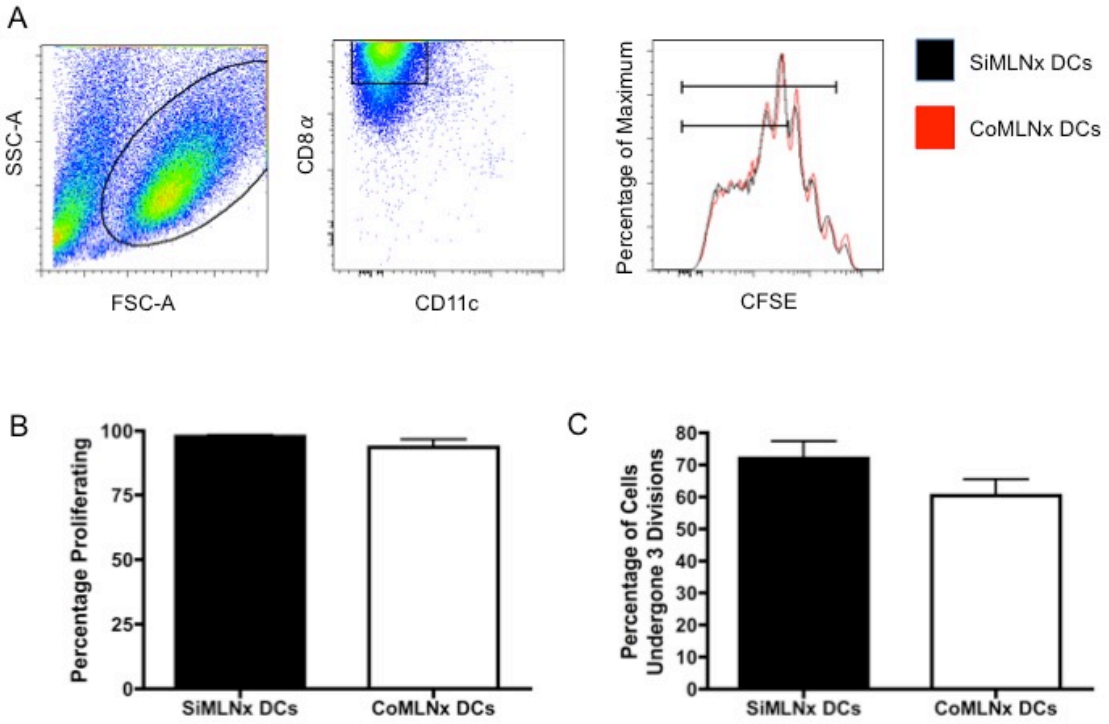

Figure 3-12 Migratory Dendritic Cells From the Small Intestine and Colon are Able to Present Antigen to Naïve T Cells.

$MHCII^+CD11c^+$ DCs from mice that had undergone siMLNx or coMLNx were FACS sorted and incubated for 2 hours with 2mg/ml ovalbumin protein at 37°C. DCs were then washed extensively and co-cultured with CFSE labelled FACS sorted $CD8^+CD62L^+$ OT-I cells for 3 days. Proliferation was assessed by CFSE dilution (A). The percentage of proliferating T cells was compared between migrating DCs from the SI and colon (B). The percentage of T cells that had undergone 3 or more divisions was also compared between siMLNx and coMLNx animals (C). Data are means and S.E.M. Results were analysed by Student's *t* test. FACS plots representative of at least 3 independent biological replicates.

T cell activation by DCs not only causes the proliferation of naïve T cells, but it also leads to the upregulation or retention of homing molecules, allowing T cells to traffic to peripheral non-lymphoid tissues. DCs from the SI and MLN cause the retention of CCR9 on T cells, resulting in these T cells having the capacity to home to the SI. $CD103^+$ DCs from the colon have been shown to be unable to cause the retention of $CCR9^+$ gut tropic T cells, making the ability to generate $CCR9^+$ T cells being described as SI specific feature (del Rio et al., 2010) (Jaensson et al., 2008). Therefore, we sought to determine if the ability to cause the retention of CCR9 expression in responding T cells was different between DCs from the siMLN and coMLN lymph. DCs were isolated by TDC performed in siMLNx and coMLNx animals as previously described. These DCs were co-cultured at varying numbers with OT-I T cells, as before, and CFSE dilution (Figure 3.13 A) and CCR9 expression was determined after three days (Figure 3.13 B and C). DCs from the siMLN and coMLN lymph were able to cause proliferation of naïve T cells; interestingly they were also both able to cause the retention of CCR9 on responding T cells equally well. Therefore, DCs from the siMLN and coMLN lymph can generate gut homing T cells.

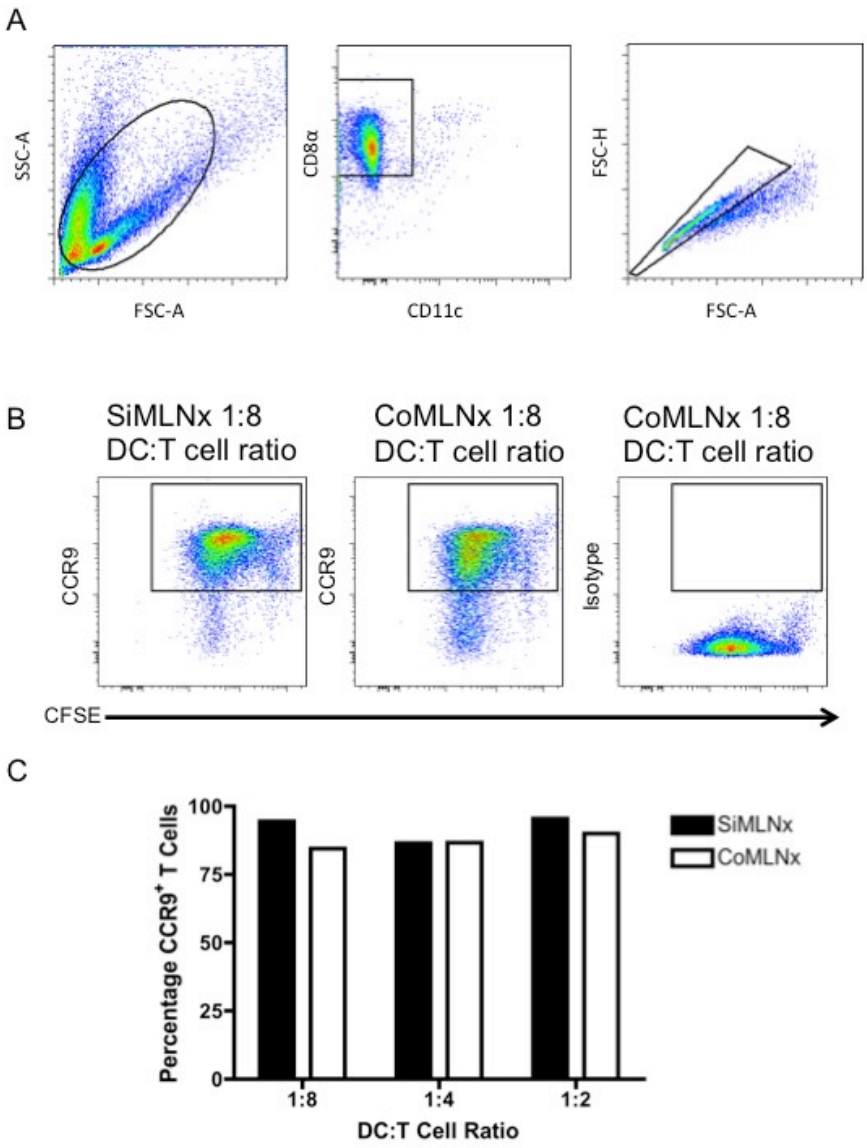

Figure 3-13 Migratory Dendritic Cells From the Small Intestine and Colon are Able to Induce CCR9 Expression in Responding T Cells.

$MHCII^+CD11c^+$ LDCs from mice that had undergone siMLNx or coMLNx were collected by thoracic duct cannulation FACS sorted and incubated for 2 hours with 2mg/ml ovalbumin protein. DCs were then washed extensively and co-cultured with CFSE labelled FACS sorted $CD8^+CD62L^+$ OT-I cells for 3 days. Single T cells were gated (A) and CCR9 expression on proliferating T cells was compared between migrating DCs from the SI and colon (B). The percentage of T cells that expressed CCR9 was compared between siMLNx and coMLNx animals at a range of DC:T cell ratios (C).

3.1.6 Dendritic Cell Subsets in the Small Intestinal and Colonic Draining Mesenteric Lymph Nodes Following Experimental Colitis

In order to investigate DC populations in the siMLN and coMLN under conditions of inflammation, a model of experimental colitis was used. In this model, colitis was induced by the addition of DSS to drinking water. This specifically induces colonic inflammation, while having little effect on the SI (Geier et al., 2009). The initiation and propagation of the inflammation induced by DSS colitis has been widely attributed to macrophages in the colon (Bain et al., 2013) (Tamoutounour et al., 2012). As there is anatomical segregation of lymphatic drainage to the MLN, any changes in DC populations in this model may have been overlooked. Therefore, DC populations were assessed using a recovery model of experimental colitis in the siMLN and coMLN. 2% DSS was added to drinking water at day -3, at day 0 animals were culled or allowed to recover for 3 or 10 days before siMLNs and coMLNs were isolated (Figure 3.14 A). Samples taken at day 0, referred to as DSS, had not yet begun to show weight loss normally associated with experimental colitis. However, there was evidence of inflammation upon examination of the colon (C.Bain, personal communication). The siMLN and coMLN were removed from animals at each time point, digested and analysed by flow cytometry. Migratory and resident DCs were gated as following; large, $B220^-$, $7AAD^-$, single, $CD64^-$ cells. Migratory DCs were $MHCII^{hi}CD11c^+$ while resident DCs were defined as $MHCII^+CD11c^{hi}$ (Figure 3.14 B). The total numbers of migratory (Figure 3.14 C) or resident DCs (Figure 3.14 D) in the siMLN or coMLN were compared between steady-state (SS), DSS, and day 3 recovery DSS (R3DSS) and day 10 recovery DSS (R10DSS). There was no significant difference in the number or percentage of DCs at any time in either the siMLN or coMLN. This was somewhat surprising, as there was significant inflammatory infiltrate in the colon caused by the break down of the epithelial barrier. Although DCs are not thought to mediate the disease, the inflammatory conditions of the colonic environment were predicted to lead to an increase in DC migration to the MLN.

Although there were no changes to overall DC numbers in the siMLN or coMLN we decided to investigate if there were changes in DC subsets that migrate to the siMLN or coMLN. As DC subsets are functionally distinct, we hypothesised that there may be an increase in the $CD103^-CD11b^+$ DC subset, as this has been shown

to be an inflammatory subset (Cerovic et al., 2012). Furthermore, cells of a similar phenotype were reported to be increased in intestinal lymph during DSS colitis (Zigmond et al., 2012). Migratory (Figure 3.15) or resident DCs (Figure 3.16) from each time point were split into four subsets based upon their expression of CD103 and CD11b. The total number of cells in each DC subset was compared between SS, DSS, R3DSS and R10DSS from the siMLN and coMLN. There were no significant differences in the number or percentage of any DC subset examined.

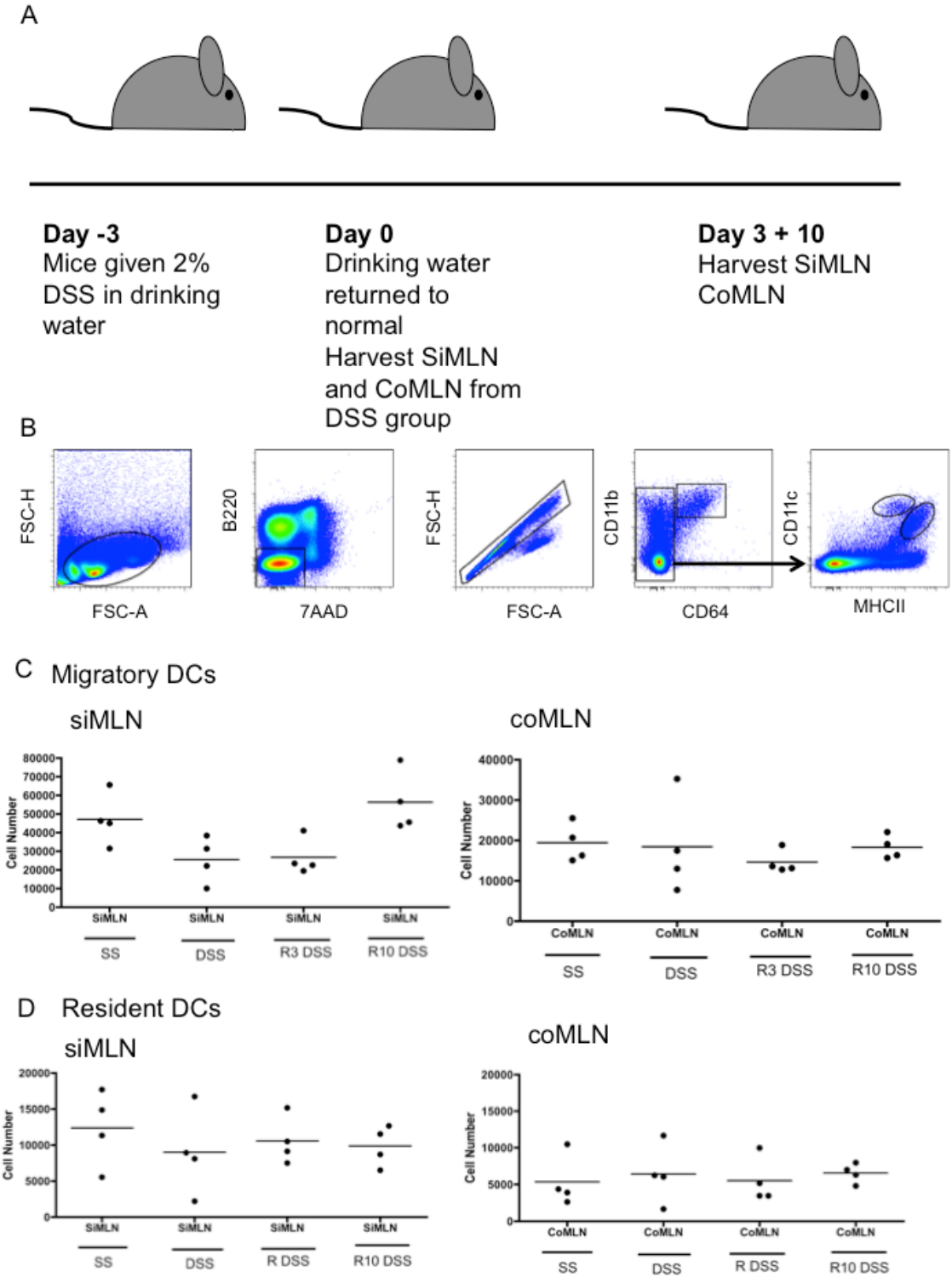

Figure 3-14 Dendritic Cell Populations are Comparable in Small Intestinal and Colonic Draining MLN During and After Experimental Colitis.

Mice received 2% DSS-supplemented drinking water at day -3, at day 0 animals with acute colitis were assessed (DSS) or drinking water was returned to normal. Animals were allowed to recover for 3 (R3 DSS) or 10 days (R10 DSS). siMLN or coMLNs were isolated, digested and analysed by flow cytometry. Migratory or blood derived DCs were gated as follows: large, $B220^-$ live, single cells were selected. $CD64^+CD11b^+$ cells were excluded and migratory DCs ($MHCII^{hi}CD11c^+$) and blood derived DCs ($MHCII^+CD11c^+$) (A). Total numbers of migratory DCs were compared between steady state (SS), DSS, R3 DSS and R10 RSS in the siMLN (C left panel) and coMLN (C right panel). Resident DCs were also compared in the siMLN (D left panel) and coMLN (D right panel). Each point represents an individual animal. Results were analysed by a two way ANOVA.

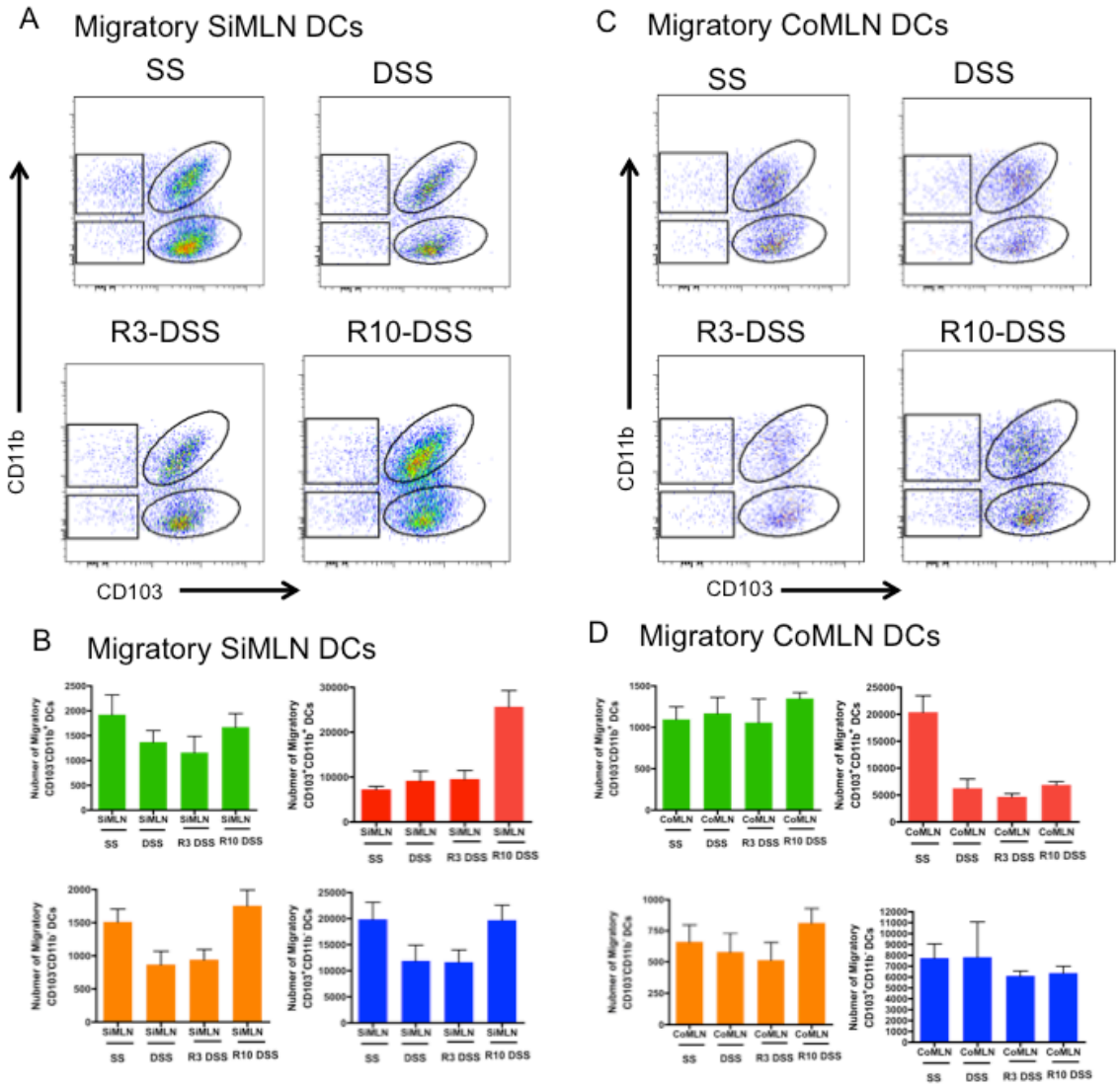

Figure 3-15 Migratory Dendritic Cell Subsets are Comparable in Small Intestinal and Colonic Draining MLN During and After Experimental Colitis

siMLN or coMLNs were isolated, digested and analysed by flow cytometer from SS, DSS, R3DSS and R10DSS animals. DC subsets from migratory DCs ($MHCII^{hi}CD11c^{+}$) were analysed based upon their expression of CD103 and CD11b. Total numbers of DC subsets from migratory DCs were compared between steady state (SS), DSS, R3 DSS and R10 RSS in the siMLN (A) and coMLN (C). Total numbers of each subset were compared between SS, DSS, R3 DSS and R10 DSS in migratory siMLN DCs (B) and in migratory coMLN DCs (D). Results were analysed by a One-Way ANOVA, with a Bonferroni post-test. Data are means and S.E.M. FACS plots representative of 4 independent biological replicates, n=4.

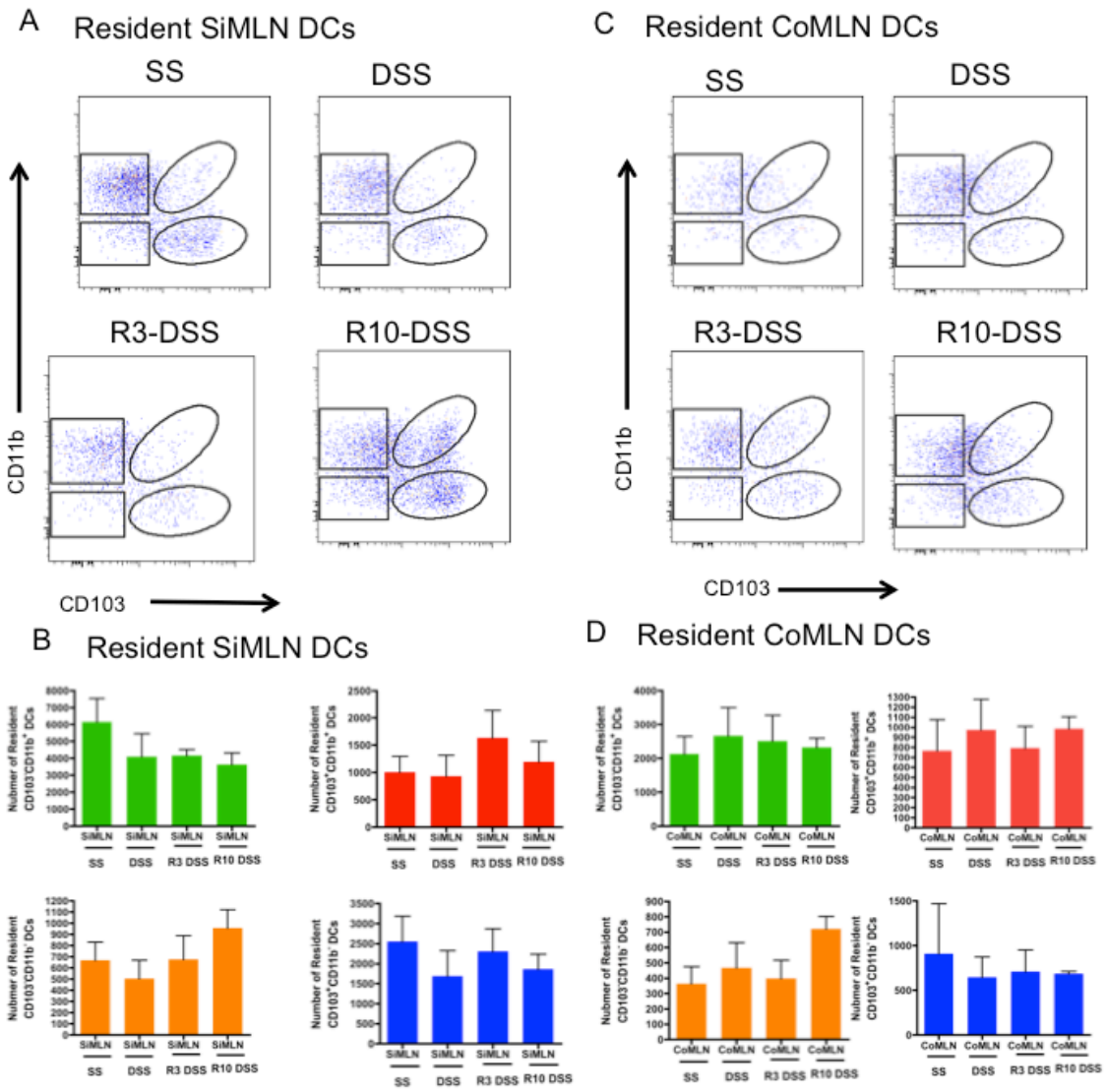

Figure 3-16 Resident Dendritic Cell Subsets are Comparable in Small Intestinal and Colonic Draining MLN During and After Experimental Colitis

siMLN or coMLNs were isolated, digested and analysed by flow cytometer from SS, DSS, R3DSS and R10DSS animals. DC subsets from resident DCs ($MHCII^{+}CD11c^{hi}$) were analysed based upon their expression of CD103 and CD11b. Total numbers of DC subsets from resident DCs were compared between steady state (SS), DSS, R3 DSS and R10 RSS in the siMLN (A) and coMLN (C). Total numbers of each subset were compared between SS, DSS, R3 DSS and R10 DSS in migratory siMLN DCs (B) and in migratory coMLN DCs (D). Results were analysed by a One-Way ANOVA, with a Bonferroni post-test. Data are means and S.E.M. FACS plots representative of 4 independent biological replicates, n=4.

Recent work in the Jung laboratory identified a population of CX3CR1^{int} population of inflammatory monocytes that expand in the colon of mice with experimental colitis. They report that the Ly6C^{lo} subset of these CX3CR1^{+} monocytes are able to migrate in the afferent lymphatics and are then able to present antigen to naïve T cells in the MLN (Zigmond et al., 2012). The Powrie laboratory also reported a similar population of E-Cadherin^{+} cells, although their analysis showed this population to be blood derived (Siddiqui et al., 2010). As experimental colitis only affects the colon, we postulated that this population of inflammatory monocytes would specifically migrate to and expand in the coMLN. Therefore, we identified a population of CD64^{+}CD11b^{+}CX3CR1^{int} cells in the siMLN and coMLN of SS, DSS, R3DSS and R10DSS (gating as in Figure 3.14 B, CX3CR1 expression 3.17 A). The number of total CD64^{+}CD11b^{+}CX3CR1^{+} monocytes was compared between SS, DSS, R3DSS and R10DSS groups in the siMLN and coMLN. There was no change in the number of these CD64^{+}CD11b^{+}CX3CR1^{+} monocytes in the siMLN (Figure 3.17 B) or coMLN (Figure 3.17 C) at any time during our recovery model of DSS colitis.

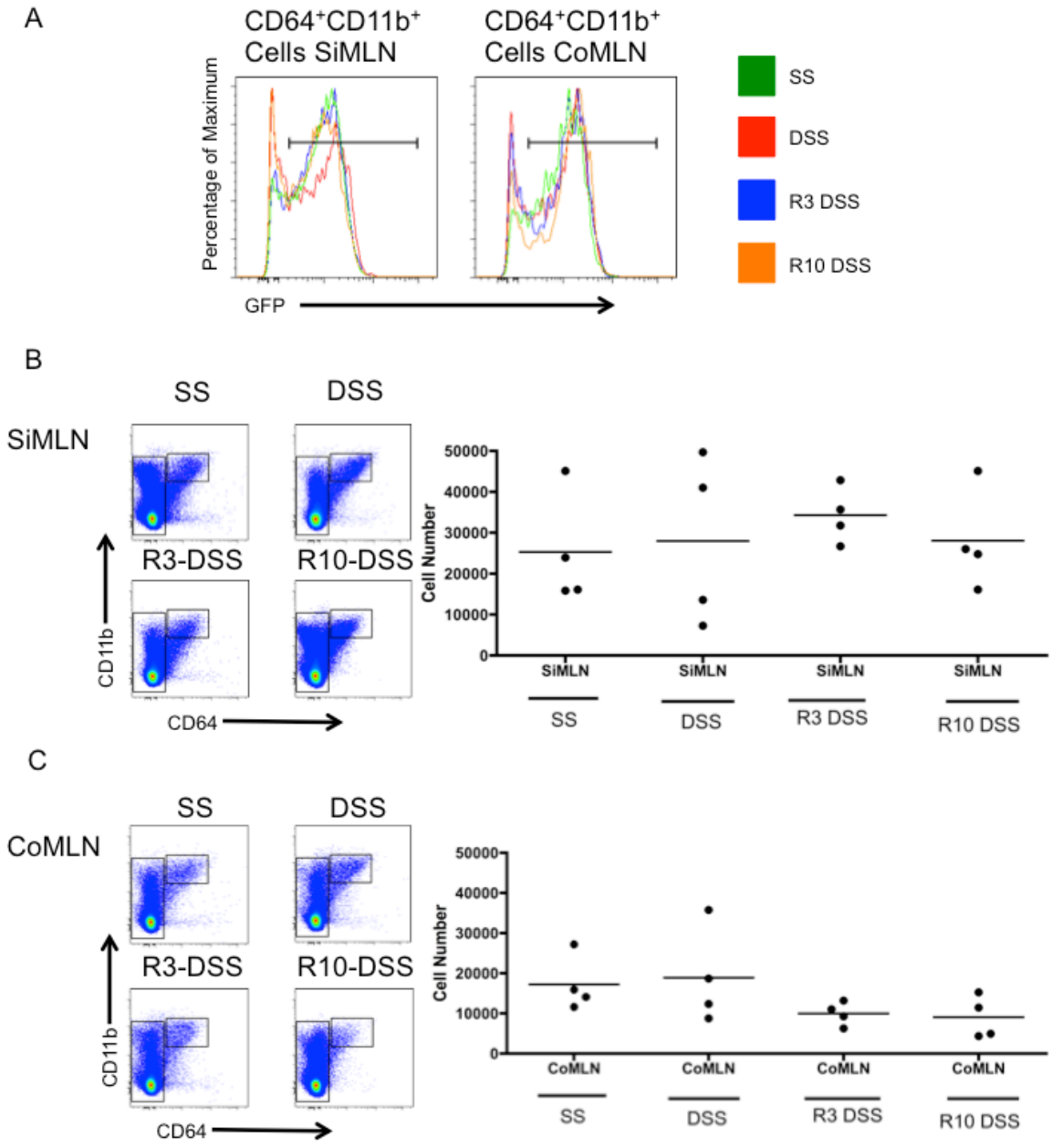

Figure 3-17 CD64$^+$CD11b$^+$CX3CR1$^+$ Cells are Unchanged in Small Intestinal and Colonic Draining MLN During and After Experimental Colitis.

siMLN or coMLNs were isolated, digested and analysed by flow cytometry from SS, DSS, R3DSS and R10DSS animals. CD64$^+$CD11b$^+$ cells were identified and expression of CX3CR1 was investigated (A). Total numbers of CD64$^+$CD11b$^+$ cells from the siMLN (B) and coMLN (C) were compared between steady state (SS), DSS, R3 DSS and R10 RSS. Each point represents an individual animal. Results were analysed by a two way ANOVA.

3.1.7 Antigen Presentation by Small Intestinal and Colonic Draining Mesenteric Lymph Node Dendritic Cells *in Vivo*

Although there were no differences in DC migration to the siMLN or coMLN following a model of experimental colitis, I wanted to further investigate the functional significance of anatomical segregation of lymphatic drainage and DC migration. Rather than concentrating upon the consequences of an inflammatory situation, antigen presentation in the steady-state was investigated. The SI is specialised for the uptake of protein, and DC are essential in the transport of antigen to the MLN where they present this to naïve T cells. Therefore, we sought to design an experiment to determine in which parts of the MLN antigen from the SI are presented to T cells. To this end, CD45.1 OT-II cells were CFSE labelled and adoptively transferred into a CD45.2 host. 24 hours later the CD45.2 animal was fed with 10mg of OVA. Three days later the siMLN, coMLN and ILNs were removed (Figure 3.18 A) and $CD45.1^{+}CD4^{+}$ T cells were identified in the lymph nodes (Figure 3.18 B). Levels of CFSE dilution were investigated as a measure of T cell proliferation. Proliferating T cells were only present in the siMLN (Figure 3.18 C), suggesting that ovalbumin which would have been taken up in the SI is only being presented to T cells in the siMLN. This is the first direct evidence that the siMLN and coMLN have specific and distinct functions.

In order to gain further insight into the preferential presentation of SI derived antigen to T cells in the siMLN we modified the previous experiment. CD45.12 OT-I T cells were CFSE labelled and adoptively transferred into a CD45.2 host. 24, 48 or 72 hours later the siMLN, coMLN and ILNs were removed (Figure 3.19 A). $CD8\alpha^{+}TCRv\alpha2^{+}$, $CD45.1^{+}CD45.2^{+}$ single cells were selected (Figure 3.19 B) and levels of proliferation were assessed by CFSE dilution in the siMLN, coMLN and ILNs were assessed after 24, 48 and 72 hours after the host was fed ovalbumin (Figure 3.19 C). After 24 hours there was no proliferation of transferred T cells, presumably as there was not enough time for the antigen to have been taken up by the DC, travel to the MLN and be presented to an OT-I T cell causing its proliferation. After 48 hours CFSE dilution was observed in the siMLN, and to some extent in the coMLN. However, levels of proliferation in the coMLN were significantly lower than in the siMLN. The small amount of proliferation of OT-I T cells in the colon may have been observed for a number of reasons. Firstly, OVA may have been taken up into the colon. This could have possible as it is water-

soluble and OVA which was not fully adsorbed in the SI could have travelled to the colon. This, combined with the extreme in sensitivity of the OT-I system may have lead us to see some proliferation of T cells in the coMLN, although to a lower extent than was observed in the siMLN. Alternatively, the lymphatics may not exclusively drain the nodes, and some siMLN afferent lymphatics may drain to the coMLN. After 72 hours CFSE was completely diluted in the siMLN, coMLN and ILN. At this this point, the antigen and T cells are likely to have been transferred into the systemic circulation. Taken together, although these data are not definitive, as the previous experiment was, support the idea that the siMLN and coMLN are functionally, as well as anatomically, separate.

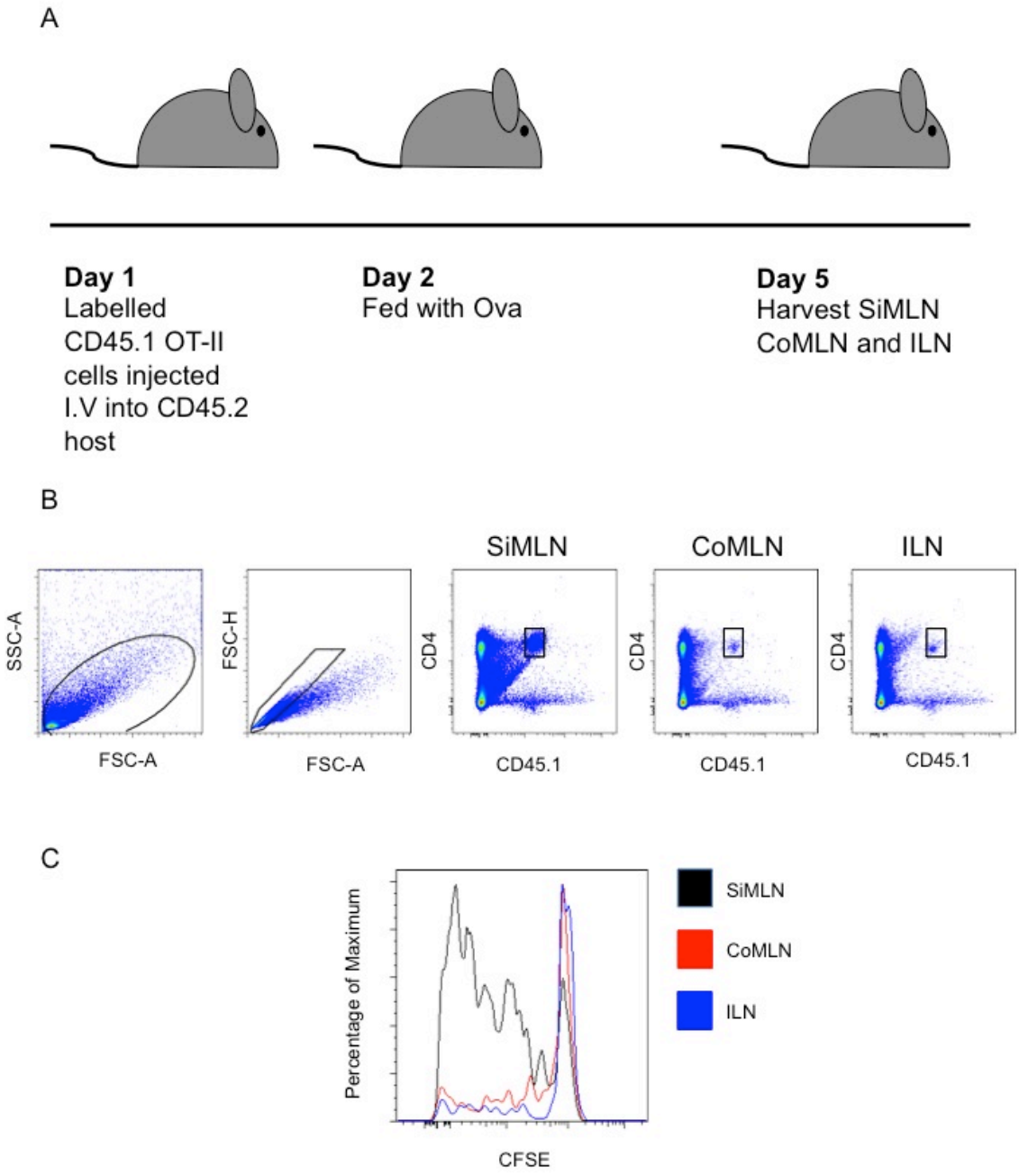

Figure 3-18 Orally Administered Antigen Preferentially Causes Proliferation of $CD4^+$ T Cells in Small Intestinal Draining Lymph Nodes.

Cells from the MLN and spleen of an OT-II CD45.1 donor were CFSE labelled and transferred to a WT CD45.2 host. 24 hours later 10 mg ovalbumin was administered orally to hosts. Three days later siMLN, coMLN and inguinal LNs (ILNs) were removed and analysed by flow cytometry (A). $CD4^+CD45.1^+$ transferred cells were identified in siMLN, coMLN and ILNs, by gating large, single $CD4^+CD45.1^+$ cells (B). Proliferation was analysed by CFSE dilution in each lymph node, siMLN (black line), coMLN (red line) and ILN (blue line) (C).

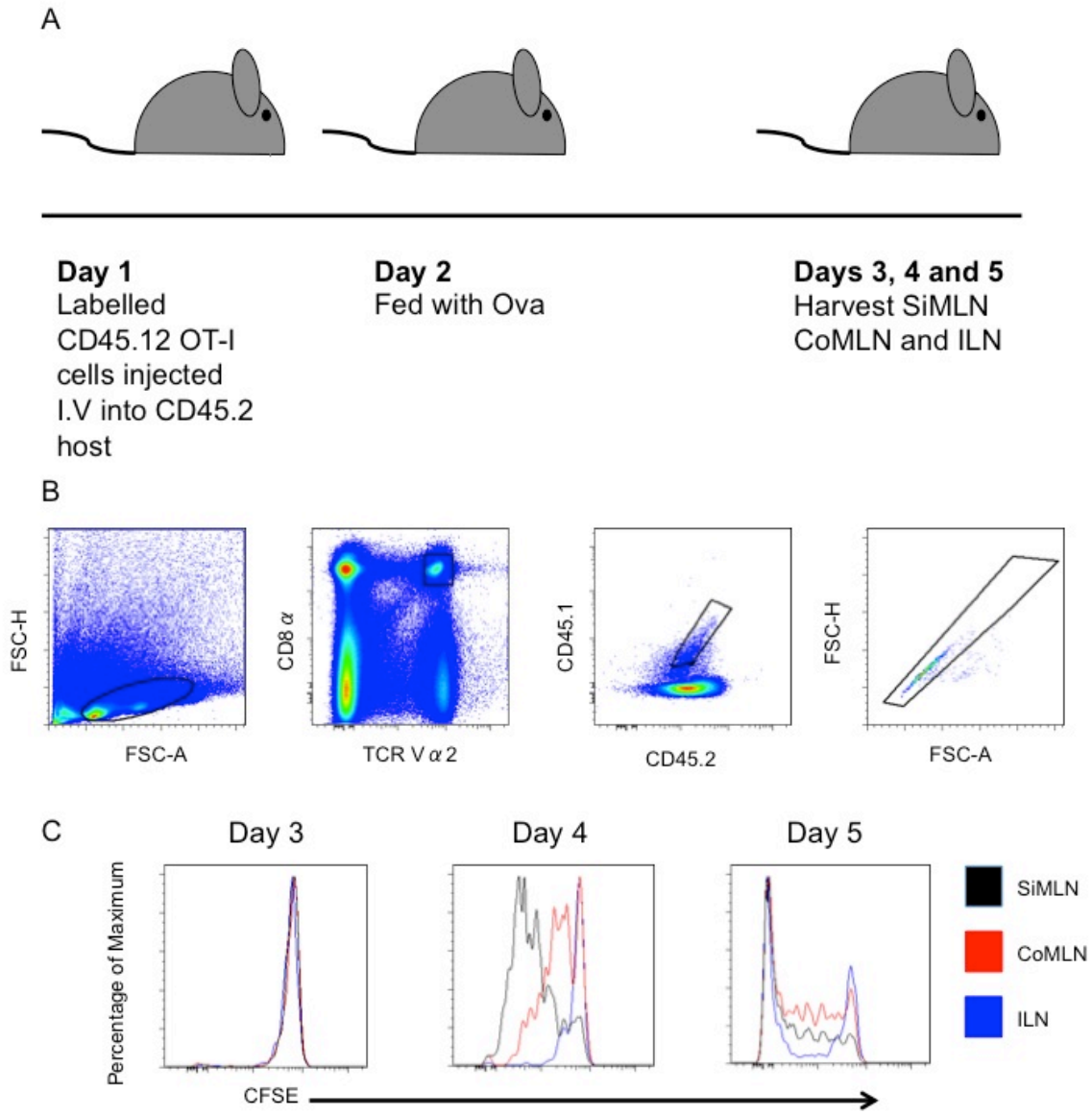

Figure 3-19 Orally Administered Antigen Causes Proliferation of CD8α$^+$ T Cells Specifically in Small Intestinal Draining Lymph Nodes.

Cells from the MLN and spleen of an OT-I CD45.12 donor were CFSE labelled and transferred to a WT CD45.2 host. 24 hours later ovalbumin was administered orally to hosts, 24, 48 and 72 hours later siMLN, coMLN and ILNs were removed and analysed by flow cytometry (A). CD8α$^+$TCRVα2$^+$, CD45.1$^+$CD45.2$^+$ single transferred cells were identified by gating large leukocytes, CD8α$^+$TCRVα2$^+$, CD45.1$^+$ CD45.2$^+$ single cells (B). Proliferation was analysed by CFSE dilution in each lymph node at day 3, day 4 and day 5. siMLN (black line), coMLN (red line) and ILN (blue line) (C).

To examine the functional consequences of the anatomical compartmentalisation of lymphatic drainage to distinct parts of the MLN we used transgenic 232-4 mice that express low levels of a cytoplasmic form of OVA only in SI enterocytes (Vezys et al., 2000). We isolated the siMLNs and coMLNs separately, stained and FACS sorted DCs. We then co-cultured the purified DCs with naïve CFSE-labelled OVA-specific OT-I ($CD8^+$) TCR-transgenic T cells. Only DCs isolated from siMLNs were able to present antigen, derived from the SI, and cause the proliferation of naïve T cells. DCs isolated from the colonic draining MLNs, were not able to cause the proliferation of naïve OT-I T cells (Figure 3.20). Together, these data demonstrate that, within the MLN chain, there is anatomical segregation of presentation of antigen derived from the SI and the colon.

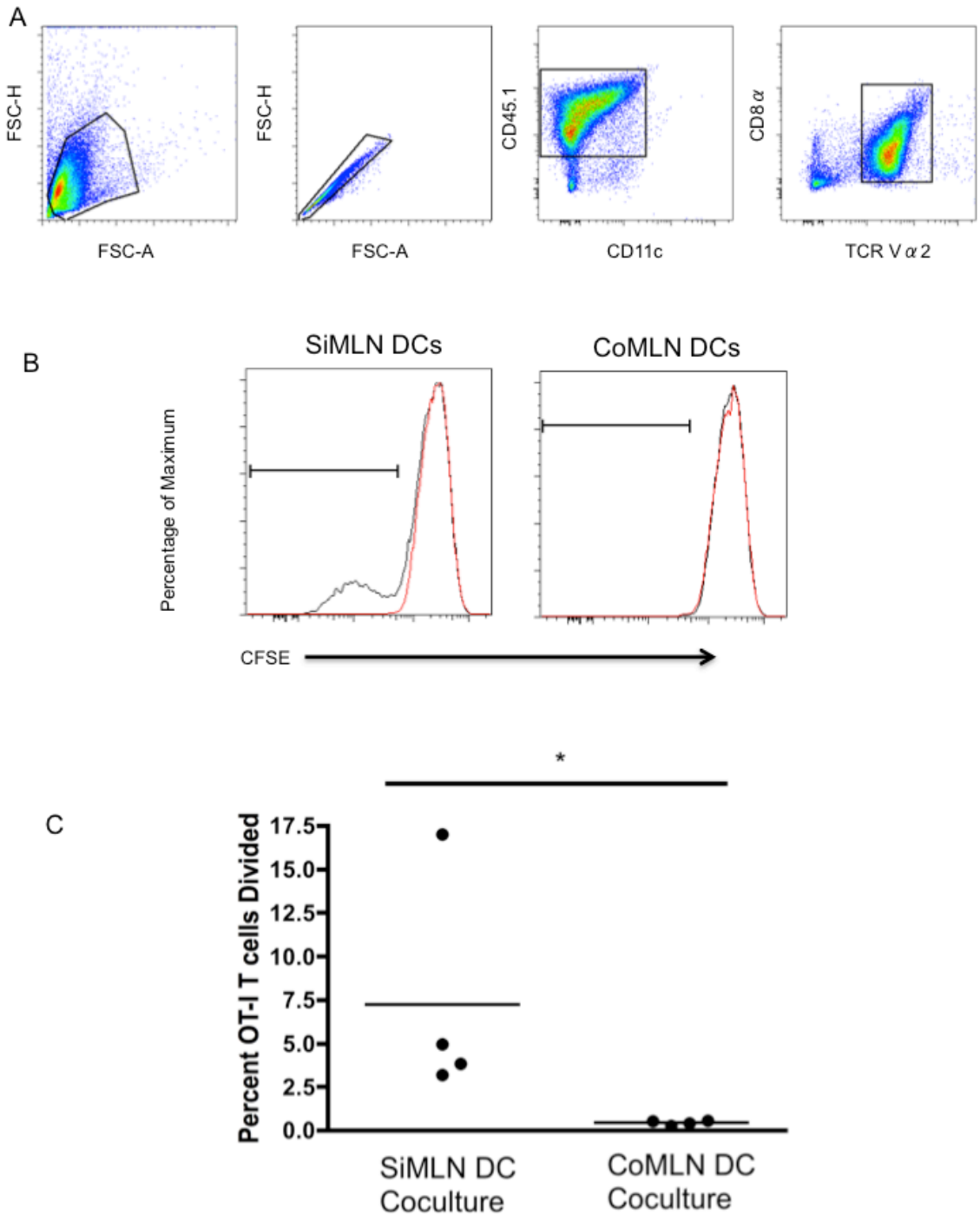

Figure 3-20 Small Intestinal Derived Ovalbumin is Only Presented to T cells in Small intestinal Draining Lymph Nodes

Small intestinal draining MLN and colonic draining MLNs were removed from 232-4 mice which express OVA only in the epithelium of the small intestine, cells were digested, and CD8α^+ DCs were sorted using a FACSAria. DCs were co-cultured at a 1:8 DC:T cell ratio with 10^5 sorted, CFSE labelled OT-I T cells. T cells were selected by gating large, single, CD45.1$^+$CD8α^+TCRVα2$^+$ cells (A). Levels of proliferation were assessed by CFSE dilution and analysed 3 days later each point represents an individual animal (B and C). Results were analysed by student's t test, asterisks denote statistical significance ($p<0.05$).

3.2 Discussion

It is not widely recognised that specific nodes within the MLN drain lymph from different regions of the intestine. Indeed, the vast majority of recent reports assume that changes in the SI and colon are reflected in the whole MLN chain. Identification of the precise LNs that drain lymph from the SI and colon is essential in order to gain an accurate understanding of the immune response. Indeed, without proper investigation of relevant LNs, important changes in cell populations may be missed entirely.

3.2.1 Identification of Draining Lymph Nodes Draining the Small Intestine and Colon

To identify which parts of the intestine supply lymph to each of the nodes of MLN chain, we first examined the lymphatic drainage from the SI and colon. To achieve this, Evans blue dye was injected into the subserosal layer of either the SI or the colon of live anaesthetised mice. This allowed direct examination of the intestinal afferent lymphatic system and the draining MLNs. Following the injection of Evans blue into the subserosal tissue of the SI, the central LNs of the MLN chain stained blue, identifying them as draining the SI, the siMLN (Figure 3.1 A). This phenomenon had previously been observed, with the identification of the middle mesenteric nodes draining the jejunum and ileum. (Balic et al., 2009; Carter and Collins, 1974; Tilney N, 1971) Previous work also identified upper MLNs, located near the pancreatic lymph nodes, that were thought to drain the stomach and duodenum (Carter and Collins, 1974). In our hands, the primary LNs draining the entire SI were the central MLNs, upper MLNs were not involved. This may be because our subserosal injections were carried out too low down the GI tract; we did not investigate the stomach, therefore cells may drain from the stomach to the upper MLNs, as is the case in rats (Tilney N, 1971). Another key difference between our work and previous studies is in the strain of animal used. We used only C56Bl/6 animals, while studies identifying upper MLNs made use of DBA/2J mice. A more recent study indirectly identified the central MLNs as draining the SI, observing a reduction of CD8α^{int} DCs specifically in siMLN following the infection with *Nippostongylus brasiliensis* (Balic et al., 2009). Similarly the central MLNs from mice infected intragastrically with *S. enteritidis,* which mainly colonises the ileum, were the first lymph nodes to be

infected (Carter and Collins, 1974). These data are consistent with our observations regarding lymphatic drainage from SI to the siMLN.

Following subserosal injection of dye into the proximal colon, dye first reached the MLN located directly adjacent to the caecum (Figure 3.1 B). This was consistent with previous reports in mice and rats (Carter and Collins, 1974; Tilney N, 1971), which identify the caecum and ascending colon draining to this "distal" MLN. Interestingly, a second LN also stained blue following injection of dye into the proximal colon. This second colon-draining MLN was at the opposite end of the main MLN chain (Figure 3.1 B). Previous studies did not identify this as draining the colon; it may have been overlooked due to its small size and unexpected location, or perhaps due to anatomical differences between mouse strains used. Previous work showed the "upper" MLNs, near the pancreas, to be draining the transverse colon (Carter and Collins, 1974). These LNs were identified as draining the colon on only one occasion in our hands. Therefore they were not routinely included in our analysis of the coMLN, as the possibility of contamination could not be ruled out and we were unable to replicate the result. Following Evans blue injection into the distal colon, the first MLN to stain blue was the LN located adjacent to the abdominal aorta (Figure 3.1 C). This was previously identified in both mice and rats, but there has been no recent investigation into this MLN (Carter and Collins, 1974; Tilney N, 1971). Although we identified one additional LN draining the colon, the majority of our work is in agreement with previous findings. Using new technology that was unavailable to earlier investigators, we then validated these observations and examined their functional relevance.

Previous studies, and our observations using Evans Blue dye, can only reveal the patterns of lymphatic drainage. They do not allow the investigation of cellular emigration from tissue or the investigation of specific populations of cells. Therefore, we further explored the anatomical segregation of lymphatic drainage from the SI and colon using kaede mice. As antigen is carried to the MLN by migratory DCs, which are responsible for the initiation of intestinal immune responses, the migration of these vital cells was specifically investigated. Kaede mice have previously been used to monitor DC migration in peripheral LNs (Tomura et al., 2008), as well B cell migration in the intestine

(Schmidt et al., 2013). Intestinal DC migration has not been investigated using this system. To analyse the migration of intestinal DCs, mice underwent a laparotomy and all accessible parts of the SI or colon were exposed to low intensity UV light for two minutes. Animals were then allowed to recover, and the siMLNs or coMLNs were examined 24 or 48 hours after photoconversion. 24 hours after exposure of the SI to UV light, significantly more photoconverted kaede-red DCs were present in the siMLN than in the coMLN (Figure 3.2). The number of kaede-red$^+$ DCs migrating into the siMLN decreased after 48 hours, however there were still significantly more kaede-red$^+$ DCs present in the siMLN than in the coMLN. Conversely, following exposure of the colon to UV light kaede-red$^+$ DCs were found only in the coMLNs, not in the siMLNs after both 24 and 48 hours (Figure 3.3). Therefore, consistent with the results with Evans blue, the anatomy of the afferent lymphatics dictates that DCs that originate in the SI drain to siMLNs, while DCs that originate in the colon drain to the coMLN. We have now clearly demonstrated, using two methods, that DCs from the SI and colon migrate to distinct areas of the MLN. Future investigations can now more precisely identify changes in cell populations that occur after interventions that specifically affect the immunology of the SI or colon.

3.2.2 Validation of Kaede Mice as a Tool to Observe DC Migration

Initial studies using transgenic kaede mice showed these to be an invaluable reagent for the investigation of DC migration. However, an important issue to address before further work was performed on these animals was to determine whether photoconversion might affect DC functions. There have been multiple studies using photoconversion of kaede mice, all of which have shown that photoconversion does not cause increased apoptosis or cell activation (Schmidt et al., 2013) (Tomura et al., 2008) (Bennett et al., 2013). These studies have been completed in either T or B cells. It was therefore essential to investigate the effect of photoconversion on DCs, particularly as stimulation of DCs can lead to increased migration from tissues to draining LNs (Turnbull et al., 2005; Yrlid et al., 2006c). Additionally we made use of a different low power UV light source than previous studies. The levels of CD80 and CD86 expression on DCs provide a measure for the level of activation of a DC. In this study BMDCs were generated using the DC specific growth factor Flt3L (Naik et al., 2005);

alternative methods for generating DCs using CSF-2 and IL-4 generate cells with a phenotype similar to inflammatory DCs rather than steady-state DCs (Naik et al., 2005). Photoconversion did not cause an increase in cell death (data not shown), or an increase in the expression of CD80 or CD86 (Figure 3.4). This suggests that photoconversion does not result in increased activation of DCs.

Another important concern regarding our experiments using kaede mice is how the laparotomy will influence DC behaviour. Previous experiments in our laboratory have investigated how MLNx affects DC activation. Although MLNx is a more invasive procedure, it begins with a laparotomy, similar to our photoconversion experiments. During these experiments there was no significant difference in the numbers of DCs in the siLP following MLNx (V. Cerovic, personal communication). In collaboration with the Mowat laboratory we investigated a model of post-operative ileus, we did not find any significant changes in the percentage of DC subsets in the SI following this procedure (C. Scott, personal communication). Therefore, it is unlikely that this less invasive photoconversion procedure will result in changes to DC populations migrating from either the SI or colon.

As we have established that kaede mice provide a suitable model to investigate DC migration in the intestine, we then investigated MHCII expression on migratory DCs in the MLN. Several groups have observed higher levels of MHCII expression in migratory DCs in LNs. It was first noted by Salomon *et al*. who identified that $MHCII^{hi}CD11c^{+}$ cells were the only cells able to transport FITC to draining LNs following FITC painting in the skin (Salomon et al., 1998). In comparison the $MHCII^{+}CD11c^{hi}$ population were labelled with FITC following i.v injection with FITC dextran, suggesting they were derived from blood borne precursors (Salomon et al., 1998). Although they claimed that the $MHCII^{hi}CD11c^{+}$ population was not responsive to Flt3L, suggesting this is not a bona-fide population of DCs, the authors only completed a relatively short-term exposure to Flt3L, only seven days. In order to observe an expansion of DCs in intestinal tissue exposure to Flt3L for up to nine days is required, therefore I suggest with longer exposure to Flt3L this $MHCII^{hi}CD11c^{+}$ population may expand. In the lung only $MHCII^{hi}CD11c^{+}$ cells were observed carrying FITC conjugated macromolecules to the thoracic LNs following intratracheal instillation

(Vermaelen et al., 2001). The convention of gating migratory DCs as $MHCII^{hi}CD11c^{+}$ has been continued in the MLN (Persson et al., 2013), although there has been no direct evidence that migratory DCs all belong to the $MHCII^{hi}$ phenotype in the intestine. Therefore, we sought to determine if migratory DCs in the intestine also displayed higher levels of MHCII in the MLN compared to resident DCs. Following photoconversion of the SI or colon, kaede-red^{+} cells were found only in the $MHCII^{hi}CD11c^{+}$ gate not the $MHCII^{+}CD11c^{hi}$ gate (Figure 3.5). This confirms that migratory DCs in the intestine have higher expression of MHCII, similar to migratory DCs in the skin and lung. Previous work in the intestine has also shown that following DC stimulation via LPS and αCD40 the distinction between $MHCII^{hi}CD11c^{+}$ and $MHCII^{+}CD11c^{hi}$ is lost (Persson et al., 2013). As the distinction between $MHCII^{hi}CD11c^{+}$ and $MHCII^{+}CD11c^{hi}$ was apparent in the MLN following photoconversion, it further suggests that there is no overt inflammation caused by photoconversion (Figure 3.5). Another important conclusion that can be drawn from this experiment is the lack of kaede-red^{+} DCs in the $MHCII^{+}CD11c^{hi}$ blood derived DC population in the MLN. This shows that all kaede-red^{+} DCs are derived from intestinal tissue, not from photoconversion of DC precursors in blood vessels overlying intestinal tissue that may then be photoconverted and migrate to the MLN (Figure 3.5). Indeed, in our hands, photocoversion of $CD45^{+}$ cells in blood was extremely inefficient with no photoconverted cells detected after two minutes (data not shown). In fact, after 24 and 48 hours there were no kaede-red^{+} DCs in other peripheral LNs such as the CLN or PLN. This would suggest that DC precursors in the blood are not converted and then migrate to LNs other than the MLN. Furthermore, it suggests that DCs do not migrate out of the LN once they reach the MLN.

3.2.3 Identification of DC subsets in the Small Intestine, Colon and Draining Lymph Nodes

Before investigating differences in DC populations between the siMLN and coMLN, it was necessary to first identify DC populations in the organ of interest. This allowed the comparison of tissues with the draining LNs. There has been some confusion in recent years in defining DCs in the both the SI and colon. This is due to phenotypic and functional overlap between DCs and macrophages. As both populations display the classical DC markers of MHCII and CD11c, it is essential that CD64 (Bain et al., 2013; Tamoutounour et al., 2012) or F4/80 (Bain

et al., 2013; Cerovic et al., 2012) be included in the analysis to exclude macrophages. Previously, CD103 has been used as a *de facto* marker of DCs in the SI and colon (Coombes et al., 2007; Johansson-Lindbom et al., 2005; Schulz et al., 2009; Sun et al., 2007). However the collection of pseudo-afferent lymph following TDC reveals that there are four phenotypically and functionally distinct subsets of DCs, identified by their expression of CD103 and CD11b, including two $CD103^-$ subsets (Cerovic et al., 2012). After excluding B cells, DCs are the only $MHCII^{hi}CD11c^+$ cells migrating in lymph, therefore we can be confident that these $CD103^-$ cells are genuine DCs. Additionally they are able to prime naïve T cells, induce the expression of gut homing molecules on responding T cells, expand in response to Flt3L and express CCR7 (Cerovic et al., 2012). The $CD103^-CD11b^+$ subset also expresses intermediate levels of the chemokine CX3CR1 (Cerovic et al., 2012). Although the levels of expression on $CD103^-CD11b^+$ DCs were not as high as intestinal macrophages, the expression of CX3CR1 has lead to much confusion in the identification of DCs. We and others, do not find $CX3CR1^{hi}$ cells in intestinal lymph (Schulz et al., 2009). However, Diehl *et al*. have recently described $CX3CR1^{hi}CD103^-$ cells in intestinal lymph both in the steady state and after treatment with antibiotics (Diehl et al., 2013). Careful analysis of the data reveals that it is extremely improbable that these $CX3CR1^{hi}$ cells represent a population of migratory macrophages. Instead, it is likely that the $CX3CR1^{hi}$ cells reported by Diehl *et al*. have been misidentified, and the cells they find are in fact $CD103^-CD11b^+$ $CX3CR1^{int}$ migratory DCs.

Following the isolation of cells from the siLP, and the exclusion of $F4/80^+$ macrophages from our analysis by excluding $F4/80^+$ cells, there were four distinct subsets of DC present (Figure 3.6). The most numerous were the $CD103^+CD11b^+$ population, followed by the $CD103^+CD11b^-$ population of DCs. Previous work has identified $CD103^+$ DCs in the intestine (Coombes et al., 2007; Johansson-Lindbom et al., 2005; Schulz et al., 2009; Sun et al., 2007). These were shown to play essential roles in the generation of $Foxp3^+$ Tregs and in the generation of gut homing T cells (Coombes et al., 2007; Jaensson et al., 2008; Sun et al., 2007). These $CD103^+$ DCs have also been shown to respond to Flt3L and derive from a pre-DC precursor (Bogunovic et al., 2009; Varol et al., 2009). Recent work by Farache *et al*. claimed $CD103^+$ DCs extend dendrites to carry bacteria from the SI in the steady-state (Farache et al., 2013). These studies

used 2-photon microscopy to identify $CD11c^{YFP+}CX3CR1^{GFP-}$ cells that are described as $CD103^+$ DCs. However, they do not directly show that $CD103^+$ DCs extend dendrites at any point. While these data may represent an interesting way in which particulate antigen can gain access to the LP, further work is required to verify what type of cells are mediating antigen uptake. Previous studies using 2-photon microscopy have shown there to be marked differences in the formation of transepithelial dendrites based upon mouse strain and in the location of formation of these dendrites (Chieppa et al., 2006) (McDole et al., 2012; Vallon-Eberhard et al., 2006). Therefore careful examination of observations is required to ensure the formation of dendrites is a genuine phenomenon, not a result of the methods used to isolate intestinal tissue for observation by 2-photon microscopy. Another recent paper describes how $CD103^+$ DCs interact with goblet cells to take up soluble antigen; similar to Farache *et al*. they made use of CD11c-YFP CX3CR1-GFP animals. These do not allow adequate identification of $CD103^+$ DCs in the LP, therefore caution should be observed when interpreting these results (McDole et al., 2012). Interestingly, McDole *et al*. did not identify the formation of trans-epithelial dendrites, although they used the same mouse model as Farache *et al*.

$CD103^+$ DC subsets have also been previously identified by their expression of CD11b, with $CD103^+CD11b^+$ and $CD103^+CD11b^-$ DCs being described (Bogunovic et al., 2009; Schulz et al., 2009; Varol et al., 2009). Recently, the $CD103^+CD11b^+$ DC population has also been shown to be dependent upon the IRF4, and these cells were essential for producing IL-6 in order to drive Th17 cell differentiation in the MLN (Persson et al., 2010). In our hands, the $CD103^+CD11b^-$ LP population was also able to express $CD8\alpha^+$. This population is dependent upon the transcription factor BatF3 (Edelson et al., 2010) and Jang *et al.,* reported this population was depleted in $CCR7^{-/-}$ mice (Jang et al., 2006). However the anatomical origin of this population has been a much debated, with many identifying it as a population originating in the SILT rather than the siLP due to the fact it is not found in $Id2^{-/-}$ animals which lack secondary lymphoid tissues (Bogunovic et al., 2009; Ginhoux et al., 2009). This is an issue that will be addressed in the following chapters.

Consistent with our findings in pseudo-afferent lymph and siLP, we also identify two populations of $CD103^-$ DCs (Figure 3.6). The $CD103^-CD11b^+$ population which express intermediate levels of CX3CR1 was identified, and has previously been shown to induce not only IFN-γ but also IL-17 expression in responding T cells. We also identify $CD103^-CD11b^-$ DCs in the siLP; these are similar to the $CD103^-CD11b^+$ DCs as they also induce IL-17 but not IFNγ. Furthermore, they are not $CX3CR1^+$ (Cerovic et al., 2012). In conclusion, here we are able to conclusively identify four distinct populations of DCs in the siLP.

The identification of DCs in the cLP has been less well documented. Rivollier *et al*. identified two populations of $MHCII^{hi}CD11c^+$ cells, expressing either intermediate or undetectable levels of F4/80 (Rivollier et al., 2012). These populations were further analysed for their expression of CD103 and CD11b. The $F4/80^{int}$ population contained populations of $CD103^+CD11b^+$ and $CD103^-CD11b^+$ cells while the $F4/80^-$ population contained only $CD103^+CD11b^-$ DCs. All these cells were able to present antigen to naïve T cells, but the $F4/80^{int}$ $CD103^-$ population was shown to be monocyte derived, and accumulated following colitis. Varol *et al*. also identified populations of $CD11c^+$ DCs; $CD103^+CD11b^-$ and $CD103^+CD11b^+$ DCs that they showed to be derived from a Flt3 dependent pathway, distinct from CX3CR1hi monocyte derived cells (Varol et al., 2009). Similarly, I have identified two populations of $F4/80^-CD103^+$ DCs in the colon (Figure 3.7). In comparison to the SI, the most numerous was the $CD103^+CD11b^-$ population. In the SI this is identified as the CD8α population, however due to the enzyme digest required to release these cells from colonic tissue, this population it is no longer $CD8\alpha^+$ (A. Aumenier personal communication). The $CD103^+CD11b^+$ subset was still present, but was a much smaller component of the overall DC population than in the SI. In contrast to the previous papers I also identify a population of $F4/80^-CD103^-CD11b^+$. This is phenotypically similar to the SI population, and recent work by Bain *et al*. has shown these do not develop from monocytes, but expand in response to Flt3L (Bain et al., 2013).

In the siMLN and coMLN we identified four distinct populations of both resident and migratory DCs (Figure 3.8). Surprisingly, although there was a small increase in $CD103^+CD11b^+$ DCs in the siMLN compared to the coMLN this was not significant. This was unexpected as $CD103^+CD11b^+$ DCs are the major population

of DCs present in the siLP. Similarly, compared to the siMLN there was an increase in coMLN $CD103^+CD11b^-$ DCs, the most numerous cLP DC population but this was not significant. There were significantly more migratory $CD103^-CD11b^+$ DCs in the siMLN compared to the coMLN. Interestingly there were significantly fewer migratory $CD103^-CD11b^-$ DCs in the coMLN compared to the siMLN, mirroring the reduction of this population in the cLP. This $CD103^-CD11b^-$ population appeared to be blood derived in the coMLN, as there were significantly more $CD103^-CD11b^-$ DCs in the $MHCII^+CD11c^{hi}$ blood-derived 'resident' DC gate than in the $MHCII^{hi}CD11c^+$ 'migratory' gate (Figure 3.8).

As we have previously shown that $CD103^-CD11b^+$ DCs are $CX3CR1^{int}$, I sought to compare levels of CX3CR1 expression between DC subsets in the siMLN and coMLN. Consistent with our previous work, migratory $CD103^+CD11b^-$ and $CD103^-CD11b^-$ were $CX3CR1^-$. Surprisingly, we found significantly higher expression of CX3CR1 on $CD103^-CD11b^+$ migratory DCs in the coMLN than in the siMLN (Figure 3.9). Furthermore, approximately half of migratory $CD103^+CD11b^+$ in the coMLN expressed CX3CR1 at intermediate levels, whereas very few $CX3CR1^+$ DCs were observed among this subset in the siMLN. The significantly higher proportion of $CD103^+CD11b^+$ and $CD103^-CD11b^+$ DCs expressing CX3CR1 in the coMLN was also observed in resident $MHCII^+CD11c^{hi}$ DCs in the coMLN. Within the resident DC population $CD103^-CD11b^-$ DCs expressed intermediate levels of CX3CR1 in both the siMLN and coMLN. The expression of CX3CR1 on DC subsets was an intriguing finding; a previous report suggested there was no difference in the proportion of $CX3CR1^+$ in $CCR7^{-/-}$ mice (Bogunovic et al., 2009). However, as DCs only express intermediate levels of CX3CR1 it is likely they were included in this analysis. Furthermore, this analysis may have missed some coMLNs that are not part of the main MLN chain, thus mainly analysing the siMLN DC populations.

Although the exact role of CX3CR1 is unknown, it has been suggested to play a role in cell survival in monocytes as the enforced expression of the antiapoptotic factor Bcl2 reverses the reduced monocyte phenotype observed in CX3CR1 deficient animals (Landsman et al., 2009). The role of CX3CR1 in inflammation is more complicated, with both pro-inflammatory and anti-inflammatory effects reported being reported. Following the stimulation of colonic DCs with CX3CR1 there is increased release of TNFα and IL-6. Conversely, inflammatory cell

infiltration and iNOS expression were reduced following the induction of DSS colitis in CX3CR1 deficient mice (Niess and Adler, 2010) (Kostadinova et al., 2010). However, its differential expression between the siMLN and coMLN is likely to be due to environment differences between the SI and colon. A major environmental difference between the SI and colon is the increased microbial load in the colon. To determine if this is the reason for increased expression of CX3CR1, DC subsets could be isolated from newborn mice that have not yet been colonised by the microbiota. Adult mice could be given antibiotics to reduce their microbial burden, and the levels of CX3CR1 on DC subsets from the siMLN and coMLN could be compared. Alternatively the microbial burden in the SI could be increased by the infection of bacteria that preferentially colonise the SI. Therefore, if the expression of CX3CR1 in DCs was affected by the presence of bacteria the levels of CX3CR1 expression in DC subsets from the siMLN would be similar to the coMLN.

3.2.4 Thoracic Duct Cannulation of Partially Mesenteric Lymphadenectomised Animals

Following the identification of these differences between the siMLN and coMLN, partial MLNx procedures were carried out. Previously, the MLNx that precedes TDC removed the entire MLN chain (Figure 3.10). I have shown these lymph nodes collect lymph not only from the SI, but also from some areas of the proximal colon. Therefore, partial MLNx procedures were performed to remove only the siMLN and others to remove only the coMLN. This will allow the unequivocal identification of migratory DC subsets from the SI and colon. TDC of mice which had undergone siMLNx revealed a significantly increased proportion of $CD103^+CD11b^+$ DCs in lymph, while lymph from coMLNx animals had significantly more $CD103^+CD11b^-$ DCs, reflecting the situation in the siLP and cLP. In comparison to the MLN, the increase in $CD103^+CD11b^+$ DCs in the siMLN and the corresponding increase of $CD103^+CD11b^-$ DCs in the coMLN were now significant (Figures 3.11). This may be due the fact that we only analyse cells directly migrating from the cLP or siLP, therefore there is likely to be little contamination from blood derived precursors. The $CD103^-CD11b^-$ population of DCs appeared to be missing following coMLNx, however the number and percentage was not significantly different to siMLNx. As the FACS plots look remarkably different, with further repeats I would suggest this would become a

statistically significant difference but due to the small size of the population this was not reflected with only five replicates. These results show that there are significant differences in the phenotypic characteristics of the DC populations that continuously migrate to the MLN from the SI and colon. In order to further investigate these subsets it could be possible to increase the rate of migration from the LP to the MLN using R848, to determine if the ratio of DC subsets in the MLNs become more similar to the ratio of DCs in the LP.

To investigate if there was any difference in the function of DCs from the siLP and cLP, total DCs were FACS sorted following TDC. Due to the small number of DCs isolated following coMLNx total $MHCII^{+}CD11c^{+}$ cells were purified to allow direct comparison between siMLNx and coMLNx DCs. This does not allow the comparison of individual subsets between the SI and colon, due to the small number of cells collected. Total lymph DCs were FACS sorted from siMLNx and coMLNx animals and cocultured with naive OT-I T cells. DCs from siMLNx and coMLNx induced the proliferation of naïve T cells equally well (Figure 3.12). To further investigate T cell priming by siMLN and coMLN DCs, the expression of CCR9 on responding T cells was compared between lymph DCs from siMLNx'd and coMLNx'd animals. DCs from siMLNx and coMLNx animals caused the retention of CCR9 on responding T cells equally well (Figure 3.13). DCs from MLN have previously been reported to support the expression of gut homing receptors such as CCR9 and $\alpha4\beta7$ (Annacker et al., 2005; Jaensson et al., 2008; Johansson-Lindbom et al., 2005; Stagg et al., 2002). However, previous work has shown that DCs purified from the colon were unable to cause the retention of CCR9 on responding T cells (Jaensson et al., 2008). In this study DCs from the MLN were still able to cause the retention of CCR9, and as T cells are essential to resolve colitis, I think it is likely that colonic DCs are able to cause the retention of CCR9 expression on responding T cells. Therefore the harsh enzymatic digestion required for the colon may affect the ability of these cells to interact with T cells and cause the retention of CCR9. Alternatively, the ability to cause the retention of CCR9 expression on responding T cells may develop in DCs only once they leave the cLP. In order to determine the fate of T cells that had been primed in the coMLN we could make use of the kaede system. Using these mice we could photoconvert entire coMLNs, then follow the journey of responding T cells at various time points.

3.2.5 Effects of Experimental Colitis Upon Dendritic Cell Subsets in the Small Intestinal or Colonic Draining Mesenteric Lymph Nodes

To investigate differences in siMLN and coMLN DCs, adding DSS to the drinking water induced colonic inflammation, and DC subsets in the siMLN and coMLN were investigated. Although recent work has suggested that DSS colitis is driven mainly by Ly6C^{hi} monocytes (Bain et al., 2013), previous work (Rivollier et al., 2012; Tamoutounour et al., 2012; Zigmond et al., 2012) identified a population of monocyte derived inflammatory DCs that increased in number following the induction of DSS colitis. We employed a recovery model of DSS colitis, to allow us to follow cell populations over an extended period of time. The increase in cell number in the colitic colon, observed by many, was not mirrored in the coMLN. Furthermore, there was no significant difference in the number of DCs isolated in the coMLN of colitic animals compared to the siMLN or to control animals (Figure 3.14). Nor was there any change in the composition of DC subsets identified by their expression of CD103 or CD11b (Figure 3.15). This and other recent work has used CD64 to distinct populations of monocytes/macrophages and DCs (Bain et al., 2013; Tamoutounour et al., 2012). As these arise from different developmental pathways and have different functions it is essential these cells be considered separately from DCs. There was no significant difference in the number of CD64^{+}CD11b^{+}CX3CR1^{+} during colitis, or recovery, in the siMLN or coMLN (Figure 3.16). This result is in contrast with the data published by Tamoutounour *et al.* who find a rapid accumulation of blood derived CD64^{+} monocytes in the MLN following T cell mediated colitis (Tamoutounour et al., 2012). Similarly, Siddiqui *et al.* observe an increase in E-cadherin^{+} monocytes in the MLN of mice with experimental colitis (Siddiqui et al., 2010). The difference between our observations and others may be due to the type of colitis induced; we used DSS to induce colitis while other reports have used a T cell transfer model (Siddiqui et al., 2010; Tamoutounour et al., 2012). Another key difference may be the duration of the induced inflammation. In our model DSS was added to drinking water for three days. In the T cell transfer model of colitis, inflammation was observed four weeks after the introduction of CD4^{+}Foxp3^{-} T cells. In contrast to previous reports that suggested these CD64^{+} monocytes were blood derived, Zigmond *et al.* report a population of CX3CR1^{+} cells that migrate to the MLN via lymph following 9 days of DSS

treatment (Zigmond et al., 2012). However, from their data it is unclear if these cells have arisen from inflammatory monocytes or are CX3CR1^{int} DCs. The elevated ability of CX3CR1^{+} cells to induce the proliferation of naïve T cells suggests these cells have been misclassified as macrophages, and actually represent the CX3CR1^{int} DCs we have shown to migrate in pseudo-afferent lymph (Cerovic et al., 2012). However, in order to precisely compare the populations of cells we find with Zigmond *et al*. it would be interesting to repeat our DSS model with 9 days of recovery. Furthermore by including additional markers, such as CD64, we could with confidence determine if these cells are DCs or macrophages.

3.2.6 Comparison of Antigen Presentation By Dendritic Cell Populations from the Small Intestinal and Colonic Draining Mesenteric Lymph Nodes

As we could not detect differences in the phenotype of the DCs in the siMLN and coMLN following colonic inflammation, we next sought to determine if siMLN and coMLN DCs acquired antigen from different anatomical locations. Although the exact mechanism by which soluble antigen gains access to the LP is unclear, there are many previous reports showing that DCs in the siLP are able to acquire soluble antigens (Chirdo et al., 2005). In fact, there is mounting evidence that antigen uptake by DCs in the LP is essential for the induction of tolerance to soluble antigens (Pabst and Mowat, 2012). We predicted that by orally administering only a small amount of antigen, the majority would be taken up in the SI before it reached the colon. In the first experiment, CD45.1 OT-II cells from the MLN and spleen were transferred into a CD45.2 host. 24 hours later the host was fed with OVA (10 mg), and three days after this levels of proliferation in the siMLN, coMLN and ILN were investigated. T cell proliferation was only detected in the siMLN (Figure 3.17). Thus, soluble OVA appears to be taken up preferentially in the SI, and this is presented specifically in the siMLN. This could reflect the *in vivo* situation that leads to generation and maintenance of oral tolerance. An interesting comparison could be drawn following the intra-rectal administration of OVA, which would presumably be absorbed by the colon. T cell proliferation in coMLN could then be compared to siMLN.

We modified this experiment to gain further insight into this process. This time LNs were analysed 24, 48 and 72 hours after OVA administration. After 24 hours there was no OT-II proliferation in any LNs (Figure 3.17). This was not unexpected as BrdU experiments indicate migratory DCs take between 24 and 48 hours to reach the MLN (Liu et al., 1998). Therefore this time point may have been too early to detect proliferation. After 48 hours proliferation was detected in both the siMLN and coMLN, but not the ILN (Figure 3.17). Although there was more proliferation in the siMLN than the coMLN, this was unexpected as our previous result suggested that SI DCs in the siMLN would present small amounts of soluble antigen and therefore only cause proliferation of T cells in the siMLN. The proliferation of T cells in the coMLN was perhaps a result of OVA passing into, and being taken up in the colon. Alternatively T cells have already begun to migrate back to the intestine. After 72 hours CFSE was completely diluted in the siMLN, coMLN and ILN. At this point the antigen and T cells are likely to have been transferred to systemic circulation. This dissemination of soluble antigen was not completely unexpected, as food protein can be detected in the blood of mice and humans after eating (Pabst and Mowat, 2012).

We decided to make use of transgenic 232-4 mice that express cytoplasmic OVA only in SI enterocytes (Vezys et al., 2000). DCs from the 232-4 siMLN were able to induce proliferation of OT-I T cells, while DCs from the coMLN were unable to induce the proliferation of OT-I T cells. These results demonstrate that antigen acquired in the SI is initially only presented to T cells in the siMLN (Figure 3.20). These data show that there is not only anatomical segregation between lymphatic drainage from the SI and the colon, but also that these distinct MLNs are functionally separate. Antigen expressed in the SI is only presented by DCs, and only causes proliferation of naïve T cells, in the siMLNs (Figure 3.20). Therefore, in future it will be beneficial to isolate and analyse these distinct MLNs separately. Independent analysis of the siMLN and coMLN will enable a more refined understanding of intestinal immune responses and is likely to lead to novel insights regarding the immunological differences between the SI and colon.

3.3 Conclusions

Here, using two distinct models, I have shown that the SI and colon drain to distinct LNs that can be analysed separately. In the future careful examination of populations of cells in these distinct LN may reveal novel phenotypic differences in the differences between immune response in the SI and colon.

In terms of DCs, I identified that there were distinct differences in the subset composition of DCs migrating from the SI and colon that I have outlined above. One of the most striking differences between the siLP and cLP, which was reflected in the lymph and coMLN to an extent, was the reduction of $CD103^-$ $CD11b^-$ DCs in the colon. We have previously shown that these cells specifically induce the production of IL-17 producing T cells in the absence of any overt stimulation (Cerovic et al., 2012). Recent work has shown that mice deficient in Th17 cells were unable to produce T cell dependent antigen specific IgA (Hirota et al., 2013). Therefore the lack of this subset in the colon may reflect a difference in the way IgA is produced between the SI and colon. This could reflect an interesting difference in the way the SI and colon respond to particulate antigen, such as microorganisms. However, much further work should be completed in order to determine the functional consequences of this.

Another interesting difference between DC subsets from the siMLN and coMLN was in the expression of CX3CR1. Specifically $CD103^+CD11b^+$ DCs from the coMLN expressing CX3CR1 while siMLN $CD103^+CD11b^+$ DCs did not express CX3CR1. This could be due to a number of reasons, such as environmental factors including the microbial burden. However, recent work in the Mowat laboratory has suggested that there may be a developmental continuum between $CD103^-CD11b^+$ DCs and $CD103^+CD11b^+$ DCs in the LP (C. Scott, personal communication). As $CD103^-CD11b^+$ DC express CX3CR1 in both the SI and colon, the increased expression of CX3CR1 in colonic $CD103^+CD11b^+$ DCs may reflect the fact that these have developed from $CD103^-CD11b^+$ DCs but have not yet downregulated CX3CR1. An interesting way to test this could be by the adoptive transfer of labelled DC precursors with detailed phenotypic analysis of the markers these cells begin to express and the markers they begin to downregulate. Further work to investigate the factors that trigger this development should be completed.

The siMLN and coMLN are functionally distinct with antigen expressed in the SI only being presented and causing proliferation of naïve T cells siMLNs. The siMLN and coMLN are likely to be exposed to different environmental antigens leading to DCs being conditioned differently. For example DCs in the SI are likely to be exposed to more dietary ligands, such as vitamin A, which is essential for the generation of $Foxp3^+$ Tregs (Mucida et al., 2009). In comparison DCs from the colon are likely to be exposed to more microbes than the SI, as the microbial burden is highest in the colon. Therefore, DCs from the colon may be better at inducing class cell switching of B cells to produce IgA than DCs from the SI, which may be better at inducing Tregs. In order to test this DCs from the SI or colon could be isolated and co-cultured with naïve T cells and the ability of these DCs to induce $Foxp3^+$ Tregs could be determined. The immune response to pathogens that preferentially colonise either the SI or the colon is likely to differ between the siMLN or coMLN, therefore infection models could be investigated.

Therefore, in future the siMLN and coMLN should be isolated and analysed separately. Independent analysis of the siMLN and coMLN will enable a more refined understanding of intestinal immune responses and is likely to lead to novel insights regarding the immunological differences between the SI and colon.

Chapter 4: Dendritic Cell Migration in Mice Lacking Peyer's Patches and Isolated Lymphoid Follicles

The organised lymphoid structures of the intestine, the PPs and ILFs, represent unique and distinct immune environments. They form along the antimesenteric axis of the SI. Cells in the PPs take up and process both soluble and particulate antigen (Kelsall and Strober, 1996). Additionally, PPs and ILFs are the only tissues with fully differentiated and functional M cells. They are therefore key locations for antigen acquisition in the SI. They also share a similar cellular composition, as they are predominantly filled with B cells and have germinal centres. Therefore, PPs and ILFs are assumed to be inductive sites for intestinal immune reactions.

Although there are many similarities between PPs and ILFs, a key difference between the structures is in their development. Although they share many of the same key developmental traits, the timing of their development differs. While PPs develop *in utero* CPs and ILFs develop post-natally. The presence of PPs in the SI is stable and is determined pre-natally while the development of ILFs is dynamic and may change in response to microbial, parasitic or viral load. Therefore, although PPs and ILFs both play important roles in inducing intestinal immune responses they must be considered as separate tissues.

Despite persistent speculation, there has been no definitive evidence to indicate whether DCs migrate from PPs and ILFs to the MLN. Recently, we described a population of DCs that express CD8α and migrate from the intestine to the MLN (Cerovic et al., 2012). Previously, the expression of CD8α was assumed to be limited to a population of blood-derived LN resident non-migratory population of DCs (Jakubzick et al., 2008) (Edelson et al., 2010). Therefore we sought to determine whether DCs are able to migrate from PPs and ILFs to the MLN. We were particularly interested in these migratory $CD103^+CD11b^-CD8\alpha^+$ DCs, as well as investigating the three other phenotypically and functionally distinct intestinal migratory DC subsets; $CD103^+CD11b^+$, $CD103^-CD11b^+$ and $CD103^-CD11b^-$ DCs. In order to complete these experiments I used two different mouse models

that lack different gut associated lymphoid tissues (GALT). I first used RORγt knock out mice that lack both PP and ILFs. Second, mice that lack only PPs but retain ILFs were generated by *in utero* exposure to LTBR-Ig, allowing the investigation of DCs migration from ILFs.

Using these two animal models, the precise anatomical origins of migratory DCs can begin to be elucidated. This will provide further insight into how DCs in the intestine can be manipulated or targeted for the development of new oral vaccines or the treatment of inflammatory bowel disease.

4.1 Results

4.1.1 Genotyping of RORγtCD3ε and CD3ε Deficient Mice

Recently Peter Lane and colleagues have developed a strain of CD3εtg26RORγt$^{neo/neo}$ (referred to as RORγtCD3ε mice, or RORγt deficient mice for the purposes of this report) mice by crossing RORγt$^{neo/neo}$ mice with CD3εtg26 (CD3ε) mice (referred to as CD3ε mice for the purposes of this report). RORγt deficient mice lack lymph nodes, PPs, and ILFs, due to the absence of LTi cells. Transgenic mice lacking murine CD3ε show completely abrogated T cell development. The combined phenotype of the RORγtCD3ε mice is a lack of T cells, NK cells and LTi cells, and the absence of MLNs, PPs and ILFs. These mice, however, still have DCs in the intestine; therefore any DCs migrating to the MLN will be LP derived.

Initially it was necessary to ensure the mice we received were of the expected genotype and phenotype to set up breeding pairs. Blood samples were taken from the tail vein of RORγtCD3ε and CD3ε deficient mice, the whole blood was processed and stained for CD3 and B220 to visualise T and B cells by flow cytometry. T and B cells were gated as live cells (Figure 4.1 A) and the presence of CD3$^+$ and B220$^+$ cells was compared (Figure 4.1 B). A B220$^+$ population was observed, however there were no CD3$^+$ cells (Figure 4.1 B). As there did not appear to be a population of T cells in either the RORγtCD3ε or CD3ε deficient mice it was assumed that these mice were of the correct phenotype.

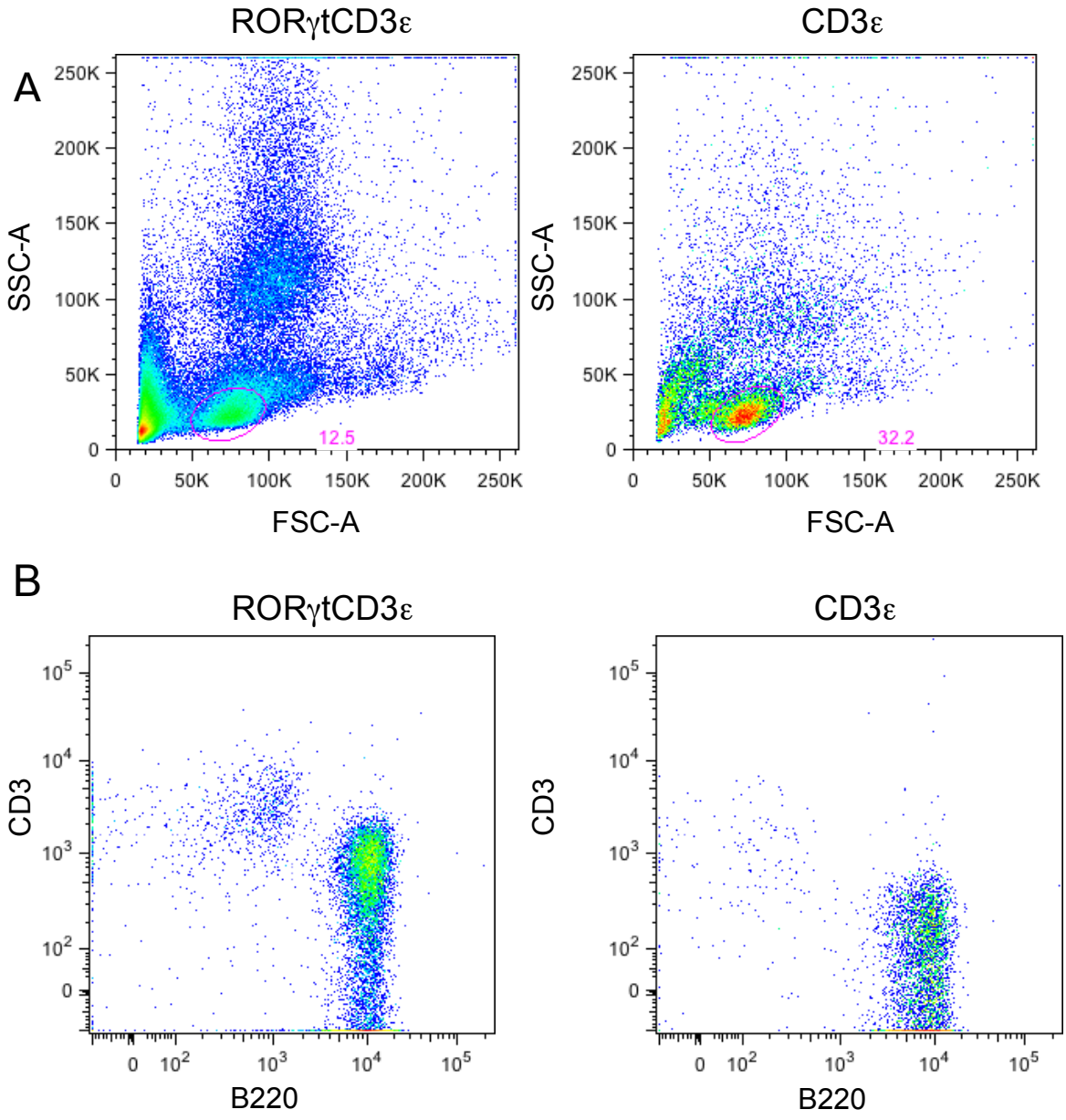

Figure 4-1 The Absence of CD3$^+$ Lymphocytes in blood samples from RORγtCD3ε and CD3ε deficient mice.

Blood samples were taken from the tail vein from RORγtCD3ε and CD3ε deficient mice, samples were processed and analysed by flow cytometry. Live cells were gated (A) and the presence of CD3$^+$ and B220$^+$ cells was examined (B). Data are representative of 16 RORγtCD3ε and 6 CD3ε deficent mice.

As the mice were of the anticipated phenotype I next wanted to ensure the mice were of the expected genotype. Therefore, a PCR was carried out on genomic DNA to confirm the genotype of these animals. As mice lacking RORγt instead have the neomycin cassette, the presence or absence of RORγt and neomycin was investigated. Tissue samples were collected by ear punch from RORγtCD3ε and CD3ε deficient mice. Genomic DNA was isolated and PCR was carried out. Primers for RORγt were designed using the Primer Blast Program and presented in Table 2.3, primers for neomycin were designed from published sequences. Primers were aligned against the murine database using BLAST (Pubmed) to ensure specificity to only the target sequence. The RORγt primers gave rise to a product with a calculated length of 190 bp and the neomycin primers gave rise to a product of 250 bp. The products of the PCR were run on a 2% agarose gel (Figure 4.2). This showed the samples from RORγtCD3ε deficient mice had the neomycin cassette but not RORγt, while the CD3ε deficient mice expressed RORγt but not the neomycin cassette. Therefore, the animals are of the expected genotype as well as phenotype.

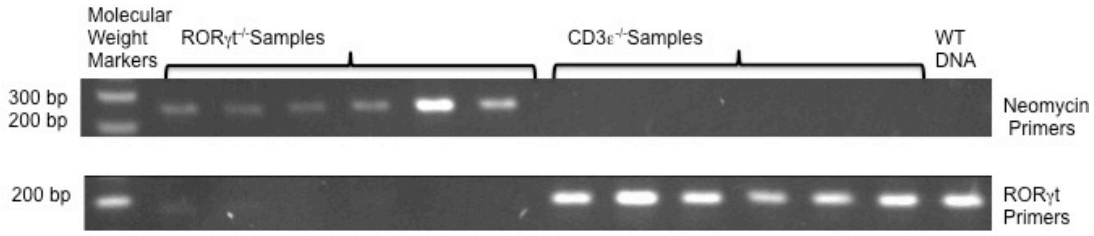

Figure 4-2 The Presence of Neomycin and RORγt Protein in RORγCD3ε and CD3ε Deficient mice.

Tissue samples were collected, genomic DNA was isolated and PCR was carried out on RORγtCD3ε and CD3ε deficient mice. Products were analysed by gel electrophoresis on a 2% agarose gel. Bands indicating expression of neomycin were only detected in RORγtCD3ε deficient mice, while RORγt expression was only detected in CD3ε deficient mice.

4.1.2 Lymphoid Tissue Development in the Small Intestine of RORγt Deficient Animals

These data allowed us to begin to investigate changes in the intestinal immune system of these animals. Firstly, the lack of PPs and ILFs was investigated using immunohistochemistry. RORγtCD3ε deficient mice lack LTi cells and therefore there should be no PPs or ILFs in the SI. In order to confirm this, longitudinal segments of SI were taken from RORγtCD3ε and CD3ε deficient mice and made into Swiss-roll sections. This allowed large areas of the SI to be visualised in one image and therefore an accurate picture of the architecture could be obtained (Moolenbeek and Ruitenberg, 1981; Pabst et al., 2005). Sections were stained with DAPI to visualise all cells, and with anti-B220. As PPs and ILFs contain large numbers of B cells, the B220 stain assists in the identification of these structures. After immunofluorescent staining, multiple overlapping high power images were generated and collated to accurately visualise the detailed architecture of the small intestine (Figure 4.3).

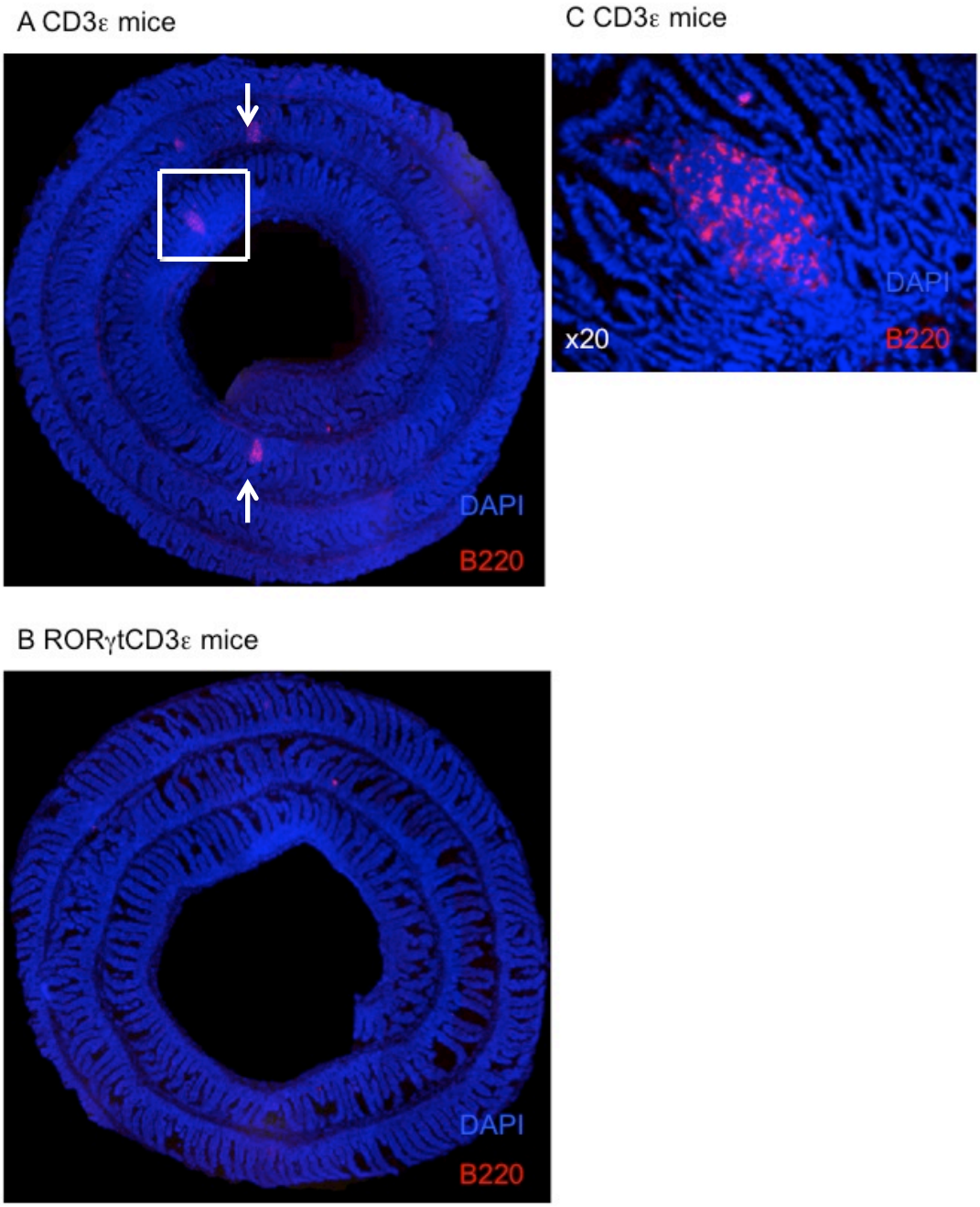

Figure 4-3 Organised Lymphoid Structures Are Absent From the Small Intestine of RORγt Deficient Mice.

Swiss roll sections were prepared from the small intestine of CD3ε mice and RORγtCD3ε deficient mice and stained with B220 to show organised lymphoid structures and with DAPI to show the structure of the intestine. Composite images of intestine from CD3ε mice (A) and RORγtCD3ε deficient mice (B) were assembled from 100-150 individual high-powered images to allow the visualisation of large areas of intestine. White arrows indicate the position of lymphoid aggregates. Selected lymphoid aggregates from CD3ε mice depicted at x20 magnification (C), taken from (A), area in box. Pictures are representative of 8 separate animals.

4.1.3 Dendritic Cell Subsets in Pseudo-Afferent Lymph, Small Intestine and Colon of RORγt Deficient Mice

Immunohistochemical analysis of Swiss-roll sections from RORγtCD3ε and CD3ε deficient mice confirmed the absence of PPs and ILFs in RORγtCD3ε deficient mice. We next investigated migratory DCs originating from the intestine of RORγtCD3ε deficient mice; as there are no GALT, any DCs migrating from the intestine will be derived from the conventional villus mucosa. First, migratory DCs from the intestine were investigated using TDC. Pseudo-afferent lymph from WT, CD3ε and RORγtCD3ε deficient mice were collected. DCs were defined as $CD19^-$ $CD11c^+MHCII^+$ (Figure 4.4 A) and analysis revealed there to be four distinct subsets migrating from the intestine in WT and CD3ε deficient mice, identified by their expression of CD11b and CD103 (Figure 4.4 B). RORγtCD3ε deficient mice had comparable percentages, and numbers of $CD103^+CD11b^+$ and $CD103^-CD11b^+$ DCs to CD3ε and WT mice. However, RORγtCD3ε deficient mice had significantly fewer $CD103^-CD11b^-$ DCs (Figure 4.4 B and C). This suggests that these $CD103^-$ $CD11b^-$ DCs are likely to migrate from either PPs or ILFs, the organised lymphoid structures that are missing in RORγtCD3ε deficient mice.

Importantly and somewhat surprisingly, the $CD103^+CD11b^-$ subset that has been reported to express CD8α was still present in the pseudo-afferent lymph of RORγtCD3ε deficient mice. In order to determine if $CD8\alpha^+$ DCs are able to migrate from the conventional villus mucosa; the expression of CD8α on DC subsets in pseudo-afferent lymph in RORγtCD3ε deficient animals was investigated (Figure 4.5). Four distinct subsets of DCs were gated as previously described and the expression of CD8α on each of these subsets was compared between WT (Figure 4.5A) and RORγtCD3ε deficient mice (Figure 4.5B). This confirmed that the $CD103^+CD11b^-$ DC subset was the only subset that was able to express CD8α. Furthermore, this subset was present in pseudo-afferent lymph from RORγt deficient mice. This shows, for the first time, that $CD8\alpha^+$ DCs are present in the non-organised lymphoid structures of the siLP and are able to migrate from there.

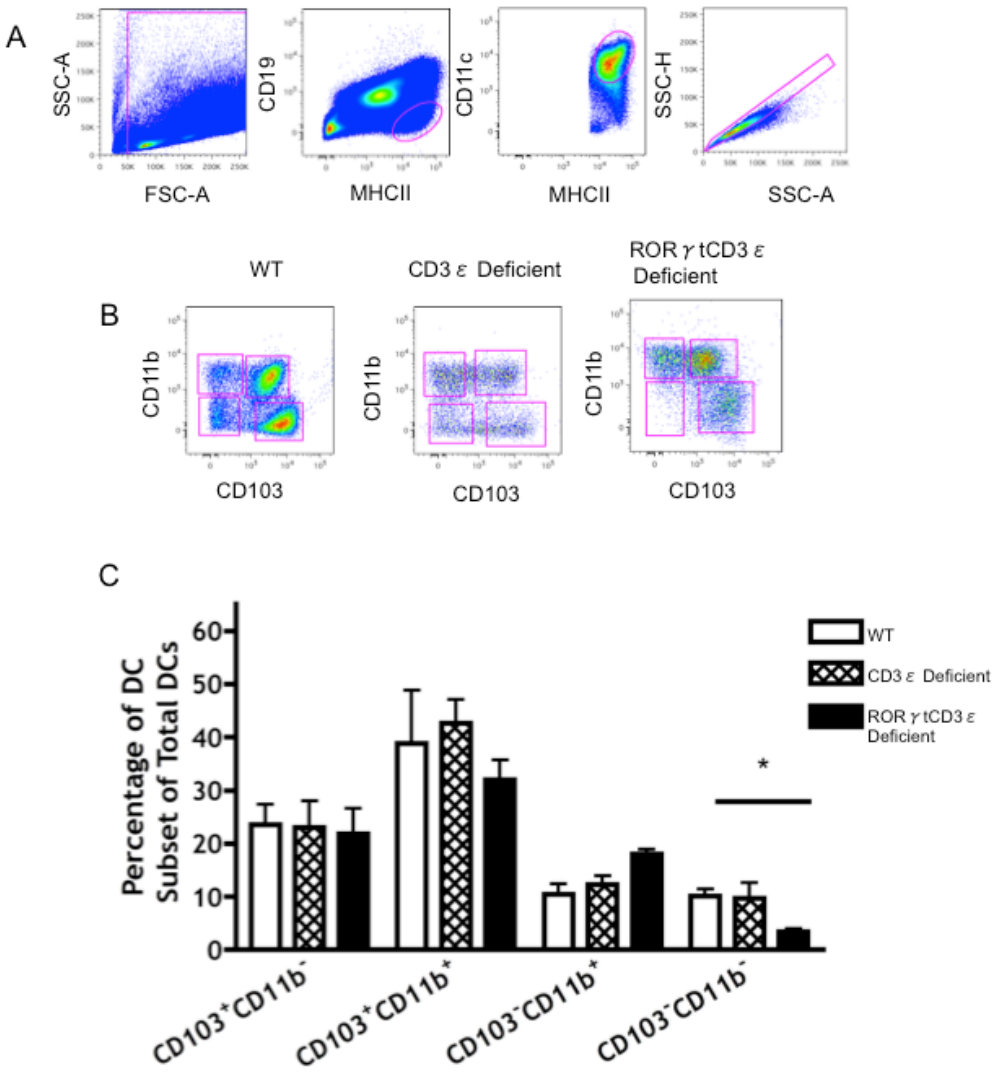

Figure 4-4 CD103$^-$CD11b$^-$ DCs Are Missing From The Lymph of RORγtCD3ε$^-$ Deficient Mice

Pseudo-afferent lymph was collected from WT, CD3ε and RORγtCD3ε deficient mice and analysed by flow cytometry. Large cells were gated, and CD19$^-$MHCII$^+$ cells were gated, and CD11c$^+$ single cells were further selected (A). These DCs were further split into four populations based upon the expression of CD103 and CD11b (B) and these four subsets were compared between WT, CD3ε and RORγtCD3ε deficient mice (C). Data are means and S.E.M. Results were analysed by ANOVA, asterisks denote statistical significance ($p<0.05$, n=6).

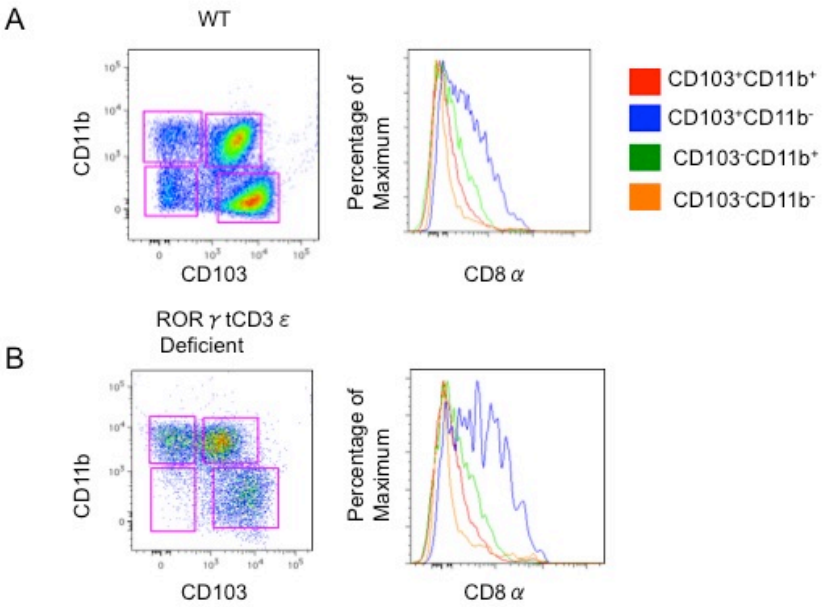

Figure 4-5 Expression of CD8α on Dendritic Cell Subsets in Lymph.

Pseudo-afferent lymph was collected from WT (A) and RORγtCD3ε deficient (B) mice and analysed by flow cytometry. DCs were gated as before and DCs were further split into four populations based upon the expression of CD103 and CD11b. Expression of CD8α on each of these four subsets was compared between WT, RORγtCD3ε deficient mice. Results are representative of at least 4 independent experiments.

Having shown that all DC subsets but the $CD103^-CD11b^-$ subset are present in pseudo-afferent lymph of RORγtCD3ε deficient mice, we first sought to understand whether this reflected the DC subsets that are present in the SI. Thus, the SI was removed, and PPs were discarded from WT and CD3ε mice. Due to the small size of ILFs we were unable to remove these before the digestion, therefore SI digests from WT and CD3ε mice will contain some contaminating ILFs. The SI was digested and a single cell suspension was stained for multi colour flow cytometry. First, large cells were gated, then live $CD45^+$, $MHCII^+$, $CD11c^+$ cells were selected, and doublets were excluded. Finally $F4/80^+$ macrophages were gated out (Figure 4.6 A). DC subsets, identified by their expression of CD103 and CD11b were examined (Figured 4.6 B) and the total numbers of DCs in each subset were compared between WT, CD3ε and RORγtCD3ε deficient mice (Figure 4.6 C). The DC subsets observed in the SI digests reflected what was found in pseudo-afferent lymph. First, there was no significant difference in the percentage or number of $CD103^+CD11b^+$ DCs or $CD103^-CD11b^+$ DCs. As in pseudo-afferent lymph, the $CD103^-CD11b^-$ subset was significantly reduced only in the SI of RORγt deficient mice, meaning this subset is likely to migrate from organised lymphoid structures present in the SI such as ILFs.

$CD103^+CD11b^-$ DCs were observed in the conventional villus mucosa of RORγtCD3ε deficient mice, suggesting that this subset of DCs which express of CD8α is not restricted to lymph nodes. We then sought to confirm these $CD103^+CD11b^-$ DCs express CD8α and are present in the siLP. Therefore, we digested and analysed DC subsets from the siLP of WT (Figure 4.7 A) and RORγtCD3ε deficient mice (Figure 4.7 B) and investigated the expression of CD8α on each of these subsets. As observed in pseudo-afferent lymph, the only major population expressing consistent levels of CD8α was the $CD103^+CD11b^-$ DCs. Although, the few cells left in the $CD103^-CD11b^-$ gate from RORγtCD3ε deficient mice also appeared to express some CD8α (Figure 4.7).

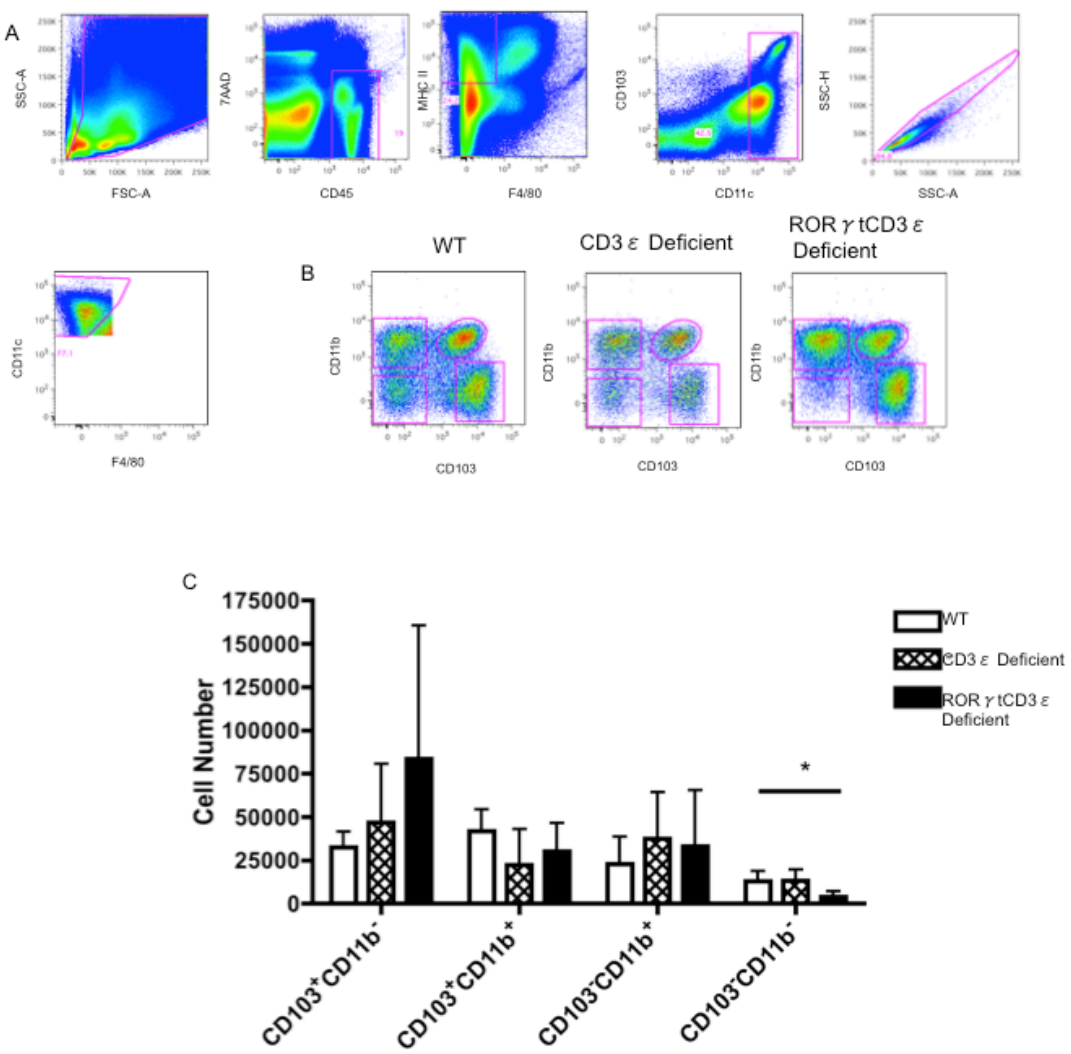

Figure 4-6 CD103$^-$CD11b$^-$ DCs Are Missing From Small Intestinal Lamina Propria of RORγt Deficient Mice.

Small intestinal LP cells were isolated as described in the methods section and cells were analysed by flow cytometry. Single cells were gated, and live leukocytes (7AAD$^-$CD45$^+$) were gated. MHCII$^+$ cells were identified and F4/80$^+$ cells were excluded and CD11c$^+$ cells were selected. These DCs were then further split into 4 populations based upon the expression of CD103 and CD11b in WT mice (A, left panel). One population of DCs was missing in RORγtCD3ε deficient mice (A and B). Data are means and S.E.M. Results were analysed by ANOVA, asterisks denote statistical significance (*$p<0.05$, n=5). FACS plots representative of 5 independent biological replicates.

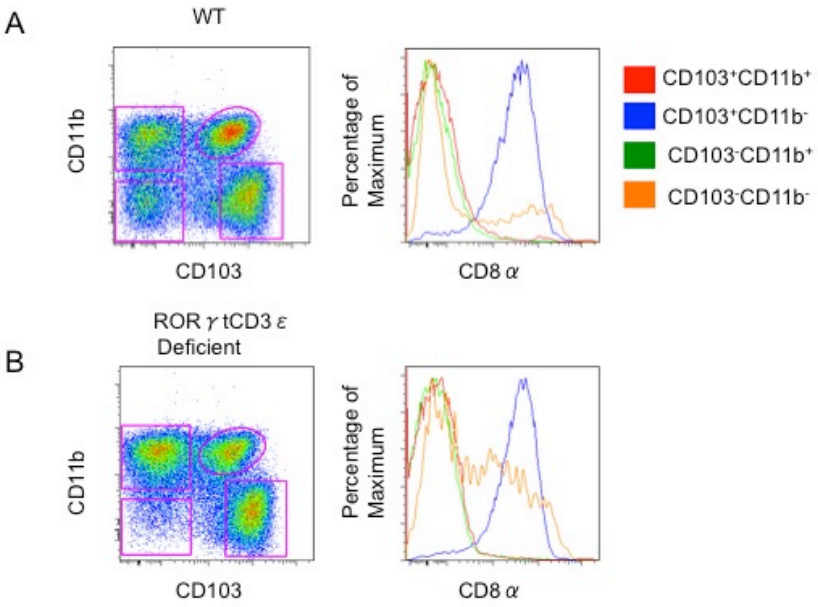

Figure 4-7 Expression of CD8α on Dendritic Cell Subsets in Small Intestinal Lamina Propria.

siLP cells were isolated and analysed by flow cytometry. Four dendritic cell subsets were identified and the expression of CD8α on each of these subsets was compared between WT (A) and RORγtCD3ε deficient (B) mice. Results are representative of at least four independent repeats.

Four DC subsets were identified in WT and CD3ε mice, while RORγtCD3ε deficient mice lack one subset of DCs, the $CD103^{-}CD11b^{-}$ DCs. As they are missing in pseudo-afferent lymph and SI digests from RORγtCD3ε deficient mice this suggests that these cells are likely to originate from GALT. We next investigated which cells were present in the cLP as we previously showed that some parts of the MLN are likely to drain the colon. PPs are present only in the SI, but ILFs are present in both the SI and colon. However colonic ILFs are distinct from those in the SI, and are able to form independently of LTi cells. Therefore, ILFs are present in the colon of RORγtCD3ε deficient mice. To investigate the DC populations therein, colons were removed from mice and single cell suspensions were generated. These were then stained with fluorescent antibodies and analysed by flow cytometry. A similar gating strategy was employed for the colon as was used for the SI; first large cells were selected, then live $CD45^{+}$ leukocytes were identified and $MHCII^{+}$, $F480^{-}$ cells were selected (Figure 4.8 A). Single, $CD11c^{+}$ cells were examined and the four populations of DCs identified by their differential expression of CD103 and CD11b (Figure 4.8 B). $CD103^{+}CD11b^{+}$ DCs were present in similar numbers in each of the mouse groups, although the number of these cells is reduced in the colon compared to the SI. $CD103^{+}CD11b^{-}$ DCs were also present in WT, CD3ε and RORγtCD3ε deficient in comparable numbers and percentages however in comparison to the SI this population is expanded in the colon. This subset is usually associated with the expression of CD8α, however I was unable to stain for this marker as the colonic digestion protocol cleaves the of CD8α antibody epitope. There was also no difference between $CD103^{-}CD11b^{+}$ DCs in the colon; as these were present in all groups of mice. In comparison to the SI, there were fewer $CD103^{-}CD11b^{-}$ DCs in WT, CD3ε or RORγtCD3ε deficient mice. This indicates that this subset does not migrate from the colon, and is specific to the SI particularly the SI GALT as this subset is specifically missing from RORγtCD3ε deficient mice. These results show there were no significant differences in the number or percentage of any DC subset in the colon between WT, CD3ε or RORγtCD3ε deficient mice (Figure 4.8 C).

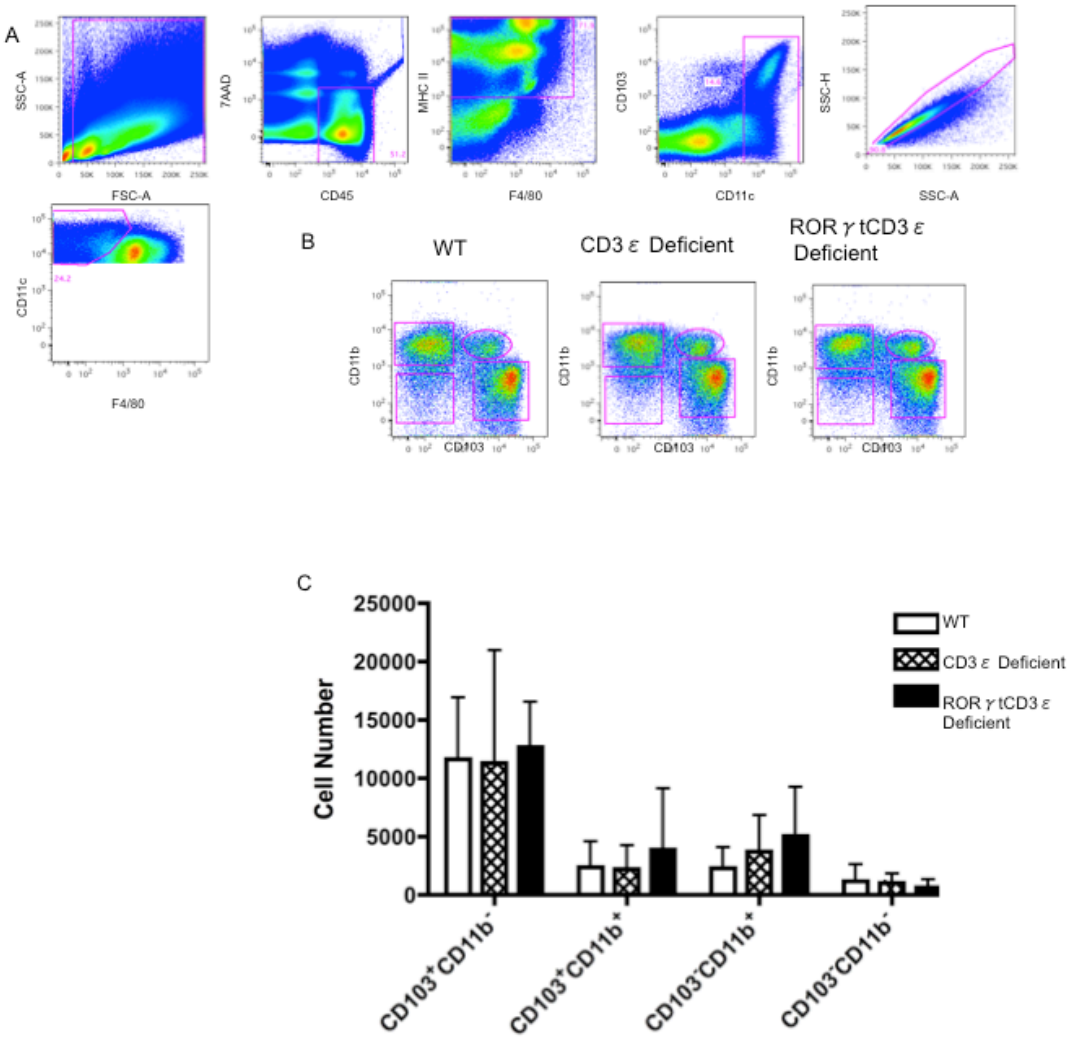

Figure 4-8 CD103$^-$CD11b$^-$ DCs Are Fewer In The Colonic Lamina Propria of WT, CD3ε and RORγtCD3ε Deficient Mice.

Colonic LP cells were isolated and cells were analysed by flow cytometry. Large cells were gated, and live leukocytes (7AAD$^-$CD45$^+$) were identified. MHCII$^+$ and F4/80$^-$ cells were gated and doublets and CD11c$^+$ cells were gated (A). These DCs were then further split into 4 populations based upon the expression of CD103 and CD11b in WT mice (B, left panel), CD3ε (B, middle panel) and RORγtCD3ε deficient mice (B, right panel). The total number of these cells were compared (C). Data are means and S.E.M. Results were analysed by ANOVA. FACS plots representative of 6 independent biological replicates.

4.1.4 Dendritic Cell Development in the Spleen and Bone Marrow of RORγt Deficient Mice

It has been previously reported that RORγt deficient mice have a defect in splenic DCs, namely that they have fewer $CD11b^+CD4^+$ DCs (P Lane, personal communication). To confirm this and to assess whether CD3ε and RORγtCD3ε deficient mice display any additional defects in resident DC populations that might affect our analyses, cells were isolated from spleens of WT, CD3ε and RORγtCD3ε deficient mice. The digestion of spleens generated a single cell suspension that was stained with fluorescent antibodies and analysed by flow cytometry. Large cells were gated then doublets and dead cells were excluded from the analysis. The presence of neutrophils and monocytes was investigated by pre-gating for $CD11b^+Ly6C^+$. Among the $CD11b^+Ly6C^+$ cells, neutrophils were defined as SSC-A^{hi} while monocytes were SSC-A^{lo} (Figure 4.9 A). pDCs were also investigated, and were identified by their expression of B220 and Ly6C. $CD11b^-$, $CD11c^+$ cells were then defined as pDCs (Figure 4.9 B). For DCs, $CD11c^+B220^-$ cells were selected and the $MHCII^+$ cells were selected. DC subsets were then classified as $CD8\alpha^+$, $CD11b^+CD4^+$ or $CD11b^+CD4^-$. There was no significant difference in the numbers or percentages of monocytes, neutrophils, or pDCs between WT, CD3ε or RORγtCD3ε deficient mice (Figure 4.9 F). There was also no significant difference between the number or percentage of $CD11c^+MHCII^+$ cells (Figure 4.9 D). We also did not see a significant difference amongst DC subsets, although there appeared to be fewer $CD11b^+CD4^+$ DCs. This suggests that RORγtCD3ε deficient mice do not have systemic defect in DC development that would have caused the lack of $CD103^-CD11b^-$ DCs in the SI and lymph.

To investigate whether there was a systemic defect in the development of RORγtCD3ε deficient DCs, we generated DCs and pDCs using BM cultured with the DC specific growth factor Flt3L. Therefore, if there were any defects in the generation of specific populations of DCs these would be detected. Cells from the femurs and tibias were isolated from WT, CD3ε and RORγtCD3ε deficient mice. These cells were cultured in the presence of Flt3L for 7 days. The phenotypes of the BMDCs generated were compared by flow cytometry. Briefly, live cells were gated and the $B220^+$ population was further gated upon PDCA-1 to identify pDCs (Figure 4.10 A and B). DCs were gated as the $B220^-$ fraction of cells

that were further gated as $CD11b^+$ or $CD11b^-$ (Figure 4.10 A and C). Both subsets were present in similar number and proportion in WT, CD3ε and RORγtCD3ε deficient mice. This confirms that there is no detectable defect in the development of DCs from precursors in RORγtCD3ε deficient mice, at least in Flt3L cultures.

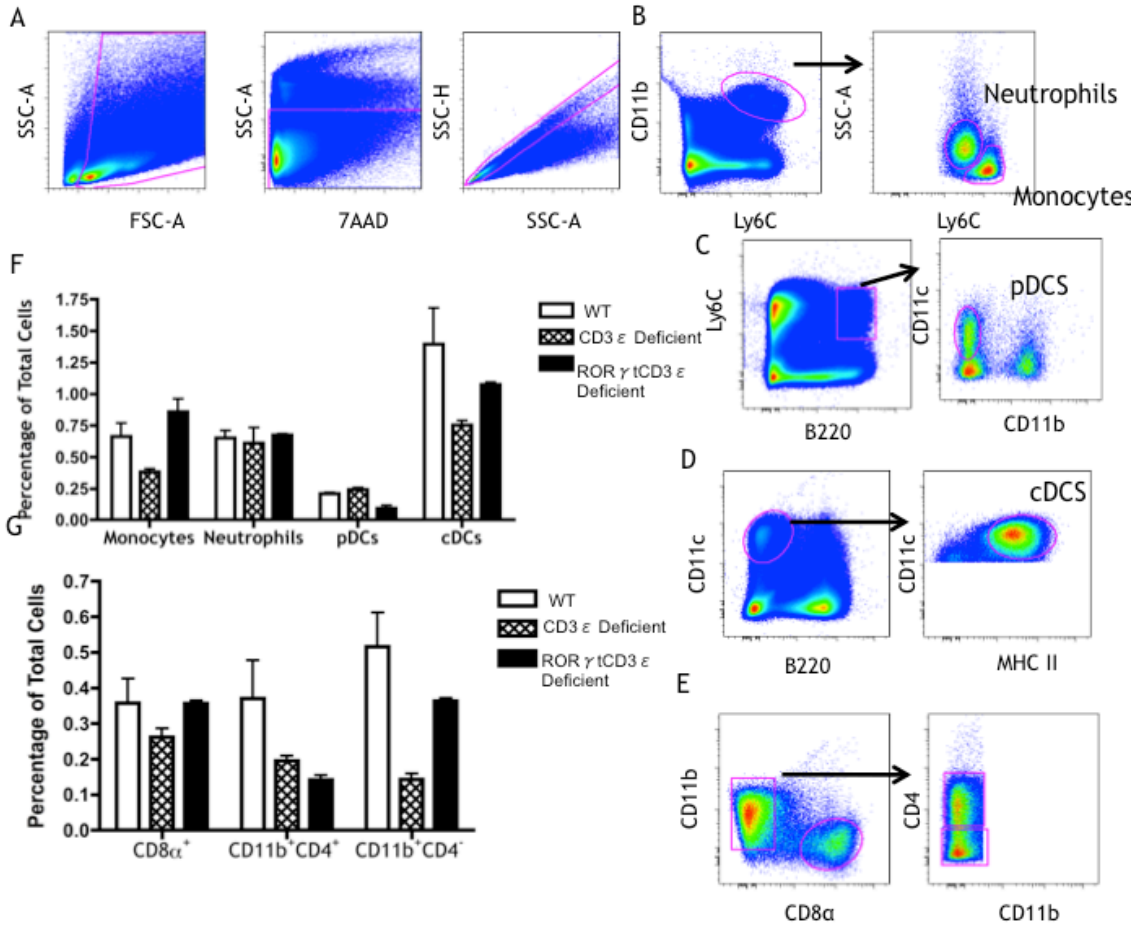

Figure 4-9 Characterisation of Cell Subsets in the Spleen of WT, CD3ε and RORγtCD3ε Deficient Mice.

Cells from the spleen of WT, CD3ε and RORγtCD3ε deficient were digested and stained for flow cytometry. Large, live, single cells were gated (A) and $CD11b^{+}Ly6C^{+}$ cells were selected and SSC^{hi} cells were then identified, as neutrophils while SSC^{lo} cells were monocytes (B). Alternatively, live single cells were gated as $Ly6C^{hi}$ $B220^{+}$ cells and the $CDllc^{+}CD11b^{-}$ cells were then identified as pDCs (C). Conventional DCs were identified as $CD11c^{+}B220^{-}$ and $MHCII^{+}$ (D), and these cells were further separated by upon their expression of CD11b, CD8α and CD4 (E). The percentage of total cells was compared (F and G) Data are means and S.E.M. and results were analysed by ANOVA, asterisks demote statistical significance (n=3). FACS plots are representative of 6 independent biological replicates.

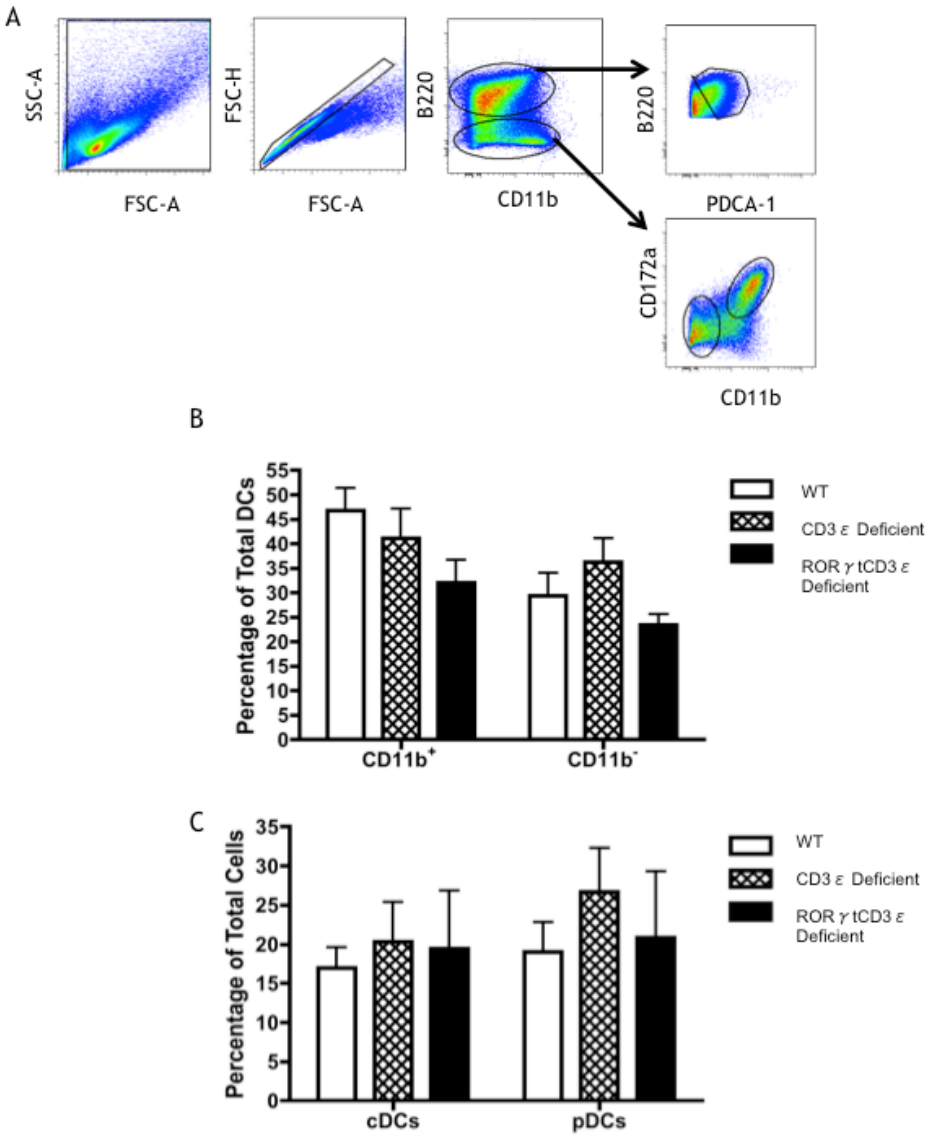

Figure 4-10 Characterisation of Cell Subsets Generated from Bone Marrow of WT, CD3ε and RORγtCD3ε Deficient Mice After Culture with Flt3L.

Cells from the bone marrow of WT, CD3ε and RORγtCD3ε deficient animals were isolated and cultured for seven days with Flt3-Ligand at 37°C. Cells were harvested and stained for flow cytometry, large single cells were gated and $B220^+$ $PDCA\text{-}1^+$ cells were identified as pDCs, while $B220^-$ cells were identified as cDCs. cDCs were further gated as $CD172a^+$ and $CD172a^-$. The percentage of DCs of cells were compared (B and C) Data are means and S.E.M. and results were analysed by ANOVA. FACS plots representative of 3 independent biological replicates. Similar results were obtained from 3 independent experiments.

4.1.5 Generation of Lymphotoxin-β Receptor Fusion Protein

The second system we used to investigate the anatomical origins of migratory DCs in the intestine involved prenatal exposure of mice to LTβR-Ig, which can inhibit lymphoid tissue organogenesis. During lymphoid tissue formation, LTo cells express the LTβR, and the LTi cells that seed the developing lymph node express the LT ligand LTα1β2. Interaction between these two molecules is required for the development of LNs and is blocked by LTβR-Ig. As lymphoid organs develop sequentially, the timing of the exposure of LTβR-Ig is crucial; injections at E14 and E16 prevent development of PPs but mesenteric, cervical, brachial and axillary lymph nodes all develop normally (Mebius, 2003). ILFs are induced to develop after birth, therefore mice exposed to LTβR-Ig at E14 and E16 lack PPs only, and while MLN and ILF formation is unaffected. Consequently, any DCs migrating to the MLN from these animals must be LP or ILF derived.

LTβR-Ig was produced from HEK293 cells stably transfected with murine LTβR-Ig expressing plasmid; the supernatant from these cells was purified by a Sepharose-protein G affinity column before being sterilised by filtration. The integrity of the protein was confirmed by SDS-PAGE (Figure 4.11). Supernatant from HEK293 containing LTβR-Ig before filtration, purified LTβR-Ig, and a molecular weight ladder were loaded into a polyacrylamide gel and coomassie blue staining was performed in order to visualise proteins. This revealed that the sterilised LTβR-Ig showed a single band of between 50 and 40 kDa, corresponding to the LTβR-Ig (48kDa). In comparison the non-purified LTβR-Ig showed a faint band corresponding to LTβR-Ig as well as smaller bands representing impurities.

Once the purity of LTβR-Ig had been established, a Bradford Assay was performed to determine the concentration of protein that was produced. Standards of BSA, and LTβR-Ig, were incubated with the Bradford reagent and their absorption of light at 562 nm was determined. Values were used to draw a standard curve (Figure 4.12), and the equation of the standard curve was used to determine that the protein concentration of LTβR-Ig was 1343.7μg/ml.

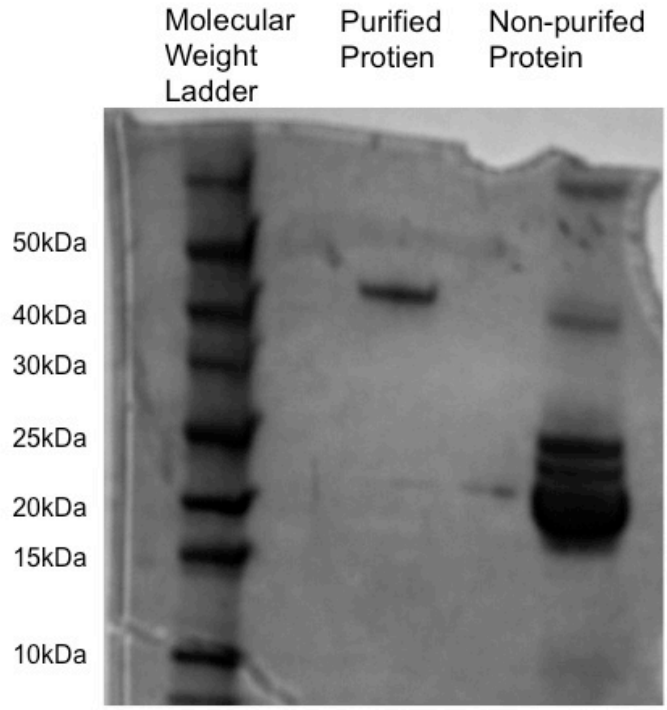

Figure 4-11 SDS-PAGE Gel of Purified LTβR-Ig.

Purified LTβR-Ig and the supernatant of the cells that produce LTβR-Ig pre purification were separated by sodium dodecyl sulphate polyacrylamide gel electrophoresis (SDS-PAGE). Lane 1 shows standard proteins, lane 2 purified LTβR-Ig and lane 3 shows LTβR-Ig pre-purification. Coomassie brilliant blue was performed following SDS-PAGE to visualise protein bands.

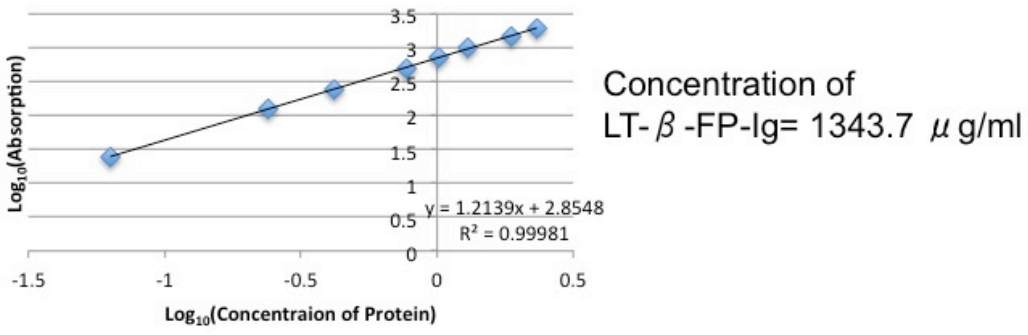

Figure 4-12 The Concentration of Purifed LTβR-Ig by Bradford Assay.

A Bradford Assay was performed on serial dilutions of BSA and purified LTβR-Ig and absorption was determined. Values were recorded, a standard curve was drawn, and the concentration of LTβR-Ig was determined.

4.1.6 Lymphoid Tissue in the Intestine of Lymphotoxin-β Receptor Fusion Protein Treated Progeny

Once the purity and concentration of LTβR-Ig was established, LTβR-Ig was injected intravenously into pregnant females at E14 and E16, to specifically block the development of PPs. Live intestinal tissue of untreated and LTβR-Ig treated progeny was examined macroscopically to check that PPs appeared to be absent and MLNs present in the LTβR-Ig treated animals as expected (Figure 4.13).

In order to confirm that LTβR-Ig progeny lack PPs, and to show that they retain ILFs, Swiss-roll sections of SI were prepared. These preparations enable detailed examination of a large area of the intestine. Sections were stained with DAPI and anti-B220 to assist in the identification of ILFs. Following immunofluorescent staining, multiple (>100) overlapping high power images were generated and manually collated to visualise the detailed architecture of the SI (Figure 4.14). This showed that WT mice contained both PPs and ILFs, while LTβR-Ig treated animals contained only ILFs, but not PPs.

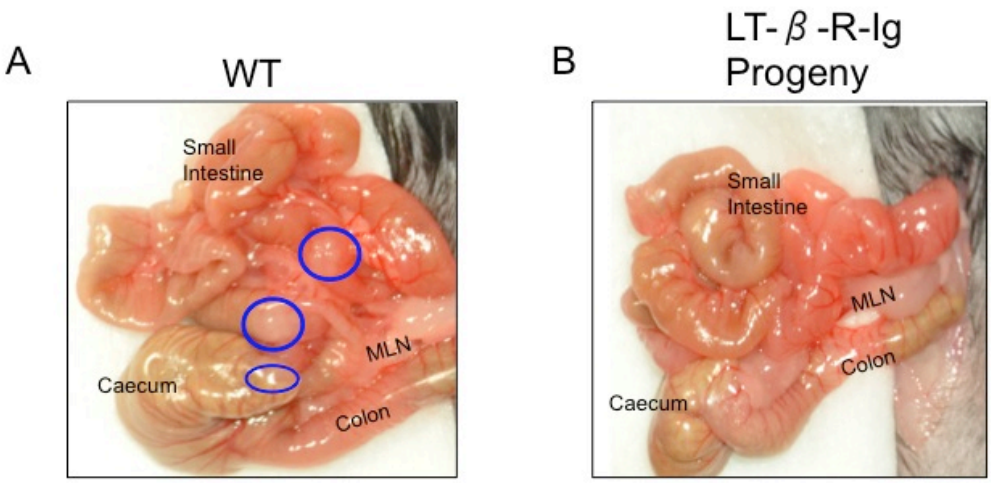

Figure 4-13 Progeny of Mice Injected With LT-βR-Ig at Embryonic Day 14 and 16 Lack Peyer's Patches But Retain Mesenteric Lymph Nodes.

Pregnant females were injected intravenously with LTβR-Ig fusion protein at embryonic days 14 and 16. 6-week-old progeny were examined for the presence of Peyer's patches PPs and MLNs and images of live intestine were captured. Visible PPs are present in WT progeny (A) and circles highlight PPs, which are missing in LT-βR-Ig progeny (B). MLNs are present in both WT and LT-βR-Ig progeny. Images are representative of 7 independent biological replicates.

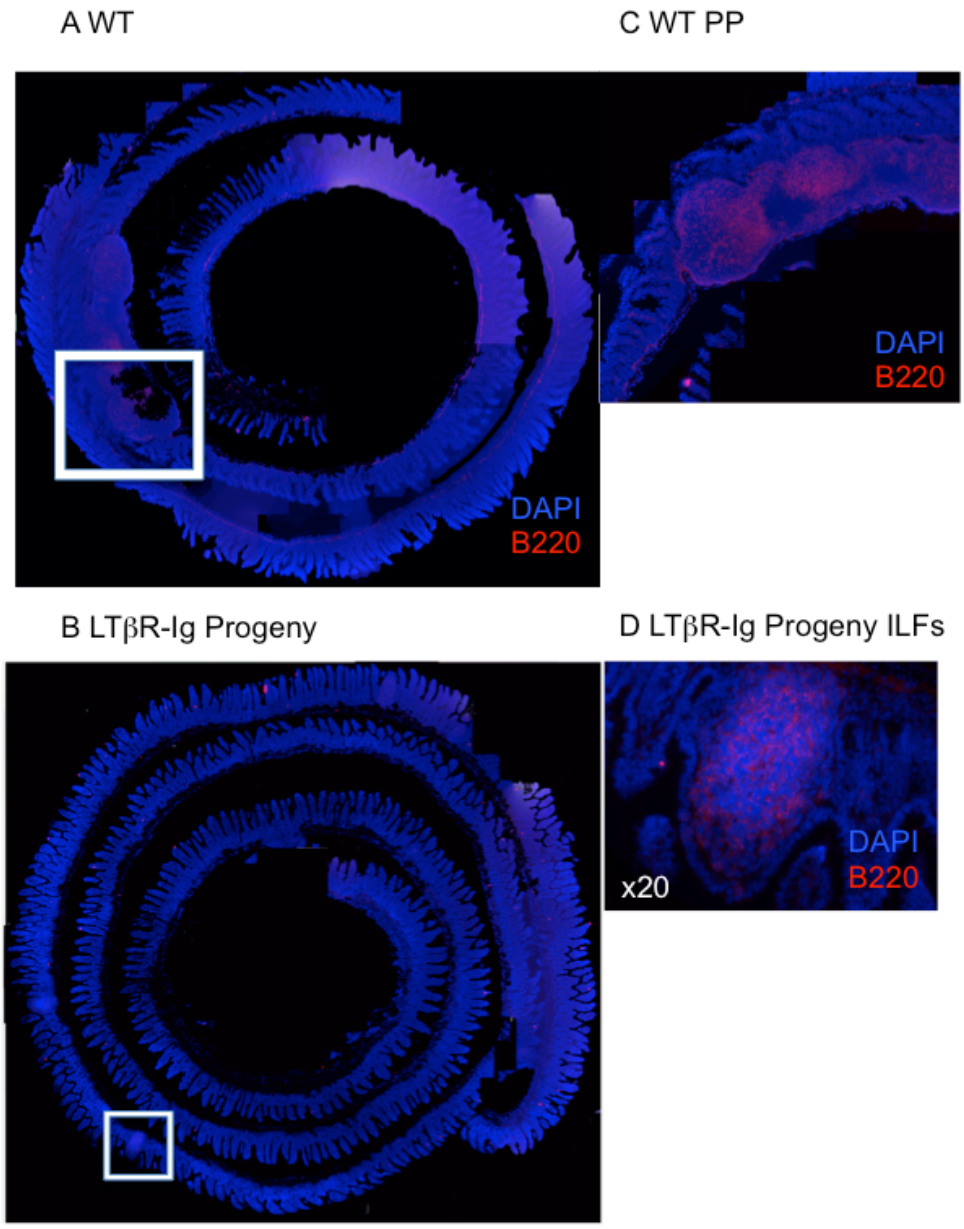

Figure 4-14 Peyer's Patches Are Absent From the Small Intestine of LTβR-Ig Treated Progeny.

Swiss roll sections were prepared from the small intestine of 6-week-old WT mice and 6-week-old LTβR-Ig treated progeny and stained with B220 to show organised lymphoid structures and DAPI to show the structure of the intestine. Composite images of intestine from WT mice (A) and LTβR-Ig Progeny (B) were assembled from 100-150 individual high-powered images using an epifluoresent microscope. WT PP depicted in (C), area indicated by white box in (A) and LTβR-Ig treated progeny ILF in (D) area indicated by white box in (B). Pictures are representative of 8 separate animals.

4.1.7 Dendritic Cell Subsets in the Mesenteric Lymph Nodes, Small Intestine, Colon and Migrating in Pseudo -Afferent Lymph of Lymphotoxin-β Receptor Fusion Protein Treated Progeny

As I have confirmed the absence of PP, but the presence of ILFs in LTβR-Ig treated progeny, the DC subsets migrating from the intestine were investigated. As there are no PPs in LTβR-Ig treated progeny, any DCs migrating from the intestine must have originated in ILFs, siLP or the cLP or colonic patches. First, migratory DCs from the intestine were investigated by TDC. Following MLNx, pseudo-afferent lymph from WT or LTβR-Ig progeny was collected overnight and was stained for flow cytometry. DCs, ($CD11c^+MHCII^+$, $CD19^-$, Figure 4.15 A) were gated and subsets were defined based upon their expression of CD103 and CD11b (Figure 4.15 B). This showed that four distinct DC subsets were present in similar numbers and percentages in both WT and LTβR-Ig progeny. In comparison to RORγtCD3ε deficient mice, the $CD103^-CD11b^-$ DC subset was present. This shows, for the first time, that all four phenotypically and functionally distinct populations of DCs that migrate from the intestine are derived from either the conventional villus mucosa or ILFs.

In order to confirm that injections of LTβR-Ig did not affect development of the MLN, or any cell populations in the MLN, the MLN was taken, digested and stained for flow cytometry. Live, single leukocytes ($7AAD^-CD45^+$ Figure 4.16 A) were gated and $CD3^-$ $B220^+CD19^+$ cells were identified as B cells (Figure 4.16 C), alternatively the $CD3^-$ fraction was gated into $CD19^-CD11c^+$ cells. These were further selected as $CD4^+$ pDCs (Figure 4.16 B). Alternatively single live leukocytes were further gated as $CD3^+$ cells and populations of T cells were identified (Figure 4.16 D). The total numbers of cells in the MLN were also investigated. There was no significant difference in the number of cells in the MLN of LTβR-Ig progeny compared to WT mice (Figure 4.16). The numbers of pDCs, B cells, $CD4^+$T cells and $CD8\alpha^+$ T cells were compared between WT mice and LTβR-Ig progeny. There was no significant difference between any of the cell populations we investigated in the MLN. This suggests that the injection of LTβR-Ig at E14 and E16 did not affect the development of the MLN, making this an excellent model in order to investigate DC migration from the intestine.

We used similar procedures to analyse cDC populations in the MLN of the LTβR-Ig treated PP null mice. This time DCs were gated; large, single leukocytes (7AAD$^-$ CD45$^+$) MHCII$^+$CD19$^-$ cells were gated (Figure 4.17 A). DCs were then analysed in three ways; as migratory DCs, which have a higher expression of MHCII; blood derived DCs that have a higher expression of CD11c; or total DCs were gated (Figure 4.17 B). This allows a more detailed analysis of DC subsets in the MLN as migratory DCs coming from the SI and blood derived DCs can be analysed separately. Therefore, any LTβR-Ig induced defect in DCs arriving from the intestine or in DC precursors seeding the MLN should be identifiable by this gating strategy. DC subsets were defined by their expression of CD103 and CD11b for migratory (Figure 4.17 C), blood derived (Figure 4.17 D) or total DCs (Figure 4.17 E). There were no significant differences between the total number or percentage of any subset of DC between WT or LTβR-Ig.

Previously I identified that distinct areas of the MLN drain lymph from the SI and colon. Therefore in order to ensure that injections of LTβR-Ig *in utero* do not affect the si*M*LN or co*M*LN, an effect that could have been missed by looking at the entire MLN, the si*M*LN and co*M*LN were isolated and examined separately. These were then digested and stained for flow cytometry. Large, live leukocytes were gated, and the CD11c$^+$B220$^-$ population was then selected. The CD3$^+$B220$^+$ and CD64$^+$ populations were excluded, as were doublets (Figure 4.18 A). The remaining populations of DCs were then gated as migratory or as blood derived DCs (Figure 4.18 B), and the four DC subsets, identified by their expression of CD103 and CD11b, were compared between si*M*LN and co*M*LN in WT mice and LTβR-Ig progeny (Figure 4.18 C and D). This analysis revealed no differences between DC populations from WT or LTβR-Ig progeny in either the si*M*LN or co*M*LN.

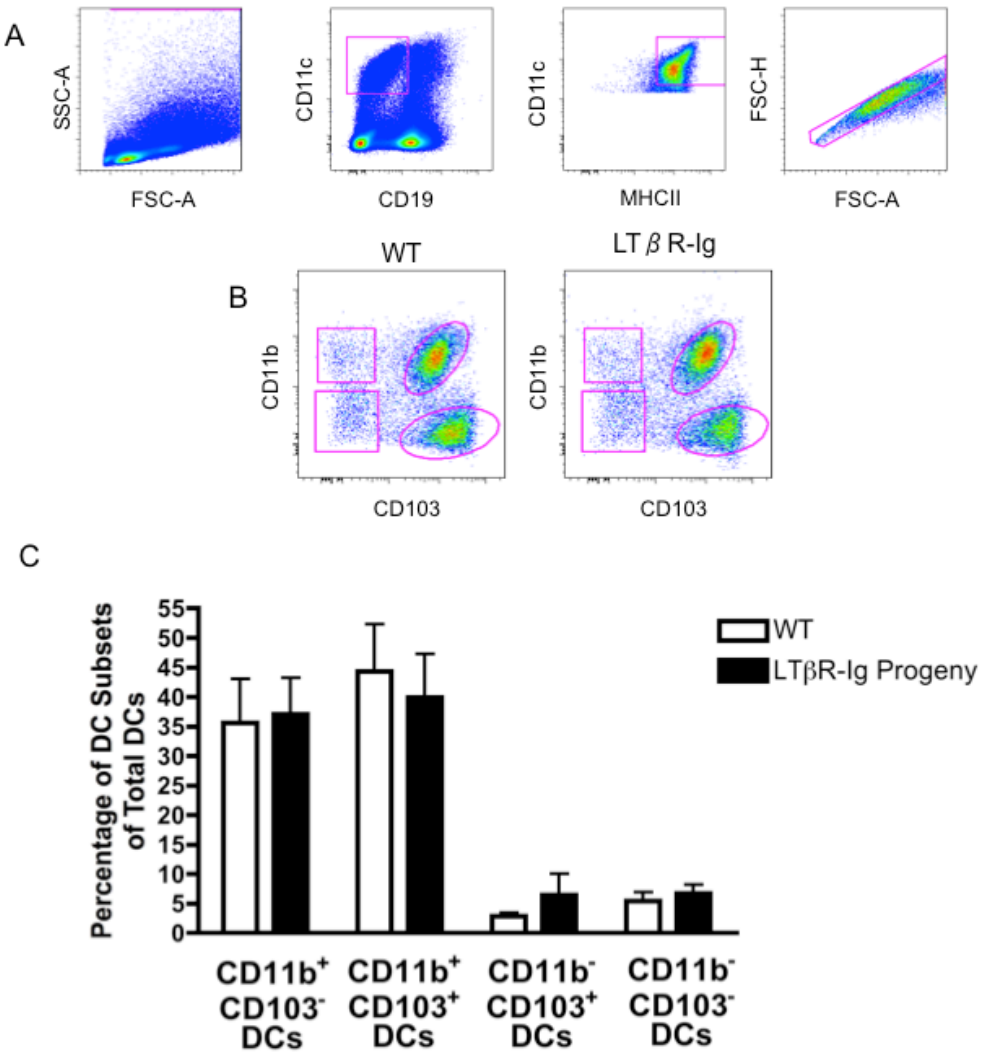

Figure 4-15 Four Subsets of DCs Are Present In The Lymph of Mice Treated *in Utero* With LTβR-Ig.

Pseudo-afferent lymph was collected from WT mice and mice treated with LTβR-Ig *in* utero and analysed by flow cytometry. Large $CD19^{-}CD11c^{+}$ cells were gated, $CD11c^{+}MHCII^{+}$ single cells were further selected as DCs (A). These DCs were further split into four populations based upon the expression of CD103 and CD11b (B) and these four subsets were compared between WT mice and mice treated *in utero* with LTβR-Ig (C). Data are means and S.E.M. Results were analysed by students *t* test, n=4.

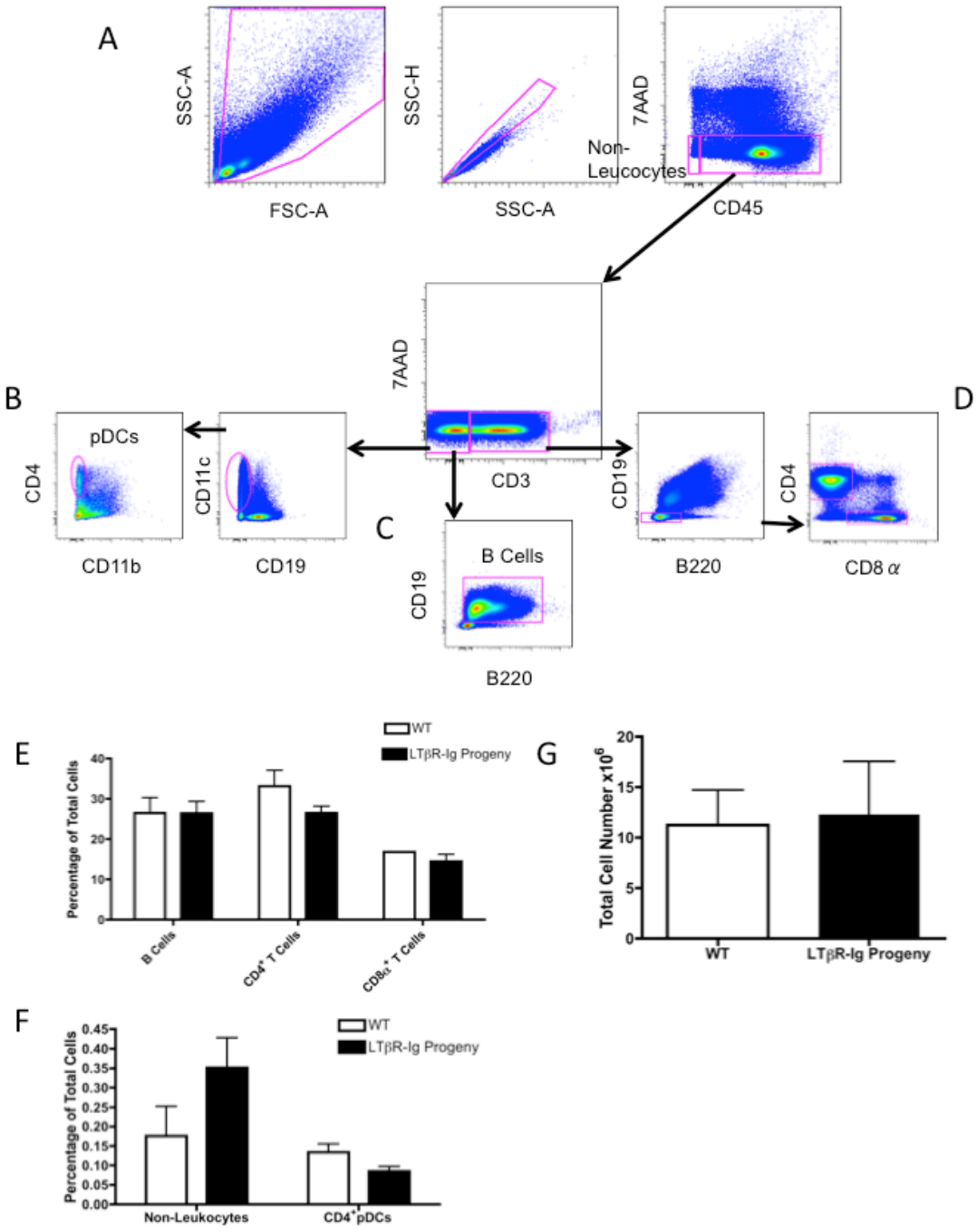

Figure 4-16 Characterisation of Cell Subsets in the MLN of WT mice and Mice Treated with LTβR-Ig *in Utero*.

Cells from the MLN of WT and 6-week-old LTβR-Ig progeny were digested and stained for flow cytometry. Large, single, live leukocytes ($7AAD^-CD45^+$) cells were gated (A) $CD3^-CD11c^+CD19^-$ cells were selected and $CD4^+CD11b^-$ cells were identified as $CD4^+$ pDCs (B). Alternatively live single $CD3^-$ $B220^+CD19^+$ leukocytes were identified as B cells (C). Single, live $CD3^+$leukocytes were gated into $CD4^+$ T cells and $CD8\alpha^+$ T cells (D). The percentages of these cells of total cells were compared (E and F), as was total cell number (G) Data are means and S.E.M. results were analysed by students *t* test. Data are means and S.E.M. FACS plots representative of 2 independent experiments, n=3.

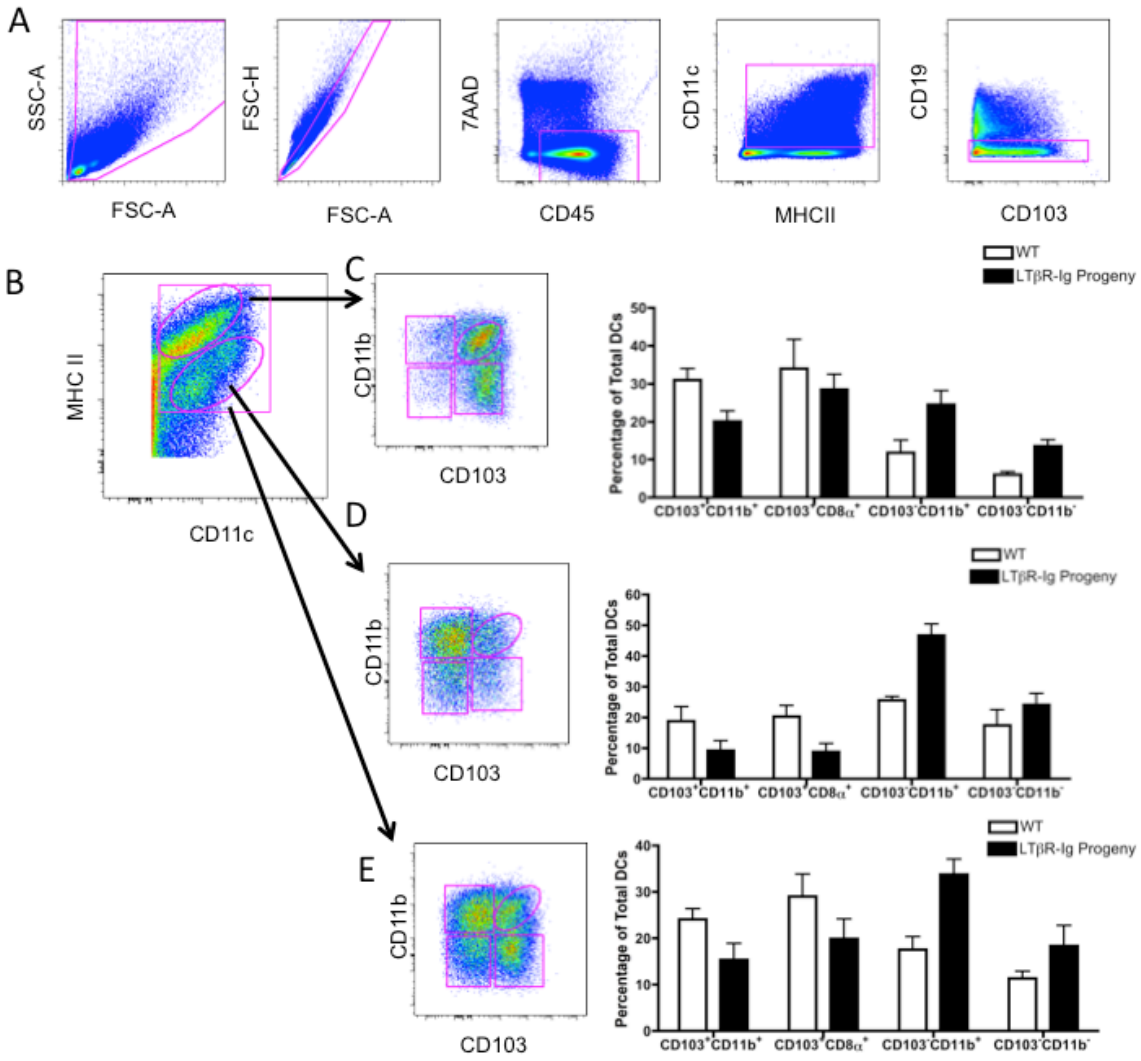

Figure 4-17 Characterisation of Migratory and Blood Derived Dendritic Cell Subsets in the MLN of WT and LTβR-Ig Progeny.

Cells from the MLN of WT and 6-week-old LTβR-Ig progeny were isolated, digested and stained for flow cytometry. Large, single, live leukocytes ($7AAD^{-}CD45^{+}$) were gated, and $CD11c^{+}$ $CD19^{-}$ cells were gated (A). Migratory ($MHCII^{hi}CD11c^{+}$) (C), blood derived ($MHCII^{+}CD11c^{hi}$) (D) and total ($CD11c^{+}MHCII^{+}$) (E) dendritic cells were further gated into four subsets based upon the expression of CD103 and CD11b. The percentage of dendritic cell subsets of total dendritic cells were compared for each type of dendritic cell and results were analysed by students *t* test. Data are means and S.E.M. FACS plots representative of 2 independent experiments, n=3.

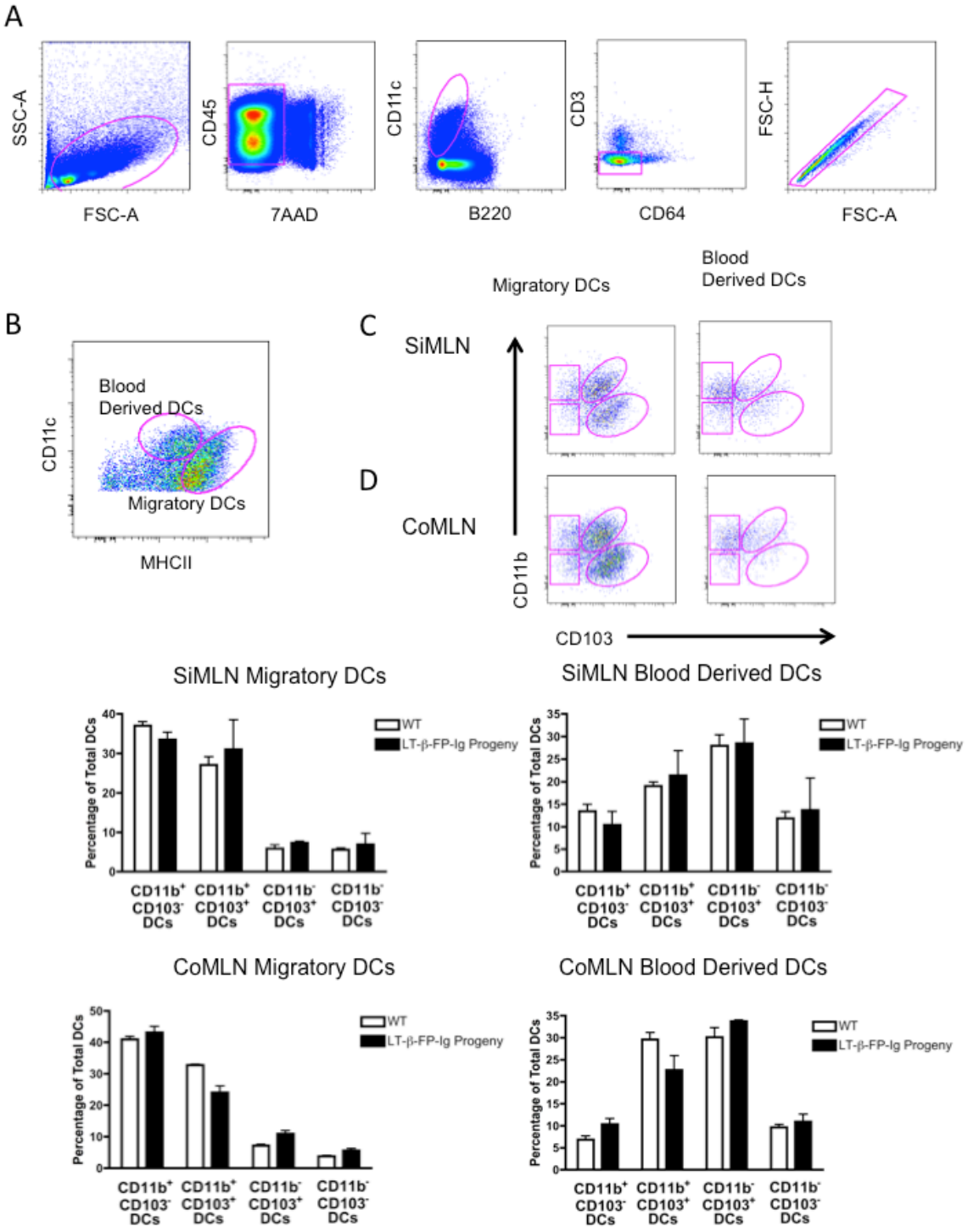

Figure 4-18 Characterisation of Dendritic Cells in Small Intestinal Draining and Colonic Draining MLN of WT and LTβR-Ig-treated Progeny.

Cells from the MLN of WT and 8-week-old LTβR-Ig-treated progeny were isolated, digested and stained for flow cytometry. Large, single, live leukocytes ($7AAD^{-}CD45^{+}$) were gated, and $CD11c^{+}$ $CD19^{-}$ cells were identified (A). Migratory ($MHCII^{hi}CD11c^{+}$), blood derived ($MHCII^{+}CD11c^{hi}$), and total ($CD11c^{+}MHCII^{+}$) dendritic cells were each divided into four subsets based upon the expression of CD103 and CD11b. The percentages of each of the DC subsets of total dendritic cells were compared for each class of dendritic cell and results were analysed by students *t* test. FACS plots representative of 8-10 independent biological replicates. Data are means and S.E.M.

Having demonstrated that all DC subsets are present in the pseudo-afferent lymph and in siMLN and coMLN of LTβR-Ig treated progeny I sought to compare these with the DC subsets that are present in the SI. The SI was removed (PPs were excised from WT mice), the SI was digested and a single cell suspension was stained for multi colour flow cytometry. As described previously, ILFs were not removed due to their size. First, large cells were gated, then live $CD45^+$, $CD11c^+CD64^-$ cells were selected and doublets were excluded. Finally $CD11c^+MHCII^+$ cells were selected and $B220^+$ cells were excluded (Figure 4.19 A). The remaining DCs subsets were compared between WT and LTβR-Ig treated progeny (Figure 4.19 B). The DC subsets in the SI reflected the populations in migrating in pseudo-afferent lymph. There were no significant differences in the number or percentage of any of the SI DC subsets between WT and LTβR-Ig treated mice.

We next investigated the DCs in the cLP (Figure 4.20). Colons were removed and a single cell suspension was generated. This was stained with fluorescent antibodies and analysed by flow cytometry. A similar gating strategy was employed for the colon as was used for the SI. DCs were then gated and four DC populations were identified in both WT and LTβR-Ig treated progeny, at similar numbers and percentages. RORγtCD3ε deficient mice also did not display any differences in the DC populations present in the colon.

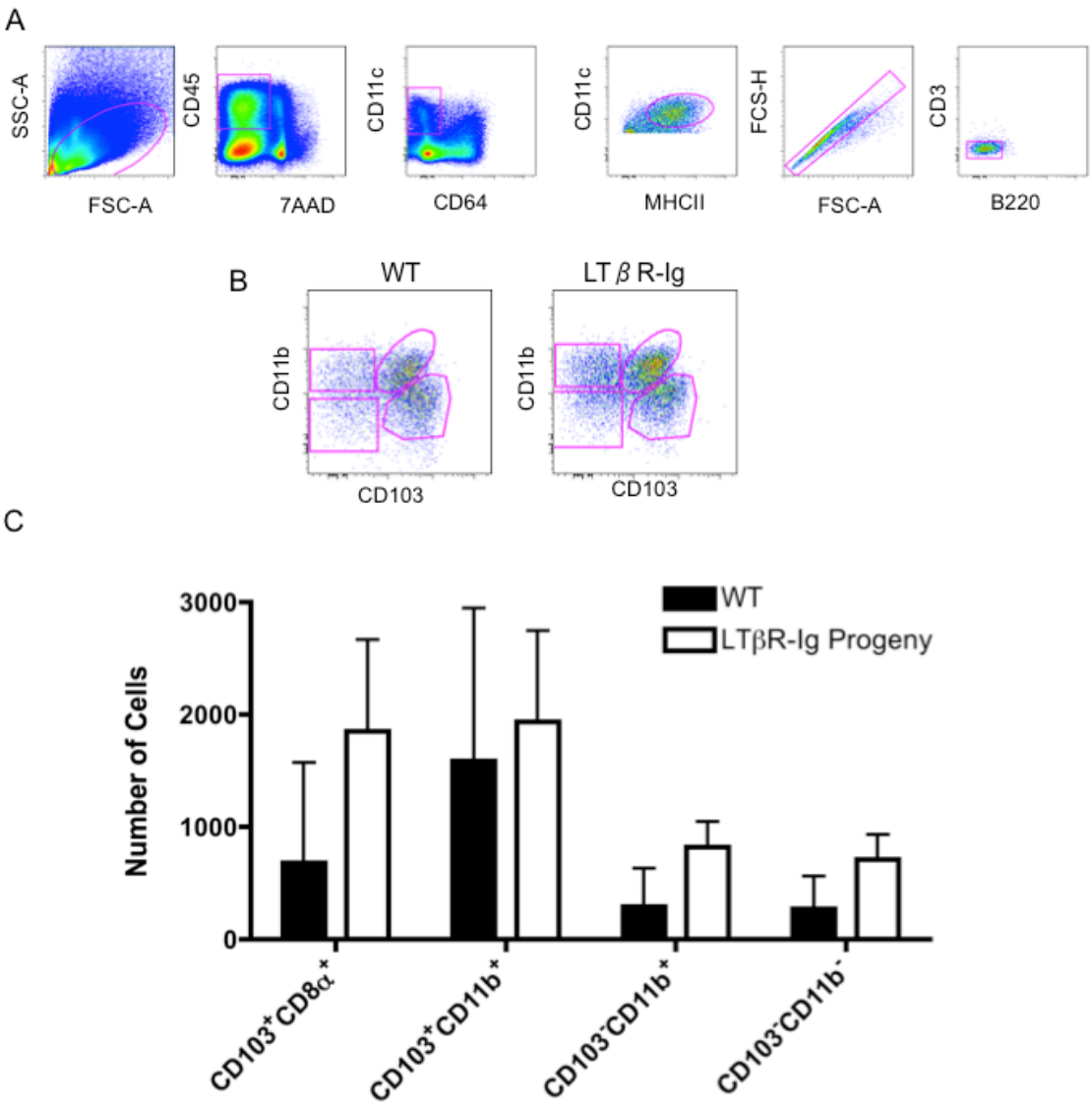

Figure 4-19 Four Dendritic Cell Subsets Are Present In The Small Intestinal Lamina Propria of Mice Treated with LTβR-Ig *in Utero*.

Cells from the siLP were isolated and cells were analysed by flow cytometry from WT and 8-week-old LTβR-Ig treated animals. Large cells were gated, and live leukocytes (7AAD-CD45+) were selected. $CD11c^{+}CD64^{-}$ $MHCII^{+}$ cells were then selected. These DCs were split into 4 populations based upon their expression of CD103 and CD11b (B). All four populations were present in mice treated with LTβR-Ig *in utero* (C). Data are means and S.E.M. and results were analysed by students *t* test. FACS plots representative of 6 independent biological replicates.

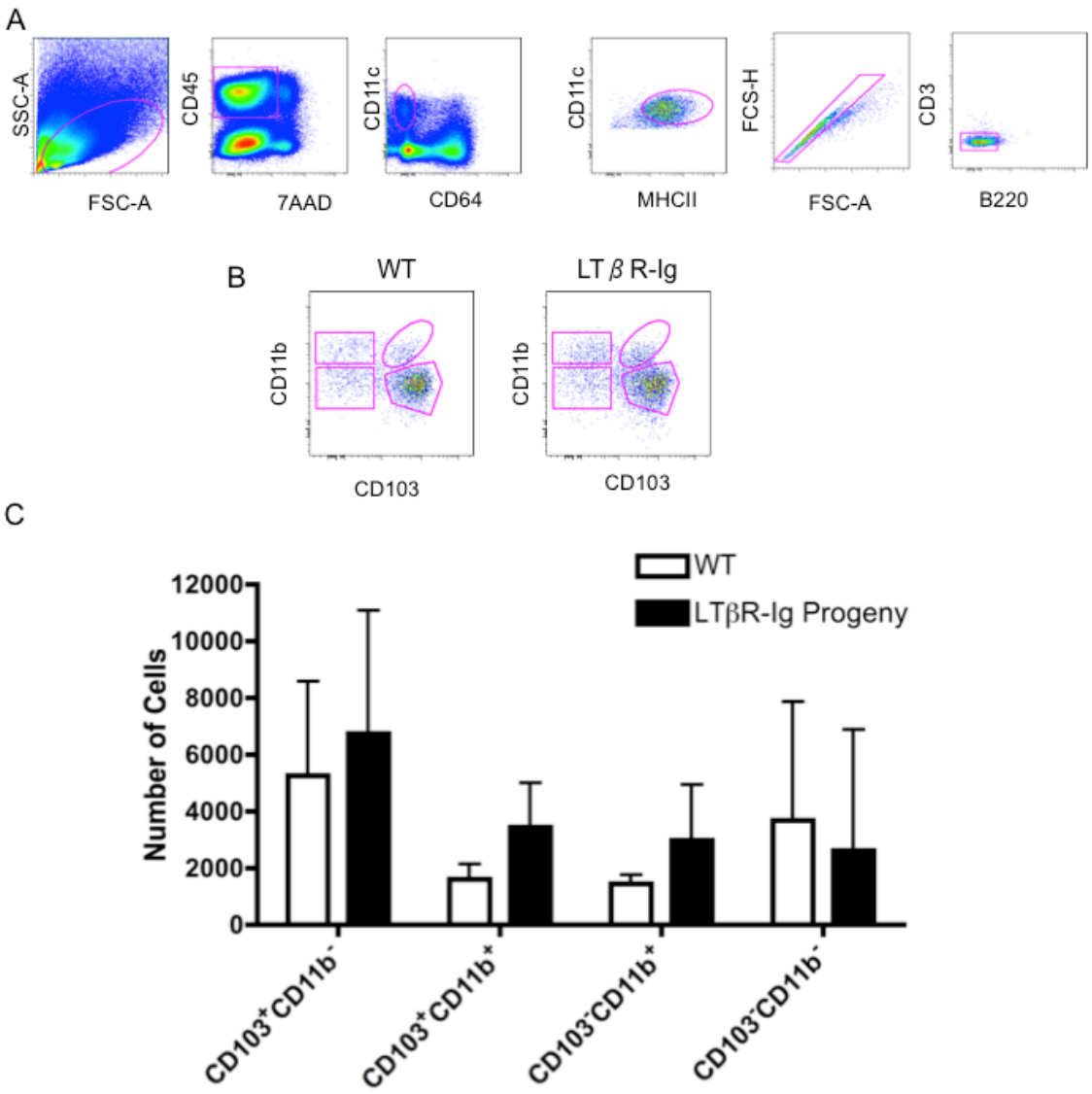

Figure 4-20 DCs from The Colonic Lamina Propria of WT, and LTβR-Ig mice.

Cells from the cLP were isolated and analysed by flow cytometry from WT and 8-week-old LTβR-Ig treated animals. Large cells were identified, and live leukocytes ($7AAD^{-}CD45^{+}$) were gated. $MHCII^{+}$ and $CD11c^{+}$ cells were gated and doublets and $F4/80^{+}$ cells were excluded (A). These DCs were then further split into 4 populations based upon their expression of CD103 and CD11b in WT mice (B, left panel) and LTβR-Ig –treated progeny (B, right panel). The total number of these cells were compared (C) Data are means and S.E.M. and results were analysed by students *t* test, (n=6). FACS plots representative of 6 independent biological replicates.

4.1.8 Development of Lymph Nodes, Spleen and Dendritic Cells in Lymphotoxin-β Receptor Fusion Protein Treated Progeny

Previously it has been shown that treatment with LTβR-Ig disrupts splenic architecture, furthermore previous work suggested there were reduced $CD4^+$ DCs in the spleen of RORγt deficient mice (P Lane, personal communication). In order to understand what effects this may have on DCs and other immune cells, we isolated the spleens of WT and LTβR-Ig treated progeny. The digestion of spleens generated a single cell suspension that was stained with fluorescent antibodies and analysed by flow cytometer. Large, live leukocytes were gated and single cells were selected (Figure 4.21 A). $CD19^+B220^+$ cells were then defined as B cells (Figure 4.21 B), $B220^+CD19^-CD11c^+$ cells were defined as pDCs (Figure 4.21 C). Alternatively, $CD3^+$ large live leukocytes were gated and $CD4^+$ T cells and $CD8\alpha^+$ T cells were identified (Figure 4.21 D). The numbers and percentages of these cells were then compared between WT and LTβR-Ig treated progeny (Figure 4.21 E and F). There were no significant differences between any of these cell populations, suggesting that LTβR-Ig did not have a general effect upon the formation of immune cells in the spleen. To specifically investigate DCs, large, live, single $CD11c^+B220^-$, $MHCII^+$ cells were gated (Figure 4.22 A). DC subsets were then classified as $CD8\alpha^+$, $CD11b^+CD4^+$ or $CD11b^+CD4^-$ DCs (Vremec et al., 2000) (Figure 4.22 B). There was no significant difference in the number of any of the DC subsets (Figure 4.22 C). This indicates that there is not a systemic defect in the development of DCs in the LTβR-Ig treated mice.

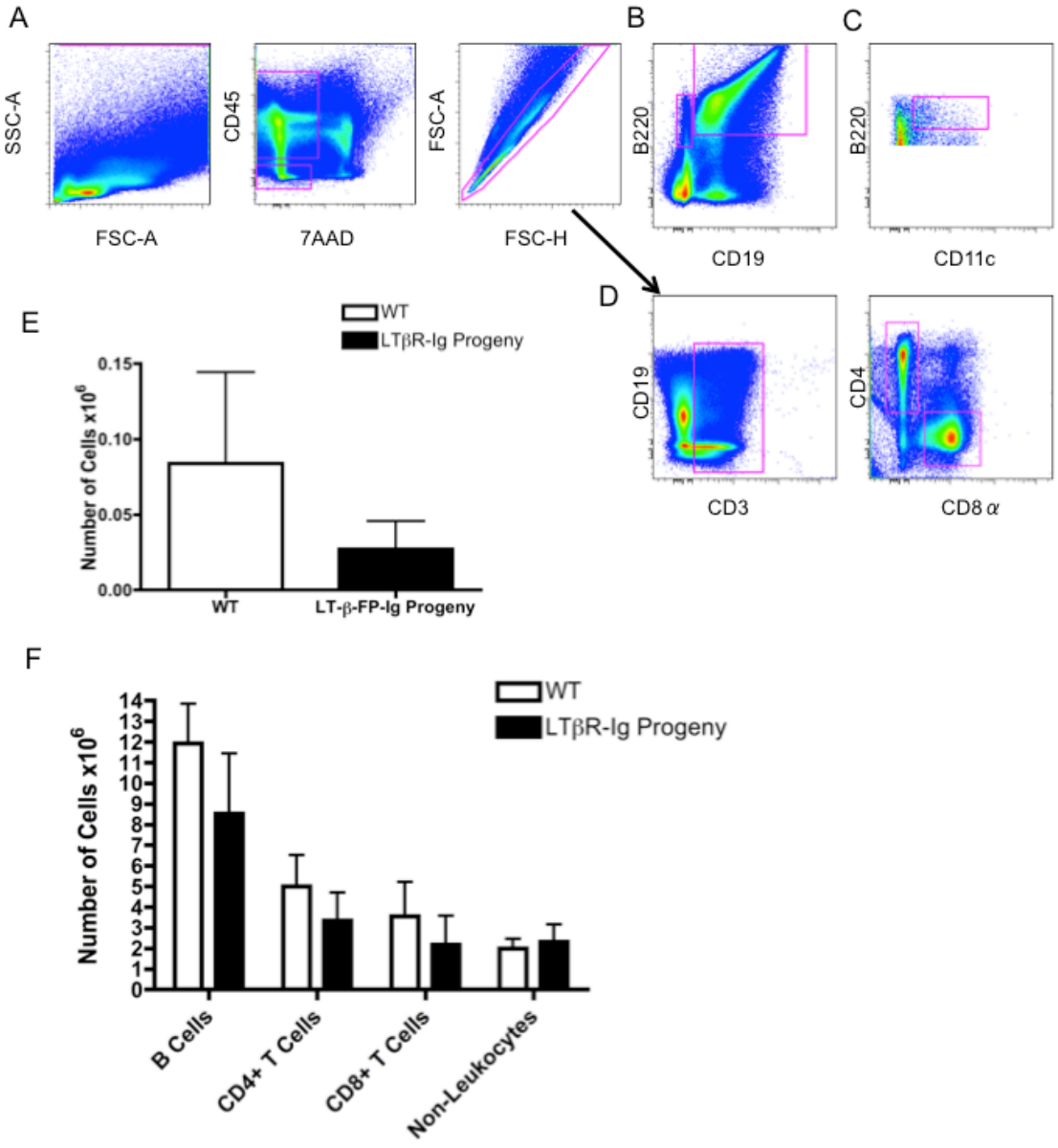

Figure 4-21 Characterisation of Cell Subsets in the Spleen of WT mice and mice treated *in Utero* with LTβR-Ig.

Spleens from WT and LTβR-Ig mice were digested and cells stained for flow cytometry from WT and 8-week-old LTβR-Ig treated animals. Large, single, live leukocytes ($CD45^+7AAD^-$), were gated (A). $B220^+CD19^+$ cells were defined as B cells (B) and $B220^+CD11c^+$ cells were identified as pDCs (C). Alternatively live single leukocytes were gated as $CD3^+$ cells, and $CD4^+$ T cells and $CD8\alpha^+$ T cells were identified (D). The total numbers of these cells were compared (E and F) Data are means and S.E.M. and results were analysed by students *t* test. (n=4). FACS plots are representative of 6 independent biological replicates.

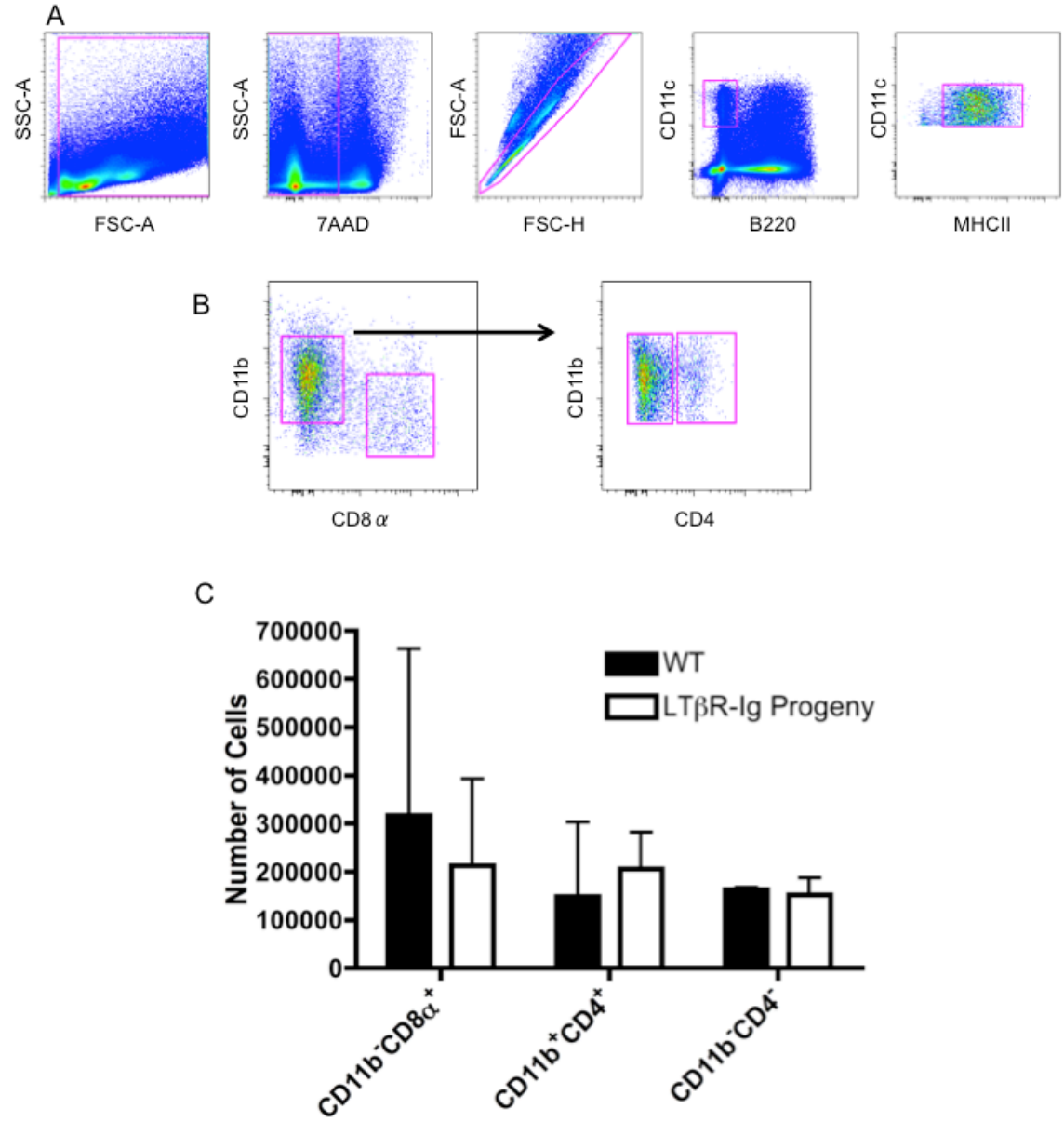

Figure 4-22 Characterisation of Dendritic Cell Subsets in the Spleen of WT and LTβR-Ig-treated mice.

Spleens of WT and LTβR-Ig-treated mice were digested and cells stained for flow cytometry from WT and 8-week-old LTβR-Ig treated animals. Large, live, single $CD11c^{+}B220^{-}$cells were gated (A) and these cells were further divided based upon their expression of CD11b, CD8α and CD4 (B). The total numbers of these DC populations were compared (C) Data are means and S.E.M. and results were analysed by students *t* test, (n=6). FACS plots representative of 6 independent biological replicates.

Injections of LTβR-Ig at E11 and E14 resulted in the complete inhibition of lymph node development (Mebius, 2003). Therefore, in order to determine whether the lymph nodes that develop at a similar time to PPs were unaffected by the injection of LTβR-Ig at E14 and E16 inguinal lymph nodes (ILN) and cervical lymph nodes (CLN) were examined. Cells were enumerated after digestion of the ILN and CLN of WT and LTβR-Ig treated mice. There were no significant differences in cell numbers between the ILN and CLNs of WT or LTβR-Ig treated mice (Figures 4.23 A and 4.24 A), suggesting that injections of LTβR-Ig did not affect the development of ILNs or CLNs. To confirm that the development of DCs in the ILN or CLNs was not affected by injections of LTβR-Ig, the DC subsets were investigated. Large, live leukocytes ($CD45^{+}7AAD^{-}$) were identified, and $B220^{-}$ $CD11c^{+}$ single cells were gated. $MHCII^{+}$ cells were then gated and DC subsets were examined based upon the expression of CD11b and CD8α (Figure 4.23 B and 4.24 B). There were no differences in DC subsets between the ILNs and CLNs of WT and LTβR-Ig treated (Figure 4.23 C and 4.24C).

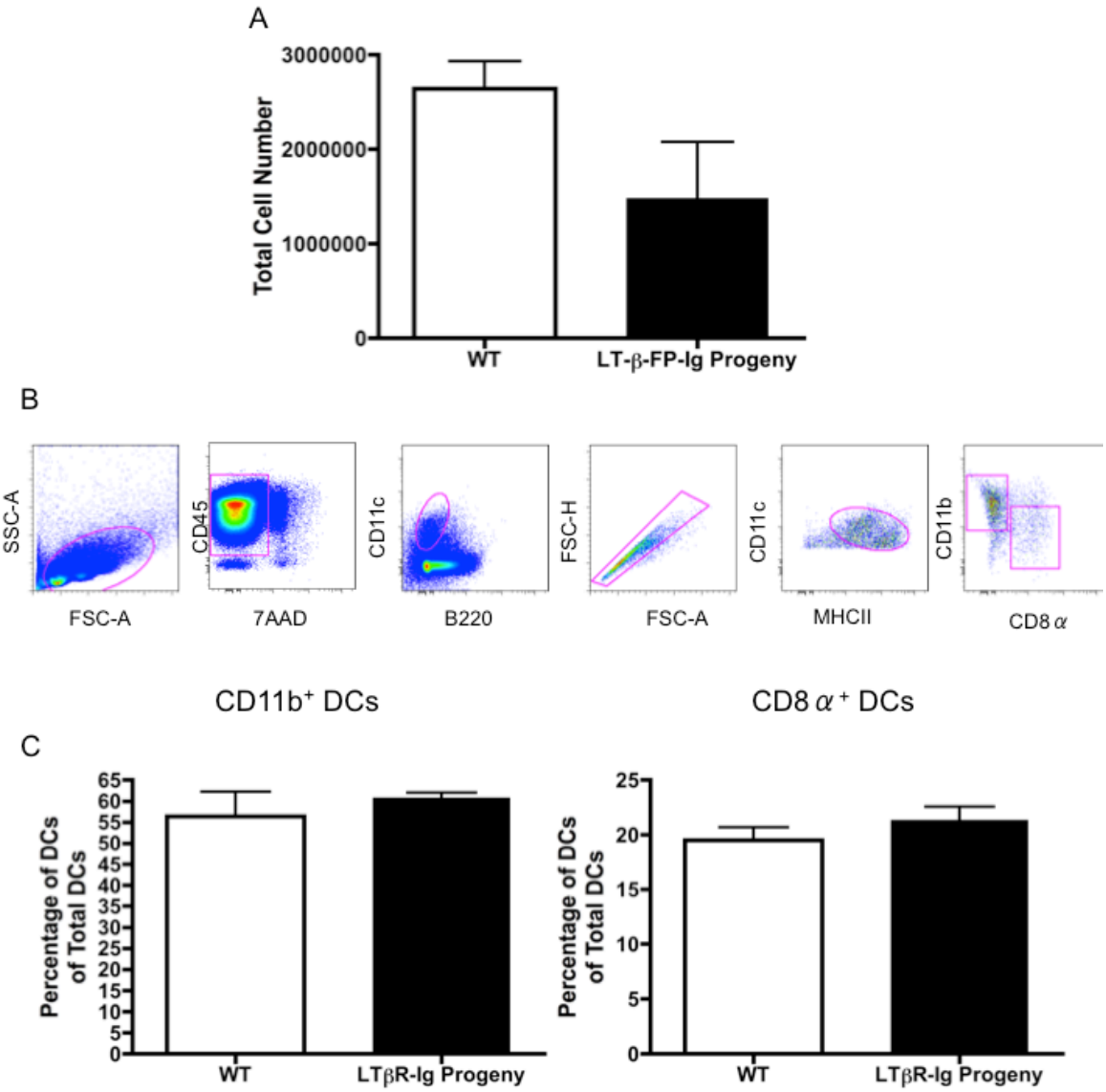

Figure 4-23 Characterisation of Dendritic Cell Subsets in the Inguinal Lymph Nodes of WT and LTβR-Ig mice.

ILNs of WT and LTβR-Ig mice were digested and cells stained for flow cytometry from WT and 8-week-old LTβR-Ig treated animals. The numbers of total cells were analysed (A). Large, live leukocytes ($CD45^{+}7AAD^{-}$), were gated and $CD11c^{+}B220^{-}$ were further selected, single $MHCII^{+}CD11c^{+}$ cells were identified as DCs and were divided into subsets based upon their expression of CD11b and CD8α (B). The percentages of $CD11b^{+}$ DCs and $CD8\alpha^{+}$ DCs were compared (C) Data are means and S.E.M. and results were analysed by students *t* test, (n=6). FACS plots representative of 6 independent biological replicates.

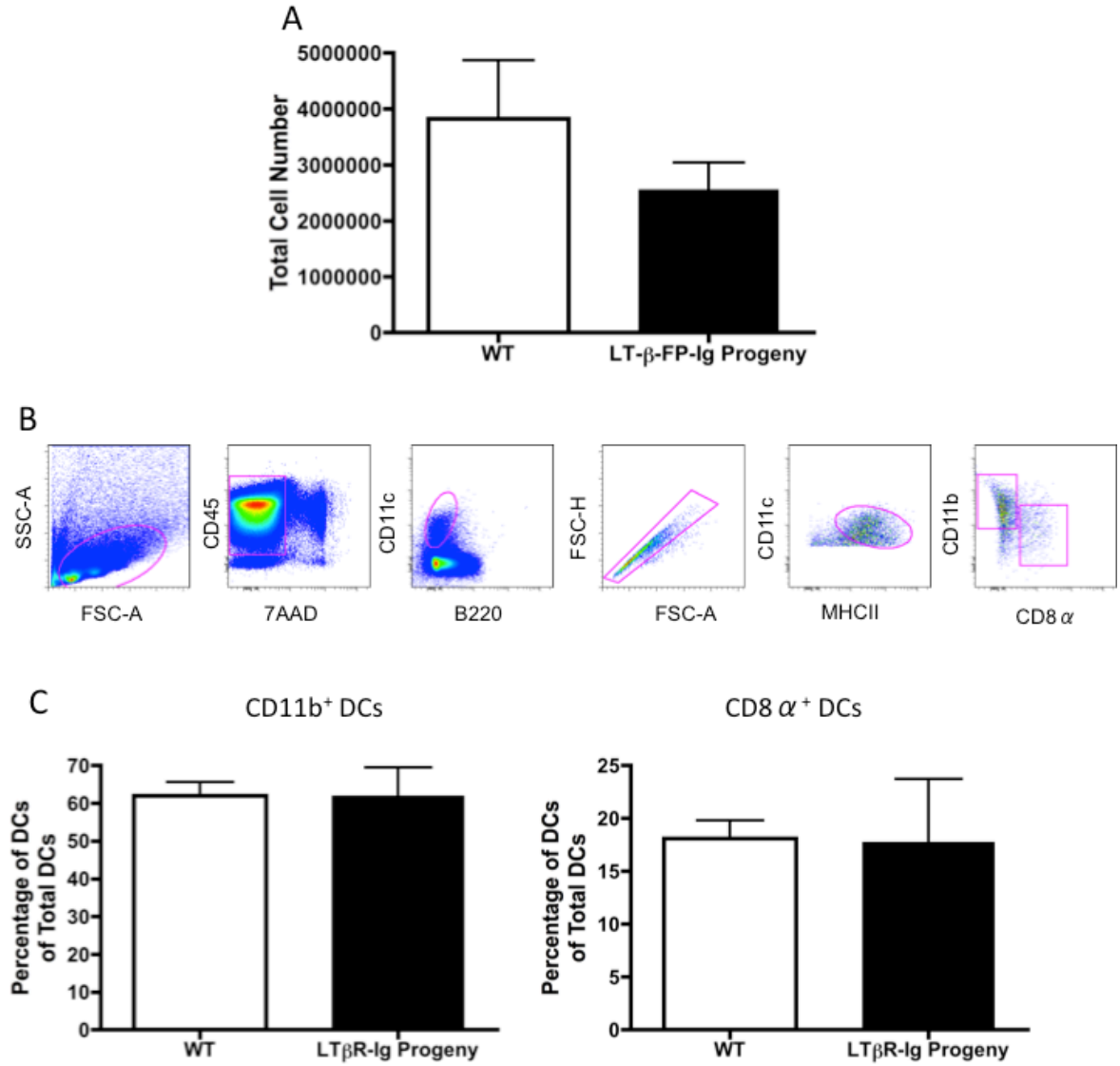

Figure 4-24 Characterisation of Dendritic Cell Subsets in the Cervical Lymph Nodes of WT and LTβR-Ig-treated mice.

CLNs of WT and LTβR-Ig-treated mice were digested and cells stained for flow cytometry from WT and 8-week-old LTβR-Ig treated animals. The numbers of total cells were analysed (A). Large, live leukocytes ($CD45^+7AAD^-$), were gated and $CD11c^+B220^-$ were further selected. Single $MHCII^+CD11c^+$ cells were identified as DCs and were further divided into subsets based upon their expression of CD11b, CD8α (B). The percentages of $CD11b^+$ DCs and $CD8\alpha^+$ DCs were compared (C) Data are means and S.E.M. and results were analysed by students *t* test. FACS plots representative of 6 independent biological replicates.

To investigate if there was a systemic defect in DCs, particularly in their development we generated DCs from BM grown in the DC specific growth factor Flt3L. Therefore, if there were any gross defects in the generation of specific populations of DCs these would be detected. Cells from the femurs and tibias were isolated from WT and LTβR-Ig treated mice. These cells were cultured in the presence of Flt3L for 7 days. The phenotypes of the BMDCs generated was compared by flow cytometry. Live cells were gated and the $CD11c^+$ population was further gated upon $MHCII^+B220^-$. The percentages of DCs were compared between WT and LTβR-Ig treated progeny (Figure 4.25 A and B). There were no significant differences in the development of DCs from BM when cultured with Flt3L. This confirms that there is no obvious defect in the development of DCs from precursors, *in vitro*, in LTβR-Ig progeny.

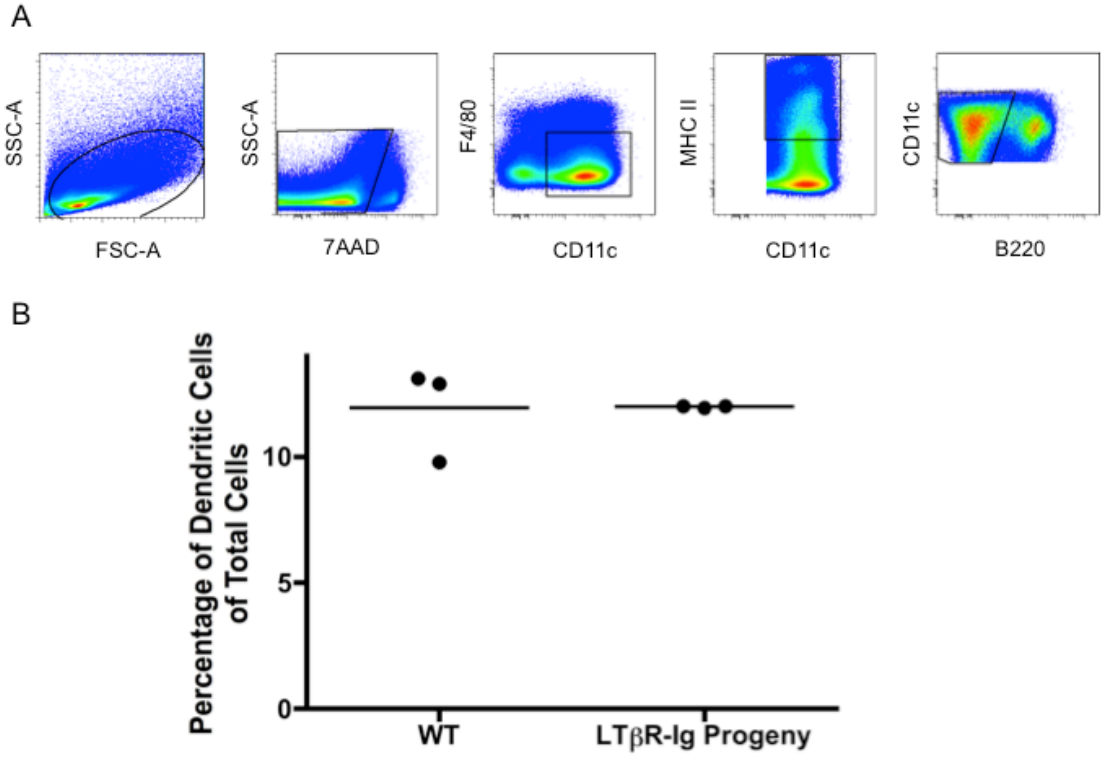

Figure 4-25 Characterisation of Dendritic Cells Generated from Bone Marrow of WT and Mice Treated *in Utero* with LTβR-Ig.

Bone Marrow Cells were isolated and cultured for seven days with Flt3L from WT and 6-week-old LTβR-Ig treated animals. Cells were harvested and stained for flow cytometry. Large, live ($7AAD^-$) $CD11c^+F4/80^-$ cells were gated, $MHCII^+$ $B220^-$ cells were identified as DCs (A). The percentage of DCs of total cells was compared (B) and results were analysed by students *t* test (n=6). FACS plots representative of 3 independent biological replicates.

4.2 Discussion

I have used two separate models lacking in specific intestinal organised lymphoid tissues to determine the origin of DC subsets in the intestine. Determining the origin of migrating DC subsets will provide key information regarding how DCs begin to initiate an immune response. The data presented here represent a significant step towards a definitive characterisation of the anatomical location of migratory DCs in the intestine.

Lymphoid tissue in the SI can be divided into effector sites that consist of lymphocytes scattered throughout the LP, or organised lymphoid tissue. Within the SI there are two distinct types of organised lymphoid tissue PPs and ILFs. PPs are formed before birth and remain fully developed throughout life; in comparison ILFs represent a spectrum of differentially developed lymphoid structures, they are a continuum of differentially developed lymphoid tissue. CPs are able to fully develop into mature ILFs in response to signals from the commensal flora, a process that is likely to continue throughout life although the function of ILFs may change with aging (Lorenz et al., 2003) (McDonald et al., 2011; Pabst et al., 2006).

The situation in the colon is remarkably different; apart from the caecal patch, PPs are completely missing. Additionally, organised colonic lymphoid structures are developmentally different to those in the SI. They can be efficiently generated in the absence of LTi cells (Lochner et al., 2011), and require different developmental signals (Knoop et al., 2011). Furthermore, the formation of ILFs in the colon does not respond to commensal flora, while ILFs in the SI are responsive to flora (Fagarasan et al., 2002; Kweon et al., 2005). Therefore, lymphoid aggregates differ between the SI and colon and should be considered separately.

4.2.1 Abrogated Lymphoid Tissue But Normal Dendritic Cell Development in RORγtCD3ε Deficient Mice

To determine the anatomical origins of each of the DCs subsets, PP-free mice were investigated. Several strains of transgenic mice have been described which lack PPs but still have intestinal DCs. Recently Peter Lane and colleagues have

developed a strain of "CD3εRORγt" mice by crossing CD3εtg26 mice (CD3ε) with RORγt deficient mice. In the intestine RORγt is required for the development of lymph nodes, PPs, CPs and therefore ILFs (Eberl and Littman, 2003). During foetal life, RORγt is exclusively expressed in LTi cells, a cell type that localises in developing lymph nodes, including MLNs, PPs and ILFs. Mature LTi cells interact with LTo cells, resulting in subsequent maturation of lymphoid tissue and the recruitment of monocytes and lymphocytes (Eberl and Littman, 2003). Therefore, because RORγt deficient mice lack LTi cells, they also lack LNs, PPs, and ILFs in the SI. However, they still posses lymphoid aggregates in the colon (Lochner et al., 2011). The combined phenotype of the RORγtCD3ε deficient mice is a lack of T cells, NK cells and LTi cells and the absence of MLNs, PPs and ILFs. Although these mice lack lymph nodes, PPs and ILFs they still have DCs in the SI (P Lane, personal communication). Therefore any DCs migrating in the afferent lymph of these mice must be derived from the siLP or colon, as there are no PPs or ILFs.

Due to the well-documented function of RORγt in LTi cells, we predicted there would be no PPs or ILFs in the intestine of RORγt deficient animals. In order to check this, Swiss-roll sections of intestine were prepared. This enabled large areas of SI to be investigated for the presence of PP or ILFs. As both PPs and ILFs are predominantly filled with B cells, sections were stained with B cell-specific B220, allowing visualisation of both PPs and ILFs. $B220^+$ structures were identified in the intestine of CD3ε deficient mice, but not RORγtCD3ε deficient mice (Figure 4.3). PPs and ILFs were easily distinguished from one another by their size, with the larger PPs containing many more germinal centres than ILFs. ILFs are much smaller than PPs, being shorter but roughly twice as thick as villi with very closely packed lymphocytes (Kanamori et al., 1996). The lack of $B220^+$ structures in the SI confirmed that RORγtCD3ε deficient mice do not contain any organised lymphoid tissue in the SI.

Previous reports suggested that RORγt deficient mice had a reduced number of $CD11b^+CD4^+$ DCs in the spleen (P.Lane, personal communication). To verify this, cells in the spleen of RORγtCD3ε deficient mice were compared to CD3ε deficient and WT mice. There were no significant differences between the numbers of neutrophils, monocytes, pDCs and cDCs between RORγtCD3ε, CD3ε and WT mice

(Figure 4.9). There were also no significant difference amongst DC subsets in the spleens of RORγtCD3ε, CD3ε deficient mice and WT mice (Figure 4.9). These results contrasted with previous reports, as we detected no significant difference between the numbers of $CD11b^+CD4^+$ DCs in the spleens of these animals. The previous reports of a specific decrease of $CD11b^+CD4^+$ DCs in the spleen of RORγtCD3ε deficient mice were important because DC subsets arise from a common precursor. Therefore this could indicate that RORγtCD3ε deficient mice have a universal DC defect, causing there to be a defect in DC generation throughout the body. Splenic $CD11b^+CD4^+$ DCs normally reside in the marginal zone of the spleen. As there is likely to be a LTα1β2 component in the development to splenic white pulp, which would likely be affected in RORγCD3ε deficient mice due to the lack of LTi cells (Vondenhoff et al., 2008), this specific defect in $CD11b^+CD4^+$ DCs may be due to a lack of appropriate signals in their environment. However, there is a level of plasticity in the development of the spleen that may explain why some DCs are able to develop normally (Glanville et al., 2009). In contrast to previous reports, we did not find a decrease in $CD11b^+CD4^+$ DCs. Therefore, this previously reported decrease may represent a transient change in the population and that there is some flexibility in the LN organisation of RORγtCD3ε deficient mice. Our data suggest that there was no systemic defect in DC development in RORγtCD3ε deficient mice, making these animals a useful model to investigate DC subsets in the intestine.

In order to further confirm that RORγtCD3ε deficient mice did not have a developmental defect in the generation of DCs, we isolated BM from RORγtCD3ε deficient mice and used this to generate BM DCs using Flt3L. There was no difference in the ability of RORγtCD3ε deficient animals to generate DC populations from BM in response to Flt3, compared to CD3ε and WT mice (Figure 4.10). Therefore, these animals do not appear to have a systemic defect in DC development, supporting their utility for investigations of DC subsets in the intestine. Despite these results it remains possible that a small defect in DC development exists. To formally exclude this possibility, precursors could be sorted and injected into WT recipients.

Although these mice provide a useful model for investigating DC subsets in the intestine, they lack all secondary lymphoid organs except a spleen. This may

cause specific effects in the intestine, for example the lack of MLNs has been shown to cause a reduction in oral tolerance. Therefore the absence of the MLN can change the immunological setting in the intestine, and may cause different subsets of DCs to migrate. Alternatively without lymphoid tissue to migrate towards, DCs may not migrate into the thoracic duct in the conventional manner. Therefore, it is important to use more than one method to investigate the anatomical origins of the DC subsets. It is also essential that DC subsets in the BM and spleen are investigated to determine if the lack of RORγtCD3ε results in a defect in the development of DC subsets in other tissues.

4.2.2 Abrogated Peyer's Patch But Normal Lymph Node and Dendritic Cell Development in LTβR-Ig Treated Progeny

In order to elucidate the difference between DCs migrating from PPs and ILFs we generated mice that lack only PPs. As previously described i.v injection of LTβR-Ig into pregnant mice at E14.5 and E17.5 results in PP-null progeny (Rennert et al., 1996; Rennert et al., 1998; Taylor et al., 2007). LTβR-Ig blocks interactions between membrane bound LTα1β2, present on the surface of lymphocytes, NK cells and LTi cells and the LTβ receptor that is expressed upon non-haematopoietic cells, such as LTo cells (Tumanov et al., 2003). Mice deficient in LTα or LTβR lack PPs and LNs, demonstrating that this interaction is essential for the development of LNs and PPs. As lymphoid organs develop sequentially, transiently blocking this interaction with LTβR-Ig allows development of specific lymphoid organs to be inhibited, without affecting other LNs. LTβR blockade on or before E17 prevents PP development, without affecting the development of the MLN. These animals will retain ILFs; in fact gestational LTβR-Ig treatment is reported to result in enhanced ILF development (Lorenz et al., 2003). Additionally, these animals retain colonic lymphoid aggregates (Lorenz et al., 2003).

In comparison to RORγtCD3ε deficient mice, which lacked all secondary lymphoid organs, mice treated with LTβR-Ig at E14 and E16 (LTβR-Ig mice) will only lack PP; other lymphoid organs will be intact. Use of LTβR-Ig provides a more precise way to remove specific lymphoid organs. However, previous studies using LTβR-Ig to remove PPs have shown that in the case of IgA producing B cells, there was

some compensation for the lack of PPs via the expansion of ILFs (Lorenz and Newberry, 2004). This potential expansion of ILFs should be borne in mind while analysing results from these animals, as it may also affect to DC subsets present in the PPs and ILFs.

Next, we used LTβR-Ig to treat pregnant female mice and confirmed that PPs were absent and ILFs were present in the offspring of the treated animals. Initial macroscopic examination of the SI revealed the presence of complete MLN and the absence of PPs in all animals treated with LTβR-Ig fusion protein *in utero* (Figure 4.13). To ascertain whether *in utero* exposure to LTβR-Ig fusion protein affected the development of ILFs, we generated multiple Swiss-roll sections of SI, which were examined using immunofluorescence microscopy. Similar to Swiss-roll sections from RORγtCD3ε and CD3ε deficient mice, sections were stained with B220 to reveal B cell rich PPs and ILFs. Examination of these sections confirmed that ILF development was not affected by *in utero* exposure to LTβR-Ig fusion protein but that PP development was abrogated (Figure 4.14). Previously it has been reported that *in utero* exposure to LTβR-Ig caused an increase in the number of ILFs after birth (Lorenz et al., 2003). Although the numbers of ILFs were not assessed here, it is possible that there was an increase in their numbers in line with previous reports.

As the development of all LNs involves the interaction between LTβR and LTα1β2 and therefore could be affected by injections of LTβR-Ig, it was essential to investigate if other LNs and cell populations within them were affected by the injection of LTβR-Ig. The numbers of neutrophils, monocytes, pDCs and other cells were not affected in the spleen of LTβR-Ig treated progeny (Figure 4.21). Furthermore, there were also no differences in the numbers or percentages of any of the DC subsets in either the ILN, CLN or spleen of mice treated with LTβR-Ig (Figures 4.23, 4.24 and 4.22 respectively). Therefore, as there was also no defect in the ability of these animals to generate DCs or other cells, this mouse model provides an excellent way to investigate the anatomical origins of DC subsets in the intestine.

4.2.3 Dendritic Cell Subsets In The Intestine of Mice Lacking Peyer's Patches or Peyer's Patches and Isolated Lymphoid Follicles

We next investigated DCs migrating from the intestine of RORγtCD3ε deficient animals and mice treated with LTβR-Ig *in utero*. As RORγtCD3ε deficient mice do not have PPs or ILFs, any DCs migrating from the intestine must originate from the siLP or colon. In comparison, animals treated with LTβR-Ig will lack only PPs, ILFs are retained, and so in these animals DCs migrating from the intestine originate from the siLP, ILFs or the colon. In order to investigate migratory DCs from the intestine, TDC was performed. There are four distinct subsets of DCs that are able to migrate in pseudo-afferent lymph from WT untreated mice, identified by their expression of CD103 and CD11b. The functions of these DC subsets was previously discussed in Chapters 1 and 3, therefore I will here concentrate upon their anatomical origins in the intestine.

In pseudo-afferent lymph, SI digests and colonic digests, RORγtCD3ε, CD3ε deficient mice and WT mice had similar percentages, and numbers of $CD103^+CD11b^+$ DCs. The pseudo-afferent lymph, SI and colonic digests of mice treated with LTβR-Ig *in utero* also had similar numbers and percentages of $CD103^+CD11b^+$ DCs. Furthermore, in mice treated with LTβR-Ig, the MLN $CD103^+CD11b^+$ DC population was unchanged compared to WT animals. $CD103^+$ DCs have been extensively investigated in the intestine, with many groups showing the majority of DCs in the both the siLP and cLP are $CD103^+$ (Jaensson et al., 2008; Johansson-Lindbom et al., 2005; Rivollier et al., 2012; Schulz et al., 2009; Varol et al., 2009). Some $CD103^+$ DCs have also been identified in PPs and in ILFs. In contrast to the LP, the majority of DCs in the GALT are $CD103^-$ (Bogunovic et al., 2009; Jaensson et al., 2008). $CD103^+CD11b^+$ DCs have previously been identified by immunohistochemistry in the siLP of mice and humans (Persson et al., 2013). The fact that $CD103^+CD11b^+$ DCs have been frequently identified in the siLP and the MLN makes their presence in the lymph of RORγtCD3ε deficient and LTβR-Ig treated mice unsurprising, as the majority of lymph cells are likely to be siLP derived. As RORγtCD3ε deficient mice do not have any SI GALT the only place from which these DCs can originate is the conventional villus mucosa. In contrast, colonic patches are still able to form in RORγtCD3ε deficient mice, and were present following digests, therefore in the

colon these CD103$^+$CD11b$^+$ DCs may be derived from either the cLP or from the colonic patches that will be present in the digest. However, they are likely to be derived mainly from the siLP as this was the largest population present in the migratory DC gate in the siMLN and there are fewer CD103$^+$CD11b$^+$ DCs in the colon.

CD103$^+$CD11b$^-$ DCs were also present in pseudo-afferent lymph in comparable percentages and numbers in RORγtCD3ε, CD3ε deficient and WT mice (Figure 4.4). Furthermore they were also able to migrate from the intestine of mice treated with LTβR-Ig (Figure 4.15). They were present in siLP and cLP digests of RORγtCD3ε deficient mice and LTβR-Ig treated animals. Additionally, they were present in the MLN of mice treated with LTβR-Ig (Figure 4.17). Our work has shown these migratory CD103$^+$CD11b$^-$ also express CD8α$^+$ in WT mice (Cerovic et al., 2012). This was perhaps surprising as previous work had suggested that CD8α$^+$ DCs were not present in the LP, but were a contaminant of resident DCs within secondary lymphoid organs, and so are not a migratory population (Jakubzick et al., 2008). More recently, however, CD11b$^-$ DCs have been identified in the LP (Fujimoto et al., 2011; Jang et al., 2006). CD8α$^+$ DCs have been identified in PPs, although the majority of these are likely to be CD103$^-$ as there are few CD103$^+$ DCs in PPs (Kelsall, 2008). In order to confirm the lymph CD103$^+$CD11b$^-$ subset in our experiments was still reproducibility CD8α$^+$, lymph from RORγtCD3ε deficient mice was stained with the CD8α specific antibody. The CD103$^+$CD11b$^-$ subset was the only subset that expressed CD8α in the lymph and SI of RORγtCD3ε deficient mice (Figures 4.5 and 4.7 respectively). We show here that CD103$^+$CD11b$^-$CD8α$^+$ DCs were present in pseudo-afferent lymph from RORγtCD3ε deficient mice and mice treated with LTβR-Ig. These data from the RORγtCD3ε deficient mice conclusively show, for the first time, that CD8α$^+$ DCs are able to migrate from the effector site of siLP in lymph.

These CD103$^+$CD11b$^-$CD8α$^+$ DCs were also present in the lymph of LTβR-Ig treated animals. Therefore, it is possible that some of these cells may also be migrating from the ILF or colon, as well as the LP. Although, if this is possible it is likely to be a small number of cells as the percentages of CD103$^+$CD11b$^-$ cells was comparable between RORγtCD3ε deficient mice and LTβR-Ig treated animals. The majority of DCs in SILT have been reported to be CD103$^-$ (Jaensson et al.,

2008). However, $CD103^+CD11b^-CD8\alpha^+$ DCs were still present in the SI digests from RORγtCD3ε deficient mice (Figure 4.6). This definitively shows, for the first time, that these cells are present in the siLP, as RORγtDE3ε deficient animals have no lymphoid tissue in the SI.

$CD103^-CD11b^+$ DCs were also identified migrating in pseudo-afferent lymph of RORγtCD3ε deficient mice and LTβR-Ig treated animals in comparable percentages and numbers to CD3ε deficient mice and WT mice (Figures 4.4 and 4.15 respectively). They were also present in SI digests and colonic digests of RORγtCD3ε deficient mice and LTβR-Ig treated mice. As outlined in Chapter 3, the majority of previous work that identified $CD11c^+MHCII^+CD103^-$ cells in the LP has misclassified these cells as DCs. Work in our laboratory has identified a genuine population of $CD103^-CD11b^+$ DCs that migrate in intestinal lymph, expand in response to Flt3L and prime naïve T cells (Cerovic et al., 2012). The majority of DCs in PPs and ILFs have also been identified as being $CD103^-$; in PPs there is population of $CD11b^+CD8\alpha^-$ DCs that are able to migrate from the subepithelial dome to the inter-follicular region after stimulation with *Toxoplasma gondii* (Cook et al., 2000). Therefore it is possible that some of these PP or ILF-derived cells are able to migrate in pseudo-afferent lymph. The published data have not yet addressed this question. However as $CD103^-CD11b^+$ DCs are present in the lymph of PP-null mice, they must also migrate from the conventional villus mucosa. This is supported by the fact these cells were also detected in SI digests from RORγtCD3ε deficient mice.

$CD103^-CD11b^-$ DCs were present in similar numbers and percentages in mice treated with LTβR-Ig and untreated WT mice (Figures 4.15 and 4.19). In comparison, this subset was significantly reduced in RORγtCD3ε deficient mice (Figures 4.4 and 4.6). Interestingly the few cells left in the $CD103^-CD11b^-$ DC gate in RORγtCD3ε deficient mice appeared to express some CD8α (Figure 4.7), although this was not the case in pseudo-afferent lymph where $CD103^-CD11b^-$ DCs were completely missing and were not analysed for their expression of CD8α (Figures 4.4 and 4.5) This may represent a false positive result as there are very few cells which were analysed for their expression of CD8α. Alternatively it may be that in the siLP these $CD103^-CD11b^-$ DCs represents a heterogeneous population of cells, containing a non-migratory $CD8\alpha^+CD103^-CD11b^-$ population of

cells that were not present in pseudo-afferent lymph. This CD103$^-$CD11b$^-$ DC subset from RORγtCD3ε deficient animals should be further investigated by analysis of surface marker expression and sorting this population and determining more about its function by microarray.

As RORγtCD3ε deficient mice lack both PPs and ILFs in the SI, while mice treated with LTβR-Ig are missing only PPs, data from pseudo-affererent lymph suggests that the CD103$^-$CD11b$^-$ DC is likely to be derived from SI ILFs. Specifically SI ILFs as this population also appeared to be reduced in the colon of WT mice (Figures 4.8, 4.20). Previously, the phenotype of ILF DCs has been investigated by manually separating ILFs from all other intestinal tissues followed by flow cytometry, or by immunohistochemistry (Jaensson et al., 2008; McDonald et al., 2010). McDonald *et al*. showed that the majority of CD11c$^+$ cells within the ILF were CD11b$^-$ although the expression of CD103 was detected in the ILF-derived DCs (McDonald et al., 2010). Jaensson *et al*. showed the majority of DCs in the SILT are CD103$^-$, however CD11b and CD8α expression were not investigated. ILFs are distinct anatomical structures in the intestine, in which DCs and B cells are closely associated with epithelial cells. The DCs that originate here are likely to have been exposed to a different immune environment than LP- or PP-derived DCs. For example, ILFs develop only as required in response to changes in the enteric flora or dietary signals (Bouskra et al., 2008; Lee et al., 2012; Lorenz et al., 2003); once the challenge has been resolved it is likely they they regress to their precursor stages (Hu et al., 2011). Therefore, ILFs can be thought of as a dynamic response to the luminal microbial burden. This specialised environment could generate the features that distinguish the ILF-DCs from the other migrating intestinal DC populations; the presence of four DC subsets in PP null animals combined with our previous findings suggest that ILF DCs possess the CD103$^-$ CD11b$^-$ surface phenotype. We have previously shown that only CD103$^-$ CD11b$^-$ DCs drive differentiation of naïve antigen-specific T cells towards an IL-17-secreting phenotype, even in the absence of exogenous stimulation (Cerovic et al., 2012). These properties make the CD103$^-$CD11b$^-$ ILF DCs an intriguing population to target for future manipulation of the intestinal immune response.

4.3 Conclusions

Here I have shown that different subsets of DCs in the intestine originate from different anatomical origins. This provides an interesting insight into the organisation of the intestinal immune response, as well as providing potential avenues by which to target specific DC subsets with defined functions.

We identified $CD103^+CD11b^+$ DCs migrating from the intestine in RORγtCD3ε deficient mice and PP-null LTβR-Ig treated mice. Therefore, these $CD103^+CD11b^+$ DCs are present in the siLP. This finding was somewhat expected as they have previously been identified as the most numerous subset in the siLP and were identified by immunofluorescence (Persson et al., 2013; Schulz et al., 2009). Earlier work has shown that migratory $CD103^+$ DCs are essential in the induction of oral tolerance to soluble antigen, via the production of RA inducing gut-homing receptors on antigen-specific T cells and promoting TGF-β dependent $Foxp3^+$ Tregs (Coombes et al., 2007; Pabst et al., 2007; Sun et al., 2007). Indeed, the induction of oral tolerance has been associated with an increase in the percentage of $CD103^+CD11b^+$ DCs (Shiokawa et al., 2009). As DCs in the siLP are able to sample small soluble antigen (Chirdo et al., 2005), the presence of $CD103^+CD11b^+$ DCs in the siLP fits with the reported ability of this cell type to gain access to small soluble molecules, migrate to the MLN and produce a tolerogenic response. More recent work has shown that $CD103^+CD11b^+$ DCs in the intestine are able to play a role in Th17 cell differentiation via the production of IL-6, under conditions of inflammation (Persson et al., 2013). Th17 cells play an essential role in protecting the intestine against extracellular bacteria and fungi in the intestine, and promoting tissue repair (Reviewed by (Huber et al., 2012)). If there is a breach in the integrity of the epithelial barrier by an infectious agent, this abundant subset of DCs is able to respond. Therefore this $CD103^+CD11b^+$ DC subset is able to not only induce a tolerogenic response to soluble antigens, but can also induce an immunogenic response in certain conditions. Thus, they are ideally located in the siLP to achieve their function.

We have also confirmed the presence of $CD103^+CD11b^-CD8\alpha^+$ DCs migrating in the intestine, and have shown that these originate from the LP. Previously, $CD8\alpha^+$ DCs were presumed to de derived only from lymphoid tissue. However we

and others, have now shown that these are located in the siLP (Cerovic et al., 2012; Fujimoto et al., 2011). In lymphoid tissues the functions of CD8α^+ DCs is to cross present exogenous antigen to CD8$^+$ T cells, which is essential in order for the generation of a CTL response. In the intestine CD103$^+$CD11b$^-$CD8α^+ DCs are also likely play a role in the cross presentation of peripheral antigen, such as intestinal epithelial cells, directly to CD8α^+ T cells (V. Cerovic, personal communication). Therefore if the function of CD8α^+ DCs is to detect apoptotic or virally infected cells they would have to be located in the siLP, as well as other peripheral tissues such as the lung (Desch et al., 2011). Here I have confirmed that CD103$^+$CD11b$^-$CD8α^+ DCs are present in the siLP, making them ideally located for the uptake of apoptotic intestinal epithelial cells. This constantly overturning population of cells is the front line of the mucosal barrier, therefore the presence of CD103$^+$CD11b$^-$CD8α^+ DCs is likely to represent a constant immune supervision of these vulnerable cells.

We recently described a genuine population of CD103$^-$CD11b$^+$ DCs that were able to migrate in pseudo-afferent lymph (Cerovic et al., 2012). Here I have shown that these cells are present in the siLP, as they were observed migrating in both RORγtCD3ε deficient mice and LTβR-Ig treated animals. As this is a newly described subset of migratory DCs, there is less information regarding its function *in vivo*. However some theories of its function, and why this subset is present in the siLP can be can be speculated from *in vitro* studies. CD103$^-$CD11b$^+$ DCs in the intestine represent only around 15% of migratory DCs, they can present antigen to naïve T cells and induce the presence of gut homing receptors on responding T cells. CD103$^-$CD11b$^+$ DCs were the only subset able to induce IFN-γ producing T cells in the absence of overt stimulation, as well as this they were are induce IL-17 producing T cells (Cerovic et al., 2012). As the majority of LP DCs are specialised to produce a tolerogenic response to harmless antigens, these DCs could represent a robust way in which the immune response can quickly respond to pathogenic challenge. Therefore their presence in the siLP alongside CD103$^+$ DCs would be essential, however a tolerogenic response would be favoured due to the larger numbers of CD103$^+$ DCs.

CD103$^-$CD11b$^-$ DCs are also a newly described population of genuine DCs in the siLP (Cerovic et al., 2012). Here, I have shown that CD103$^-$CD11b$^-$ DCs migrate

from SI ILFs, as these were missing in RORγtCD3ε deficient mice but present in LTβR-Ig progeny. Furthermore, this population did not appear to be present following cLP digests of WT mice. This is the smallest population of DCs in the siLP, accounting for less than 10% of total DCs. It also exclusively induced IL-17 producing T cells in the absence of overt stimulation (Cerovic et al., 2012). Recent work has shown that mice deficient in Th17 cells were unable to produce T cell dependent antigen specific IgA (Hirota et al., 2013). As ILFs are a dynamic lymphoid tissue that are able to produce antigen specific IgA, an IL-17 producing subset of $CD103^{-}CD11b^{-}$ DCs originating from here is a reasonable conclusion.

The data I have presented here show that three functionally distinct subsets of DCs are able to migrate from the siLP, while one subset of $CD103^{-}CD11b^{-}$ DCs are likely to migrate from ILFs. However, it does not discount the possibility that some DCs may also originate from PPs.

Chapter 5: Dendritic Cell Migration From Peyer's Patches to the Mesenteric Lymph Nodes

PPs are secondary lymphoid organs that form part of the GALT. They are sites for the initiation of both immunostimulatory and immunomodulatory responses in the SI (Sato and Iwasaki, 2005). They share common features with other secondary LNs, such as the presence of follicular B cell and T cell regions. However they also have unique features such as the presence of M cells for the capture and processing of particulate luminal antigen, and the ability to initiate antigen specific immune responses against M cell derived antigen (Kraehenbuhl and Neutra, 2000). DCs are present throughout the PPs, where they are essential for the processing and presentation of antigen. Iwasaki and Kelsall identified three populations of DCs based upon their expression of CD11b and CD8α. They showed these different subsets had distinct functions, and were present in discrete parts of the PP (Iwasaki and Kelsall, 2001). In contrast others have used CD103 and CD11b to define DC subsets in the PPs, where they also identify three subsets (Bogunovic et al., 2009).

Although we have shown that no specific MLN or intestinal lymph DC subset was missing from PP-free mice, we did not directly investigate whether migration of DCs from PPs to MLN was possible. This is a long-standing area of uncertainty in the field. Previous reports have suggested that there may be some migration from the PP to the MLN in rodents, however this has not been directly assessed (Macpherson and Uhr, 2004). MacPherson and Uhr demonstrated commensal bacteria were able to gain access to the MLN, however they did not show if this was via the PP or the siLP. Similarly, Pron *et al*. demonstrated in rats that *Listeria monocytogenes* was present in the MLN following intra luminal administration (Pron et al., 2001). Although, similar to MacPherson and Uhr, they did not provide direct evidence that PP DCs were transporting bacteria to the MLN.

It is important to understand if PP DCs are able to migrate to the MLN for a number of reasons. Firstly PP and LP DCs are likely to transport antigen acquired via different routes, fully functional M cells are only present in GALT therefore PPs are specialised for the uptake of particulate antigen (Knoop et al., 2009; McDole et al., 2012). Secondly, the microenvironment differs between the PPs and the MLN. For example, PPs DCs have been shown to produce higher levels of TGF-β than MLN DCs; upon bacterial stimulation this was present with a concomitant rise in IL-6 that may promote the synthesis of secretory IgA (Fink and Frokiaer, 2008). Therefore DCs from PPs may be specialised for class switching to IgA and have been shown to preferentially induce a Th2 type response (Iwasaki and Kelsall, 1999). Although DCs from the PP and MLN share considerable functional overlap, there are some key differences meaning they likely to play different physiological roles. For example delayed-type hypersensitivity responses were not inhibited by the adoptive transfer of PP DCs from OVA fed mice, but upon transfer of DCs from siLP this delayed type hypersensitivity was inhibited (Chirdo et al., 2005). Therefore MLN DCs are required for systemic tolerance to orally administered antigen, PP DCs alone appear unable to generate this type of response. Furthermore, there have been reports that PP mononuclear cells were not as proficient in causing proliferation of naïve T cells as MLN mononuclear cells (Jump and Levine, 2002). Therefore, it is essential to determine if DCs can migrate to the MLN and identify these cells in the context of recent advances in the identification of phenotypically and functionally distinct DC populations in the mucosa.

5.1 Results

5.1.1 Dendritic Cells from the Peyer's Patches Migrate to the Mesenteric Lymph Nodes in Kaede Mice

To determine if DCs are able to migrate from PPs to the MLN, we used a PP-photoconversion protocol similar to a recently-described method (Cyster and Schwab, 2012) for the photoconversion of PP in kaede mice. As described in Chapter 3 kaede mice express the kaede protein that is irreversibly photoconverted by UV light. This makes them an excellent tool to investigate DC migration in the intestine. In this experiment, all visible PPs were photoconverted for 2 minutes each while the MLN and LP were shielded from the

violet light. The animal was allowed to recover and 24 hours later siMLN and coMLN were removed, digested separately, and the numbers and percentage of kaede-red$^+$ DCs were assessed. Cells were stained with antibodies for flow cytometry and analysed. The gating strategy was consistent throughout the experiment. First, large cells were gated, and dead B220$^+$ cells, and doublets were excluded. MHCII$^+$CD11c$^+$ DCs were selected (Figure 5.1 A), and kaede-red$^+$ DCs were identified in the siMLN (Figure 5.1 B). They were not present in the coMLN (Figure 5.1 C). This was the first direct evidence that DCs are able to migrate from PPs to the MLN. Specifically, DCs migrate from the PP to the siMLN, which I have shown to specifically drain the SI, where the PPs are located.

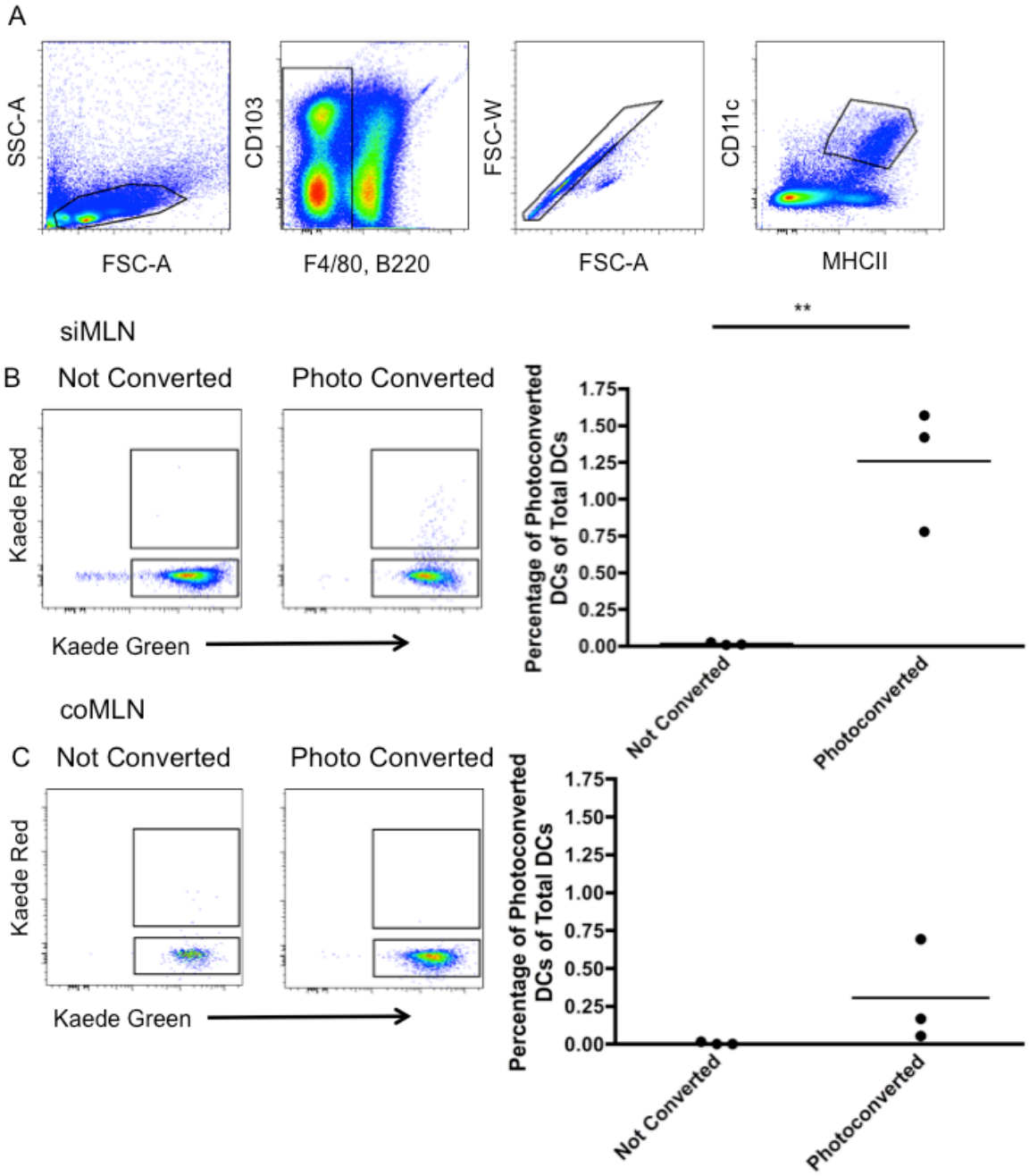

Figure 5-1 DCs Originating in the Peyer's Patches Migrate to Specific Parts of the Mesenteric Lymph Node.

The PPs of photoconvertible kaede mice were exposed to violet light for two minutes each, avoiding the surrounding SI. The siMLN and coMLN were removed 24 hours later and digested. DCs were gated as $F4/80^{-}B220^{-}$, single $MHCII^{+}CD11c^{+}$ cells (A) and kaede-red^{+} DCs were observed and analysed in the siMLN (B) and coMLN (C). Results are representative of three separate experiments with similar results and each point represents and individual animal. A students *t* test was performed **$p<0.01$.

To interpret these data, it was important to investigate how efficient photoconversion was in PPs. This would allow an estimation of how effective the photoconversion technique was for PP DCs. Thus, PPs were removed from mice that had not undergone photoconversion, from mice immediately after photoconversion was performed, and from mice that had undergone photoconversion 24 hours previously. PPs were carefully isolated from the SI and digested to produce a single cell suspension. These cells were labelled for flow cytometry and DCs were gated as large, live, $B220^-$, single cells, $MHCII^+CD11c^+$ cells (Figure 5.2 A). The percentage of kaede-red^+ cells amongst these DCs was assessed (Figure 5.2 B). There were significantly more kaede-red^+ DCs in PPs immediately after photoconversion (70%) than in to mice that had not undergone photoconversion. The percentage, and the total number (data not shown), of kaede-red^+ DCs significantly decreased to around 50% after 24 hours (Figure 5.2 C). Therefore, approximately 70% of DCs were photoconverted in the PP. Subsequently; approximately 1% of DCs in the siMLN became photoconverted, as shown above. Thus, we can conclude that around 1.4% of DCs in the siMLN were of PP origin at 24 hours.

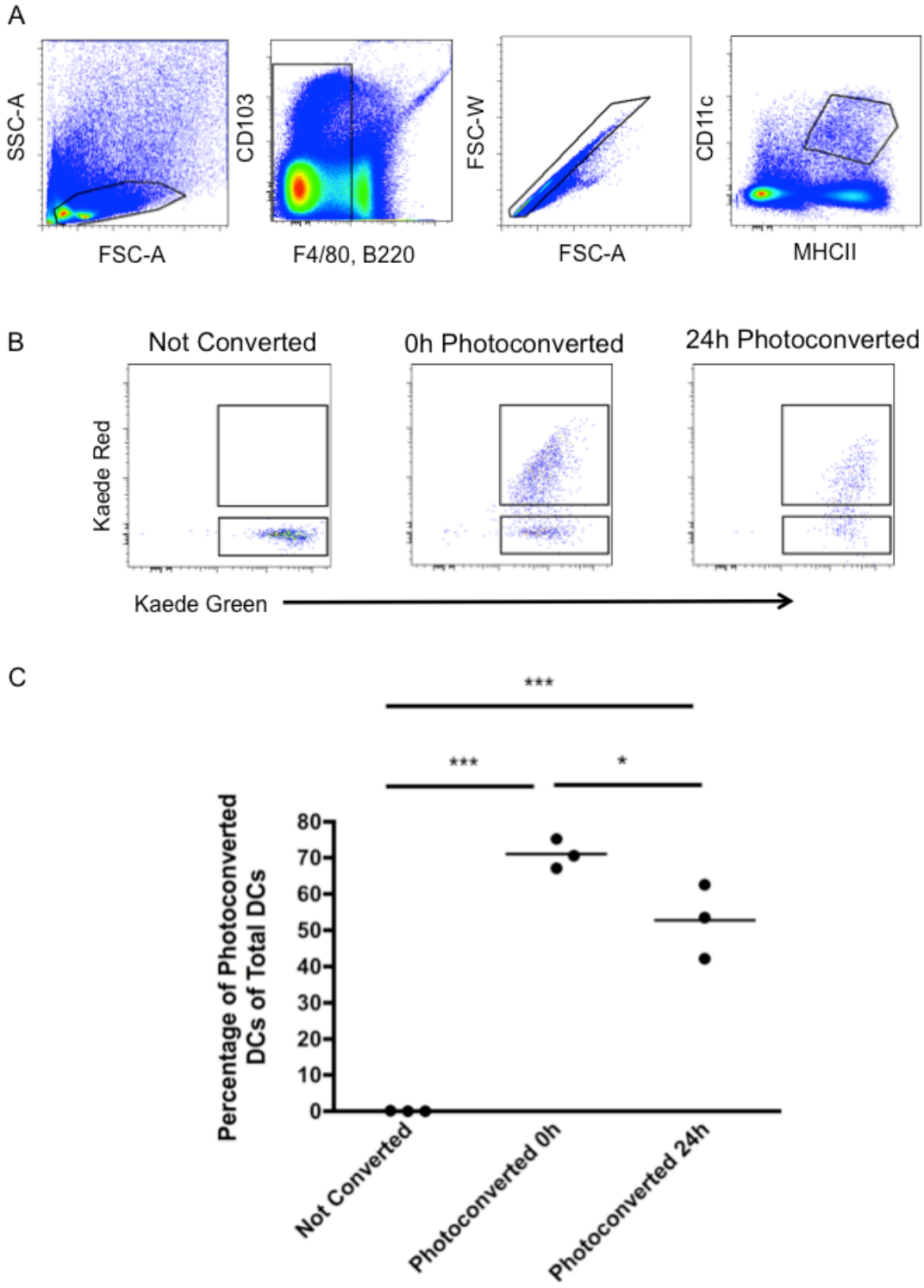

Figure 5-2 Peyer's Patch DCs Express Kaede-Red After Photoconversion.

The PPs of photoconvertible kaede mice were exposed to violet light for two minutes each, avoiding the surrounding SI. PPs were isolated, pooled and digested from individual animals that either did not undergo photoconversion, immediately after photoconversion, or 24 hours after photoconversion. DCs were gated as F4/80$^-$B220$^-$, single MHCII$^+$CD11c$^+$ cells (A) and the presence of kaede-red$^+$ DCs was observed and analysed for each group (B and C). Each point represents PPs pooled from an individual animal. A one way ANOVA was performed, *p<0.05, ***P<0.001.

In order to confirm there was no contamination from the siLP during the photoconversion of PPs, resulting in kaede-red$^+$ DCs from the siLP contaminating our analysis, I digested the SI immediately after photoconversion. Any DCs in the siLP that were accidentally labelled should be evident in the siLP digestion. Once the SI was isolated, PPs were carefully removed and the SI was digested. Cells were labelled and analysed by flow cytometry. Large, live, CD45$^+$, B220$^-$, CD64$^-$ cells were selected. MHCII$^+$CD11c$^+$ single DCs were gated (Figure 5.3 A) and the presence of kaede-red$^+$ cells was investigated (Figure 5.3 B). There were no kaede-red$^+$ DCs in the SI immediately after photoconversion (Figure 5.3 C). The entire SI was acquired following photoconversion, to ensure that no contaminating cells were missed. In fact, there were no photoconverted cells at all in the siLP (data not shown). Therefore, it can be concluded that the photoconversion of PPs does not result in the detectable photoconversion of DCs in the LP. Thus all kaede-red$^+$ cells have originated from the PPs, and are not the result of contamination by the photoconversion of DCs in the LP.

As an additional control, I wanted to ascertain whether the kaede-red$^+$ DCs detected in the MLN were migrating from PP, or were contaminating photoconverted cells directly from the siMLN and coMLN during the PP-photoconversion technique. Therefore the siMLN and coMLN were isolated and digested immediately after PP-photoconversion. Cells were labelled for flow cytometry and DCs were gated as large, CD45$^+$, B220$^-$, live, single, MHCII$^+$CD11c$^+$ cells (Figure 5.4 A). The expression of kaede-red in DCs in the siMLN (Figure 5.4 B) and coMLN (Figure 5.4 C) were compared. There were no kaede-red$^+$ cells in either the siMLN or coMLN immediately after PP photoconversion. Therefore, the photoconversion of PPs does not result in photoconversion of cells directly in the siMLN or coMLN.

Taken together, these results confirm that following PP photoconversion the only kaede-red$^+$ DCs were in the PPs. There was no photoconversion of DCs in the siLP, siMLN or coMLN, meaning it is unlikely that the presence of kaede-red$^+$ DCs in the siMLN was due to accidental photoconversion of tissues other than the PPs. Therefore, approximately 1.4% of DCs in the siMLN are of PP origin. These experiments offer the first direct evidence that PP DCs are able to migrate to the MLN.

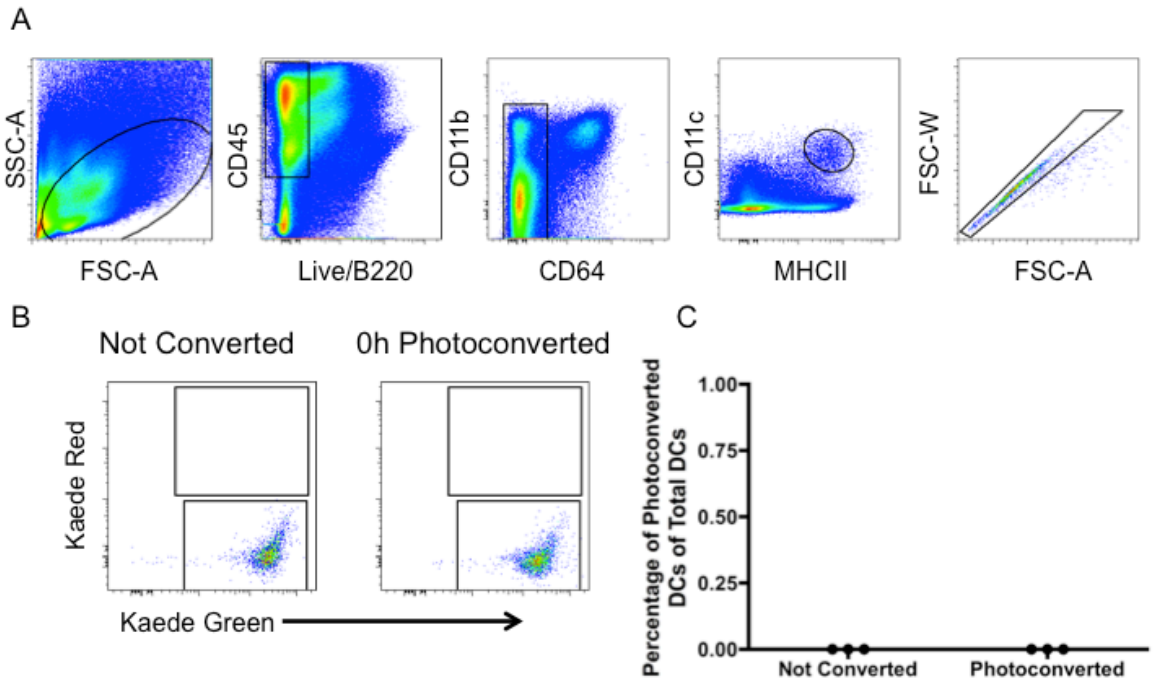

Figure 5-3 Lamina Propria DCs Do Not Express Kaede-Red After Peyer's Patch Photoconversion.

The PPs of photoconvertible kaede mice were exposed to violet light for two minutes each, avoiding the surrounding SI. siLP was isolated and digested from animals that did not undergo photoconversion and from animals immediately after photoconversion. DCs were gated as live $CD45^{+}$, $CD64^{-}$, single $MHCII^{+}CD11c^{+}$ cells (A) and the presence of kaede-red^{+} DCs was observed and analysed for each group (B and C). Each point represents an individual animal and a students *t* test was performed.

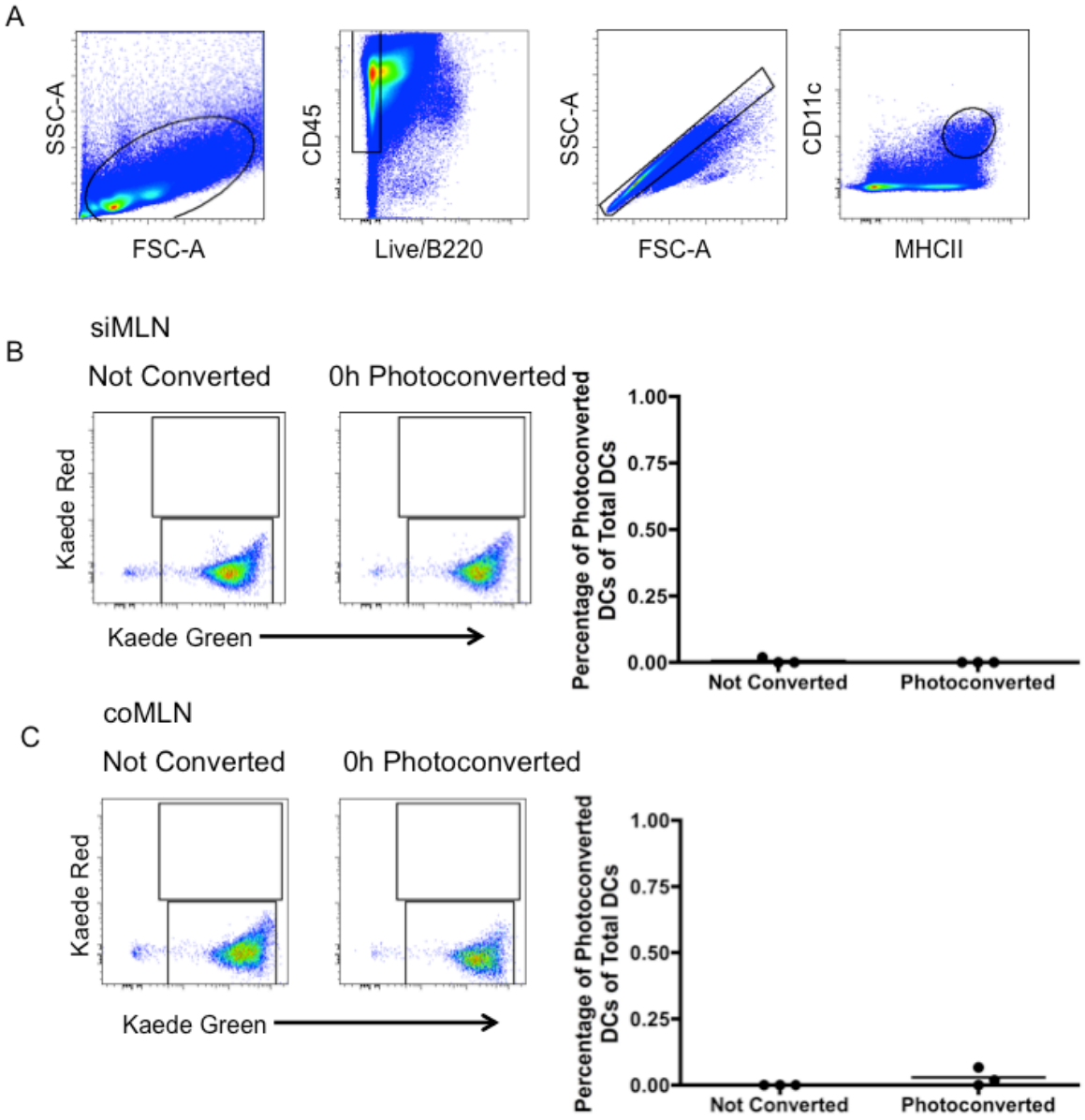

Figure 5-4 Small Intestinal Draining MLN and Colonic Draining MLN DCs Do Not Express Kaede-Red Immediately After Peyer's Patch Photoconversion.

The PPs of photoconvertible kaede mice were exposed to violet light for two minutes each, avoiding the surrounding SI. siMLN and coMLN were isolated and digested from animals that did not undergo photoconversion and from animals immediately after photoconversion. DCs were gated gated as live $CD45^{+}$, $B220^{-}$, single $MHCII^{+}CD11c^{+}$ cells (A) and the presence of kaede-red^{+} DCs was observed and analysed for siMLN and coMLN (B and C). Each point represents an individual animal and a students *t* test was performed.

5.1.2 Dendritic Cells Migrating From Peyer's Patches to the Mesenteric Lymph Nodes Expand In Response to Flt3 Ligand

Next I addressed the ontogeny of these DCs migrating from the PP, by determining if they would expand in response to the DC specific growth factor Flt3L. Kaede mice were treated with recombinant Flt3L for 10 days; this is known to result in the specific expansion of DCs (Cerovic et al., 2012; Schulz et al., 2009). After the treatment of kaede mice with Flt3L for 9 days, I performed photoconversion of the PPs and gave the final administration of Flt3L.

I confirmed that PP DCs expanded in response to 9 days treatment with Flt3L. PPs were carefully excised from the SI and digested to form a single cell suspension. Cells were then labelled and analysed for flow cytometry. DCs were gated as large, $B220^-$, $F4/80^-$, single, $CD11c^+MHCII^+$ cells (Figure 5.5 A). The administration of Flt3L resulted in a significant increase in the number and percentage of DCs in the PP (Figure 5.5 B). This confirms, in line with previous reports, that Flt3L expands the DC populations in the PP.

Mice were allowed to recover overnight, and the siMLN and coMLN were removed. These were digested separately and labelled and analysed by flow cytometry, DCs were gated as large, $B220^-$, $F4/80^-$, single, $MHCII^+CD11c^+$ cells (Figure 5.6 A). Cells that had not undergone photoconversion were used to define the gates for kaede-red^+ cells (Figure 5.6 B). In mice that had undergone photoconversion there was a significant increase in kaede-red^+ DCs in the siMLN. These kaede-red^+ DCs were not present in the coMLN (Figure 5.6 C). In mice that had been treated with Flt3L there was a significant increase in the percentage and number of kaede-red^+ DCs (Figure 5.6 D). As we have previously shown that these kaede-red^+ DCs were derived from the PPs after PP photoconversion, we can conclude that these kaede-red^+ cells in the siMLN are PP derived.

Therefore, taken together our data demonstrate that the PP DCs that migrate to the siMLN expand in response to Flt3L. As Flt3L is a DC specific growth factor this confirms that the migrating kaede-red^+ PP-derived population we observe are *bona-fide* DCs.

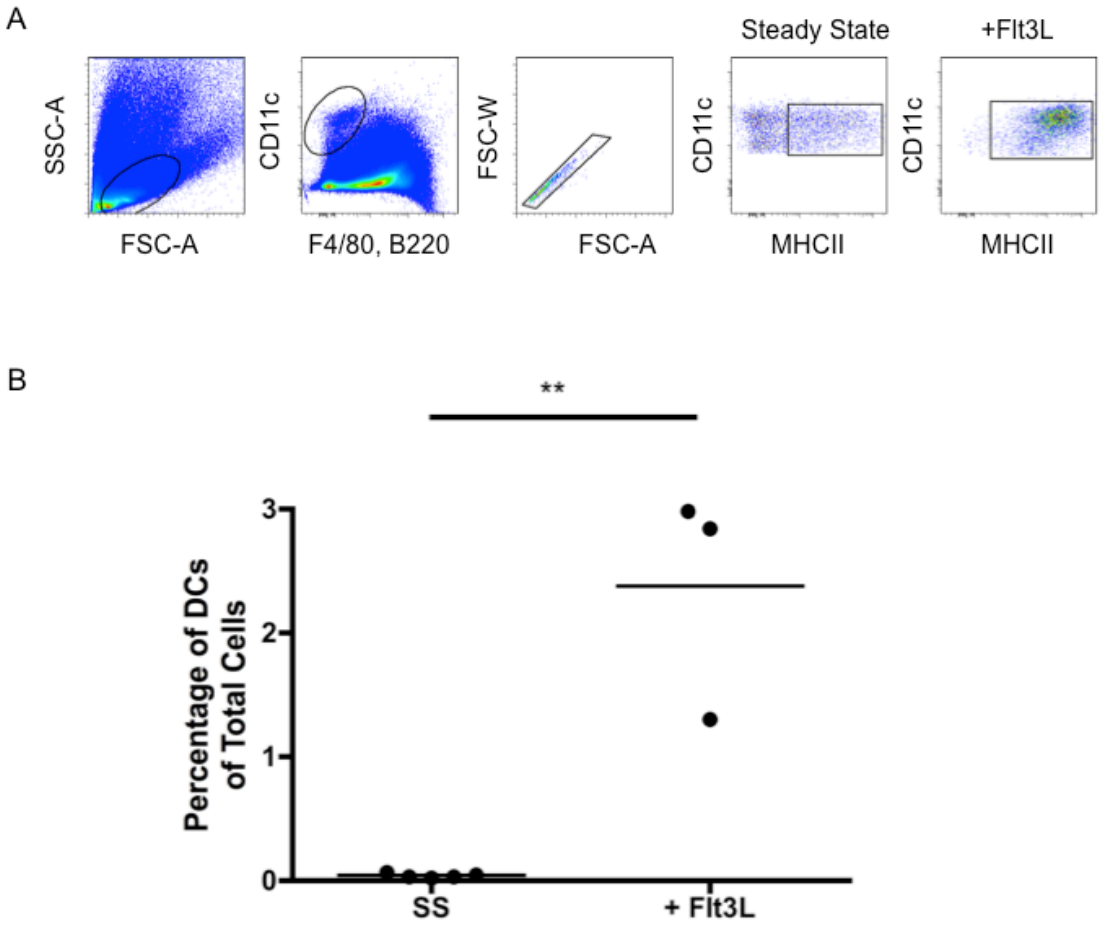

Figure 5-5 Peyer's Patch Dendritic Cells Expand In Response to Flt3 Ligand.

Photoconvertable kaede mice were injected for 10 days with Flt3L i.p and Peyer's patches were removed and digested. DCs were gated as large, $CD11c^{+}$, $F4/80^{-}$, $B220^{-}$ $MHCII^{+}$ cells (A) and the percentage of DCs among total cells was observed and analysed (B). Results are representative of two separate experiments with similar results and each point represents an individual animal. A students *t* test was performed, **p<0.01.

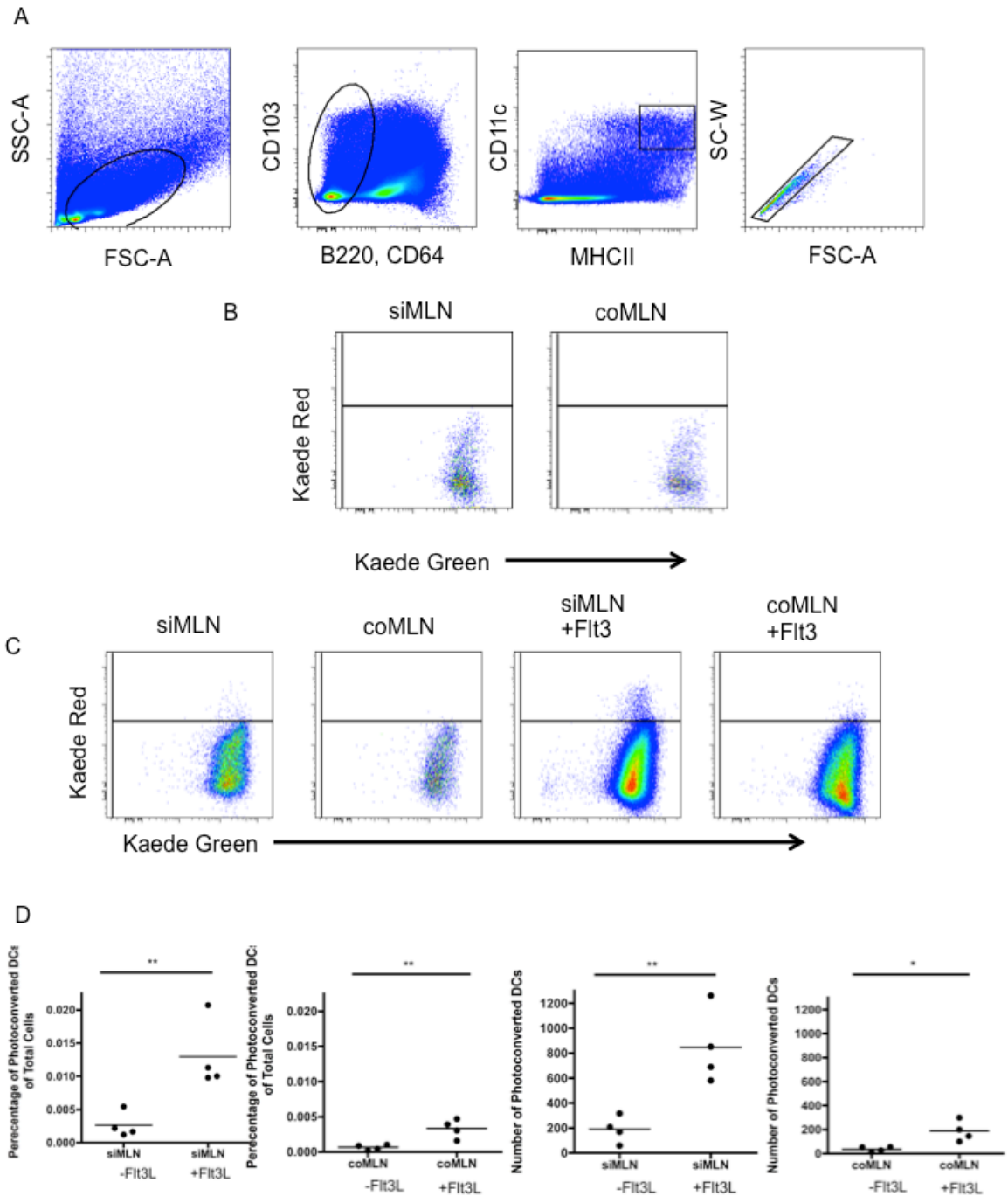

Figure 5-6 Migratory Peyer's Patch Dendritic Cells in the MLN Expand In Response to Flt3 Ligand.

Photoconvertable kaede mice were injected for 10 days with Flt3L i.p, after 9 days the PPs of photoconvertible kaede mice were exposed to violet light for two minutes each, avoiding the surrounding SI. 24 hours later the siMLN and coMLN were removed, digested and stained for flow cytometry. DCs were gated as $B220^{-}$, $CD64^{-}$, $MHCII^{+}CD11c^{+}$ single cells (A) and the presence of kaede-red^{+} DCs in the siMLN and coMLN of non-photoconverted mice (B), and the siMLN and coMLN of photoconverted mice with and without Flt3L was assessed(C). The percentage of kaede-red^{+} DCs of total cells was analysed (D). Results are representative of two separate experiments with similar results and each point represents an individual animal. A students *t* test was performed. * $p<0.05$, ** $p<0.01$.

5.1.3 Dendritic Cells From Peyer's Patches Migrate in Pseudo-Afferent Lymph

I next wanted to confirm that these migratory PP DCs were able to migrate in pseudo-afferent lymph, a defining feature of DCs. Kaede mice underwent MLNx and 5-6 weeks later TDC was performed. Following cannulation, PP photoconversion was performed. Animals were then allowed to recover and pseudo-afferent lymph was collected overnight. The lymph was processed and stained with antibodies for analysis by flow cytometry. Large, $MHCII^+$, $CD19^-$, $CD11c^+$ single DCs were gated (Figure 5.7 A) and the presence of kaede-red^+ DCs was assessed (Figure 5.7 B). There were significantly more kaede-red^+ DCs in the lymph of mice that had undergone PP photoconversion compared to animals that had not undergone PP photoconversion (Figure 5.7 C). Interestingly following PP photoconversion, approximately 8% of DCs migrating in lymph were kaede-red^+ indicating they were of PP origin.

5.1.4 Subsets of DCs Migrating From the Peyer's Patches to the Mesenteric Lymph Node

As described in previous chapters, we have identified four distinct subsets of DCs that are able to migrate from the SI to the MLN. Therefore, I investigated whether DCs that migrate from the PP were of any specific DC subset. Following the cannulation of kaede mice that had undergone PP photoconversion, cells were analysed by flow cytometry. DCs were gated as large, $CD19^-$, $MHCII^+$, $CD11c^+$, single cells (Figure 5.8 A). These DCs were then split into four subsets based on their expression of CD11b and CD103, as were PP DCs (Figure 5.8 B). The percentage of each DC subset was compared between PP DCs, photoconverted kaede-red^+ DCs from lymph and non-photoconverted kaede-$green^+$ DCs from lymph. There was no significant difference in the percentage of $CD103^+CD11b^-$ DCs, $CD103^-CD11b^+$ DCs, or $CD103^-CD11b^-$ DCs between PP DCs, kaede-red^+ lymph DCs and kaede-$green^+$ lymph DCs (Figure 5.8 C). In comparison, there were significantly more $CD103^+CD11b^+$ DCs among the kaede-$green^+$ siLP derived DCs, than there were $CD103^+CD11b^+$ DCs among the PP and kaede-red^+ DCs migrating in lymph (Figure 5.8 C). There were no significant differences in the percentage of any DC subset between PP DCs and kaede-red^+ DCs migrating in lymph following in PP photoconversion. Thus, the subset

composition of kaede-red^{+} DCs reflects that seen in the PPs, providing additional evidence that these DCs are PP derived.

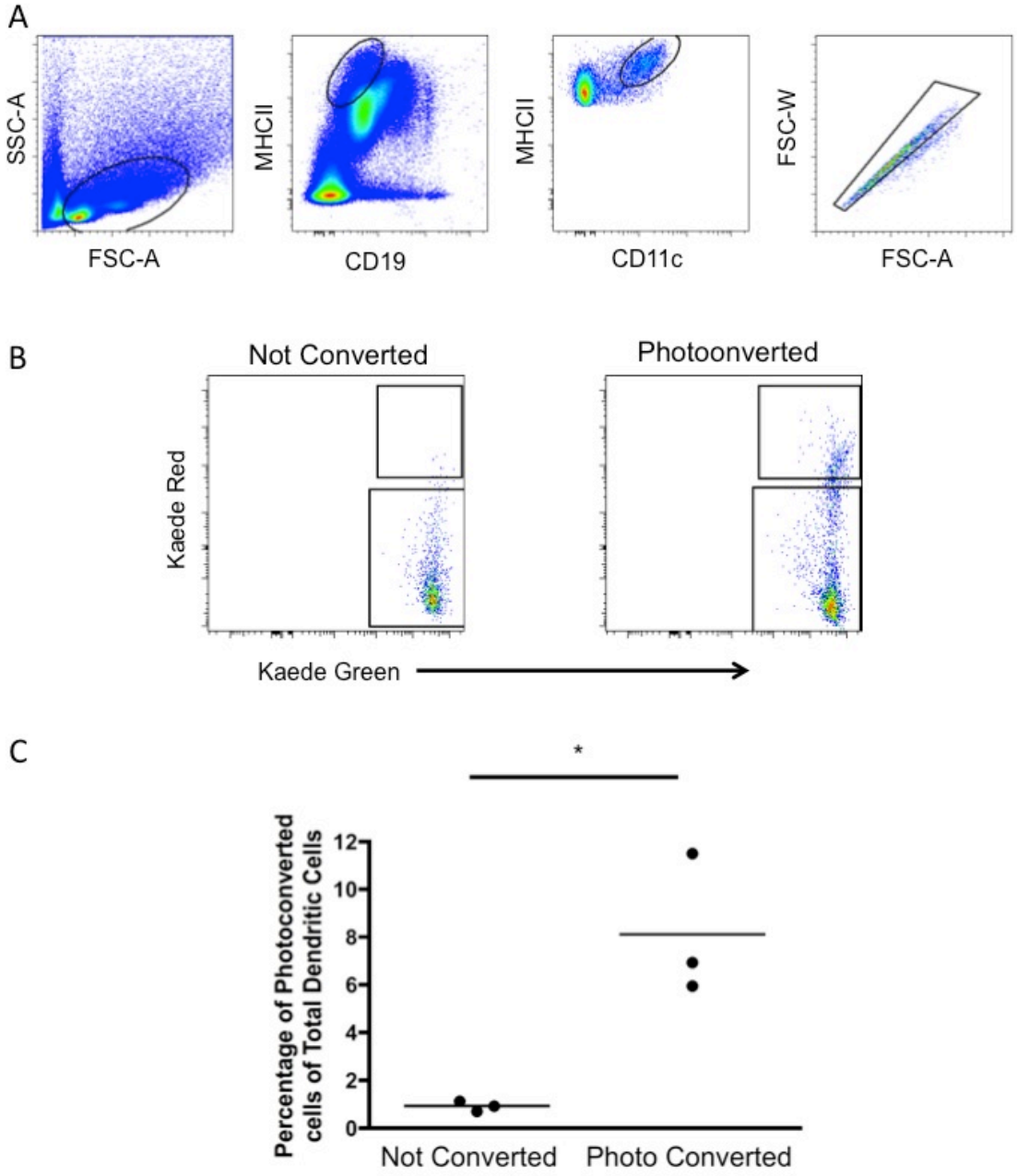

Figure 5-7 Migratory Peyer's Patch Dendritic Cells Migrate in Lymph.

Photoconvertible kaede mice underwent MLNx, 5-6 weeks later thoracic duct cannulation was performed. PPs were then exposed to violet light for two minutes each, avoiding the surrounding SI. Pseudo-afferent lymph was collected overnight then processed and stained for flow cytometry. DCs were gated as $CD19^-$, $MHCII^+$, $CD11c^+$ single cells (A), and the presence of kaede-red^+ DCs in the lymph of non-photoconverted animals and photoconverted animals was compared (B). The percentage of kaede-red^+ DCs among total DCs was analysed (C). Each point represents an individual animal. A students *t* test was performed. *$p<0.05$.

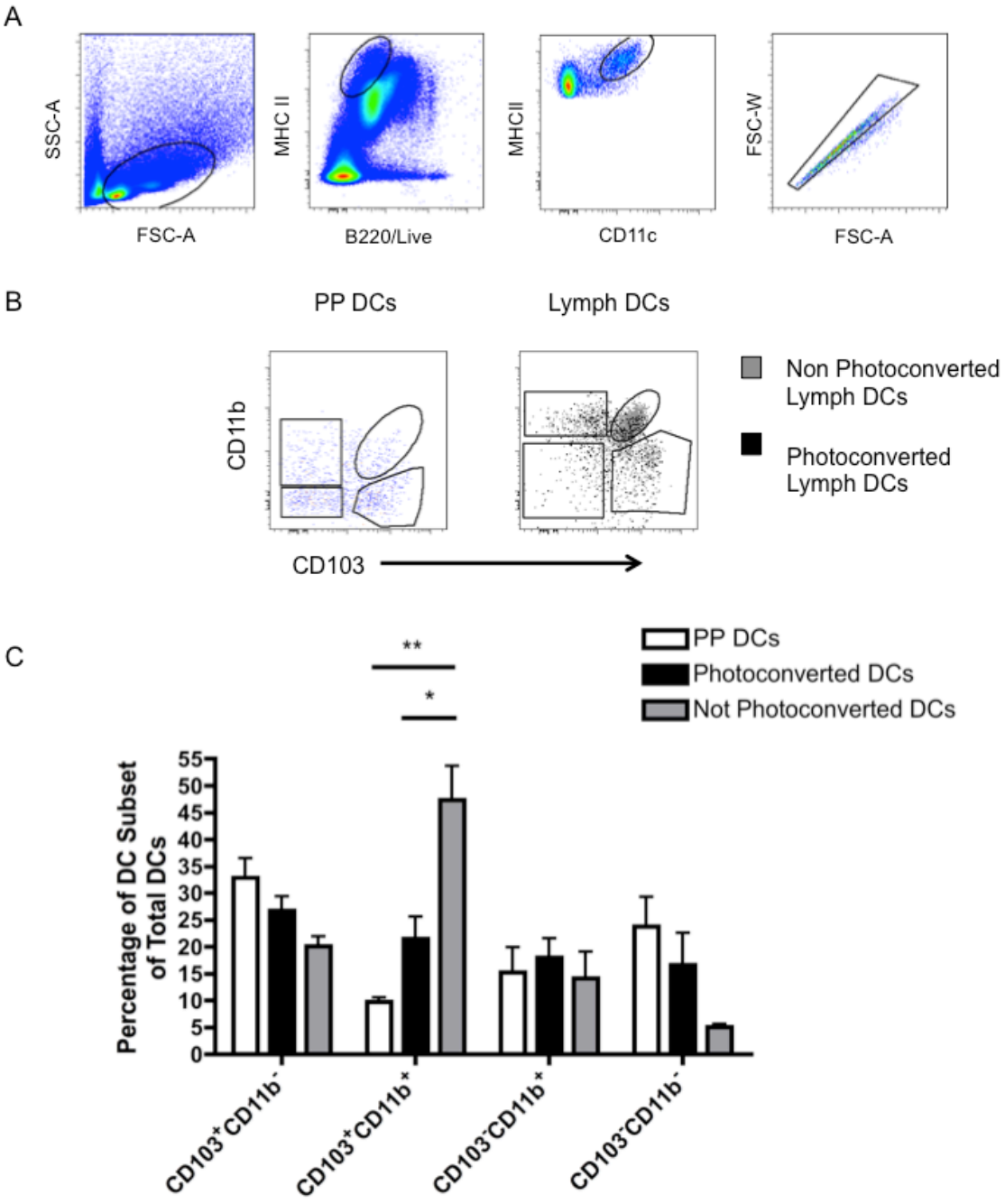

Figure 5-8 Subsets of Migratory Peyer's Patch Dendritic Cells In Psuedo-Afferent Lymph.

Photoconvertible kaede mice underwent MLNx, 5-6 weeks later thoracic duct cannulation was performed. PPs of photoconvertible kaede mice were then exposed to violet light for two minutes each, avoiding the surrounding SI. Pseudo-afferent lymph was collected overnight then processed and stained for flow cytometry. DCs were gated as large, live, $B220^{-}$, $MHCII^{+}CD11c^{+}$ single cells (A), and four distinct subsets of DCs based upon their CD103 and CD11b expression were identified in kaede-red^{-} DCs, kaede-red^{+} DCs and PP DCs (B). The percentage of each subset of total DCs was assessed and analysed (C). Results are presented as mean of 10 individual animals, error bars represent S.E.M. A one-way ANOVA was performed *$p<0.05$, **$p<0.01$.

5.1.5 Dendritic Cells from the Peyer's Patches Migrate to the Mesenteric Lymph Nodes Following FITC Injection

In order to confirm a proportion of PP DCs migrate to the siMLN, and to investigate the molecular mechanisms that control this migration, we performed FITC injections into the PPs. FITC injections into the PP were pioneered by the Pabst group, and involve the injection of a precise small volume of liquid under high pressure using a micro-injector. This allows the labelling of cells within the PPs, without labelling the surrounding LP.

We performed the FITC injection technique into all accessible PPs. 24 hours later the siMLN and coMLN were removed and digested separately. Cells were labelled for flow cytometry and large, $B220^-$, $MHCII^+CD11c^+$ single cells were selected as DCs (Figure 5.9 A). The presence of $FITC^+$ cells amongst DCs in the siMLN and coMLN were compared to mice that had received a PP injection of PBS (Figure 5.9 B). There were significantly more $FITC^+$ DCs in the siMLN of animals that had undergone PP $FITC^+$ injection than in the coMLN, and no $FITC^+$ DCs were detectable in the siMLN or coMLN of animals that had received PP injections of PBS (Figure 5.9 C). This indicates, in line with our kaede experiments that PP DCs are able to migrate to the siMLN. Consistent with our previous data these migratory PP DCs were found specifically in the siMLN, not the coMLN.

In order to confirm that the FITC we were injecting did not contaminate the surrounding siLP, leading to a false positive result, the siLP was isolated, digested and the presence of $FITC^+$ cells was assessed after the injection of PBS or FITC into PPs and after subserosal injection of FITC into the tissue surrounding the PPs. The SI was then isolated, digested and stained for flow cytometry. DCs were gated as large, $CD45^+$ live, $B220^-$, $CD11c^+$ $MHCII^+$ cells (Figure 5.10 A). The presence of $FITC^+$ DCs following the injection of PBS into PPs, the injection of FITC into PPs, and the subserosal injection of FITC into the SI tissue surrounding the PPs was investigated (Figure 5.10 B). There were no $FITC^+$ DCs in the SI following the injection of PBS into PPs, nor were there any following FITC injection of PPS. In comparison there was a significant population of $FITC^+$ DCs following the subserosal injection of FITC into the SI (Figure 5.10 C). Therefore, following FITC injection into the PPs there is no FITC leakage into the surrounding SI.

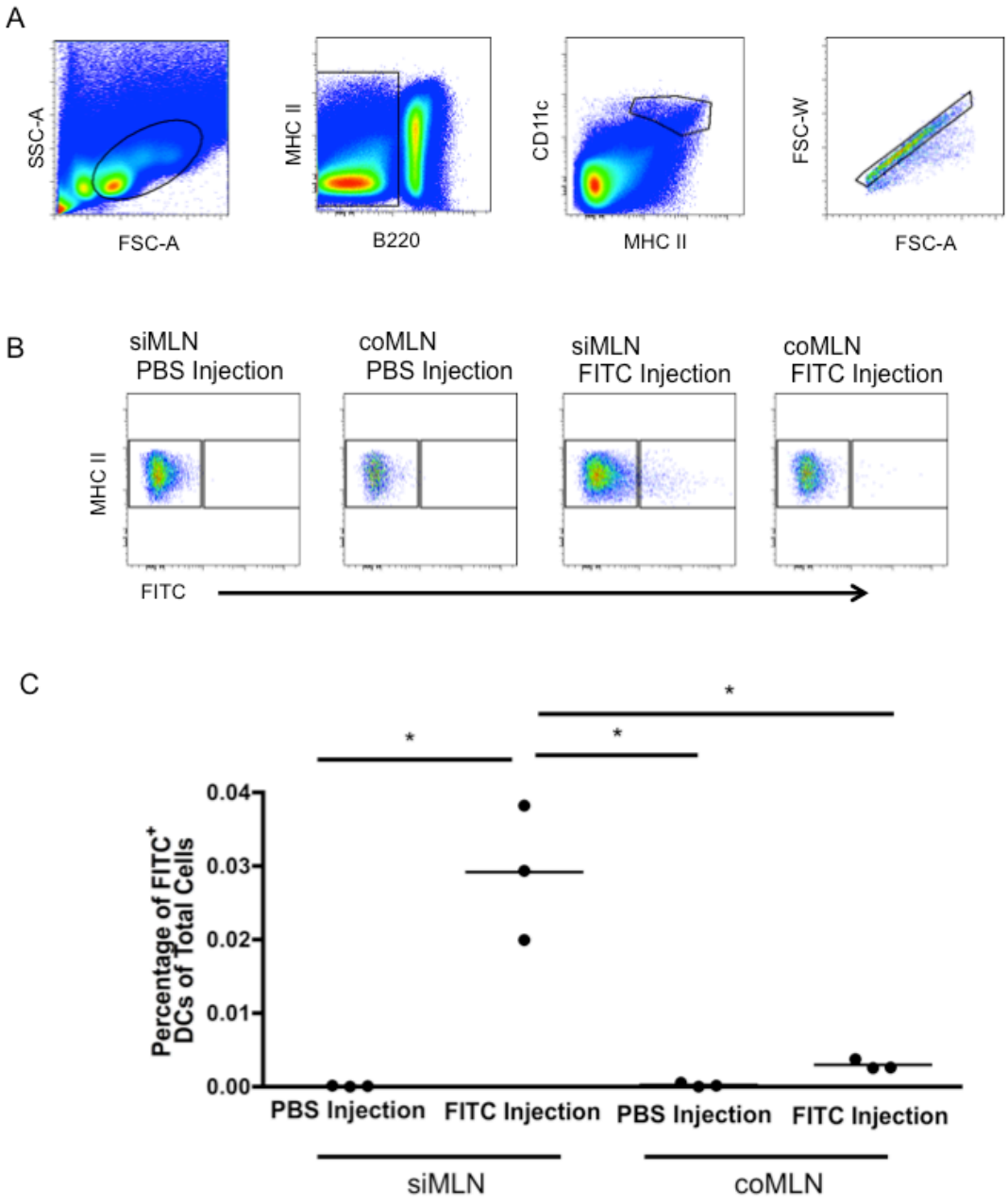

Figure 5-9 Peyer's Patch Dendritic Cells Migrate to the Small Intestinal Draining MLN Following FITC Injection.

All accessible PPs were microinjected with FITC. 24 hours later the siMLN and coMLN were isolated, digested separately and stained for flow cytometry. DCs were gated as large, $B220^-$, $MHCII^+CD11c^+$ single cells (A), and the presence of $FITC^+$ DCs in the siMLN and coMLN of FITC injected and non-injected mice was assessed (B). The percentage of $FITC^+$ DCs of total cells was assessed (C). Results show one individual experiment, but are representative of at least 6 separate experiments with similar results. Each point represents an individual animal. A two way ANOVA was performed *$p<0.05$.

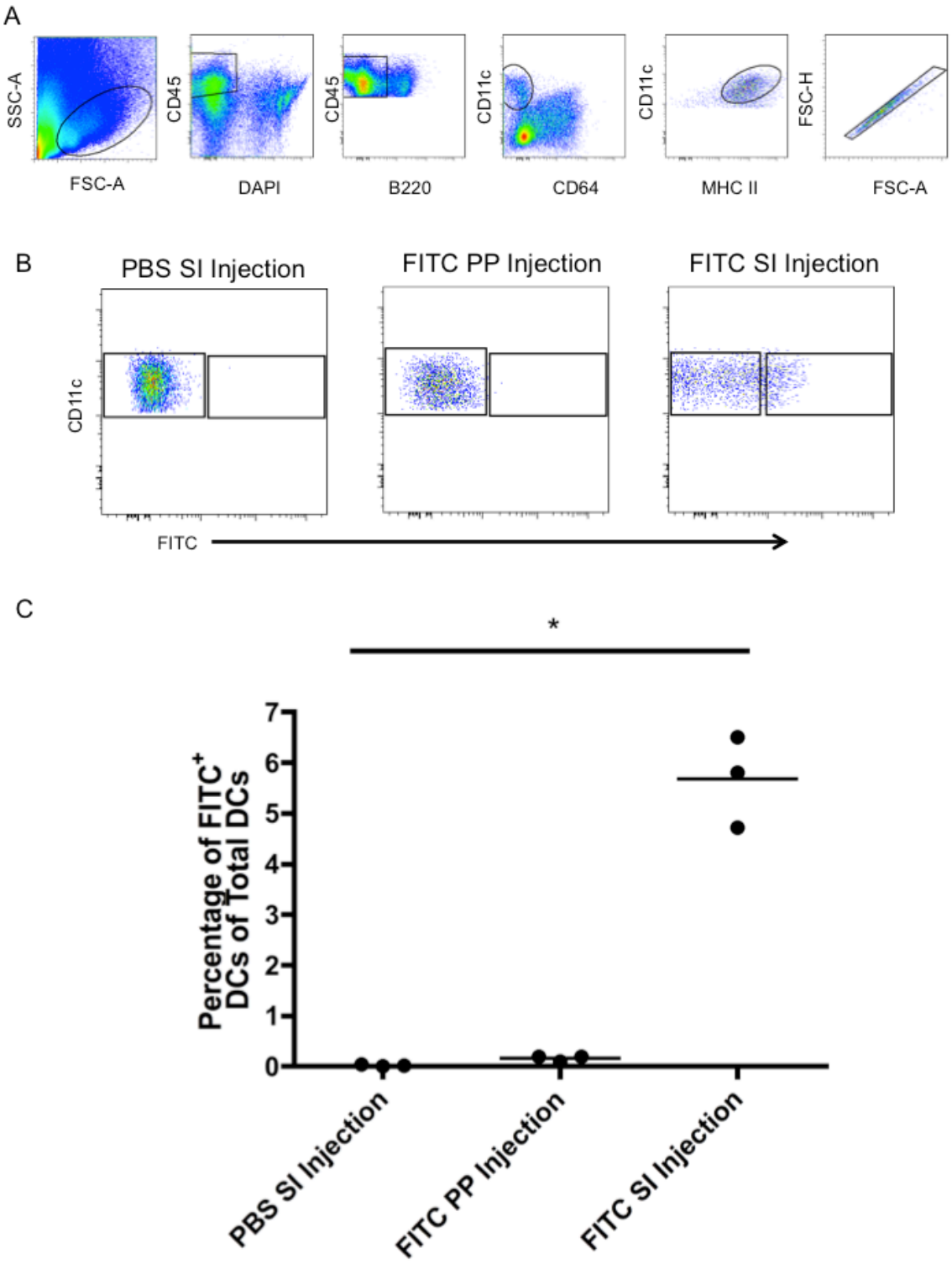

Figure 5-10 FITC$^+$ DCs Are Not Present in the Small Intestinal Lamina Propria Following Peyer's Patch Injection.

All accessible PPs were microinjected with FITC, or the surrounding SI was subserosally injected with FITC. Immediately after the SI was removed, digested and stained for flow cytometry. DCs were gated as large, live, CD45$^+$, B220$^-$, CD11c$^+$, CD64$^-$, MHCII$^+$ single cells (A) and the presence of FITC$^+$ DCs was assessed (B). The percentage of FITC$^+$ DCs of total DCs was assessed (C). Each point represents an individual animal. A one way ANOVA was performed with post test. *$p<0.05$.

5.1.6 Dendritic Cells Migrating From Peyer's Patches to the Mesenteric Lymph Nodes Do Not Expand In Response to R848 or Cholera Toxin

Cholera toxin (CT) is a powerful mucosal adjuvant, and has previously been shown to increase the numbers of mature DCs in the MLN (Anjuere et al., 2004). Additionally, it has been shown to mobilise DCs within the PPs, with a rapid influx of DCs into the FAE followed by DC migration from the SED to T cell areas of the PP after 24 hours (Anosova et al., 2008). The TLR7/8 ligand, R848, has also been shown to have a powerful effect upon mucosal DCs. Following oral administration of R848 there is a complete loss of LP DCs with a responding increase in the MLN, as well as a dramatically altered distribution of PP DCs (Yrlid et al., 2006c). Therefore, we decided to investigate the effects of CT and R848 upon the migration of PP DCs to the siMLN.

FITC injections were performed and 10μg of CT or 10μg R848 or PBS was administered orally once the animal was fully recovered. 24 hours later the siMLN was isolated, enzymatically digested, stained for flow cytometry and analysed. DCs were gated as large, $B220^-$, single; $MHCII^+CD11c^+$ cells (Figure 5. 11 A). $FITC^+$ DCs were gated, and compared between animals that had received oral PBS, CT or R848 (Figure 5.11 B and C). There was no significant increase in the percentage of $FITC^+$ DCs of total cells in the siMLN after any of the treatments.

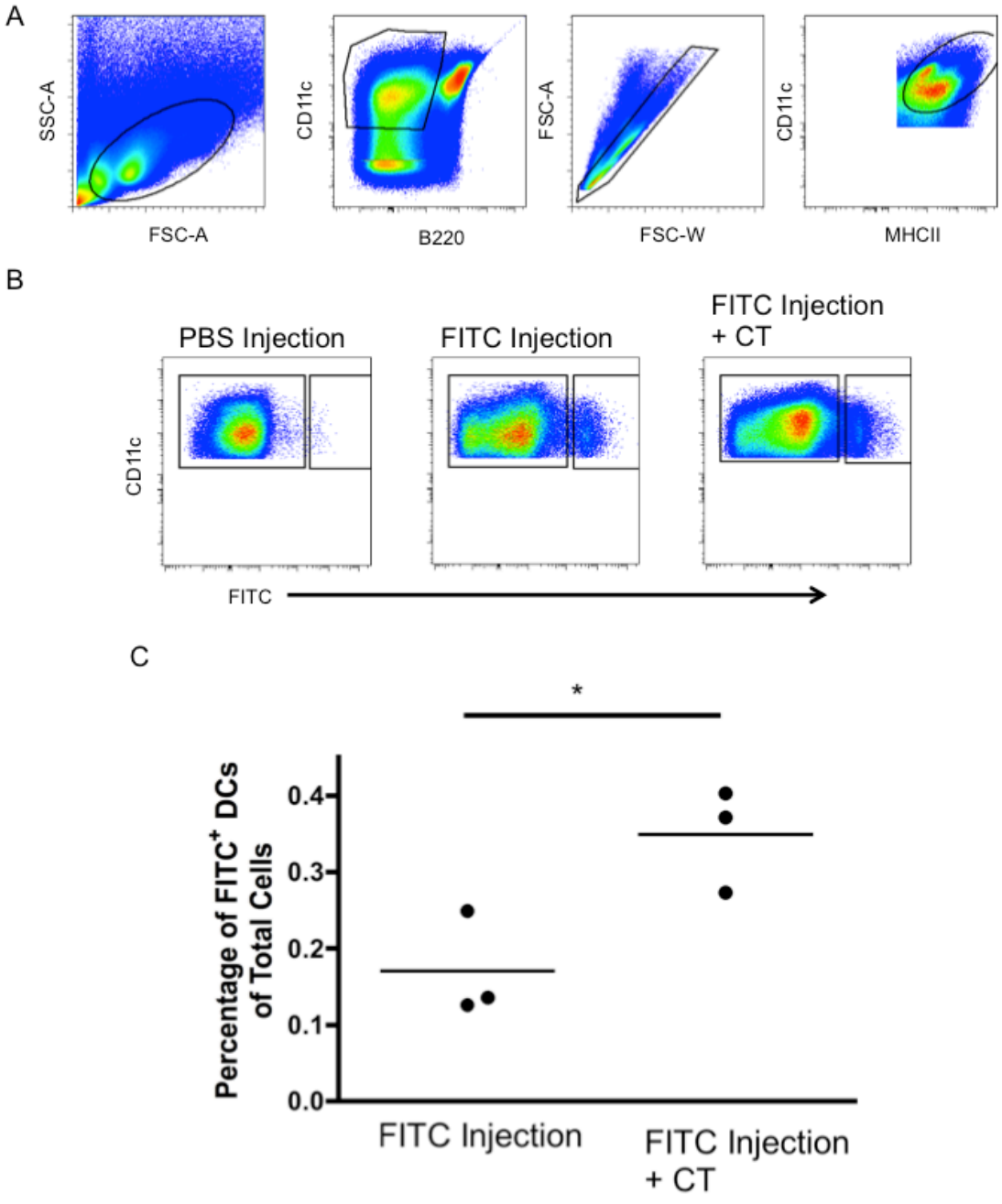

Figure 5-11 Neither Cholera Toxin or R848 Increase Peyer's Patch Dendritic Cells Migration to the Small Intestinal Draining MLN.

All accessible PPs were microinjected with FITC. Immediately after mice had recovered they were fed with either PBS, cholera toxin or R848. 24 hours later the siMLN were digested separately and stained for flow cytometry. The presence of $FITC^+$ DCs in the siMLN of mice fed PBS, CT or R848 was assessed (B). The percentage of $FITC^+$ DCs of total cells was assessed (C). Each point represents an individual animal. A one-way ANOVA was performed.

5.1.7 Dendritic Cells Migrating From Peyer's Patches to the Mesenteric Lymph Nodes Are Dependent Upon CCR7 and S1PR

A defining feature of migratory DCs is their expression of CCR7, which enables their constitutive migration to LNs (Jang et al., 2006). Consequently genetic deficiency in CCR7 results in a loss of all migratory DCs in the MLN, and therefore a lack of recognition of fed antigen by T cells in the MLN (Worbs et al., 2006). Therefore, FITC injections were performed in $CCR7^{-/-}$ mice to confirm that DCs migrating from the PP to the MLN were bona-fide DCs. Following FITC injection into WT and $CCR7^{-/-}$ mice the siMLN was isolated digested and stained for flow cytometry. Large, $B220^{-}$, $MHCII^{+}CD11c^{+}$ single cells were gated as DCs (Figure 5.12 A), and the percentage of $FITC^{+}$ DCs of total DCs was assessed in WT and $CCR7^{-/-}$ animals (Figure 5.12 B and C). Injection of FITC into PPs of $CCR7^{-/-}$ mice revealed that significantly fewer $FITC^{+}$ DCs were detected in $CCR7^{-/-}$ mice, again confirming that these are likely to be *bona-fide* migratory DCs.

The immunosuppressant FTY720 induces the sequestration of circulating mature lymphocytes in lymphoid tissues, including PPs by acting upon one of the five S1P receptors (Yanagawa and Onoe, 2003). There have also been reports suggesting that it may also affect DC migration; Lan *et al*. reported that animals treated with an analogue of FTY720 showed reduced transendothelial migration towards CCL19 (Lan et al., 2005). However, *in vivo* reports suggested that blocking of S1P receptors did not have an effect upon the number of DCs migrating from the intestine in pseudo-afferent lymph of rats (S. Milling, personal communication). Therefore, we decided to investigate the effect of FTY720 upon the migration of DCs from the PPs to the siMLN. Immediately prior to FITC injections, 20μg FTY720 was administered and siMLN were isolated 24 hours later. The siMLN was digested and stained for flow cytometry. DCs were gated as large, $B220^{-}$ $MHCII^{+}CD11c^{+}$ single cells (Figure 5.13 A). The number and percentage of $FITC^{+}$ DCs was assessed (Figure 5.13 B and C). There were significantly fewer PP migratory DCs detected in the MLN of mice following treatment with FTY720. These experiments were performed alongside the FITC injection of $CCR7^{-/-}$ mice therefore they share controls.

The fact that FTY720 inhibits migration of DCs from the PP to the MLN indicates that this process is dependent upon one of the sphingosine-1-phosphate

receptors (S1PRs); FTY720 acts upon five separate S1PRs to block S1PR-dependent cell migration. We therefore sought to determine which of these G protein coupled receptors is expressed upon PP migratory DCs, and controls the migration of PP migratory DCs. Therefore we repeated the PP FITC injections in mice that lack S1PR3, $EDG3^{-/-}$. 24 hours after FITC injection, the siMLN was digested and stained for flow cytometry. DCs were gated as large, $B220^{-}$ $MHCII^{+}CD11c^{+}$ single cells (Figure 5.14 A). The number and percentage of $FITC^{+}$ DCs was assessed (Figure 5.14 B and C). In the $EDG3^{-/-}$ mice no defects were observed in the migration of DCs from the PP, indicating that S1PR3 does not control the migration of PP DCs to the MLN.

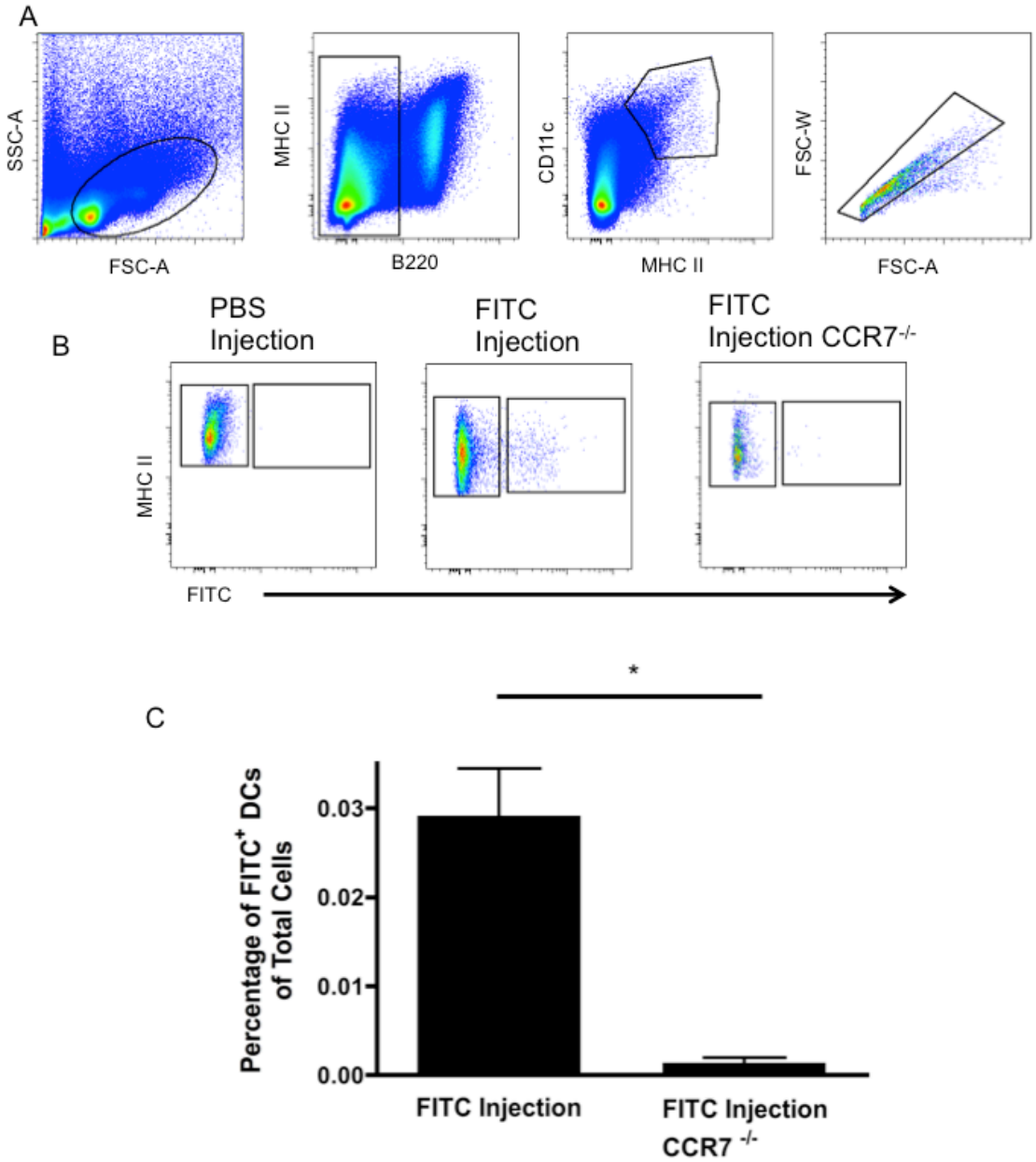

Figure 5-12 Peyer's Patch Dendritic Cells That Migrate to the Small Intestinal Draining MLN Following FITC Injection Are Missing from CCR7$^{-/-}$ Mice.

All accessible PPs were microinjected in WT and CCR7$^{-/-}$ mice. 24 hours later the small intestinal draining MLN were isolated, digested and stained for flow cytometry. DCs were gated as large, B220^{-}, CD11c^{+}MHCII^{+} single cells (A), and the presence of FITC^{+} DCs in the MLN of WT and CCR7$^{-/-}$ mice was assessed (B). The percentage of FITC^{+} DCs of total cells was analysed (C). Results are representative of 2 separate experiments with similar results. Data are means and S.E.M. A students *t* test was performed. *p<0.05, n=3 per group.

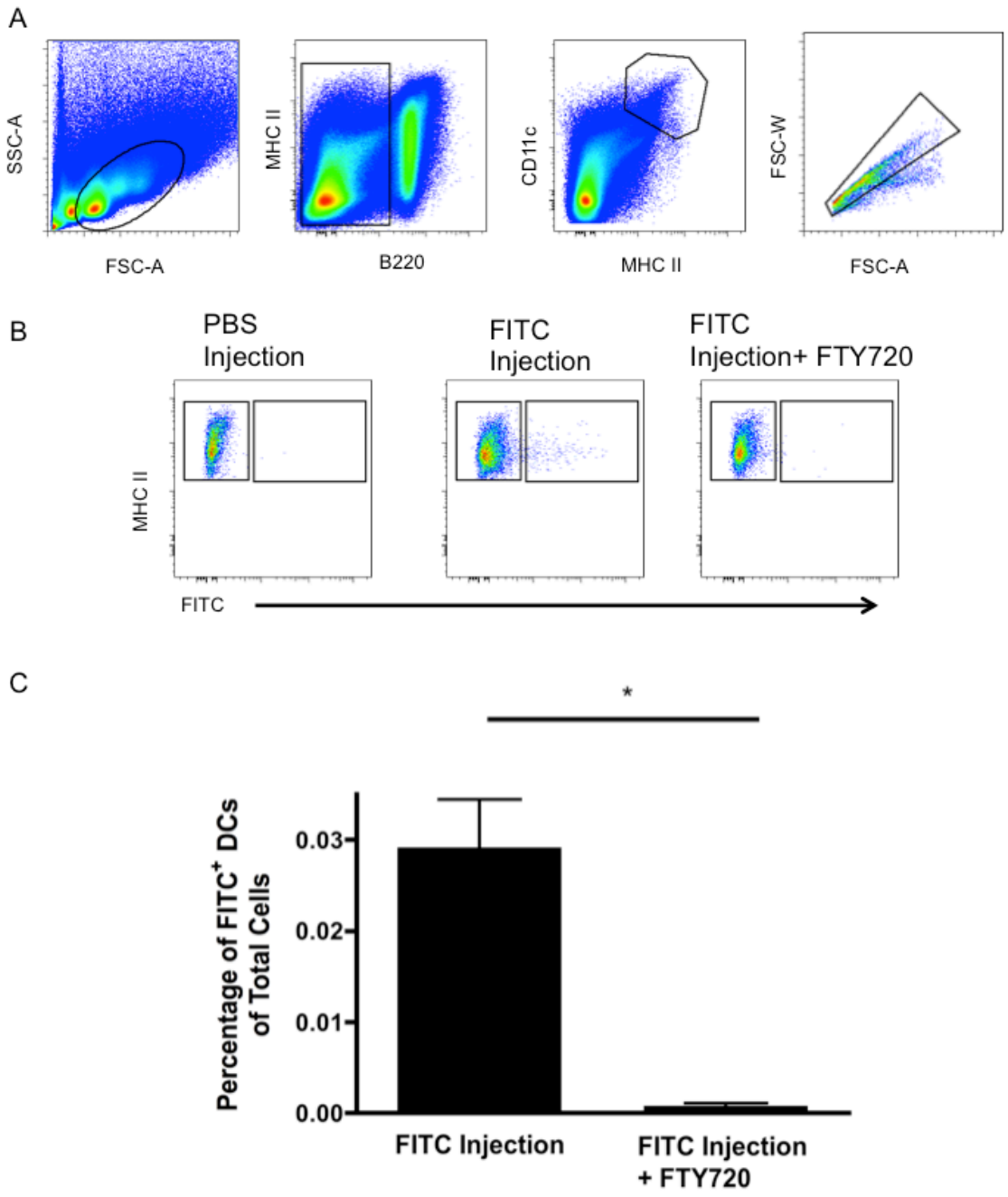

Figure 5-13 Peyer's Patch Dendritic Cells That Migrate to the Small Intestinal Draining MLN Following FITC Injection are Missing In FTY720 Treated Animals.

Before performing FITC injections into each accessible Peyer's patch animals were fed with FTY720 and mice fed with PBS. 24 hours later the small intestinal draining MLN were isolated, digested and stained for flow cytometry. DCs were gated as large, $B220^-$, $CD11c^+MHCII^+$ single cells (A), and the presence of $FITC^+$ DCs in the MLN of untreated and FTY720 treated mice was assessed (B). The percentage of $FITC^+$ DCs of total cells was assessed (C). Results are representative of at lease 2 separate experiments with similar results. Data are means and S.E.M. A students *t* test was performed. *$p<0.05$, n=6.

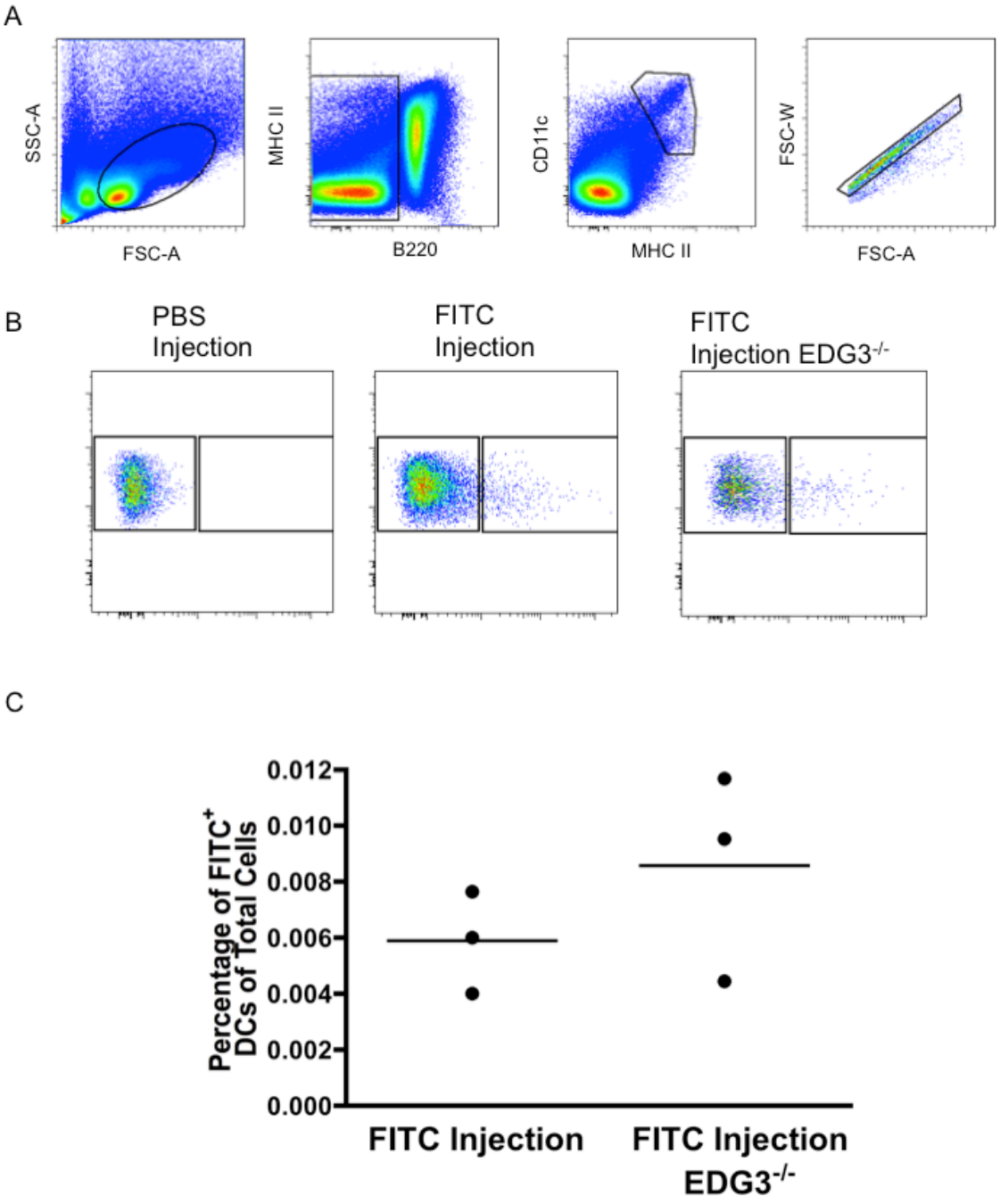

Figure 5-14 Peyer's Patch Dendritic Cells That Migrate to the Small Intestinal Draining MLN Following FITC Injection Are Present In EDG3$^{-/-}$ Mice.

All accessible PPs were microinjected in WT and EDG3$^{-/-}$ mice. 24 hours later the small intestinal draining MLN were isolated, digested and stained for flow cytometry. DCs were gated as large, B220^{-}, CD11c^{+}MHCII^{+} single cells (A), and the presence of FITC^{+} DCs in the siMLN of WT and EDG3$^{-/-}$ mice was assessed (B). The percentage of FITC^{+} DCs of total cells was analysed (C). Results are representative of at least 2 separate experiments with similar results and each point represents an individual animal. A students *t* test was performed.

5.1.8 Subsets of DCs Migrating From the Peyer's Patches to the Mesenteric Lymph Node

Next, the phenotype of DCs migrating from the PPs to the siMLN following FITC injection was investigated. As described previously, PP migratory DCs isolated following kaede experiments were more similar to PP DCs. This was demonstrated by a reduction in $CD103^+CD11b^+$ kaede-red^+ DCs in the MLN compared to kaede-$green^+$ DCs. Making the kaede-red^+ DCs in the MLN more similar to PP DCs. Therefore, 24 hours after FITC injections into the PPs the siMLN was removed, digested and stained for flow cytometry. DCs were gated as large $B220^-$, $MHCII^+CD11c^+$ single cells and $FITC^+$ and $FITC^-$ DCs were gated (Figure 5.15A), the four DC subsets were identified based upon the expression of CD103 and CD11b (Figure 5.15 B). There were no significant differences in the percentage of any DC subset between the $FITC^+$ or $FITC^-$ DC populations (Figure 5.15 C). This was in contrast with results from kaede experiments, in which the percentage of $CD103^+CD11b^+$ DC was significantly lower in PP migratory DCs compared to LP migratory DCs. Next, the same $FITC^+$ DC subsets from the siMLN were compared to PP DCs (Figure 5.15 D). There was no significant difference between the proportions of DCs in each subset, when compared between $FITC^+$ DCs in the siMLN and PP DCs (Figure 5.15 E).

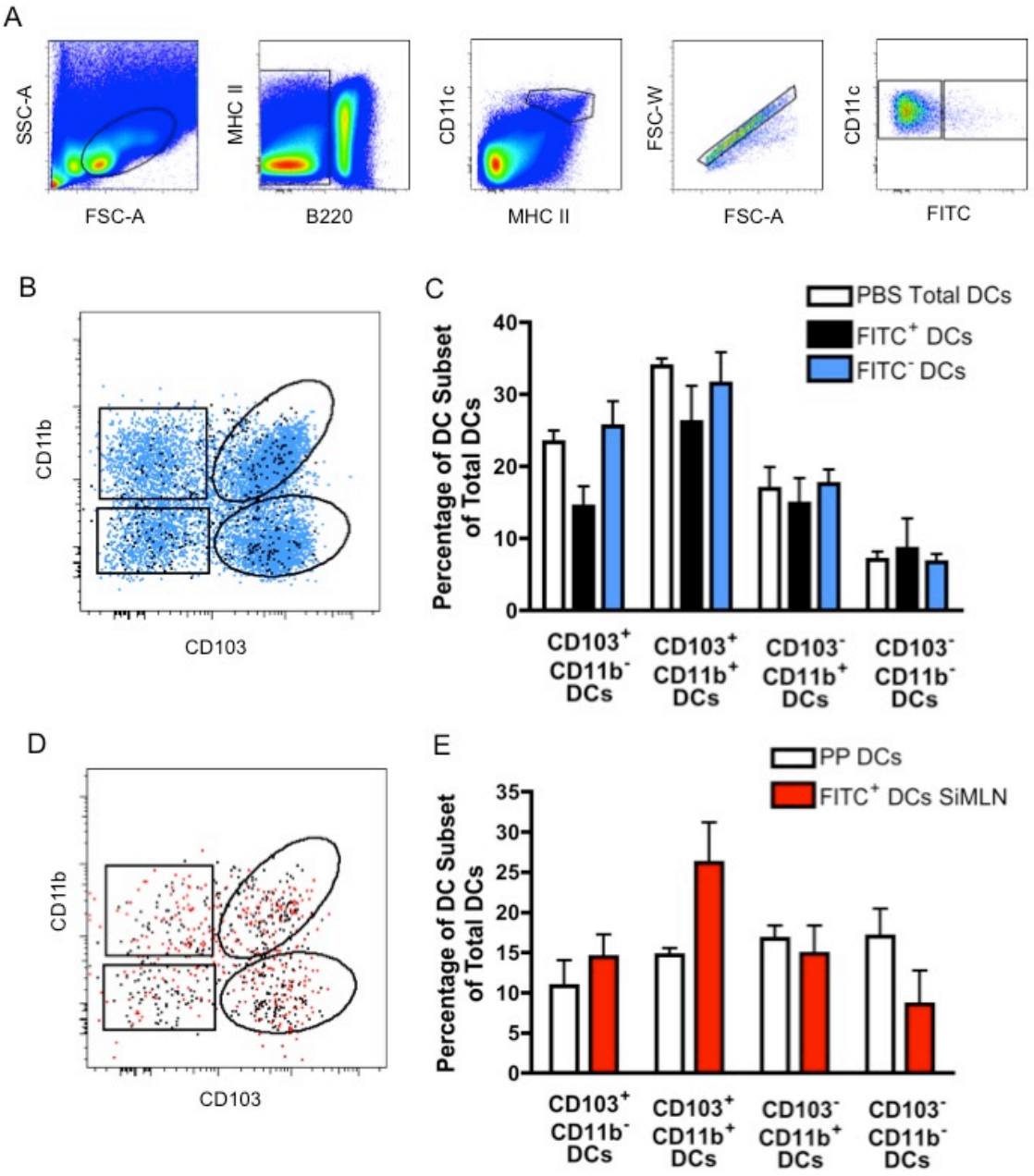

Figure 5-15 Subsets of Migratory Peyer's Patch Dendritic Cells in the Small Intestinal Draining MLN Following FITC Injection.

All accessible PPs were microinjected in mice. 24 hours later the small intestinal draining MLN were isolated, digested and stained for flow cytometry. DCs were gated as large, $B220^-$, $CD11c^+MHCII^+$ single cells (A), and four distinct subsets of MLN DCs based upon CD103 and CD11b expression were gated in $FITC^+$ DCs, $FITC^-$ DCs, and in the total DCs of PBS injected mice in the MLN were gated (B). The percentage of each subset of total DCs was assessed and analysed (C). $FITC^+$ DC subsets were also compared to total PP DC subsets (D) and and the percentage of each subset of total DCs was assessed and analysed (E). A one-way ANOVA was used to compare different conditions (C) and a two way ANOVA was performed to compare subsets from the PP and MLN (E). Data are means and S.E.M. N=6 for MLN, n=3 for PP DC subsets.

5.2 Discussion

Conclusively determining whether PP DCs are able to migrate to the MLN is essential. DCs migrating from PPs to the MLN represent an important pathway by which antigen, which has been acquired in an immunologically distinct environment can reach the MLN. Here we present, using two different experimental approaches, definitive evidence that DCs can migrate from the PP to the MLN.

PPs consist of large B cell follicles with intervening T cell areas; they are separated from the intestinal lumen by a single layer of cells known as the follicle-associated epithelium. One of the most significant features of the follicle-associated epithelium is the presence of fully differentiated functional M cells (Kraehenbuhl and Neutra, 2000). M cells are capable of promiscuously binding to a wide variety of antigens expressed upon the surface of bacteria and viruses to transport these antigenic materials across the intestinal barrier. This process is particularly suited to the uptake of large particulate antigen, such as bacteria (Schulz and Pabst, 2013). Immediately under the follicle-associated epithelium is the DC rich subepithelial dome. DCs in this region are ideally located to capture antigen transported into the PP by M cells. Following antigen uptake, DCs are able to migrate to the T cell rich areas known as the interfollicular region (Iwasaki and Kelsall, 2000).

There is evidence to show that organised lymphoid structures in the SI are necessary for the recognition of particulate antigens (Macpherson et al., 2008). The role of PP DCs in the induction of oral tolerance is less clear; it has been reported that targeting antigen to M cells can facilitate the induction of tolerance (Suzuki et al., 2008), however others have shown that there is normal oral tolerance in PP-null mice (Spahn et al., 2001; Spahn et al., 2002). In comparison, mice lacking both PP and MLN have decreased oral tolerance and this defect can be rescued by restoring the development of the MLN (Spahn et al., 2002). Furthermore the removal of MLN, or the inability of DCs to migrate to the MLN results in a complete lack of oral tolerance (Worbs et al., 2006). Therefore, while the MLN is essential for the generation of oral tolerance, DCs isolated directly from PPs may behave in a different manner. For instance,

delayed-type hypersensitivity to orally primed antigen was reduced upon adoptive transfer of DCs from the MLN, but not PPs (Chirdo et al., 2005).

Instead, DCs in the PP are likely to play a key role in the immune response to commensal and pathogenic bacteria by driving the production of IgA. The production of IL-10, TGF-β and IL-6 by PP DCs results in the secretion of IL-4 and IL-10 from responding $CD4^+$ T cells, and all of these cytokines play a role in class switching to IgA (Sato et al., 2003) (Iwasaki and Kelsall, 1999) (Brandtzaeg and Johansen, 2005). Additionally, DCs are able to directly present antigen to B, cells inducing them to undergo class switching to IgA via the production of IL-5, Il-6 and retinoic acid (Mora et al., 2006). IgA class switching is not confined to PP DCs, as PP-deficient mice induced IgA production in the MLN, and IgA class switching has been demonstrated in GALT (Yamamoto et al., 2000). Therefore, in order to manipulate the intestinal immune system with specificity it is essential to understand where antigens and acquired, and in which tissues they are presented.

5.2.1 Dendritic Cells from the Peyer's Patches Migrate to the Mesenteric Lymph Nodes

Previous work has provided indirect evidence that DCs are able to migrate from PPs to the MLN (Macpherson and Uhr, 2004; Pron et al., 2001). Macpherson and Uhr first showed that DCs carrying the commensal bacteria *Enterobacter colacae* were present in the MLN. Since these bacteria were likely to be primarily taken up in the PPs, and were observed in the MLN, the authors postulated that bacteria were transported to the MLN by PP-derived DCs. However, macrophages in the MLN were also found to contain bacteria. As it is well documented that macrophages do not migrate from the intestine to the MLN (Schulz et al., 2009), this suggests that the movement of bacteria from PP to the MLN may not be entirely cell dependent; bacteria free in lymph may thus migrate to the MLN. Alternatively, there may be some transfer of bacteria between cells. This work, therefore, does not conclusively show that DCs migrate from the PP to the MLN. Similarly Pron *et al.* showed that *L. monocytogenes* specifically gained entry into PPs, and were found in the MLN (Pron et al., 2001). However, similar to Macpherson and Uhr, there remained the possibility that bacteria could either migrate in a non-cell dependent manner or be transferred between cells.

Therefore, this was not conclusive evidence that DCs can migrate from the PPs to the MLN.

In contrast, there have been others that have argued that DCs do not migrate from the PPs. For example, due to the abundance of chemokines essential for DC trafficking within the PPs, it was suggested that DCs would be contained to the PP (Kelsall, 2008). In addition, Bogunovic *et al.* suggested that there was no migration from PPs to the MLN because in $Id2^{-/-}$ mice, which lack PPs and ILFs, there was a specific lack of $CD103^{+}CD11b^{-}$ DCs (Bogunovic et al., 2009). This led the authors to postulate that these cells were specifically from lymphoid tissues in the intestine, and were therefore not a migratory population. The suggestion that DCs do not migrate from the PP to the MLN under steady-state conditions has been further perpetuated by a study in minipigs, in which the authors compared the phenotypes of DCs in the PPs, MLNs and pseudo-afferent lymph and concluded that DCs were unable to migrate from PP to the MLN (Bimczok et al., 2005). However this study was incomplete as they did not deplete PPs or label PPs to investigate this further.

Together these conflicting studies do not fully address the question whether DCs migrate from PP to the MLN. Using several novel approaches we are now able to definitively show that DCs are able to migrate from the PPs to the MLN.

Firstly, photoconvertible kaede mice were used to address the question of whether DCs migrate from PP to the MLN. We were able to specifically photoconvert DCs in PPs, without affecting DCs in the surrounding LP or the MLN. Immediately following photoconversion of PPs, we showed that approximately 70% PPs DCs were photoconverted (Figure 5.2). This decreased to around 50% after 24 hours, and correspondingly we were able to detect photoconverted DCs in the MLN (Figure 5.1). As we know that we label only around 70% of PP DCs, we are able to calculate that approximately 1.4% of all DCs in the MLN were of PP origin. Specifically, the PP DCs migrated to the siMLN, not the coMLN. This was expected, as we showed in Chapter 3 that there is anatomical segregation of drainage to the MLN, and PPs are located only in the SI. These PP DC migration data further validate our conclusion regarding the anatomical segregation of lymphatic drainage in the intestine. As antigen acquired in the PPs is specifically carried only to the siMLN, this may contribute

to the functional differences between the siMLN and coMLN. We were also able to identify these photoconverted PP DCs migrating in pseudo-afferent lymph following TDC. This confirms that these cells are a population of bona-fide migratory DCs (Figure 5.7). In accordance with the results in kaede mice, we were also able to detect DCs migrating from PPs to the siMLN following FITC injections into the PP (Figure 5.9). This technique also only labels cells in the PP, without labelling cells in the surrounding LP (Figure 5.10). Therefore, using two separate techniques DCs were observed migrating from PPs to the MLN.

The results from the kaede mice and FITC injections both indicate that DCs are able, under specific circumstances, to migrate from one secondary lymphoid tissue (PP) to another (the MLN). This migration of DCs in efferent lymphatic vessels is highly unusual and has not been observed in other tissues or species in the steady-state (Cerovic et al., 2012; Schwartz-Cornil et al., 2006) (Howard et al., 1995). There have been reports in sheep that topical administration of the chemical carcinogen 7,12-dimethylbenz(a)antharcene (DMBA) or Beryllium may cause the migration of Langerhan cells or DCs in efferent lymphatics, traversing the LN (Dandie et al., 1994; Hall and Smith, 1971). However, these conditions do not represent the physiological steady-state, nor the normal response to a pathogen, and the observed DC migration may have been cause by major disturbances due to the toxicity of the adjuvants administered. Although our studies require laparotomy, and may therefore not fully represent the steady-state, we have not previously observed the migration of detectable numbers of DCs in efferent lymphatics (Cerovic et al., 2012). Further experiments using particulate fluorescent particles, or antigen that has been targeted to M cells, both of which should be taken up specifically by the PPs, could be used to investigate this process under steady-state conditions.

5.2.2 Dendritic Cells Migrating From Peyer's Patches to the Mesenteric Lymph Nodes Expand In Response to Flt3 Ligand

Flt3L and its receptor Flt3 represent the major interaction that drive the generation of steady-state DC subsets from BM progenitors *in vivo* (Naik et al., 2005). Additionally *in vitro* Flt3L generated DCs have a close phenotypical correspondence to splenic resident DC subsets, in comparison to the cells generated in CFS-2 cultures that resemble inflammatory DCs (Inaba et al., 1992).

In the intestine we found that LP DCs expressed levels of Flt3 mRNA 100 times higher than macrophages (Cerovic et al., 2012). Furthermore, we showed that administration of recombinant Flt3L induced a significant expansion of DCs in the LP and intestinal lymph without affecting the number of macrophages (Cerovic et al., 2012).

Therefore, we hypothesised that the administration of Flt3L would increase the number and percentage of DCs migrating from the PPs to the MLN. In line with previous reports (Castellaneta et al., 2004), we found a significant increase in the number and percentage of PP DCs following the administration of Flt3L (Figure 5.5). Following the photoconversion of PPs in Flt3L treated kaede mice, compared to kaede mice that did not receive Flt3L; there was a significant increase in the number of PP DCs migrating to the MLN. As Flt3L is a DC specific growth factor, this strongly indicates that PP-migratory cells that we have described are bona-fide DCs.

5.2.3 Proportions of Dendritic Cells Migrating From Peyer's Patches to the Mesenteric Lymph Nodes Do Not Increase in Response to R848 or Cholera Toxin

As we had shown that PP DCs migrating to the MLN expand in response to Flt3L, we sought to determine if conditions of inflammation could result in an increase of this population. We first investigated the DCs' response to the TLR7/8 agonist R848. Previous work has demonstrated that orally-administered R848 induced a 20 to 30-fold increase in DC output from the intestine (Yrlid et al., 2006c). This increase in DC migration was likely due to total release of DCs from the LP. Although no decrease in the total numbers of DCs in the PP was observed, there was an altered distribution of PP DCs. In response to R848, DCs from the subepithelial dome moved into the interfollicular T cell areas (Yrlid et al., 2006c). Thus, although R848 does not empty the PPs of DCs, it can induce DC migration within the MLN. Therefore, we investigated the effect of R848 administration on DC migration from the PPs to the MLN. Following administration of R848 there was no increase in DCs migrating from the PP to the MLN (Figure 5.11). Therefore, the response to R848 represents a difference between LP DCs and PP DCs. R848 induces migration of DCs from the LP, and this process is TNFα and IFNα dependent (Yrlid et al., 2006c). PP responsiveness to

these cytokines could be investigated, and this may reveal an important functional difference between PP and LP derived DCs. In order to investigate this further, DC egress in response to TNFα or IFNα may be studied. This would allow us to determine if there is one particular cytokine which PP DCs respond differently to compared to LP DCs. Alternatively DC migration from the PP to the MLN can be investigated under conditions of inflammation caused by a bacterial agent, rather than an adjuvant, in the PP could be compared to R848.

Next, we investigated the effect of CT on DCs migrating from PPs to the MLN. Unlike R848, CT is a large complex molecule with a mass of around 85 kDa. Additionally it has previously been shown to rapidly gain access to the PPs via M cells, where it is delivered to the subepithelal dome region (Frey et al., 1996; Shreedhar et al., 2003). Like R848, it has been shown to induce the migration of DCs within the PP without affecting the overall number of PP DCs (Anjuere et al., 2004). CT was able to induce the migration of subepithelial DCs to interfollicular T cell areas (Anosova et al., 2008). Therefore, we hypothesised that the number of PP DCs migrating to the MLN would be increased following the administration of CT. However, there was no significant increase in the migration of PP DCs to the MLN following the administration of CT (Figure 5.11). Initially this was surprising, as previous work has shown that administration of CT results in DC maturation and upregulation of CCR7 (Bagley et al., 2002). In contrast, it was also shown that administration of CT results in the migration of DCs towards the follicle associated epithelium (Anosova et al., 2008), rather than towards T cell zones as an upregualtion of CCR7 would suggest. Instead CT may result in the increased expression of CCL20 in the follicle associated epithelium, as has been shown in other the villus epithelium (Anjuere et al., 2004). Therefore upon CT administration there may be upregulation of CCL20 and CCL19 in the follicle associated epithelium which may provide a stronger signal for DCs to migrate towards, compared to T cell zones or draining lymphatic vessels. This may explain the apparent lack of increase in DC migration from the PPs to the draining MLN. Further time points could be investigated to determine if once DCs migrate out of the follicle associated epithelium there would be a resultant increase in DC migration to the MLN.

These results show that there was no significant increase in DC migration form the PP to the MLN following the administration of R848 or CT. In order to further investigate these cells other mucosal adjuvants such as heat-liable enterotoxin from *E. coli* could be investigated to determine if these can cause and increase of PP migratory DCs. Furthermore the effect of pathogens that specifically target PP M cells for their entry, such as *L. monocytogenes* or *S. enterica*, upon PP DC migration could be investigated. This may give us further insight into the mechanism of action, or function of these cells and provide key insights into ways to manipulate these PP migratory DCs.

5.2.4 Dendritic Cells Migrating From Peyer's Patches to the Mesenteric Lymph Nodes Are Dependent Upon CCR7 and S1PR

Under both steady-state and pro-inflammatory conditions migratory DCs must express the lymph node homing chemokine receptor CCR7. The inability to do so, in $CCR7^{-/-}$ mice, leads to a defect in DC migration to lymph nodes and results in less than one tenth the number of DCs in the lymph node (Jang et al., 2006; Randolph et al., 2005). In the intestine, $CCR7^{-/-}$ mice have normal numbers of PPs as well as normal populations of DCs in the LP (Worbs et al., 2006). However, as LP DCs are unable to migrate to the MLN there is a defect in the generation of oral tolerance (Worbs et al., 2006). Therefore, we hypothesised that the migration of PP DCs to the MLN would be abolished in $CCR7^{-/-}$ mice. To test this hypothesis, we performed FITC injections in these animals. The results showed that the migration of PP DCs to the MLN was dependent upon CCR7 (Figure 5.12). This further confirms that these cells are genuine migratory DCs; they behave in a similar way to DCs from non-lymphoid tissue. This conclusively shows that the movement of antigen from PPs is cell dependent, specifically DC dependent, because without CCR7 there were no $FITC^{+}$ DCs in the MLN. Therefore, this is the first time that it has been conclusively shown that the transport of material from PPs to the MLN is cell dependent.

Next we investigated the effects of FTY720 upon DCs migrating from PPs to the MLN. FTY720 is phosphorylated *in vivo* to its active metabolite, which can bind one of the five S1PRs. *In vivo* it can act to render lymphocytes unresponsive to S1P, thus depriving them of a signal required to egress from lymphoid organs. Its effect upon DCs in the lung and skin has also been investigated. It has been

shown that FTY720 caused a reduction in DCs migrating from the lung to the mediastinal LNs, in both mice that had been challenged with allergen and in naïve mice (Idzko et al., 2006). Similarly, following FITC skin paining there was a decrease in DCs migrating to the draining LN (Czeloth et al., 2005). The mechanism of action of FTY720 upon DCs remains controversial, with some attributing its effects to be due to an impaired response to CCR7 (Lan et al., 2005). Others attribute its effects to a downregulation of S1PR1 (Czeloth et al., 2005). When a FTY720 analogue was previously administered to rats, a decrease in the number of DCs migrating in lymph following TDC of MLNx animals was not observed (S Milling, personal communication). Therefore, although FTY720 does not appear to affect the majority of intestinal DCs, we investigated the effect of FTY720 upon DCs migrating from PPs to the MLN. Following FTY720 administration, the migration of DCs from the PPs to the MLN was abolished (Figure 5.13). This suggests that the molecular mechanism controlling the migration of DCs from the PPs is unlike that used by DCs that migrate from the conventional villus mucosa. The ability of PP DCs to migrate to the MLN in an S1P dependent manner is line with the ability of these cells to migrate from one secondary lymphoid organ to another, such as T or B cells.

We next investigated which of the S1PRs might be required for DCs to migrate from the PP to the MLN. Previous work has shown that signaling through S1PR1 and S1PR3 mediated migration, while the action of S1PR2 antagonised it (Sanchez and Hla, 2004). Therefore, we made use of $EDG3^{-/-}$ mice, which are deficient in S1PR3, to investigate if this was essential for PP DCs migration to the MLN. We found that in $EDG3^{-/-}$ mice there was no change in the number or percentage of DCs migrating from the PPs to the MLN (Figure 5.14). Previous *in vitro* work has shown that S1PR3 is essential for the mature DC migration and their endocytotic capability (Maeda et al., 2007). Therefore, it may be that the PP DCs that migrate to the MLN may be similar to LP DCs, which migrate in a 'semi-mature' state (Milling et al., 2010), and hence were unaffected by the lack of S1PR3 signalling. Future work could make use of the wide array of pharmacological agents and mouse models that can specifically target each of the S1PR signalling pathways to determine specifically which of the S1PRs FTY720 is acting upon to abolish the migration of PP DCs to the MLN.

5.2.5 Subsets of DCs Migrating From the Peyer's Patches to the Mesenteric Lymph Node

We next examined the subsets of DCs migrating from the PPs to the MLN. Much work has investigated DC subsets in the MLN, identified by their expression of CD103, CD11b and CD8α. As we have used CD103 and CD11b to define DC subsets, we continue to use these markers to investigate the DC subsets from the PP in the MLN. Much of the previous work in PPs used CD11b and CD8α to investigate DC subsets (Iwasaki and Kelsall, 2001). This showed there were three subsets of $CD11c^+$ DC subsets in the PP, present in different locations. $CD8\alpha^+$ DCs were observed within the interfollicular regions of the PPs and were shown to express CCR7. $CD11b^+$ DCs were observed in the subepithelial dome and were able to upregulate CCR7 and migrate to the interfollicular regions. $CD11b^+$ DCs express CCR6. Additionally a third, double negative subset was found in both the interfollicular region and the subepithelial dome (Iwasaki and Kelsall, 2001). More recent work has shown this double negative subset may be comprised of two subsets, separated by their expression of CX3CR1 and lysozyme M (Lelouard et al., 2012). $CD103^+$ DCs have also been identified in the PPs (Bogunovic et al., 2009; Jaensson et al., 2008). Although the majority of DCs in the PPs are $CD103^-$, currently it is unclear how these relate to the previously defined subsets.

Following photoconversion of PPs, subsets of migratory PP DCs in the MLN were investigated. Photoconverted DCs were compared to non-converted DCs in the MLN and PP DCs. There was only one significant difference when comparing between DC subsets in the PPs, photoconverted DCs in the MLN, and non-photoconverted DCs in the MLN. We found that there were significantly fewer $CD103^+CD11b^+$ photoconverted DCs from PPs in the MLN, compared to non-converted DCs. These non-converted DCs are likely to represent mostly DCs derived from the LP, as we have shown that we photoconvert the majority of DCs from the PP. There were also significantly fewer $CD103^+CD11b^+$ DCs in PPs compared to the MLN (Figure 5.8). These data indicate that the photoconverted DCs in the MLN have a surface phenotype highly very similar to of PP DCs. As $CD103^+CD11b^+$ DCs are the most numerous subset in the siLP, this is consistent with the fact that photoconverted DCs in the MLN are PP derived. In comparison, following FITC injection, although there were fewer $FITC^+$ $CD103^+CD11b^+$ DCs in the MLN compared to $FITC^-$ DCs, this difference was not significant. There were

no significant differences between DC subsets amongst FITC$^+$ DCs from PP in the MLN and FITC$^-$ DCs in the MLN. There were also no significant differences between FITC$^+$ DCs in the MLN and PP DCs (Figure 5.15). The reason for the difference is subset composition between kaede-red$^+$ DCs and FITC$^+$ DCs in the MLN may be due to a number of factors. Firstly, investigations of subsets of DCs following photoconversion have been completed on a larger sample size. Therefore, in further repeats of FITC injections the difference in CD103$^+$CD11b$^+$ cells between FITC$^+$ and FITC$^-$ DCs may become significant. Another reason for the observed difference in subset composition of DCs migrating to the MLN following photoconversion or FITC injection may be due to the labelling technique used. FITC is a soluble molecule, while photoconversion induces a conformational change in proteins present within cells. It is be possible that FITC is transferred to DCs within the MLN in a different manner than photoconverted kaede. These data show that migration from the PP to the MLN is not a property of only one specific subset of DCs. Further work is required to define the properties of the DCs that migrate from the PP to the MLN, and the molecular mechanisms that control this migration.

5.3 Conclusions

We show here that migrating DC populations that reach the MLN can be separated, both by their specific tissue of origin, and by the molecular mechanisms that control their migration. These findings demonstrate a new way by which the intestinal immune system communicates. Furthermore, they open new avenues for controlling the functions of intestinal DCs, and therefore manipulating the intestinal immune response, with exquisite precision.

DC migration from PPs to the MLN is likely to be the main route by which particulate antigen gains access to the MLN in the steady-state, although this should be further verified. Therefore, these DCs represent an opportunity to discover novel functions of the intestinal immune system, and to manipulate them. For example, this PP to MLN route is likely to be the way in which commensal bacteria and pathogenic bacteria gain access to the MLN. Therefore a possible treatment strategy could be to target these DCs via M cells in the context of bacterial infections to prevent their dissemination. Alternatively, increasing migration of PP DCs to the MLN may prove to be beneficial under some conditions, for example when inducing vaccine responses using particulate antigen. However, to maximize these opportunities we first must fully understand the function of these cells.

The function of the DCs that migrate to the MLN from the PPs remain unclear; it may be that in order to generate an effective T cell response, a proportion of PP DCs must first migrate to the MLN. Previous work has shown that PP DCs were less efficient in inducing antigen-specific T cell activation *in vivo* (Chirdo et al., 2005). Indeed, some work has suggested that they may in fact suppress T cell responses *in vitro* (Jump and Levine, 2002). The cooperation between PP and MLN to promote a functional T cell response has already been demonstrated (Kwa et al., 2006). Kwa *et al*. showed that the immune response to *Eimeria vermiformis*, which requires a rapid Th1 response, was delayed in PP-null mice. They attributed this to an observed delay in the increase of $CD11b^+$ DCs in the MLN, presumably originating from PPs.

Further work should be carried out to investigate the functions of these cells. Primarily a full phenotypic analysis should be performed, using available antibodies and mRNA expression analysis, as the presence of up or down regulated molecules may generate insights into the functions of these cells. Second, these cells should be purified and used to stimulate naïve T cells *in vitro* and *in vivo*. This would begin to give and idea of the type of immune response these DCs are specailised to perform.

Additionally, it would be interesting to study these DCs under conditions of bacterial infection to determine their role. This may also provide insight into mechanisms by which the systemic immune response remains ignorant of intestinal microbiota, and how this ignorance breached in some conditions. Furthermore, investigating the migration of these DCs that may carry commensal microorganisms following treatment with antibiotics to disturb the normal microbiota may also provide interesting insights into how these cells react under conditions of dysbiosis.

Finally, these cells may provide a novel way to generate oral vaccines with exquisite specificity, as they appear to be distinct from LP DCs. Determining the functional differences between these PP migratory DCs and LP DCs therefore is of paramount importance.

Chapter 6: Final Discussion

In the preceding chapters I have provided a comprehensive, detailed and up to date examination of the migration of DC subsets in the intestine. In addition, I have discussed the relevance of my results to published data regarding the functions of these subsets. In this final chapter I will provide an overview of the novel insights into DC migration I have described, and give an account of how these may allow us to manipulate the intestinal immune system.

I have shown that the SI and colon drain to distinct LNs, which can be analysed separately. I have also shown that different subsets of DCs in the intestine originate in different anatomical locations, with all but one DC subset being present in the siLP. Surprisingly, $CD103^{+}CD8\alpha^{+}$ DCs are not restricted to intestinal lymphoid tissues and are present in the siLP, while $CD103^{-}CD11b^{-}$ DCs are derived only from ILFs in the SI. Furthermore, I have conclusively demonstrated, for the first time, that DCs are able to migrate from PPs to the siMLN. These data are depicted in figure 6.1.

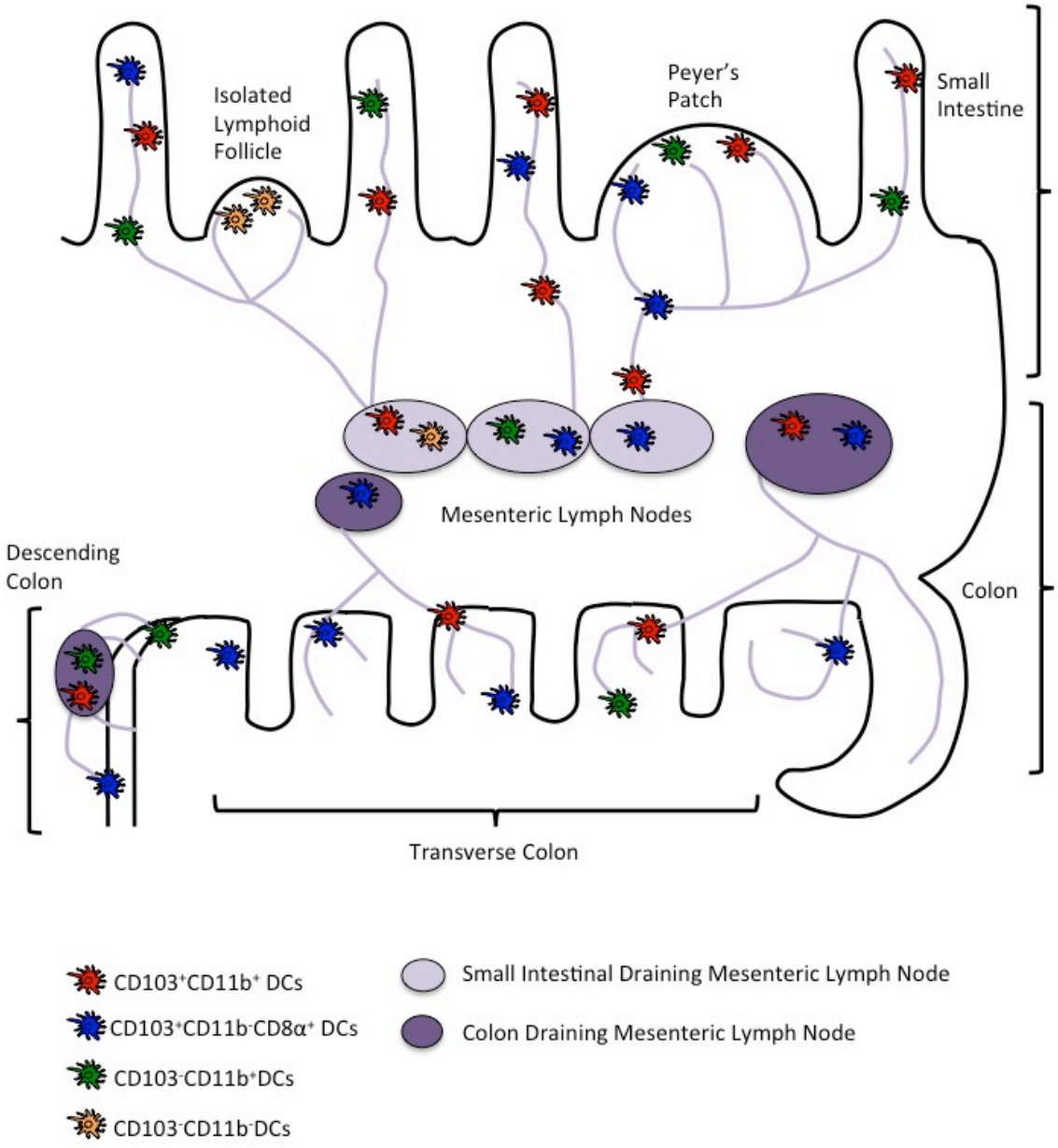

Figure 6-1 Dendritic Cell Subsets in the Small Intestine and Colon and Draining Mesenteric Lymph Nodes.

The lymphatics of the small intestine (SI) and colon drain to distinct parts of the MLN: the siMLN and coMLN respectively. Afferent lymphatic vessels are depicted in purple. $CD103^{+}CD11b^{+}$ (red), $CD103^{+}CD11b^{-}CD8\alpha^{+}$ (blue), and $CD103^{-}CD11b^{+}$ (green) dendritic cells (DCs) are located in the SI lamina propria, Peyer's patches (PPs) and colon. The draining lymph nodes for each of these distinct anatomical locations are depicted. $CD103^{-}CD11b^{-}$ (orange) DCs are present only in SI isolated lymphoid tissues (ILFs), and migrate to the siMLN.

I have described the anatomical segregation between lymphatic drainage of DCs in the SI and colon. Future work examining immune responses in the SI and colon should isolate these LNs separately: independent analyses of the siMLN and coMLN will enable a more refined understanding of intestinal immune responses. This may reveal much about differences in DC biology between the SI and colon, both in the steady-state and under conditions of inflammation. Additionally, small changes in cell populations that may have been missed entirely may now become apparent upon careful examination of specific draining LNs. Differences in lymphatic drainage to distinct parts of the MLN may, in part, explain the mechanism by which different immune responses are achived in the SI and colon. For example, food proteins in the SI induce both local and systemic tolerance, while in the colon there is no systemic response to bacteria, meaning the immune system is acting differently. This allows the immune system to respond differently to food and bacteria depending upon their location in the intestinal tract. Because these different responses are initiated in the anatomically-distinct siMLN and coMLN, it is likely that DCs in the siMLN and coMLN are functionally distinct. These differences could be exploited to target the type of immune response required by specific oral vaccines. For example to generate a systemic immune response to a pathogen that may enter via the intestine or other routes, it would be preferable to target DCs in the SI.

Another key difference between the SI and colon is in disease models. For example UC causes a massive influx of cells in the cLP accompanied by inflammation, yet there is little change in the siLP. One theory to explain the difference in effect in the SI and colon is that T cells primed in the siMLN by DCs from the SI selectively home to the siLP, while colonic DCs prime T cells in the coMLN which home to the colon. Differential homing, induced in the siMLN or coMLN would require SI- or colon-specific T cell homing receptors, the blocking of which may ameliorate inflammatory symptoms of disease. If indeed such T cell specific homing molecules exist, there are many applications by which their upregulation, or down-regulation may enhance tolerance or alleviate diseases.

An intriguing difference between the SI and colon was apparent in their DC subset compositions. The SI had the largest population of $CD103^+CD11b^+$ DCs, while in the colon the $CD103^+CD8\alpha^+$ DCs were the largest subset. These $CD103^+$

subsets share considerable functional overlap in terms of the generation of oral tolerance (Welty et al., 2013) but the functional relevance of this change in subset composition needs further investigation. The differences in DC subset composition are likely to reflect differences in the cytokine microenvironments between the SI and colon. Recent work in the Mowat laboratory has shown that there may be a developmental continuum between $CD103^-CD11b^+$ DCs and $CD103^+CD11b^+$ DCs in the LP (C. Scott, personal communication). As $CD103^-$ DCs display a more immunogenic phenotype, the reduced number of the $CD103^+CD11b^+$ DCs in the colon compared to the SI may be due to a more immunogenic environment in the colon compared to the SI, which prevents the differentiation of these cells into $CD103^+CD11b^+$ DCs. $CD103^+CD11b^+$ DCs have been shown to be essential for the generation of a Th17 response, which, in the SI, this is essential in order to mount a response to *Citrobacter rodentium* (Ivanov et al., 2009). Therefore, the differences between $CD103^+CD11b^+$ DCs in the SI and colon may have evolved to counter the different microbial species present in the tissues. Furthermore, an exacerbated Th17 response is associated with CD (Ogino et al., 2013), so it may be beneficial for the colon to have an expanded population of $CD103^+CD8\alpha^+$ DCs, instead of $CD103^+CD11b^+$ DCs. These $CD103^+CD8\alpha^+$ DCs that are able to mediate many of the same tolerogenic responses as $CD103^+CD11b^+$ DCs, while being less likely to induce pathogenic Th17 responses. The consequences of these newly-identified differences between DC migration in the SI and colon are far reaching. They should be considered in the context of immune responses in the SI and colon.

I have shown that different subsets of DCs in the intestine originate from different anatomical locations. This provides an interesting insight into the organisation of the intestinal immune response, as well as providing potential avenues by which to target specific DC subsets with defined functions. First, I showed that $CD103^+CD11b^+$, $CD103^+CD11b^-CD8\alpha^+$ and $CD103^-CD11b^+$ DCs were all present in the siLP and cLP. Of these subsets, the presence of $CD8\alpha^+$ DCs was most notable. It had been suggested that $CD8\alpha^+$ DCs were only present in organised lymphoid tissues. However, we and others, have now conclusively shown that $CD8\alpha^+$ DCs are present in other tissues, including the LP and lung (Cerovic et al., 2012; Desch et al., 2011; Fujimoto et al., 2011). $CD8\alpha^+$ DCs are the only DC subset capable of cross-presenting exogenously derived antigen and

inducing a strong CTL response. The observation that CD8α^+ DCs are present in the LP provides a mechanism by which DCs are able to instigate a primary immune response to virally infected cells in the intestine. This information can also be used to manipulate the immune system. As such, targeting CD8α^+ DCs will result in a strong CTL response which would be beneficial for anti-viral and anti-tumour immunity. These cells can now be specifically targeted in both the SI and colon to provide new treatment avenues.

My data show that three functionally distinct subsets of DCs are able to migrate from the siLP and cLP, while one subset of CD103$^-$CD11b$^-$ DCs is likely to migrate from SI ILFs. This ILF-resident population of DCs warrants much further study, and is likely to represent an excellent opportunity to specifically target the generation of a SI immune response. The CD103$^-$CD11b$^-$ DCs induce the production IL-17 from developing T cells, even without exogenous stimulation. Therefore, the ability to target this population of DCs would be useful in generating a Th17 type response. Compared to DCs from the LP, CD103$^-$CD11b$^-$ DCs would perhaps present an easier target. They are only present in the SI, specifically within ILFs. Therefore, by targeting ILFs, one can specifically target CD103$^-$CD11b$^-$ DCs which may allow for a more controlled activation of the immune response.

I have also presented data that show that DCs are able to migrate from PPs to the siMLN. This is a long-standing area of controversy in the field. Previous reports have suggested that there may be some migration of DCs from the PP to the MLN, however this has never been directly assessed (Macpherson and Uhr, 2004). It is important to understand whether or not PP DCs are able to migrate to the MLN because PP and LP DCs are likely to transport different types of antigen, acquired via different routes (Knoop et al., 2009; McDole et al., 2012), in different microenvironments (Ermund et al., 2013; Hirota et al., 2013; Schulz et al., 2009), and are therefore likely to play different physiological roles.

DCs from the PPs can acquire antigen via M cells, which are specialised for the uptake of large particulate antigen. Therefore, data presented in this thesis shows how particulate antigen is able to gain access to the MLN, from DCs in the PP that migrate to the MLN. Targeting this PP-migratory DC subset via M cell

specific agents, such as anti-GP-2, represents a truly unique way to manipulate the immune system (Hase et al., 2009a). However, many questions remain unanswered regarding these DCs. Their physiological functions, for instance, remain unclear. I postulate that the migration of DCs to the MLN from the PP may be necessary to initiate T cell responses in the MLN against PP derived antigen. Although there are naive T cells in PPs they are present at lower levels compared to other lymphatic tissues, therefore DCs may have to migrate to the MLN to achieve an effective T cell response. Furthermore, it is unclear what type of an immune response is preferentially induced in by PP migratory DCs. PP DCs have been associated with an antigen dependent Th2 type response; therefore this novel population of migratory DCs may also be expected to induce a Th2 type response (Yoshida et al., 2002b).

Further questions remain regarding the mechanisms controlling the migration of PP DCs to the MLN. Migratory PP DCs were missing from the MLN of $CCR7^{-/-}$ mice; therefore they are likely to migrate in response to CCL19 and CCL21. However PPs contain CCL19 and CCL21 expressing cells, so it remains to be determined how PP DCs appear selectively able to migrate towards IFRs of the PP, while others migrate towards CCL19 and CCL21 from the MLN. It would be interesting to determine if there are areas, close to the PP-draining lymphatic vessels, where expression of CCL19 and CCL21 is weaker thus giving the PP DC the opportunity to migrate to the MLN. Furthermore, the molecular mechanisms controlling migration of PP DCs are unlike those used by DCs that migrate from the conventional villus mucosa. The migration of PP DCs is controlled by S1P, while LP DC migration is unaffected by blocking S1P signalling. This suggests that there are fundamental differences between PP and LP migratory DCs, making PP migratory DCs an attractive population for further investigation.

I show here that migrating DC populations that reach the MLN can be separated, both by their specific tissue of origin, and by the molecular mechanisms that control their migration. These findings demonstrate a new way by which the intestinal immune system communicates. Furthermore, they open new avenues for controlling the functions of intestinal DCs, and therefore manipulating the intestinal immune response, with exquisite precision. Finally, these cells may provide a novel tool to generate oral vaccines with enhanced specificity, as they

appear to be distinct from LP DCs. Determining the functional differences between these PP migratory DCs and LP DCs is therefore of paramount importance.

6.1 Conclusions

Experiments presented in this thesis have added to existing knowledge by providing a detailed analysis of DC subsets and their migration from specific areas in the intestine. I have demonstrated the anatomical segregation of lymphatic drainage between the SI and colon and I have identified a novel pathway by which PP DC can access the MLN. Future work will should now investigate the roles played by these DCs in the prevention of disease, and should aim to target these cells to exploit their full immunogenic potential.

Chapter 7: References

Adachi, S., H. Yoshida, K. Honda, K. Maki, K. Saijo, K. Ikuta, T. Saito, and S.I. Nishikawa. 1998. Essential role of IL-7 receptor alpha in the formation of Peyer's patch anlage. *Int Immunol* 10:1-6.

Aguzzi, A., and N.J. Krautler. 2010. Characterizing follicular dendritic cells: A progress report. *Eur J Immunol* 40:2134-2138.

Alimzhanov, M.B., D.V. Kuprash, M.H. Kosco-Vilbois, A. Luz, R.L. Turetskaya, A. Tarakhovsky, K. Rajewsky, S.A. Nedospasov, and K. Pfeffer. 1997. Abnormal development of secondary lymphoid tissues in lymphotoxin beta-deficient mice. *Proceedings of the National Academy of Sciences of the United States of America* 94:9302-9307.

Alvarez, D., E.H. Vollmann, and U.H. von Andrian. 2008. Mechanisms and consequences of dendritic cell migration. *Immunity* 29:325-342.

Anderson, M.S., and J.A. Bluestone. 2005. The NOD mouse: a model of immune dysregulation. *Annu Rev Immunol* 23:447-485.

Anjuere, F., C. Luci, M. Lebens, D. Rousseau, C. Hervouet, G. Milon, J. Holmgren, C. Ardavin, and C. Czerkinsky. 2004. In vivo adjuvant-induced mobilization and maturation of gut dendritic cells after oral administration of cholera toxin. *Journal of immunology* 173:5103-5111.

Annacker, O., J.L. Coombes, V. Malmstrom, H.H. Uhlig, T. Bourne, B. Johansson-Lindbom, W.W. Agace, C.M. Parker, and F. Powrie. 2005. Essential role for CD103 in the T cell-mediated regulation of experimental colitis. *J Exp Med* 202:1051-1061.

Anosova, N.G., S. Chabot, V. Shreedhar, J.A. Borawski, B.L. Dickinson, and M.R. Neutra. 2008. Cholera toxin, E. coli heat-labile toxin, and non-toxic derivatives induce dendritic cell migration into the follicle-associated epithelium of Peyer's patches. *Mucosal Immunol* 1:59-67.

Ansel, K.M., V.N. Ngo, P.L. Hyman, S.A. Luther, R. Forster, J.D. Sedgwick, J.L. Browning, M. Lipp, and J.G. Cyster. 2000. A chemokine-driven positive feedback loop organizes lymphoid follicles. *Nature* 406:309-314.

Auffray, C., D.K. Fogg, E. Narni-Mancinelli, B. Senechal, C. Trouillet, N. Saederup, J. Leemput, K. Bigot, L. Campisi, M. Abitbol, T. Molina, I. Charo, D.A. Hume, A. Cumano, G. Lauvau, and F. Geissmann. 2009. CX3CR1+ CD115+ CD135+ common macrophage/DC precursors and the role of CX3CR1 in their response to inflammation. *The Journal of experimental medicine* 206:595-606.

Ayabe, T., D.P. Satchell, C.L. Wilson, W.C. Parks, M.E. Selsted, and A.J. Ouellette. 2000. Secretion of microbicidal alpha-defensins by intestinal Paneth cells in response to bacteria. *Nature immunology* 1:113-118.

Bagley, K.C., S.F. Abdelwahab, R.G. Tuskan, T.R. Fouts, and G.K. Lewis. 2002. Cholera toxin and heat-labile enterotoxin activate human monocyte-derived dendritic cells and dominantly inhibit cytokine production through a cyclic AMP-dependent pathway. *Infect Immun* 70:5533-5539.

Bain, C.C., C.L. Scott, H. Uronen-Hansson, S. Gudjonsson, O. Jansson, O. Grip, M. Guilliams, B. Malissen, W.W. Agace, and A.M. Mowat. 2013. Resident and pro-inflammatory macrophages in the colon represent alternative context-dependent fates of the same Ly6Chi monocyte precursors. *Mucosal immunology* 6:498-510.

Balic, A., K.A. Smith, Y. Harcus, and R.M. Maizels. 2009. Dynamics of CD11c(+) dendritic cell subsets in lymph nodes draining the site of intestinal nematode infection. *Immunology letters* 127:68-75.

Balmer, J.E., and R. Blomhoff. 2002. Gene expression regulation by retinoic acid. *J Lipid Res* 43:1773-1808.

Baluk, P., J. Fuxe, H. Hashizume, T. Romano, E. Lashnits, S. Butz, D. Vestweber, M. Corada, C. Molendini, E. Dejana, and D.M. McDonald. 2007. Functionally specialized junctions between endothelial cells of lymphatic vessels. *The Journal of experimental medicine* 204:2349-2362.

Baptista, A.P., B.J. Olivier, G. Goverse, M. Greuter, M. Knippenberg, K. Kusser, R.G. Domingues, H. Veiga-Fernandes, A.D. Luster, A. Lugering, T.D. Randall, T. Cupedo, and R.E. Mebius. 2013. Colonic patch and colonic SILT development are independent and differentially regulated events. *Mucosal immunology* 6:511-521.

Barnden, M.J., J. Allison, W.R. Heath, and F.R. Carbone. 1998. Defective TCR expression in transgenic mice constructed using cDNA-based alpha- and beta-chain genes under the control of heterologous regulatory elements. *Immunology and cell biology* 76:34-40.

Behrens, G., M. Li, C.M. Smith, G.T. Belz, J. Mintern, F.R. Carbone, and W.R. Heath. 2004. Helper T cells, dendritic cells and CTL Immunity. *Immunol Cell Biol* 82:84-90.

Belz, G.T., G.M. Behrens, C.M. Smith, J.F. Miller, C. Jones, K. Lejon, C.G. Fathman, S.N. Mueller, K. Shortman, F.R. Carbone, and W.R. Heath. 2002. The CD8alpha(+) dendritic cell is responsible for inducing peripheral self-tolerance to tissue-associated antigens. *The Journal of experimental medicine* 196:1099-1104.

Ben Suleiman, Y., M. Yoshida, S. Nishiumi, H. Tanaka, T. Mimura, K. Nobutani, K. Yamamoto, M. Takenaka, A. Aoganghua, I. Miki, H. Ota, S. Takahashi, H. Matsui, M. Nakamura, R.S. Blumberg, and T. Azuma. 2012. Neonatal Fc receptor for IgG (FcRn) expressed in the gastric epithelium regulates bacterial infection in mice. *Mucosal immunology* 5:87-98.

Bennett, J.S., D.M. Stroud, J.R. Becker, and D.M. Roden. 2013. Proliferation of embryonic cardiomyocytes in zebrafish requires the sodium channel scn5Lab. *Genesis* 51:562-574.

Bimczok, D., E.N. Sowa, H. Faber-Zuschratter, R. Pabst, and H.J. Rothkotter. 2005. Site-specific expression of CD11b and SIRPalpha (CD172a) on dendritic cells: implications for their migration patterns in the gut immune system. *Eur J Immunol* 35:1418-1427.

Bjerknes, M., and H. Cheng. 1999. Clonal analysis of mouse intestinal epithelial progenitors. *Gastroenterology* 116:7-14.

Blum, J.S., P.A. Wearsch, and P. Cresswell. 2013. Pathways of antigen processing. *Annu Rev Immunol* 31:443-473.

Bogunovic, M., F. Ginhoux, J. Helft, L. Shang, D. Hashimoto, M. Greter, K. Liu, C. Jakubzick, M.A. Ingersoll, M. Leboeuf, E.R. Stanley, M. Nussenzweig, S.A. Lira, G.J. Randolph, and M. Merad. 2009. Origin of the lamina propria dendritic cell network. *Immunity* 31:513-525.

Borghesi, C., M.J. Taussig, and C. Nicoletti. 1999. Rapid appearance of M cells after microbial challenge is restricted at the periphery of the follicle-associated epithelium of Peyer's patch. *Lab Invest* 79:1393-1401.

Bouskra, D., C. Brezillon, M. Berard, C. Werts, R. Varona, I.G. Boneca, and G. Eberl. 2008. Lymphoid tissue genesis induced by commensals through NOD1 regulates intestinal homeostasis. *Nature* 456:507-510.

Brandtzaeg, P., and F.E. Johansen. 2005. Mucosal B cells: phenotypic characteristics, transcriptional regulation, and homing properties. *Immunol Rev* 206:32-63.

Braun, A., T. Worbs, G.L. Moschovakis, S. Halle, K. Hoffmann, J. Bolter, A. Munk, and R. Forster. 2011. Afferent lymph-derived T cells and DCs use different chemokine receptor CCR7-dependent routes for entry into the lymph node and intranodal migration. *Nat Immunol* 12:879-887.

Brinkmann, V., M.D. Davis, C.E. Heise, R. Albert, S. Cottens, R. Hof, C. Bruns, E. Prieschl, T. Baumruker, P. Hiestand, C.A. Foster, M. Zollinger, and K.R. Lynch. 2002. The immune modulator FTY720 targets sphingosine 1-phosphate receptors. *J Biol Chem* 277:21453-21457.

Carter, P.B., and F.M. Collins. 1974. The route of enteric infection in normal mice. *The Journal of experimental medicine* 139:1189-1203.

Cassani, B., E.J. Villablanca, F.J. Quintana, P.E. Love, A. Lacy-Hulbert, W.S. Blaner, T. Sparwasser, S.B. Snapper, H.L. Weiner, and J.R. Mora. 2011. Gut-tropic T cells that express integrin alpha4beta7 and CCR9 are required for induction of oral immune tolerance in mice. *Gastroenterology* 141:2109-2118.

Castellaneta, A., M. Abe, A.E. Morelli, and A.W. Thomson. 2004. Identification and characterization of intestinal Peyer's patch interferon-alpha producing (plasmacytoid) dendritic cells. *Human immunology* 65:104-113.

Cella, M., A. Fuchs, W. Vermi, F. Facchetti, K. Otero, J.K. Lennerz, J.M. Doherty, J.C. Mills, and M. Colonna. 2009. A human natural killer cell subset provides an innate source of IL-22 for mucosal immunity. *Nature* 457:722-725.

Cerovic, V., S.A. Houston, C.L. Scott, A. Aumeunier, U. Yrlid, A.M. Mowat, and S.W. Milling. 2012. Intestinal CD103- dendritic cells migrate in lymph and prime effector T cells. *Mucosal Immunol- In Press*

Cerutti, A. 2008. The regulation of IgA class switching. *Nat Rev Immunol* 8:421-434.

Cerutti, A., and M. Rescigno. 2008. The biology of intestinal immunoglobulin A responses. *Immunity* 28:740-750.

Chabot, S., J.S. Wagner, S. Farrant, and M.R. Neutra. 2006. TLRs regulate the gatekeeping functions of the intestinal follicle-associated epithelium. *Journal of immunology* 176:4275-4283.

Chang, W.W., and C.P. Leblond. 1971. Renewal of the epithelium in the descending colon of the mouse. I. Presence of three cell populations: vacuolated-columnar, mucous and argentaffin. *Am J Anat* 131:73-99.

Chiba, S., T. Nagai, T. Hayashi, Y. Baba, S. Nagai, and S. Koyasu. 2011. Listerial invasion protein internalin B promotes entry into ileal Peyer's patches in vivo. *Microbiol Immunol* 55:123-129.

Chieppa, M., M. Rescigno, A.Y. Huang, and R.N. Germain. 2006. Dynamic imaging of dendritic cell extension into the small bowel lumen in response to epithelial cell TLR engagement. *J Exp Med* 203:2841-2852.

Chionh, Y.T., J.L. Wee, A.L. Every, G.Z. Ng, and P. Sutton. 2009. M-cell targeting of whole killed bacteria induces protective immunity against gastrointestinal pathogens. *Infect Immun* 77:2962-2970.

Chirdo, F.G., O.R. Millington, H. Beacock-Sharp, and A.M. Mowat. 2005. Immunomodulatory dendritic cells in intestinal lamina propria. *Eur J Immunol* 35:1831-1840.

Clark, M.A., B.H. Hirst, and M.A. Jepson. 1998. M-cell surface beta1 integrin expression and invasin-mediated targeting of Yersinia pseudotuberculosis to mouse Peyer's patch M cells. *Infect Immun* 66:1237-1243.

Colino, J., Y. Shen, and C.M. Snapper. 2002. Dendritic cells pulsed with intact Streptococcus pneumoniae elicit both protein- and polysaccharide-specific immunoglobulin isotype responses in vivo through distinct mechanisms. *The Journal of experimental medicine* 195:1-13.

Cook, D.N., D.M. Prosser, R. Forster, J. Zhang, N.A. Kuklin, S.J. Abbondanzo, X.D. Niu, S.C. Chen, D.J. Manfra, M.T. Wiekowski, L.M. Sullivan, S.R. Smith, H.B. Greenberg, S.K. Narula, M. Lipp, and S.A. Lira. 2000. CCR6 mediates dendritic cell localization, lymphocyte homeostasis, and immune responses in mucosal tissue. *Immunity* 12:495-503.

Coombes, J.L., and F. Powrie. 2008. Dendritic cells in intestinal immune regulation. *Nat Rev Immunol* 8:435-446.

Coombes, J.L., K.R. Siddiqui, C.V. Arancibia-Carcamo, J. Hall, C.M. Sun, Y. Belkaid, and F. Powrie. 2007. A functionally specialized population of mucosal CD103+ DCs induces Foxp3+ regulatory T cells via a TGF-beta and retinoic acid-dependent mechanism. *J Exp Med* 204:1757-1764.

Cresswell, P. 1996. Invariant chain structure and MHC class II function. *Cell* 84:505-507.

Crotty, S. 2011. Follicular helper CD4 T cells (TFH). *Annu Rev Immunol* 29:621-663.

Cuff, C.A., R. Sacca, and N.H. Ruddle. 1999. Differential induction of adhesion molecule and chemokine expression by LTalpha3 and LTalphabeta in inflammation elucidates potential mechanisms of mesenteric and peripheral lymph node development. *Journal of immunology* 162:5965-5972.

Cupedo, T., W. Jansen, G. Kraal, and R.E. Mebius. 2004. Induction of secondary and tertiary lymphoid structures in the skin. *Immunity* 21:655-667.

Cyster, J.G. 2005. Chemokines, sphingosine-1-phosphate, and cell migration in secondary lymphoid organs. *Annu Rev Immunol* 23:127-159.

Cyster, J.G., K.M. Ansel, K. Reif, E.H. Ekland, P.L. Hyman, H.L. Tang, S.A. Luther, and V.N. Ngo. 2000. Follicular stromal cells and lymphocyte homing to follicles. *Immunol Rev* 176:181-193.

Cyster, J.G., and S.R. Schwab. 2012. Sphingosine-1-phosphate and lymphocyte egress from lymphoid organs. *Annu Rev Immunol* 30:69-94.

Czeloth, N., G. Bernhardt, F. Hofmann, H. Genth, and R. Forster. 2005. Sphingosine-1-phosphate mediates migration of mature dendritic cells. *Journal of immunology* 175:2960-2967.

Czeloth, N., A. Schippers, N. Wagner, W. Muller, B. Kuster, G. Bernhardt, and R. Forster. 2007. Sphingosine-1 phosphate signaling regulates positioning of dendritic cells within the spleen. *Journal of immunology* 179:5855-5863.

Dalod, M., T.P. Salazar-Mather, L. Malmgaard, C. Lewis, C. Asselin-Paturel, F. Briere, G. Trinchieri, and C.A. Biron. 2002. Interferon alpha/beta and interleukin 12 responses to viral infections: pathways regulating dendritic cell cytokine expression in vivo. *The Journal of experimental medicine* 195:517-528.

Dandie, G.W., F.Y. Watkins, S.J. Ragg, P.E. Holloway, and H.K. Muller. 1994. The migration of Langerhans' cells into and out of lymph nodes draining normal, carcinogen and antigen-treated sheep skin. *Immunology and cell biology* 72:79-86.

Dejardin, E., N.M. Droin, M. Delhase, E. Haas, Y. Cao, C. Makris, Z.W. Li, M. Karin, C.F. Ware, and D.R. Green. 2002. The lymphotoxin-beta receptor induces different patterns of gene expression via two NF-kappaB pathways. *Immunity* 17:525-535.

del Rio, M.L., G. Bernhardt, J.I. Rodriguez-Barbosa, and R. Forster. 2010. Development and functional specialization of CD103+ dendritic cells. *Immunol Rev* 234:268-281.

den Haan, J.M., S.M. Lehar, and M.J. Bevan. 2000. CD8(+) but not CD8(-) dendritic cells cross-prime cytotoxic T cells in vivo. *The Journal of experimental medicine* 192:1685-1696.

Denning, T.L., Y.C. Wang, S.R. Patel, I.R. Williams, and B. Pulendran. 2007. Lamina propria macrophages and dendritic cells differentially induce regulatory and interleukin 17-producing T cell responses. *Nat Immunol* 8:1086-1094.

Desch, A.N., G.J. Randolph, K. Murphy, E.L. Gautier, R.M. Kedl, M.H. Lahoud, I. Caminschi, K. Shortman, P.M. Henson, and C.V. Jakubzick. 2011. CD103+ pulmonary dendritic cells preferentially acquire and present apoptotic cell-associated antigen. *J Exp Med* 208:1789-1797.

Diao, J., E. Winter, C. Cantin, W. Chen, L. Xu, D. Kelvin, J. Phillips, and M.S. Cattral. 2006. In situ replication of immediate dendritic cell (DC) precursors contributes to conventional DC homeostasis in lymphoid tissue. *Journal of immunology* 176:7196-7206.

Dickinson, B.L., K. Badizadegan, Z. Wu, J.C. Ahouse, X. Zhu, N.E. Simister, R.S. Blumberg, and W.I. Lencer. 1999. Bidirectional FcRn-dependent IgG transport in a polarized human intestinal epithelial cell line. *J Clin Invest* 104:903-911.

Diehl, G.E., R.S. Longman, J.X. Zhang, B. Breart, C. Galan, A. Cuesta, S.R. Schwab, and D.R. Littman. 2013. Microbiota restricts trafficking of bacteria to mesenteric lymph nodes by CX(3)CR1(hi) cells. *Nature* 494:116-120.

Donaldson, D.S., A. Kobayashi, H. Ohno, H. Yagita, I.R. Williams, and N.A. Mabbott. 2012. M cell-depletion blocks oral prion disease pathogenesis. *Mucosal immunology* 5:216-225.

Dons, E.M., G. Raimondi, D.K. Cooper, and A.W. Thomson. 2012. Induced regulatory T cells: mechanisms of conversion and suppressive potential. *Human immunology* 73:328-334.

Dougall, W.C., M. Glaccum, K. Charrier, K. Rohrbach, K. Brasel, T. De Smedt, E. Daro, J. Smith, M.E. Tometsko, C.R. Maliszewski, A. Armstrong, V. Shen, S. Bain, D. Cosman, D. Anderson, P.J. Morrissey, J.J. Peschon, and J. Schuh. 1999. RANK is essential for osteoclast and lymph node development. *Genes Dev* 13:2412-2424.

Dubois, B., Joubert, G. Gomez de Aguero, M. Gouanvic, M. Goubier, A, and D. Kaiserlian. 2009. Sequential role of plasmacytoid dendritic cells and regulatory T cells in oral tolerance. *Gastroenterology* 137:1019-28

Eberl, G. 2005. Inducible lymphoid tissues in the adult gut: recapitulation of a fetal developmental pathway? *Nat Rev Immunol* 5:413-420.

Eberl, G., and D.R. Littman. 2003. The role of the nuclear hormone receptor RORgammat in the development of lymph nodes and Peyer's patches. *Immunol Rev* 195:81-90.

Eberl, G., and D.R. Littman. 2004. Thymic origin of intestinal alphabeta T cells revealed by fate mapping of RORgammat+ cells. *Science* 305:248-251.

Edelson, B.T., W. Kc, R. Juang, M. Kohyama, L.A. Benoit, P.A. Klekotka, C. Moon, J.C. Albring, W. Ise, D.G. Michael, D. Bhattacharya, T.S. Stappenbeck, M.J. Holtzman, S.S. Sung, T.L. Murphy, K. Hildner, and K.M. Murphy. 2010. Peripheral CD103+ dendritic cells form a unified subset developmentally related to CD8alpha+ conventional dendritic cells. *The Journal of experimental medicine* 207:823-836.

Edwards, A.D., S.S. Diebold, E.M. Slack, H. Tomizawa, H. Hemmi, T. Kaisho, S. Akira, and C. Reis e Sousa. 2003. Toll-like receptor expression in murine DC subsets: lack of TLR7 expression by CD8 alpha+ DC correlates with unresponsiveness to imidazoquinolines. *European journal of immunology* 33:827-833.

El Shikh, M.E., R.M. El Sayed, A.K. Szakal, and J.G. Tew. 2009. T-independent antibody responses to T-dependent antigens: a novel follicular dendritic cell-dependent activity. *J Immunol* 182:3482-3491.

Ermund, A., A. Schuette, M.E. Johansson, J.K. Gustafsson, and G.C. Hansson. 2013. Gastrointestinal mucus layers have different properties depending on location - 1. Studies of mucus in mouse stomach, small intestine, Peyer's patches and colon. *American journal of physiology. Gastrointestinal and liver physiology*

Fagarasan, S., M. Muramatsu, K. Suzuki, H. Nagaoka, H. Hiai, and T. Honjo. 2002. Critical roles of activation-induced cytidine deaminase in the homeostasis of gut flora. *Science* 298:1424-1427.

Farache, J., I. Koren, I. Milo, I. Gurevich, K.W. Kim, E. Zigmond, G.C. Furtado, S.A. Lira, and G. Shakhar. 2013. Luminal bacteria recruit CD103+ dendritic cells into the intestinal epithelium to sample bacterial antigens for presentation. *Immunity* 38:581-595.

Fazilleau, N., L. Mark, L.J. McHeyzer-Williams, and M.G. McHeyzer-Williams. 2009. Follicular helper T cells: lineage and location. *Immunity* 30:324-335.

Fink, L.N., and H. Frokiaer. 2008. Dendritic cells from Peyer's patches and mesenteric lymph nodes differ from spleen dendritic cells in their

response to commensal gut bacteria. *Scandinavian journal of immunology* 68:270-279.

Finke, D., H. Acha-Orbea, A. Mattis, M. Lipp, and J. Kraehenbuhl. 2002. CD4+CD3- cells induce Peyer's patch development: role of alpha4beta1 integrin activation by CXCR5. *Immunity* 17:363-373.

Fleeton, M.N., N. Contractor, F. Leon, J.D. Wetzel, T.S. Dermody, and B.L. Kelsall. 2004. Peyer's patch dendritic cells process viral antigen from apoptotic epithelial cells in the intestine of reovirus-infected mice. *J Exp Med* 200:235-245.

Fogg, D.K., C. Sibon, C. Miled, S. Jung, P. Aucouturier, D.R. Littman, A. Cumano, and F. Geissmann. 2006. A clonogenic bone marrow progenitor specific for macrophages and dendritic cells. *Science* 311:83-87.

Fonteneau, J.F., M. Larsson, A.S. Beignon, K. McKenna, I. Dasilva, A. Amara, Y.J. Liu, J.D. Lifson, D.R. Littman, and N. Bhardwaj. 2004. Human immunodeficiency virus type 1 activates plasmacytoid dendritic cells and concomitantly induces the bystander maturation of myeloid dendritic cells. *Journal of virology* 78:5223-5232.

Forster, R., A. Schubel, D. Breitfeld, E. Kremmer, I. Renner-Muller, E. Wolf, and M. Lipp. 1999. CCR7 coordinates the primary immune response by establishing functional microenvironments in secondary lymphoid organs. *Cell* 99:23-33.

Frey, A., K.T. Giannasca, R. Weltzin, P.J. Giannasca, H. Reggio, W.I. Lencer, and M.R. Neutra. 1996. Role of the glycocalyx in regulating access of microparticles to apical plasma membranes of intestinal epithelial cells: implications for microbial attachment and oral vaccine targeting. *The Journal of experimental medicine* 184:1045-1059.

Fujimoto, K., T. Karuppuchamy, N. Takemura, M. Shimohigoshi, T. Machida, Y. Haseda, T. Aoshi, K.J. Ishii, S. Akira, and S. Uematsu. 2011. A new subset of CD103+CD8alpha+ dendritic cells in the small intestine expresses TLR3, TLR7, and TLR9 and induces Th1 response and CTL activity. *Journal of immunology* 186:6287-6295.

Fukuyama, S., T. Hiroi, Y. Yokota, P.D. Rennert, M. Yanagita, N. Kinoshita, S. Terawaki, T. Shikina, M. Yamamoto, Y. Kurono, and H. Kiyono. 2002. Initiation of NALT organogenesis is independent of the IL-7R, LTbetaR, and NIK signaling pathways but requires the Id2 gene and CD3(-)CD4(+)CD45(+) cells. *Immunity* 17:31-40.

Fukuyama, S., and H. Kiyono. 2007. Neuroregulator RET initiates Peyer's-patch tissue genesis. *Immunity* 26:393-395.

Geier, M.S., C.L. Smith, R.N. Butler, and G.S. Howarth. 2009. Small-intestinal manifestations of dextran sulfate sodium consumption in rats and assessment of the effects of Lactobacillus fermentum BR11. *Dig Dis Sci* 54:1222-1228.

Geiger, T.L., and S. Tauro. 2012. Nature and nurture in Foxp3(+) regulatory T cell development, stability, and function. *Human immunology* 73:232-239.

Geissmann, F., M.G. Manz, S. Jung, M.H. Sieweke, M. Merad, and K. Ley. 2010. Development of monocytes, macrophages, and dendritic cells. *Science* 327:656-661.

Ginhoux, F., K. Liu, J. Helft, M. Bogunovic, M. Greter, D. Hashimoto, J. Price, N. Yin, J. Bromberg, S.A. Lira, E.R. Stanley, M. Nussenzweig, and M. Merad. 2009. The origin and development of nonlymphoid tissue CD103+ DCs. *J Exp Med* 206:3115-3130.

Glanville, S.H., V. Bekiaris, E.J. Jenkinson, P.J. Lane, G. Anderson, and D.R. Withers. 2009. Transplantation of embryonic spleen tissue reveals a role for adult non-lymphoid cells in initiating lymphoid tissue organization. *European journal of immunology* 39:280-289.

Glaysher, B.R., and N.A. Mabbott. 2007. Isolated lymphoid follicle maturation induces the development of follicular dendritic cells. *Immunology* 120:336-344.

Goubier, A., B. Dubois, H. Gheit, G. Joubert, F. Villard-Truc, C. Asselin-Paturel, G. Trinchieri, and D. Kaiserlian. 2008. Plasmacytoid dendritic cells mediate oral tolerance. *Immunity* 29:464-475.

Greter, M., J. Helft, A. Chow, D. Hashimoto, A. Mortha, J. Agudo-Cantero, M. Bogunovic, E.L. Gautier, J. Miller, M. Leboeuf, G. Lu, C. Aloman, B.D. Brown, J.W. Pollard, H. Xiong, G.J. Randolph, J.E. Chipuk, P.S. Frenette, and M. Merad. 2012. GM-CSF controls nonlymphoid tissue dendritic cell homeostasis but is dispensable for the differentiation of inflammatory dendritic cells. *Immunity* 36:1031-1046.

Guermonprez, P., J. Valladeau, L. Zitvogel, C. Thery, and S. Amigorena. 2002. Antigen presentation and T cell stimulation by dendritic cells. *Annu Rev Immunol* 20:621-667.

Gunn, M.D., S. Kyuwa, C. Tam, T. Kakiuchi, A. Matsuzawa, L.T. Williams, and H. Nakano. 1999. Mice lacking expression of secondary lymphoid organ chemokine have defects in lymphocyte homing and dendritic cell localization. *The Journal of experimental medicine* 189:451-460.

Hadis, U., B. Wahl, O. Schulz, M. Hardtke-Wolenski, A. Schippers, N. Wagner, W. Muller, T. Sparwasser, R. Forster, and O. Pabst. 2011. Intestinal tolerance requires gut homing and expansion of FoxP3+ regulatory T cells in the lamina propria. *Immunity* 34:237-246.

Hall, J.G., and M.E. Smith. 1971. Studies on the afferent and efferent lymph of lymph nodes draining the site of application of fluorodinitrobenzene (FDNB). *Immunology* 21:69-79.

Hase, K., K. Kawano, T. Nochi, G.S. Pontes, S. Fukuda, M. Ebisawa, K. Kadokura, T. Tobe, Y. Fujimura, S. Kawano, A. Yabashi, S. Waguri, G. Nakato, S. Kimura, T. Murakami, M. Iimura, K. Hamura, S. Fukuoka, A.W. Lowe, K. Itoh, H. Kiyono, and H. Ohno. 2009a. Uptake through glycoprotein 2 of

FimH(+) bacteria by M cells initiates mucosal immune response. *Nature* 462:226-230.

Hase, K., S. Kimura, H. Takatsu, M. Ohmae, S. Kawano, H. Kitamura, M. Ito, H. Watarai, C.C. Hazelett, C. Yeaman, and H. Ohno. 2009b. M-Sec promotes membrane nanotube formation by interacting with Ral and the exocyst complex. *Nat Cell Biol* 11:1427-1432.

Hashi, H., H. Yoshida, K. Honda, S. Fraser, H. Kubo, M. Awane, A. Takabayashi, H. Nakano, Y. Yamaoka, and S. Nishikawa. 2001. Compartmentalization of Peyer's patch anlagen before lymphocyte entry. *Journal of immunology* 166:3702-3709.

Heath, W.R., and F.R. Carbone. 2001. Cross-presentation, dendritic cells, tolerance and immunity. *Annu Rev Immunol* 19:47-64.

Hegazy, A.N., M. Peine, C. Helmstetter, I. Panse, A. Frohlich, A. Bergthaler, L. Flatz, D.D. Pinschewer, A. Radbruch, and M. Lohning. 2010. Interferons direct Th2 cell reprogramming to generate a stable GATA-3(+)T-bet(+) cell subset with combined Th2 and Th1 cell functions. *Immunity* 32:116-128.

Hermiston, M.L., and J.I. Gordon. 1995. Organization of the crypt-villus axis and evolution of its stem cell hierarchy during intestinal development. *Am J Physiol* 268:G813-822.

Hirota, K., J.E. Turner, M. Villa, J.H. Duarte, J. Demengeot, O.M. Steinmetz, and B. Stockinger. 2013. Plasticity of Th17 cells in Peyer's patches is responsible for the induction of T cell-dependent IgA responses. *Nature immunology* 14:372-379.

Hogquist, K.A., S.C. Jameson, and M.J. Bevan. 1995. Strong agonist ligands for the T cell receptor do not mediate positive selection of functional CD8+ T cells. *Immunity* 3:79-86.

Honda, K., H. Nakano, H. Yoshida, S. Nishikawa, P. Rennert, K. Ikuta, M. Tamechika, K. Yamaguchi, T. Fukumoto, T. Chiba, and S.I. Nishikawa. 2001. Molecular basis for hematopoietic/mesenchymal interaction during initiation of Peyer's patch organogenesis. *The Journal of experimental medicine* 193:621-630.

Hooper, L.V., and A.J. Macpherson. 2010. Immune adaptations that maintain homeostasis with the intestinal microbiota. *Nat Rev Immunol* 10:159-169.

Howard, C.J., P. Sopp, J. Brownlie, K.R. Parsons, and L.S. Lee. 1995. Phenotypic variation and functional differences within dendritic cells isolated from afferent lymph. *Adv Exp Med Biol* 378:105-107.

Hu, S., K. Yang, J. Yang, M. Li, and N. Xiong. 2011. Critical roles of chemokine receptor CCR10 in regulating memory IgA responses in intestines. *Proceedings of the National Academy of Sciences of the United States of America* 108:E1035-1044.

Huang, F.P., N. Platt, M. Wykes, J.R. Major, T.J. Powell, C.D. Jenkins, and G.G. MacPherson. 2000. A discrete subpopulation of dendritic cells transports apoptotic intestinal epithelial cells to T cell areas of mesenteric lymph nodes. *J Exp Med* 191:435-444.

Huber, S., N. Gagliani, and R.A. Flavell. 2012. Life, death, and miracles: Th17 cells in the intestine. *European journal of immunology* 42:2238-2245.

Idzko, M., H. Hammad, M. van Nimwegen, M. Kool, T. Muller, T. Soullie, M.A. Willart, D. Hijdra, H.C. Hoogsteden, and B.N. Lambrecht. 2006. Local application of FTY720 to the lung abrogates experimental asthma by altering dendritic cell function. *J Clin Invest* 116:2935-2944.

Idzko, M., E. Panther, S. Corinti, A. Morelli, D. Ferrari, Y. Herouy, S. Dichmann, M. Mockenhaupt, P. Gebicke-Haerter, F. Di Virgilio, G. Girolomoni, and J. Norgauer. 2002. Sphingosine 1-phosphate induces chemotaxis of immature and modulates cytokine-release in mature human dendritic cells for emergence of Th2 immune responses. *Faseb J* 16:625-627.

Inaba, K., M. Inaba, N. Romani, H. Aya, M. Deguchi, S. Ikehara, S. Muramatsu, and R.M. Steinman. 1992. Generation of large numbers of dendritic cells from mouse bone marrow cultures supplemented with granulocyte/macrophage colony-stimulating factor. *The Journal of experimental medicine* 176:1693-1702.

Inaba, K., S. Turley, F. Yamaide, T. Iyoda, K. Mahnke, M. Inaba, M. Pack, M. Subklewe, B. Sauter, D. Sheff, M. Albert, N. Bhardwaj, I. Mellman, and R.M. Steinman. 1998. Efficient presentation of phagocytosed cellular fragments on the major histocompatibility complex class II products of dendritic cells. *The Journal of experimental medicine* 188:2163-2173.

Ivanov, II, K. Atarashi, N. Manel, E.L. Brodie, T. Shima, U. Karaoz, D. Wei, K.C. Goldfarb, C.A. Santee, S.V. Lynch, T. Tanoue, A. Imaoka, K. Itoh, K. Takeda, Y. Umesaki, K. Honda, and D.R. Littman. 2009. Induction of intestinal Th17 cells by segmented filamentous bacteria. *Cell* 139:485-498.

Ivanov, II, L. Frutos Rde, N. Manel, K. Yoshinaga, D.B. Rifkin, R.B. Sartor, B.B. Finlay, and D.R. Littman. 2008. Specific microbiota direct the differentiation of IL-17-producing T-helper cells in the mucosa of the small intestine. *Cell Host Microbe* 4:337-349.

Iwasaki, A., and B.L. Kelsall. 1999. Freshly isolated Peyer's patch, but not spleen, dendritic cells produce interleukin 10 and induce the differentiation of T helper type 2 cells. *The Journal of experimental medicine* 190:229-239.

Iwasaki, A., and B.L. Kelsall. 2000. Localization of distinct Peyer's patch dendritic cell subsets and their recruitment by chemokines macrophage inflammatory protein (MIP)-3alpha, MIP-3beta, and secondary lymphoid organ chemokine. *J Exp Med* 191:1381-1394.

Iwasaki, A., and B.L. Kelsall. 2001. Unique functions of CD11b+, CD8 alpha+, and double-negative Peyer's patch dendritic cells. *J Immunol* 166:4884-4890.

Iwata, M., A. Hirakiyama, Y. Eshima, H. Kagechika, C. Kato, and S.Y. Song. 2004. Retinoic acid imprints gut-homing specificity on T cells. *Immunity* 21:527-538.

Iyoda, T., S. Shimoyama, K. Liu, Y. Omatsu, Y. Akiyama, Y. Maeda, K. Takahara, R.M. Steinman, and K. Inaba. 2002. The CD8+ dendritic cell subset selectively endocytoses dying cells in culture and in vivo. *The Journal of experimental medicine* 195:1289-1302.

Jackson, D.G. 2009. Immunological functions of hyaluronan and its receptors in the lymphatics. *Immunol Rev* 230:216-231.

Jaensson, E., H. Uronen-Hansson, O. Pabst, B. Eksteen, J. Tian, J.L. Coombes, P.L. Berg, T. Davidsson, F. Powrie, B. Johansson-Lindbom, and W.W. Agace. 2008. Small intestinal CD103+ dendritic cells display unique functional properties that are conserved between mice and humans. *J Exp Med* 205:2139-2149.

Jakubzick, C., M. Bogunovic, A.J. Bonito, E.L. Kuan, M. Merad, and G.J. Randolph. 2008. Lymph-migrating, tissue-derived dendritic cells are minor constituents within steady-state lymph nodes. *The Journal of experimental medicine* 205:2839-2850.

Jang, M.H., M.N. Kweon, K. Iwatani, M. Yamamoto, K. Terahara, C. Sasakawa, T. Suzuki, T. Nochi, Y. Yokota, P.D. Rennert, T. Hiroi, H. Tamagawa, H. Iijima, J. Kunisawa, Y. Yuki, and H. Kiyono. 2004. Intestinal villous M cells: an antigen entry site in the mucosal epithelium. *Proc Natl Acad Sci U S A* 101:6110-6115.

Jang, M.H., N. Sougawa, T. Tanaka, T. Hirata, T. Hiroi, K. Tohya, Z. Guo, E. Umemoto, Y. Ebisuno, B.G. Yang, J.Y. Seoh, M. Lipp, H. Kiyono, and M. Miyasaka. 2006. CCR7 is critically important for migration of dendritic cells in intestinal lamina propria to mesenteric lymph nodes. *J Immunol* 176:803-810.

Jeffrey, M., L. Gonzalez, A. Espenes, C.M. Press, S. Martin, M. Chaplin, L. Davis, T. Landsverk, C. MacAldowie, S. Eaton, and G. McGovern. 2006. Transportation of prion protein across the intestinal mucosa of scrapie-susceptible and scrapie-resistant sheep. *The Journal of pathology* 209:4-14.

Johansson-Lindbom, B., M. Svensson, O. Pabst, C. Palmqvist, G. Marquez, R. Forster, and W.W. Agace. 2005. Functional specialization of gut CD103+ dendritic cells in the regulation of tissue-selective T cell homing. *J Exp Med* 202:1063-1073.

Johansson-Lindbom, B., M. Svensson, M.A. Wurbel, B. Malissen, G. Marquez, and W. Agace. 2003. Selective generation of gut tropic T cells in gut-associated lymphoid tissue (GALT): requirement for GALT dendritic cells and adjuvant. *J Exp Med* 198:963-969.

Johnson, L.A., S. Clasper, A.P. Holt, P.F. Lalor, D. Baban, and D.G. Jackson. 2006. An inflammation-induced mechanism for leukocyte transmigration across lymphatic vessel endothelium. *The Journal of experimental medicine* 203:2763-2777.

Johnson, L.A., and D.G. Jackson. 2008. Cell traffic and the lymphatic endothelium. *Ann N Y Acad Sci* 1131:119-133.

Johnson, L.A., and D.G. Jackson. 2010. Inflammation-induced secretion of CCL21 in lymphatic endothelium is a key regulator of integrin-mediated dendritic cell transmigration. *Int Immunol* 22:839-849.

Johnson, L.A., and D.G. Jackson. 2013. The chemokine CX3CL1 promotes trafficking of dendritic cells through inflamed lymphatics. *J Cell Sci* 126:5259-5270.

Jones, B.D., N. Ghori, and S. Falkow. 1994. Salmonella typhimurium initiates murine infection by penetrating and destroying the specialized epithelial M cells of the Peyer's patches. *The Journal of experimental medicine* 180:15-23.

Josefowicz, S.Z., and A. Rudensky. 2009. Control of regulatory T cell lineage commitment and maintenance. *Immunity* 30:616-625.

Jump, R.L., and A.D. Levine. 2002. Murine Peyer's patches favor development of an IL-10-secreting, regulatory T cell population. *Journal of immunology* 168:6113-6119.

Jung, S., J. Aliberti, P. Graemmel, M.J. Sunshine, G.W. Kreutzberg, A. Sher, and D.R. Littman. 2000. Analysis of fractalkine receptor CX(3)CR1 function by targeted deletion and green fluorescent protein reporter gene insertion. *Mol Cell Biol* 20:4106-4114.

Kadowaki, N., S. Ho, S. Antonenko, R.W. Malefyt, R.A. Kastelein, F. Bazan, and Y.J. Liu. 2001. Subsets of human dendritic cell precursors express different toll-like receptors and respond to different microbial antigens. *J Exp Med* 194:863-869.

Kamath, A.T., S. Henri, F. Battye, D.F. Tough, and K. Shortman. 2002. Developmental kinetics and lifespan of dendritic cells in mouse lymphoid organs. *Blood* 100:1734-1741.

Kanamori, Y., K. Ishimaru, M. Nanno, K. Maki, K. Ikuta, H. Nariuchi, and H. Ishikawa. 1996. Identification of novel lymphoid tissues in murine intestinal mucosa where clusters of c-kit+ IL-7R+ Thy1+ lympho-hemopoietic progenitors develop. *J Exp Med* 184:1449-1459.

Karsunky, H., M. Merad, A. Cozzio, I.L. Weissman, and M.G. Manz. 2003. Flt3 ligand regulates dendritic cell development from Flt3+ lymphoid and myeloid-committed progenitors to Flt3+ dendritic cells in vivo. *The Journal of experimental medicine* 198:305-313.

Kelly, K.A., and R. Scollay. 1992. Seeding of neonatal lymph nodes by T cells and identification of a novel population of CD3-CD4+ cells. *European journal of immunology* 22:329-334.

Kelsall, B. 2008. Recent progress in understanding the phenotype and function of intestinal dendritic cells and macrophages. *Mucosal Immunol* 1:460-469.

Kelsall, B.L., and W. Strober. 1996. Distinct populations of dendritic cells are present in the subepithelial dome and T cell regions of the murine Peyer's patch. *J Exp Med* 183:237-247.

Kim, D., R.E. Mebius, J.D. MacMicking, S. Jung, T. Cupedo, Y. Castellanos, J. Rho, B.R. Wong, R. Josien, N. Kim, P.D. Rennert, and Y. Choi. 2000. Regulation of peripheral lymph node genesis by the tumor necrosis factor family member TRANCE. *J Exp Med* 192:1467-1478.

Kim, M.Y., G. Anderson, A. White, E. Jenkinson, W. Arlt, I.L. Martensson, L. Erlandsson, and P.J. Lane. 2005. OX40 ligand and CD30 ligand are expressed on adult but not neonatal CD4+CD3- inducer cells: evidence that IL-7 signals regulate CD30 ligand but not OX40 ligand expression. *Journal of immunology* 174:6686-6691.

Kim, S.H., D.I. Jung, I.Y. Yang, J. Kim, K.Y. Lee, T. Nochi, H. Kiyono, and Y.S. Jang. 2011. M cells expressing the complement C5a receptor are efficient targets for mucosal vaccine delivery. *European journal of immunology* 41:3219-3229.

Kinnebrew, M.A., C.G. Buffie, G.E. Diehl, L.A. Zenewicz, I. Leiner, T.M. Hohl, R.A. Flavell, D.R. Littman, and E.G. Pamer. 2012. Interleukin 23 production by intestinal CD103(+)CD11b(+) dendritic cells in response to bacterial flagellin enhances mucosal innate immune defense. *Immunity* 36:276-287.

Knoop, K.A., B.R. Butler, N. Kumar, R.D. Newberry, and I.R. Williams. 2011. Distinct developmental requirements for isolated lymphoid follicle formation in the small and large intestine: RANKL is essential only in the small intestine. *Am J Pathol* 179:1861-1871.

Knoop, K.A., N. Kumar, B.R. Butler, S.K. Sakthivel, R.T. Taylor, T. Nochi, H. Akiba, H. Yagita, H. Kiyono, and I.R. Williams. 2009. RANKL is necessary and sufficient to initiate development of antigen-sampling M cells in the intestinal epithelium. *Journal of immunology* 183:5738-5747.

Kobayashi, A., D.S. Donaldson, T. Kanaya, S. Fukuda, J.K. Baillie, T.C. Freeman, H. Ohno, I.R. Williams, and N.A. Mabbott. 2012. Identification of novel genes selectively expressed in the follicle-associated epithelium from the meta-analysis of transcriptomics data from multiple mouse cell and tissue populations. *DNA Res* 19:407-422.

Kono, M., Y. Mi, Y. Liu, T. Sasaki, M.L. Allende, Y.P. Wu, T. Yamashita, and R.L. Proia. 2004. The sphingosine-1-phosphate receptors S1P1, S1P2, and S1P3 function coordinately during embryonic angiogenesis. *J Biol Chem* 279:29367-29373.

Kostadinova, F.I., T. Baba, Y. Ishida, T. Kondo, B.K. Popivanova, and N. Mukaida. 2010. Crucial involvement of the CX3CR1-CX3CL1 axis in dextran sulfate sodium-mediated acute colitis in mice. *Journal of leukocyte biology* 88:133-143.

Kraehenbuhl, J.P., and M.R. Neutra. 2000. Epithelial M cells: differentiation and function. *Annu Rev Cell Dev Biol* 16:301-332.

Kropshofer, H., G.J. Hammerling, and A.B. Vogt. 1999. The impact of the non-classical MHC proteins HLA-DM and HLA-DO on loading of MHC class II molecules. *Immunol Rev* 172:267-278.

Kurts, C., B.W. Robinson, and P.A. Knolle. 2010. Cross-priming in health and disease. *Nat Rev Immunol* 10:403-414.

Kwa, S.F., P. Beverley, and A.L. Smith. 2006. Peyer's patches are required for the induction of rapid Th1 responses in the gut and mesenteric lymph nodes during an enteric infection. *Journal of immunology* 176:7533-7541.

Kweon, M.N., M. Yamamoto, P.D. Rennert, E.J. Park, A.Y. Lee, S.Y. Chang, T. Hiroi, M. Nanno, and H. Kiyono. 2005. Prenatal blockage of lymphotoxin beta receptor and TNF receptor p55 signaling cascade resulted in the acceleration of tissue genesis for isolated lymphoid follicles in the large intestine. *Journal of immunology* 174:4365-4372.

Laffont, S., K.R. Siddiqui, and F. Powrie. 2010. Intestinal inflammation abrogates the tolerogenic properties of MLN CD103+ dendritic cells. *Eur J Immunol* 40:1877-1883.

Lambrecht, B.N., B. Salomon, D. Klatzmann, and R.A. Pauwels. 1998. Dendritic cells are required for the development of chronic eosinophilic airway inflammation in response to inhaled antigen in sensitized mice. *Journal of immunology* 160:4090-4097.

Lan, Y.Y., A. De Creus, B.L. Colvin, M. Abe, V. Brinkmann, P.T. Coates, and A.W. Thomson. 2005. The sphingosine-1-phosphate receptor agonist FTY720 modulates dendritic cell trafficking in vivo. *Am J Transplant* 5:2649-2659.

Landsman, L., L. Bar-On, A. Zernecke, K.W. Kim, R. Krauthgamer, E. Shagdarsuren, S.A. Lira, I.L. Weissman, C. Weber, and S. Jung. 2009. CX3CR1 is required for monocyte homeostasis and atherogenesis by promoting cell survival. *Blood* 113:963-972.

Lane, P.J., F.M. McConnell, D. Withers, F. Gaspal, M. Saini, and G. Anderson. 2009. Lymphoid tissue inducer cells: bridges between the ancient innate and the modern adaptive immune systems. *Mucosal immunology* 2:472-477.

Lee, J.S., M. Cella, K.G. McDonald, C. Garlanda, G.D. Kennedy, M. Nukaya, A. Mantovani, R. Kopan, C.A. Bradfield, R.D. Newberry, and M. Colonna. 2012. AHR drives the development of gut ILC22 cells and postnatal lymphoid tissues via pathways dependent on and independent of Notch. *Nature immunology* 13:144-151.

Lee, Y., R.K. Chin, P. Christiansen, Y. Sun, A.V. Tumanov, J. Wang, A.V. Chervonsky, and Y.X. Fu. 2006. Recruitment and activation of naive T cells in the islets by lymphotoxin beta receptor-dependent tertiary lymphoid structure. *Immunity* 25:499-509.

Lelouard, H., M. Fallet, B. de Bovis, S. Meresse, and J.P. Gorvel. 2012. Peyer's patch dendritic cells sample antigens by extending dendrites through M cell-specific transcellular pores. *Gastroenterology* 142:592-601 e593.

Lelouard, H., S. Henri, B. De Bovis, B. Mugnier, A. Chollat-Namy, B. Malissen, S. Meresse, and J.P. Gorvel. 2010. Pathogenic bacteria and dead cells are internalized by a unique subset of Peyer's patch dendritic cells that express lysozyme. *Gastroenterology* 138:173-184 e171-173.

Lenschow, D.J., T.L. Walunas, and J.A. Bluestone. 1996. CD28/B7 system of T cell costimulation. *Annu Rev Immunol* 14:233-258.

Lewis, K.L., M.L. Caton, M. Bogunovic, M. Greter, L.T. Grajkowska, D. Ng, A. Klinakis, I.F. Charo, S. Jung, J.L. Gommerman, Ivanov, II, K. Liu, M. Merad, and B. Reizis. 2011. Notch2 receptor signaling controls functional differentiation of dendritic cells in the spleen and intestine. *Immunity* 35:780-791.

Liu, K., and M.C. Nussenzweig. 2010. Origin and development of dendritic cells. *Immunol Rev* 234:45-54.

Liu, L., M. Zhang, C. Jenkins, and G.G. MacPherson. 1998. Dendritic cell heterogeneity in vivo: two functionally different dendritic cell populations in rat intestinal lymph can be distinguished by CD4 expression. *Journal of immunology* 161:1146-1155.

Lochner, M., C. Ohnmacht, L. Presley, P. Bruhns, M. Si-Tahar, S. Sawa, and G. Eberl. 2011. Microbiota-induced tertiary lymphoid tissues aggravate inflammatory disease in the absence of RORgamma t and LTi cells. *J Exp Med* 208:125-134.

Lorenz, R.G., D.D. Chaplin, K.G. McDonald, J.S. McDonough, and R.D. Newberry. 2003. Isolated lymphoid follicle formation is inducible and dependent upon lymphotoxin-sufficient B lymphocytes, lymphotoxin beta receptor, and TNF receptor I function. *J Immunol* 170:5475-5482.

Lorenz, R.G., and R.D. Newberry. 2004. Isolated lymphoid follicles can function as sites for induction of mucosal immune responses. *Ann N Y Acad Sci* 1029:44-57.

Lu, K.T., Y. Kanno, J.L. Cannons, R. Handon, P. Bible, A.G. Elkahloun, S.M. Anderson, L. Wei, H. Sun, J.J. O'Shea, and P.L. Schwartzberg. 2011. Functional and epigenetic studies reveal multistep differentiation and plasticity of in vitro-generated and in vivo-derived follicular T helper cells. *Immunity* 35:622-632.

Luther, S.A., K.M. Ansel, and J.G. Cyster. 2003. Overlapping roles of CXCL13, interleukin 7 receptor alpha, and CCR7 ligands in lymph node development. *The Journal of experimental medicine* 197:1191-1198.

Lynch, P.M., F.A. Delano, and G.W. Schmid-Schonbein. 2007. The primary valves in the initial lymphatics during inflammation. *Lymphatic research and biology* 5:3-10.

MacDonald, K.P., V. Rowe, H.M. Bofinger, R. Thomas, T. Sasmono, D.A. Hume, and G.R. Hill. 2005. The colony-stimulating factor 1 receptor is expressed on dendritic cells during differentiation and regulates their expansion. *Journal of immunology* 175:1399-1405.

Macpherson, A.J., K.D. McCoy, F.E. Johansen, and P. Brandtzaeg. 2008. The immune geography of IgA induction and function. *Mucosal immunology* 1:11-22.

Macpherson, A.J., E. Slack, M.B. Geuking, and K.D. McCoy. 2009. The mucosal firewalls against commensal intestinal microbes. *Semin Immunopathol* 31:145-149.

Macpherson, A.J., and T. Uhr. 2004. Induction of protective IgA by intestinal dendritic cells carrying commensal bacteria. *Science* 303:1662-1665.

Maeda, Y., H. Matsuyuki, K. Shimano, H. Kataoka, K. Sugahara, and K. Chiba. 2007. Migration of CD4 T cells and dendritic cells toward sphingosine 1-phosphate (S1P) is mediated by different receptor subtypes: S1P regulates the functions of murine mature dendritic cells via S1P receptor type 3. *Journal of immunology* 178:3437-3446.

Mandala, S., R. Hajdu, J. Bergstrom, E. Quackenbush, J. Xie, J. Milligan, R. Thornton, G.J. Shei, D. Card, C. Keohane, M. Rosenbach, J. Hale, C.L. Lynch, K. Rupprecht, W. Parsons, and H. Rosen. 2002. Alteration of lymphocyte trafficking by sphingosine-1-phosphate receptor agonists. *Science* 296:346-349.

Mangan, P.R., L.E. Harrington, D.B. O'Quinn, W.S. Helms, D.C. Bullard, C.O. Elson, R.D. Hatton, S.M. Wahl, T.R. Schoeb, and C.T. Weaver. 2006. Transforming growth factor-beta induces development of the T(H)17 lineage. *Nature* 441:231-234.

Mantis, N.J., M.C. Cheung, K.R. Chintalacharuvu, J. Rey, B. Corthesy, and M.R. Neutra. 2002. Selective adherence of IgA to murine Peyer's patch M cells: evidence for a novel IgA receptor. *Journal of immunology* 169:1844-1851.

Mantis, N.J., N. Rol, and B. Corthesy. 2011. Secretory IgA's complex roles in immunity and mucosal homeostasis in the gut. *Mucosal immunology* 4:603-611.

Manz, M.G., D. Traver, T. Miyamoto, I.L. Weissman, and K. Akashi. 2001. Dendritic cell potentials of early lymphoid and myeloid progenitors. *Blood* 97:3333-3341.

McDole, J.R., L.W. Wheeler, K.G. McDonald, B. Wang, V. Konjufca, K.A. Knoop, R.D. Newberry, and M.J. Miller. 2012. Goblet cells deliver luminal antigen to CD103+ dendritic cells in the small intestine. *Nature* 483:345-349.

McDonald, K.G., M.R. Leach, K.W. Brooke, C. Wang, L.W. Wheeler, E.K. Hanly, C.W. Rowley, M.S. Levin, M. Wagner, E. Li, and R.D. Newberry. 2012. Epithelial expression of the cytosolic retinoid chaperone cellular retinol binding protein II is essential for in vivo imprinting of local gut dendritic cells by lumenal retinoids. *The American journal of pathology* 180:984-997.

McDonald, K.G., M.R. Leach, C. Huang, C. Wang, and R.D. Newberry. 2011. Aging impacts isolated lymphoid follicle development and function. *Immun Ageing* 8:1.

McDonald, K.G., J.S. McDonough, B.K. Dieckgraefe, and R.D. Newberry. 2010. Dendritic cells produce CXCL13 and participate in the development of murine small intestine lymphoid tissues. *The American journal of pathology* 176:2367-2377.

McDonald, K.G., J.S. McDonough, C. Wang, T. Kucharzik, I.R. Williams, and R.D. Newberry. 2007. CC chemokine receptor 6 expression by B lymphocytes is essential for the development of isolated lymphoid follicles. *The American journal of pathology* 170:1229-1240.

McKenna, H.J., K.L. Stocking, R.E. Miller, K. Brasel, T. De Smedt, E. Maraskovsky, C.R. Maliszewski, D.H. Lynch, J. Smith, B. Pulendran, E.R. Roux, M. Teepe, S.D. Lyman, and J.J. Peschon. 2000. Mice lacking flt3 ligand have deficient hematopoiesis affecting hematopoietic progenitor cells, dendritic cells, and natural killer cells. *Blood* 95:3489-3497.

Mebius, R.E. 2003. Organogenesis of lymphoid tissues. *Nat Rev Immunol* 3:292-303.

Mebius, R.E., and G. Kraal. 2005. Structure and function of the spleen. *Nat Rev Immunol* 5:606-616.

Mebius, R.E., P. Rennert, and I.L. Weissman. 1997. Developing lymph nodes collect CD4+CD3- LTbeta+ cells that can differentiate to APC, NK cells, and follicular cells but not T or B cells. *Immunity* 7:493-504.

Mebius, R.E., P.R. Streeter, S. Michie, E.C. Butcher, and I.L. Weissman. 1996. A developmental switch in lymphocyte homing receptor and endothelial vascular addressin expression regulates lymphocyte homing and permits CD4+ CD3- cells to colonize lymph nodes. *Proceedings of the National Academy of Sciences of the United States of America* 93:11019-11024.

Mellman, I., and R.M. Steinman. 2001. Dendritic cells: specialized and regulated antigen processing machines. *Cell* 106:255-258.

Meynell, H.M., N.W. Thomas, P.S. James, J. Holland, M.J. Taussig, and C. Nicoletti. 1999. Up-regulation of microsphere transport across the follicle-associated epithelium of Peyer's patch by exposure to Streptococcus pneumoniae R36a. *Faseb J* 13:611-619.

Milling, S., and G. MacPherson. 2010. Isolation of rat intestinal lymph DC. *Methods Mol Biol* 595:281-297.

Milling, S., U. Yrlid, V. Cerovic, and G. MacPherson. 2010. Subsets of migrating intestinal dendritic cells. *Immunol Rev* 234:259-267.

Milling, S.W., U. Yrlid, C. Jenkins, C.M. Richards, N.A. Williams, and G. MacPherson. 2007. Regulation of intestinal immunity: effects of the oral adjuvant Escherichia coli heat-labile enterotoxin on migrating dendritic cells. *Eur J Immunol* 37:87-99.

Mishra, R.S., S. Basu, Y. Gu, X. Luo, W.Q. Zou, R. Mishra, R. Li, S.G. Chen, P. Gambetti, H. Fujioka, and N. Singh. 2004. Protease-resistant human prion protein and ferritin are cotransported across Caco-2 epithelial cells: implications for species barrier in prion uptake from the intestine. *J Neurosci* 24:11280-11290.

Moodycliffe, A.M., V. Shreedhar, S.E. Ullrich, J. Walterscheid, C. Bucana, M.L. Kripke, and L. Flores-Romo. 2000. CD40-CD40 ligand interactions in vivo regulate migration of antigen-bearing dendritic cells from the skin to draining lymph nodes. *The Journal of experimental medicine* 191:2011-2020.

Moolenbeek, C., and E.J. Ruitenberg. 1981. The "Swiss roll": a simple technique for histological studies of the rodent intestine. *Lab Anim* 15:57-59.

Mora, J.R., M.R. Bono, N. Manjunath, W. Weninger, L.L. Cavanagh, M. Rosemblatt, and U.H. Von Andrian. 2003. Selective imprinting of gut-homing T cells by Peyer's patch dendritic cells. *Nature* 424:88-93.

Mora, J.R., G. Cheng, D. Picarella, M. Briskin, N. Buchanan, and U.H. von Andrian. 2005. Reciprocal and dynamic control of CD8 T cell homing by dendritic cells from skin- and gut-associated lymphoid tissues. *J Exp Med* 201:303-316.

Mora, J.R., M. Iwata, B. Eksteen, S.Y. Song, T. Junt, B. Senman, K.L. Otipoby, A. Yokota, H. Takeuchi, P. Ricciardi-Castagnoli, K. Rajewsky, D.H. Adams, and U.H. von Andrian. 2006. Generation of gut-homing IgA-secreting B cells by intestinal dendritic cells. *Science* 314:1157-1160.

Mora, J.R., M. Iwata, and U.H. von Andrian. 2008. Vitamin effects on the immune system: vitamins A and D take centre stage. *Nat Rev Immunol* 8:685-698.

Mori, S., H. Nakano, K. Aritomi, C.R. Wang, M.D. Gunn, and T. Kakiuchi. 2001. Mice lacking expression of the chemokines CCL21-ser and CCL19 (plt mice) demonstrate delayed but enhanced T cell immune responses. *The Journal of experimental medicine* 193:207-218.

Mosmann, T.R., and R.L. Coffman. 1989. TH1 and TH2 cells: different patterns of lymphokine secretion lead to different functional properties. *Annu Rev Immunol* 7:145-173.

Mowat, A.M. 2003. Anatomical basis of tolerance and immunity to intestinal antigens. *Nat Rev Immunol* 3:331-341.

Moyron-Quiroz, J.E., J. Rangel-Moreno, L. Hartson, K. Kusser, M.P. Tighe, K.D. Klonowski, L. Lefrancois, L.S. Cauley, A.G. Harmsen, F.E. Lund, and T.D. Randall. 2006. Persistence and responsiveness of immunologic memory in the absence of secondary lymphoid organs. *Immunity* 25:643-654.

Moyron-Quiroz, J.E., J. Rangel-Moreno, K. Kusser, L. Hartson, F. Sprague, S. Goodrich, D.L. Woodland, F.E. Lund, and T.D. Randall. 2004. Role of inducible bronchus associated lymphoid tissue (iBALT) in respiratory immunity. *Nat Med* 10:927-934.

Mucida, D., K. Pino-Lagos, G. Kim, E. Nowak, M.J. Benson, M. Kronenberg, R.J. Noelle, and H. Cheroutre. 2009. Retinoic acid can directly promote TGF-beta-mediated Foxp3(+) Treg cell conversion of naive T cells. *Immunity* 30:471-472; author reply 472-473.

Murai, M., O. Turovskaya, G. Kim, R. Madan, C.L. Karp, H. Cheroutre, and M. Kronenberg. 2009. Interleukin 10 acts on regulatory T cells to maintain expression of the transcription factor Foxp3 and suppressive function in mice with colitis. *Nature immunology* 10:1178-1184.

Murphy, K.M., and B. Stockinger. 2010. Effector T cell plasticity: flexibility in the face of changing circumstances. *Nature immunology* 11:674-680.

Nagatake, T., S. Fukuyama, D.Y. Kim, K. Goda, O. Igarashi, S. Sato, T. Nochi, H. Sagara, Y. Yokota, A.M. Jetten, T. Kaisho, S. Akira, H. Mimuro, C. Sasakawa, Y. Fukui, K. Fujihashi, T. Akiyama, J. Inoue, J.M. Penninger, J. Kunisawa, and H. Kiyono. 2009. Id2-, RORgammat-, and LTbetaR-independent initiation of lymphoid organogenesis in ocular immunity. *The Journal of experimental medicine* 206:2351-2364.

Naik, S.H. 2008. Demystifying the development of dendritic cell subtypes, a little. *Immunology and cell biology* 86:439-452.

Naik, S.H., D. Metcalf, A. van Nieuwenhuijze, I. Wicks, L. Wu, M. O'Keeffe, and K. Shortman. 2006. Intrasplenic steady-state dendritic cell precursors that are distinct from monocytes. *Nature immunology* 7:663-671.

Naik, S.H., A.I. Proietto, N.S. Wilson, A. Dakic, P. Schnorrer, M. Fuchsberger, M.H. Lahoud, M. O'Keeffe, Q.X. Shao, W.F. Chen, J.A. Villadangos, K. Shortman, and L. Wu. 2005. Cutting edge: generation of splenic CD8+ and CD8- dendritic cell equivalents in Fms-like tyrosine kinase 3 ligand bone marrow cultures. *J Immunol* 174:6592-6597.

Naik, S.H., P. Sathe, H.Y. Park, D. Metcalf, A.I. Proietto, A. Dakic, S. Carotta, M. O'Keeffe, M. Bahlo, A. Papenfuss, J.Y. Kwak, L. Wu, and K. Shortman. 2007. Development of plasmacytoid and conventional dendritic cell subtypes from single precursor cells derived in vitro and in vivo. *Nature immunology* 8:1217-1226.

Nasr, I.W., M. Reel, M.H. Oberbarnscheidt, R.H. Mounzer, F.K. Baddoura, N.H. Ruddle, and F.G. Lakkis. 2007. Tertiary lymphoid tissues generate effector and memory T cells that lead to allograft rejection. *Am J Transplant* 7:1071-1079.

Neutra, M.R., A. Frey, and J.P. Kraehenbuhl. 1996. Epithelial M cells: gateways for mucosal infection and immunization. *Cell* 86:345-348.

Neutra, M.R., N.J. Mantis, and J.P. Kraehenbuhl. 2001. Collaboration of epithelial cells with organized mucosal lymphoid tissues. *Nat Immunol* 2:1004-1009.

Niess, J.H., and G. Adler. 2010. Enteric flora expands gut lamina propria CX3CR1+ dendritic cells supporting inflammatory immune responses under normal and inflammatory conditions. *Journal of immunology* 184:2026-2037.

Niess, J.H., S. Brand, X. Gu, L. Landsman, S. Jung, B.A. McCormick, J.M. Vyas, M. Boes, H.L. Ploegh, J.G. Fox, D.R. Littman, and H.C. Reinecker. 2005. CX3CR1-mediated dendritic cell access to the intestinal lumen and bacterial clearance. *Science* 307:254-258.

O'Shea, J.J., and W.E. Paul. 2010. Mechanisms underlying lineage commitment and plasticity of helper CD4+ T cells. *Science* 327:1098-1102.

Ochando, J.C., C. Homma, Y. Yang, A. Hidalgo, A. Garin, F. Tacke, V. Angeli, Y. Li, P. Boros, Y. Ding, R. Jessberger, G. Trinchieri, S.A. Lira, G.J. Randolph, and J.S. Bromberg. 2006. Alloantigen-presenting plasmacytoid dendritic cells mediate tolerance to vascularized grafts. *Nat Immunol* 7:652-662.

Ogino, T., J. Nishimura, S. Barman, H. Kayama, S. Uematsu, D. Okuzaki, H. Osawa, N. Haraguchi, M. Uemura, T. Hata, I. Takemasa, T. Mizushima, H. Yamamoto, K. Takeda, Y. Doki, and M. Mori. 2013. Increased Th17-Inducing Activity of CD14(+) CD163(low) Myeloid Cells in Intestinal Lamina Propria of Patients With Crohn's Disease. *Gastroenterology* 145:1380-1391 e1381.

Ohl, L., G. Henning, S. Krautwald, M. Lipp, S. Hardtke, G. Bernhardt, O. Pabst, and R. Forster. 2003. Cooperating mechanisms of CXCR5 and CCR7 in development and organization of secondary lymphoid organs. *The Journal of experimental medicine* 197:1199-1204.

Ohl, L., M. Mohaupt, N. Czeloth, G. Hintzen, Z. Kiafard, J. Zwirner, T. Blankenstein, G. Henning, and R. Forster. 2004. CCR7 governs skin dendritic cell migration under inflammatory and steady-state conditions. *Immunity* 21:279-288.

Okuda, M., A. Togawa, H. Wada, and S. Nishikawa. 2007. Distinct activities of stromal cells involved in the organogenesis of lymph nodes and Peyer's patches. *Journal of immunology* 179:804-811.

Oldenhove, G., N. Bouladoux, E.A. Wohlfert, J.A. Hall, D. Chou, L. Dos Santos, S. O'Brien, R. Blank, E. Lamb, S. Natarajan, R. Kastenmayer, C. Hunter, M.E. Grigg, and Y. Belkaid. 2009. Decrease of Foxp3+ Treg cell number and acquisition of effector cell phenotype during lethal infection. *Immunity* 31:772-786.

Onai, N., A. Obata-Onai, M.A. Schmid, T. Ohteki, D. Jarrossay, and M.G. Manz. 2007. Identification of clonogenic common Flt3+M-CSFR+ plasmacytoid and conventional dendritic cell progenitors in mouse bone marrow. *Nature immunology* 8:1207-1216.

Onai, N., A. Obata-Onai, R. Tussiwand, A. Lanzavecchia, and M.G. Manz. 2006. Activation of the Flt3 signal transduction cascade rescues and enhances type I interferon-producing and dendritic cell development. *The Journal of experimental medicine* 203:227-238.

Owen, R.L. 1999. Uptake and transport of intestinal macromolecules and microorganisms by M cells in Peyer's patches--a personal and historical perspective. *Semin Immunol* 11:157-163.

Pabst, O., G. Bernhardt, and R. Forster. 2007. The impact of cell-bound antigen transport on mucosal tolerance induction. *J Leukoc Biol* 82:795-800.

Pabst, O., H. Herbrand, M. Friedrichsen, S. Velaga, M. Dorsch, G. Berhardt, T. Worbs, A.J. Macpherson, and R. Forster. 2006. Adaptation of solitary intestinal lymphoid tissue in response to microbiota and chemokine receptor CCR7 signaling. *J Immunol* 177:6824-6832.

Pabst, O., H. Herbrand, T. Worbs, M. Friedrichsen, S. Yan, M.W. Hoffmann, H. Korner, G. Bernhardt, R. Pabst, and R. Forster. 2005. Cryptopatches and isolated lymphoid follicles: dynamic lymphoid tissues dispensable for the generation of intraepithelial lymphocytes. *Eur J Immunol* 35:98-107.

Pabst, O., and A.M. Mowat. 2012. Oral tolerance to food protein. *Mucosal Immunol* 5:232-239.

Pascale, F., V. Contreras, M. Bonneau, A. Courbet, S. Chilmonczyk, C. Bevilacqua, M. Epardaud, V. Niborski, S. Riffault, A.M. Balazuc, E. Foulon, L. Guzylack-Piriou, B. Riteau, J. Hope, N. Bertho, B. Charley, and I. Schwartz-Cornil. 2008. Plasmacytoid dendritic cells migrate in afferent skin lymph. *J Immunol* 180:5963-5972.

Persson, E.K., E. Jaensson, and W.W. Agace. 2010. The diverse ontogeny and function of murine small intestinal dendritic cell/macrophage subsets. *Immunobiology* 215:692-697.

Persson, E.K., H. Uronen-Hansson, M. Semmrich, A. Rivollier, K. Hagerbrand, J. Marsal, S. Gudjonsson, U. Hakansson, B. Reizis, K. Kotarsky, and W.W. Agace. 2013. IRF4 transcription-factor-dependent CD103(+)CD11b(+) dendritic cells drive mucosal T helper 17 cell differentiation. *Immunity* 38:958-969.

Pham, T.H., P. Baluk, Y. Xu, I. Grigorova, A.J. Bankovich, R. Pappu, S.R. Coughlin, D.M. McDonald, S.R. Schwab, and J.G. Cyster. 2010. Lymphatic endothelial cell sphingosine kinase activity is required for lymphocyte egress and lymphatic patterning. *The Journal of experimental medicine* 207:17-27.

Pham, T.H., T. Okada, M. Matloubian, C.G. Lo, and J.G. Cyster. 2008. S1P1 receptor signaling overrides retention mediated by G alpha i-coupled receptors to promote T cell egress. *Immunity* 28:122-133.

Possot, C., S. Schmutz, S. Chea, L. Boucontet, A. Louise, A. Cumano, and R. Golub. 2011. Notch signaling is necessary for adult, but not fetal, development of RORgammat(+) innate lymphoid cells. *Nature immunology* 12:949-958.

Pron, B., C. Boumaila, F. Jaubert, P. Berche, G. Milon, F. Geissmann, and J.L. Gaillard. 2001. Dendritic cells are early cellular targets of Listeria monocytogenes after intestinal delivery and are involved in bacterial spread in the host. *Cell Microbiol* 3:331-340.

Pugh, C.W., G.G. MacPherson, and H.W. Steer. 1983. Characterization of nonlymphoid cells derived from rat peripheral lymph. *J Exp Med* 157:1758-1779.

Qi, H., J.G. Egen, A.Y. Huang, and R.N. Germain. 2006. Extrafollicular activation of lymph node B cells by antigen-bearing dendritic cells. *Science* 312:1672-1676.

Randall, T.D., D.M. Carragher, and J. Rangel-Moreno. 2008. Development of secondary lymphoid organs. *Annu Rev Immunol* 26:627-650.

Randolph, G.J. 2001. Dendritic cell migration to lymph nodes: cytokines, chemokines, and lipid mediators. *Semin Immunol* 13:267-274.

Randolph, G.J., V. Angeli, and M.A. Swartz. 2005. Dendritic-cell trafficking to lymph nodes through lymphatic vessels. *Nat Rev Immunol* 5:617-628.

Randolph, G.J., S. Beaulieu, S. Lebecque, R.M. Steinman, and W.A. Muller. 1998. Differentiation of monocytes into dendritic cells in a model of transendothelial trafficking. *Science* 282:480-483.

Rathinasamy, A., N. Czeloth, O. Pabst, R. Forster, and G. Bernhardt. 2010. The origin and maturity of dendritic cells determine the pattern of sphingosine 1-phosphate receptors expressed and required for efficient migration. *Journal of immunology* 185:4072-4081.

Reis e Sousa, C., S. Hieny, T. Scharton-Kersten, D. Jankovic, H. Charest, R.N. Germain, and A. Sher. 1997. In vivo microbial stimulation induces rapid CD40 ligand-independent production of interleukin 12 by dendritic cells and their redistribution to T cell areas. *The Journal of experimental medicine* 186:1819-1829.

Rennert, P.D., J.L. Browning, R. Mebius, F. Mackay, and P.S. Hochman. 1996. Surface lymphotoxin alpha/beta complex is required for the development of peripheral lymphoid organs. *J Exp Med* 184:1999-2006.

Rennert, P.D., D. James, F. Mackay, J.L. Browning, and P.S. Hochman. 1998. Lymph node genesis is induced by signaling through the lymphotoxin beta receptor. *Immunity* 9:71-79.

Rescigno, M., M. Urbano, B. Valzasina, M. Francolini, G. Rotta, R. Bonasio, F. Granucci, J.P. Kraehenbuhl, and P. Ricciardi-Castagnoli. 2001. Dendritic cells express tight junction proteins and penetrate gut epithelial monolayers to sample bacteria. *Nat Immunol* 2:361-367.

Rey, J., N. Garin, F. Spertini, and B. Corthesy. 2004. Targeting of secretory IgA to Peyer's patch dendritic and T cells after transport by intestinal M cells. *Journal of immunology* 172:3026-3033.

Rimoldi, M., and M. Rescigno. 2005. Uptake and presentation of orally administered antigens. *Vaccine* 23:1793-1796.

Rivollier, A., J. He, A. Kole, V. Valatas, and B.L. Kelsall. 2012. Inflammation switches the differentiation program of Ly6Chi monocytes from antiinflammatory macrophages to inflammatory dendritic cells in the colon. *J Exp Med* 209:139-155.

Rodriguez, A., A. Regnault, M. Kleijmeer, P. Ricciardi-Castagnoli, and S. Amigorena. 1999. Selective transport of internalized antigens to the cytosol for MHC class I presentation in dendritic cells. *Nat Cell Biol* 1:362-368.

Rosen, H., P.J. Gonzalez-Cabrera, M.G. Sanna, and S. Brown. 2009. Sphingosine 1-phosphate receptor signaling. *Annu Rev Biochem* 78:743-768.

Rosen, H., M.G. Sanna, S.M. Cahalan, and P.J. Gonzalez-Cabrera. 2007. Tipping the gatekeeper: S1P regulation of endothelial barrier function. *Trends Immunol* 28:102-107.

Rosen, H., R.C. Stevens, M. Hanson, E. Roberts, and M.B. Oldstone. 2013. Sphingosine-1-phosphate and its receptors: structure, signaling, and influence. *Annu Rev Biochem* 82:637-662.

Salazar-Gonzalez, R.M., J.H. Niess, D.J. Zammit, R. Ravindran, A. Srinivasan, J.R. Maxwell, T. Stoklasek, R. Yadav, I.R. Williams, X. Gu, B.A. McCormick, M.A. Pazos, A.T. Vella, L. Lefrancois, H.C. Reinecker, and S.J. McSorley. 2006. CCR6-mediated dendritic cell activation of pathogen-specific T cells in Peyer's patches. *Immunity* 24:623-632.

Salomon, B., J.L. Cohen, C. Masurier, and D. Klatzmann. 1998. Three populations of mouse lymph node dendritic cells with different origins and dynamics. *Journal of immunology* 160:708-717.

Sanchez, T., and T. Hla. 2004. Structural and functional characteristics of S1P receptors. *J Cell Biochem* 92:913-922.

Saraiva, M., and A. O'Garra. 2010. The regulation of IL-10 production by immune cells. *Nat Rev Immunol* 10:170-181.

Sato, A., M. Hashiguchi, E. Toda, A. Iwasaki, S. Hachimura, and S. Kaminogawa. 2003. CD11b+ Peyer's patch dendritic cells secrete IL-6 and induce IgA secretion from naive B cells. *Journal of immunology* 171:3684-3690.

Sato, A., and A. Iwasaki. 2005. Peyer's patch dendritic cells as regulators of mucosal adaptive immunity. *Cell Mol Life Sci* 62:1333-1338.

Satoh-Takayama, N., C.A. Vosshenrich, S. Lesjean-Pottier, S. Sawa, M. Lochner, F. Rattis, J.J. Mention, K. Thiam, N. Cerf-Bensussan, O. Mandelboim, G. Eberl, and J.P. Di Santo. 2008. Microbial flora drives interleukin 22 production in intestinal NKp46+ cells that provide innate mucosal immune defense. *Immunity* 29:958-970.

Satpathy, A.T., W. Kc, J.C. Albring, B.T. Edelson, N.M. Kretzer, D. Bhattacharya, T.L. Murphy, and K.M. Murphy. 2012. Zbtb46 expression distinguishes classical dendritic cells and their committed progenitors from other immune lineages. *The Journal of experimental medicine* 209:1135-1152.

Scheu, S., J. Alferink, T. Potzel, W. Barchet, U. Kalinke, and K. Pfeffer. 2002. Targeted disruption of LIGHT causes defects in costimulatory T cell activation and reveals cooperation with lymphotoxin beta in mesenteric lymph node genesis. *J Exp Med* 195:1613-1624.

Schmidt, T.H., O. Bannard, E.E. Gray, and J.G. Cyster. 2013. CXCR4 promotes B cell egress from Peyer's patches. *The Journal of experimental medicine* 210:1099-1107.

Schnorrer, P., G.M. Behrens, N.S. Wilson, J.L. Pooley, C.M. Smith, D. El-Sukkari, G. Davey, F. Kupresanin, M. Li, E. Maraskovsky, G.T. Belz, F.R. Carbone, K. Shortman, W.R. Heath, and J.A. Villadangos. 2006. The dominant role of CD8+ dendritic cells in cross-presentation is not dictated by antigen capture. *Proceedings of the National Academy of Sciences of the United States of America* 103:10729-10734.

Schoenberger, S.P., R.E. Toes, E.I. van der Voort, R. Offringa, and C.J. Melief. 1998. T-cell help for cytotoxic T lymphocytes is mediated by CD40-CD40L interactions. *Nature* 393:480-483.

Schraml, B.U., J. van Blijswijk, S. Zelenay, P.G. Whitney, A. Filby, S.E. Acton, N.C. Rogers, N. Moncaut, J.J. Carvajal, and C. Reis e Sousa. 2013. Genetic tracing via DNGR-1 expression history defines dendritic cells as a hematopoietic lineage. *Cell* 154:843-858.

Schulz, O., S.S. Diebold, M. Chen, T.I. Naslund, M.A. Nolte, L. Alexopoulou, Y.T. Azuma, R.A. Flavell, P. Liljestrom, and C. Reis e Sousa. 2005. Toll-like receptor 3 promotes cross-priming to virus-infected cells. *Nature* 433:887-892.

Schulz, O., E. Jaensson, E.K. Persson, X. Liu, T. Worbs, W.W. Agace, and O. Pabst. 2009. Intestinal CD103+, but not CX3CR1+, antigen sampling cells migrate in lymph and serve classical dendritic cell functions. *J Exp Med* 206:3101-3114.

Schulz, O., and O. Pabst. 2013. Antigen sampling in the small intestine. *Trends Immunol* 34:155-161.

Schwartz-Cornil, I., M. Epardaud, and M. Bonneau. 2006. Cervical duct cannulation in sheep for collection of afferent lymph dendritic cells from head tissues. *Nat Protoc* 1:874-879.

Shiokawa, A., K. Tanabe, N.M. Tsuji, R. Sato, and S. Hachimura. 2009. IL-10 and IL-27 producing dendritic cells capable of enhancing IL-10 production of T cells are induced in oral tolerance. *Immunology letters* 125:7-14.

Shreedhar, V.K., B.L. Kelsall, and M.R. Neutra. 2003. Cholera toxin induces migration of dendritic cells from the subepithelial dome region to T- and B-cell areas of Peyer's patches. *Infect Immun* 71:504-509.

Siddiqui, K.R., S. Laffont, and F. Powrie. 2010. E-cadherin marks a subset of inflammatory dendritic cells that promote T cell-mediated colitis. *Immunity* 32:557-567.

Sinha, R.K., C. Park, I.Y. Hwang, M.D. Davis, and J.H. Kehrl. 2009. B lymphocytes exit lymph nodes through cortical lymphatic sinusoids by a mechanism independent of sphingosine-1-phosphate-mediated chemotaxis. *Immunity* 30:434-446.

Spahn, T.W., A. Fontana, A.M. Faria, A.J. Slavin, H.P. Eugster, X. Zhang, P.A. Koni, N.H. Ruddle, R.A. Flavell, P.D. Rennert, and H.L. Weiner. 2001. Induction of oral tolerance to cellular immune responses in the absence of Peyer's patches. *European journal of immunology* 31:1278-1287.

Spahn, T.W., H.L. Weiner, P.D. Rennert, N. Lugering, A. Fontana, W. Domschke, and T. Kucharzik. 2002. Mesenteric lymph nodes are critical for the induction of high-dose oral tolerance in the absence of Peyer's patches. *Eur J Immunol* 32:1109-1113.

Spiegel, S., and S. Milstien. 2003. Sphingosine-1-phosphate: an enigmatic signalling lipid. *Nat Rev Mol Cell Biol* 4:397-407.

Spits, H., D. Artis, M. Colonna, A. Diefenbach, J.P. Di Santo, G. Eberl, S. Koyasu, R.M. Locksley, A.N. McKenzie, R.E. Mebius, F. Powrie, and E. Vivier. 2013. Innate lymphoid cells--a proposal for uniform nomenclature. *Nat Rev Immunol* 13:145-149.

Spits, H., and T. Cupedo. 2012. Innate lymphoid cells: emerging insights in development, lineage relationships, and function. *Annu Rev Immunol* 30:647-675.

Stagg, A.J., M.A. Kamm, and S.C. Knight. 2002. Intestinal dendritic cells increase T cell expression of alpha4beta7 integrin. *European journal of immunology* 32:1445-1454.

Steinman, R.M., and Z.A. Cohn. 1973. Identification of a novel cell type in peripheral lymphoid organs of mice. I. Morphology, quantitation, tissue distribution. *J Exp Med* 137:1142-1162.

Steinman, R.M., M. Pack, and K. Inaba. 1997. Dendritic cells in the T-cell areas of lymphoid organs. *Immunol Rev* 156:25-37.

Stephensen, C.B. 2001. Vitamin A, infection, and immune function. *Annu Rev Nutr* 21:167-192.

Sun, C.M., J.A. Hall, R.B. Blank, N. Bouladoux, M. Oukka, J.R. Mora, and Y. Belkaid. 2007. Small intestine lamina propria dendritic cells promote de novo generation of Foxp3 T reg cells via retinoic acid. *The Journal of experimental medicine* 204:1775-1785.

Sun, Z., D. Unutmaz, Y.R. Zou, M.J. Sunshine, A. Pierani, S. Brenner-Morton, R.E. Mebius, and D.R. Littman. 2000. Requirement for RORgamma in thymocyte survival and lymphoid organ development. *Science* 288:2369-2373.

Suzuki, H., S. Sekine, K. Kataoka, D.W. Pascual, M. Maddaloni, R. Kobayashi, K. Fujihashi, H. Kozono, and J.R. McGhee. 2008. Ovalbumin-protein sigma 1 M-cell targeting facilitates oral tolerance with reduction of antigen-specific CD4+ T cells. *Gastroenterology* 135:917-925.

Svensson, M., B. Johansson-Lindbom, F. Zapata, E. Jaensson, L.M. Austenaa, R. Blomhoff, and W.W. Agace. 2008. Retinoic acid receptor signaling levels and antigen dose regulate gut homing receptor expression on CD8+ T cells. *Mucosal Immunol* 1:38-48.

Tabeta, K., P. Georgel, E. Janssen, X. Du, K. Hoebe, K. Crozat, S. Mudd, L. Shamel, S. Sovath, J. Goode, L. Alexopoulou, R.A. Flavell, and B. Beutler. 2004. Toll-like receptors 9 and 3 as essential components of innate immune defense against mouse cytomegalovirus infection. *Proceedings of the National Academy of Sciences of the United States of America* 101:3516-3521.

Takeda, K., and S. Akira. 2005. Toll-like receptors in innate immunity. *Int Immunol* 17:1-14.

Tal, O., H.Y. Lim, I. Gurevich, I. Milo, Z. Shipony, L.G. Ng, V. Angeli, and G. Shakhar. 2011. DC mobilization from the skin requires docking to immobilized CCL21 on lymphatic endothelium and intralymphatic crawling. *The Journal of experimental medicine* 208:2141-2153.

Tamoutounour, S., S. Henri, H. Lelouard, B. de Bovis, C. de Haar, C.J. van der Woude, A.M. Woltman, Y. Reyal, D. Bonnet, D. Sichien, C.C. Bain, A.M. Mowat, C. Reis e Sousa, L.F. Poulin, B. Malissen, and M. Guilliams. 2012. CD64 distinguishes macrophages from dendritic cells in the gut and reveals the Th1-inducing role of mesenteric lymph node macrophages during colitis. *European journal of immunology* 42:3150-3166.

Tang, F., Q. Du, and Y.J. Liu. 2010. Plasmacytoid dendritic cells in antiviral immunity and autoimmunity. *Sci China Life Sci* 53:172-182.

Taylor, R.T., S.R. Patel, E. Lin, B.R. Butler, J.G. Lake, R.D. Newberry, and I.R. Williams. 2007. Lymphotoxin-independent expression of TNF-related activation-induced cytokine by stromal cells in cryptopatches, isolated lymphoid follicles, and Peyer's patches. *Journal of immunology* 178:5659-5667.

Teoh, D., L.A. Johnson, T. Hanke, A.J. McMichael, and D.G. Jackson. 2009. Blocking development of a CD8+ T cell response by targeting lymphatic recruitment of APC. *Journal of immunology* 182:2425-2431.

Tew, J.G., J. Wu, M. Fakher, A.K. Szakal, and D. Qin. 2001. Follicular dendritic cells: beyond the necessity of T-cell help. *Trends Immunol* 22:361-367.

Tezuka, H., and T. Ohteki. 2010. Regulation of intestinal homeostasis by dendritic cells. *Immunol Rev* 234:247-258.

Tilney N, L. 1971. Patterns of lymphatic drainage in the adult laboratory rat. *J Anat* 109:14.

Tomura, M., N. Yoshida, J. Tanaka, S. Karasawa, Y. Miwa, A. Miyawaki, and O. Kanagawa. 2008. Monitoring cellular movement in vivo with photoconvertible fluorescence protein "Kaede" transgenic mice. *Proc Natl Acad Sci U S A* 105:10871-10876.

Travis, S., and I. Menzies. 1992. Intestinal permeability: functional assessment and significance. *Clin Sci (Lond)* 82:471-488.

Tsuji, M., N. Komatsu, S. Kawamoto, K. Suzuki, O. Kanagawa, T. Honjo, S. Hori, and S. Fagarasan. 2009. Preferential generation of follicular B helper T cells from Foxp3+ T cells in gut Peyer's patches. *Science* 323:1488-1492.

Tsuji, M., K. Suzuki, H. Kitamura, M. Maruya, K. Kinoshita, Ivanov, II, K. Itoh, D.R. Littman, and S. Fagarasan. 2008. Requirement for lymphoid tissue-inducer cells in isolated follicle formation and T cell-independent immunoglobulin A generation in the gut. *Immunity* 29:261-271.

Tumanov, A.V., D.V. Kuprash, and S.A. Nedospasov. 2003. The role of lymphotoxin in development and maintenance of secondary lymphoid tissues. *Cytokine Growth Factor Rev* 14:275-288.

Turnbull, E.L., U. Yrlid, C.D. Jenkins, and G.G. Macpherson. 2005. Intestinal dendritic cell subsets: differential effects of systemic TLR4 stimulation on migratory fate and activation in vivo. *Journal of immunology* 174:1374-1384.

Uematsu, S., M.H. Jang, N. Chevrier, Z. Guo, Y. Kumagai, M. Yamamoto, H. Kato, N. Sougawa, H. Matsui, H. Kuwata, H. Hemmi, C. Coban, T. Kawai, K.J. Ishii, O. Takeuchi, M. Miyasaka, K. Takeda, and S. Akira. 2006. Detection of pathogenic intestinal bacteria by Toll-like receptor 5 on intestinal CD11c+ lamina propria cells. *Nat Immunol* 7:868-874.

Vallon-Eberhard, A., L. Landsman, N. Yogev, B. Verrier, and S. Jung. 2006. Transepithelial pathogen uptake into the small intestinal lamina propria. *J Immunol* 176:2465-2469.

van de Pavert, S.A., B.J. Olivier, G. Goverse, M.F. Vondenhoff, M. Greuter, P. Beke, K. Kusser, U.E. Hopken, M. Lipp, K. Niederreither, R. Blomhoff, K. Sitnik, W.W. Agace, T.D. Randall, W.J. de Jonge, and R.E. Mebius. 2009. Chemokine CXCL13 is essential for lymph node initiation and is induced by retinoic acid and neuronal stimulation. *Nature immunology* 10:1193-1199.

Varol, C., A. Vallon-Eberhard, E. Elinav, T. Aychek, Y. Shapira, H. Luche, H.J. Fehling, W.D. Hardt, G. Shakhar, and S. Jung. 2009. Intestinal lamina propria dendritic cell subsets have different origin and functions. *Immunity* 31:502-512.

Varona, R., R. Villares, L. Carramolino, I. Goya, A. Zaballos, J. Gutierrez, M. Torres, A.C. Martinez, and G. Marquez. 2001. CCR6-deficient mice have impaired leukocyte homeostasis and altered contact hypersensitivity and delayed-type hypersensitivity responses. *J Clin Invest* 107:R37-45.

Veiga-Fernandes, H., M.C. Coles, K.E. Foster, A. Patel, A. Williams, D. Natarajan, A. Barlow, V. Pachnis, and D. Kioussis. 2007. Tyrosine kinase receptor RET is a key regulator of Peyer's patch organogenesis. *Nature* 446:547-551.

Velaga, S., H. Herbrand, M. Friedrichsen, T. Jiong, M. Dorsch, M.W. Hoffmann, R. Forster, and O. Pabst. 2009. Chemokine receptor CXCR5 supports solitary intestinal lymphoid tissue formation, B cell homing, and induction of intestinal IgA responses. *Journal of immunology* 182:2610-2619.

Vermaelen, K.Y., I. Carro-Muino, B.N. Lambrecht, and R.A. Pauwels. 2001. Specific migratory dendritic cells rapidly transport antigen from the airways to the thoracic lymph nodes. *The Journal of experimental medicine* 193:51-60.

Vezys, V., S. Olson, and L. Lefrancois. 2000. Expression of intestine-specific antigen reveals novel pathways of CD8 T cell tolerance induction. *Immunity* 12:505-514.

Villadangos, J.A., R.A. Bryant, J. Deussing, C. Driessen, A.M. Lennon-Dumenil, R.J. Riese, W. Roth, P. Saftig, G.P. Shi, H.A. Chapman, C. Peters, and H.L. Ploegh. 1999. Proteases involved in MHC class II antigen presentation. *Immunol Rev* 172:109-120.

Voehringer, D., K. Shinkai, and R.M. Locksley. 2004. Type 2 immunity reflects orchestrated recruitment of cells committed to IL-4 production. *Immunity* 20:267-277.

Vondenhoff, M.F., G.E. Desanti, T. Cupedo, J.Y. Bertrand, A. Cumano, G. Kraal, R.E. Mebius, and R. Golub. 2008. Separation of splenic red and white pulp occurs before birth in a LTalphabeta-independent manner. *Journal of leukocyte biology* 84:152-161.

Vondenhoff, M.F., M. Greuter, G. Goverse, D. Elewaut, P. Dewint, C.F. Ware, K. Hoorweg, G. Kraal, and R.E. Mebius. 2009a. LTbetaR signaling induces cytokine expression and up-regulates lymphangiogenic factors in lymph node anlagen. *Journal of immunology* 182:5439-5445.

Vondenhoff, M.F., S.A. van de Pavert, M.E. Dillard, M. Greuter, G. Goverse, G. Oliver, and R.E. Mebius. 2009b. Lymph sacs are not required for the initiation of lymph node formation. *Development* 136:29-34.

Vremec, D., J. Pooley, H. Hochrein, L. Wu, and K. Shortman. 2000. CD4 and CD8 expression by dendritic cell subtypes in mouse thymus and spleen. *Journal of immunology* 164:2978-2986.

Vremec, D., M. Zorbas, R. Scollay, D.J. Saunders, C.F. Ardavin, L. Wu, and K. Shortman. 1992. The surface phenotype of dendritic cells purified from mouse thymus and spleen: investigation of the CD8 expression by a subpopulation of dendritic cells. *The Journal of experimental medicine* 176:47-58.

Wagner, N., J. Lohler, E.J. Kunkel, K. Ley, E. Leung, G. Krissansen, K. Rajewsky, and W. Muller. 1996. Critical role for beta7 integrins in formation of the gut-associated lymphoid tissue. *Nature* 382:366-370.

Wang, B., C. Biron, J. She, K. Higgins, M.J. Sunshine, E. Lacy, N. Lonberg, and C. Terhorst. 1994. A block in both early T lymphocyte and natural killer cell development in transgenic mice with high-copy numbers of the human CD3E gene. *Proc Natl Acad Sci U S A* 91:9402-9406.

Welty, N.E., C. Staley, N. Ghilardi, M.J. Sadowsky, B.Z. Igyarto, and D.H. Kaplan. 2013. Intestinal lamina propria dendritic cells maintain T cell homeostasis but do not affect commensalism. *The Journal of experimental medicine* 210:2011-2024.

Wendland, M., N. Czeloth, N. Mach, B. Malissen, E. Kremmer, O. Pabst, and R. Forster. 2007. CCR9 is a homing receptor for plasmacytoid dendritic cells to the small intestine. *Proceedings of the National Academy of Sciences of the United States of America* 104:6347-6352.

Wigle, J.T., and G. Oliver. 1999. Prox1 function is required for the development of the murine lymphatic system. *Cell* 98:769-778.

Wilke, C.M., K. Bishop, D. Fox, and W. Zou. 2011. Deciphering the role of Th17 cells in human disease. *Trends Immunol* 32:603-611.

Wilson, C.L., A.J. Ouellette, D.P. Satchell, T. Ayabe, Y.S. Lopez-Boado, J.L. Stratman, S.J. Hultgren, L.M. Matrisian, and W.C. Parks. 1999. Regulation of intestinal alpha-defensin activation by the metalloproteinase matrilysin in innate host defense. *Science* 286:113-117.

Wilson, N.S., L.J. Young, F. Kupresanin, S.H. Naik, D. Vremec, W.R. Heath, S. Akira, K. Shortman, J. Boyle, E. Maraskovsky, G.T. Belz, and J.A. Villadangos. 2008. Normal proportion and expression of maturation markers in migratory dendritic cells in the absence of germs or Toll-like receptor signaling. *Immunol Cell Biol* 86:200-205.

Withers, D.R., M.Y. Kim, V. Bekiaris, S.W. Rossi, W.E. Jenkinson, F. Gaspal, F. McConnell, J.H. Caamano, G. Anderson, and P.J. Lane. 2007. The role of lymphoid tissue inducer cells in splenic white pulp development. *European journal of immunology* 37:3240-3245.

Woerly, G., P. Lacy, A.B. Younes, N. Roger, S. Loiseau, R. Moqbel, and M. Capron. 2002. Human eosinophils express and release IL-13 following CD28-dependent activation. *Journal of leukocyte biology* 72:769-779.

Worbs, T., U. Bode, S. Yan, M.W. Hoffmann, G. Hintzen, G. Bernhardt, R. Forster, and O. Pabst. 2006. Oral tolerance originates in the intestinal immune system and relies on antigen carriage by dendritic cells. *J Exp Med* 203:519-527.

Wu, Y., and Y. Liu. 1994. Viral induction of co-stimulatory activity on antigen-presenting cells bypasses the need for CD4+ T-cell help in CD8+ T-cell responses. *Curr Biol* 4:499-505.

Wykes, M., A. Pombo, C. Jenkins, and G.G. MacPherson. 1998. Dendritic cells interact directly with naive B lymphocytes to transfer antigen and initiate class switching in a primary T-dependent response. *Journal of immunology* 161:1313-1319.

Yamamoto, M., P. Rennert, J.R. McGhee, M.N. Kweon, S. Yamamoto, T. Dohi, S. Otake, H. Bluethmann, K. Fujihashi, and H. Kiyono. 2000. Alternate mucosal immune system: organized Peyer's patches are not required for IgA responses in the gastrointestinal tract. *J Immunol* 164:5184-5191.

Yamazaki, S., D. Dudziak, G.F. Heidkamp, C. Fiorese, A.J. Bonito, K. Inaba, M.C. Nussenzweig, and R.M. Steinman. 2008. CD8+ CD205+ splenic dendritic cells are specialized to induce Foxp3+ regulatory T cells. *Journal of immunology* 181:6923-6933.

Yanagawa, Y., and K. Onoe. 2003. CCR7 ligands induce rapid endocytosis in mature dendritic cells with concomitant up-regulation of Cdc42 and Rac activities. *Blood* 101:4923-4929.

Yang, R., Q. Liu, J.L. Grosfeld, and M.D. Pescovitz. 1994. Intestinal venous drainage through the liver is a prerequisite for oral tolerance induction. *J Pediatr Surg* 29:1145-1148.

Yewdell, J.W., C.C. Norbury, and J.R. Bennink. 1999. Mechanisms of exogenous antigen presentation by MHC class I molecules in vitro and in vivo: implications for generating CD8+ T cell responses to infectious agents, tumors, transplants, and vaccines. *Adv Immunol* 73:1-77.

Yokota, Y., A. Mansouri, S. Mori, S. Sugawara, S. Adachi, S. Nishikawa, and P. Gruss. 1999. Development of peripheral lymphoid organs and natural killer cells depends on the helix-loop-helix inhibitor Id2. *Nature* 397:702-706.

Yoshida, H., A. Naito, J. Inoue, M. Satoh, S.M. Santee-Cooper, C.F. Ware, A. Togawa, and S. Nishikawa. 2002a. Different cytokines induce surface lymphotoxin-alphabeta on IL-7 receptor-alpha cells that differentially engender lymph nodes and Peyer's patches. *Immunity* 17:823-833.

Yoshida, M., S.M. Claypool, J.S. Wagner, E. Mizoguchi, A. Mizoguchi, D.C. Roopenian, W.I. Lencer, and R.S. Blumberg. 2004. Human neonatal Fc receptor mediates transport of IgG into luminal secretions for delivery of antigens to mucosal dendritic cells. *Immunity* 20:769-783.

Yoshida, M., K. Kobayashi, T.T. Kuo, L. Bry, J.N. Glickman, S.M. Claypool, A. Kaser, T. Nagaishi, D.E. Higgins, E. Mizoguchi, Y. Wakatsuki, D.C. Roopenian, A. Mizoguchi, W.I. Lencer, and R.S. Blumberg. 2006. Neonatal Fc receptor for IgG regulates mucosal immune responses to luminal bacteria. *J Clin Invest* 116:2142-2151.

Yoshida, T., S. Hachimura, M. Ishimori, F. Kinugasa, W. Ise, M. Totsuka, A. Ametani, and S. Kaminogawa. 2002b. Antigen presentation by Peyer's patch cells can induce both Th1- and Th2-type responses depending on antigen dosage, but a different cytokine response pattern from that of spleen cells. *Biosci Biotechnol Biochem* 66:963-969.

Yrlid, U., V. Cerovic, S. Milling, C.D. Jenkins, L.S. Klavinskis, and G.G. MacPherson. 2006a. A distinct subset of intestinal dendritic cells responds selectively to oral TLR7/8 stimulation. *European journal of immunology* 36:2639-2648.

Yrlid, U., V. Cerovic, S. Milling, C.D. Jenkins, J. Zhang, P.R. Crocker, L.S. Klavinskis, and G.G. MacPherson. 2006b. Plasmacytoid dendritic cells do not migrate in intestinal or hepatic lymph. *J Immunol* 177:6115-6121.

Yrlid, U., S.W. Milling, J.L. Miller, S. Cartland, C.D. Jenkins, and G.G. MacPherson. 2006c. Regulation of intestinal dendritic cell migration and activation by plasmacytoid dendritic cells, TNF-alpha and type 1 IFNs after feeding a TLR7/8 ligand. *J Immunol* 176:5205-5212.

Zhang, X., H. Huang, J. Yuan, D. Sun, W.S. Hou, J. Gordon, and J. Xiang. 2005. CD4-8- dendritic cells prime CD4+ T regulatory 1 cells to suppress antitumor immunity. *Journal of immunology* 175:2931-2937.

Zhang, X., L. Izikson, L. Liu, and H.L. Weiner. 2001. Activation of CD25(+)CD4(+) regulatory T cells by oral antigen administration. *Journal of immunology* 167:4245-4253.

Zhang, X., M.A. Munegowda, J. Yuan, Y. Wei, and J. Xiang. 2010. Optimal TLR9 signal converts tolerogenic CD4-8- DCs into immunogenic ones capable of stimulating antitumor immunity via activating CD4+ Th1/Th17 and NK cell responses. *Journal of leukocyte biology* 88:393-403.

Zhao, X., A. Sato, C.S. Dela Cruz, M. Linehan, A. Luegering, T. Kucharzik, A.K. Shirakawa, G. Marquez, J.M. Farber, I. Williams, and A. Iwasaki. 2003. CCL9 is secreted by the follicle-associated epithelium and recruits dome region Peyer's patch CD11b+ dendritic cells. *J Immunol* 171:2797-2803.

Zhu, J., and W.E. Paul. 2008. CD4 T cells: fates, functions, and faults. *Blood* 112:1557-1569.

Zigmond, E., C. Varol, J. Farache, E. Elmaliah, A.T. Satpathy, G. Friedlander, M. Mack, N. Shpigel, I.G. Boneca, K.M. Murphy, G. Shakhar, Z. Halpern, and S. Jung. 2012. Ly6C hi monocytes in the inflamed colon give rise to proinflammatory effector cells and migratory antigen-presenting cells. *Immunity* 37:1076-1090.

Zuany-Amorim, C., C. Ruffie, S. Haile, B.B. Vargaftig, P. Pereira, and M. Pretolani. 1998. Requirement for gammadelta T cells in allergic airway inflammation. *Science* 280:1265-1267.